Molecular changes in egg tempera paint dosimeters as tools to monitor the museum environment

Molecular changes in egg tempera paint dosimeters as tools to monitor the museum environment

ACADEMISCH PROEFSCHRIFT

ter verkrijging van de graad van doctor

aan de Universiteit van Amsterdam

op gezag van de Rector Magnificus

prof. dr. J.J.M. Franse,

ten overstaan van een door het college voor promoties ingestelde

commissie, in het openbaar te verdedigen in de Aula der Universiteit

op donderdag 29 november 2001, te 10.00 uur

door

Oscar Franciscus van den Brink

geboren te Bilthoven

Promotor:

Prof. Dr. J.J. Boon

Examination Committee:

Prof. Dr. C.J. Elsevier
Prof. Dr. P.G. Kistemaker
Prof. Dr. C.G. de Koster
Prof. Dr. J. Verhoeven
Dr. D. Saunders

MOLART Reports

MOLART - Molecular Aspects of Ageing of Painted Art - is a 5-year co-operative project between art historians, restorers, analytical chemists and technical physicists funded by the Netherlands Organisation for Scientific Research (NWO). Technical support and advice is given by Shell-SRTCA (Amsterdam), AKZO Nobel (Arnhem), Instituut Collectie Nederland (ICN, Amsterdam) and the Dutch art museums. The project was launched on 1 February 1995 and will end early 2002. The object of MOLART is to contribute to the development of a scientific framework for the conservation of painted art on the molecular level. The focus of MOLART is the determination of the present chemical and physical condition of works of art produced in the period from the 15th to the 20th century. Studies of historical paint manufacturing and workshop practice must give insight into the nature of the painters' media and the painting technique used originally. Fundamental studies on varnishes, paint and colorants are undertaken to understand the molecular aspects of ageing since this is thought to be a main cause for the continued need to treat paintings.

This thesis is the fourth in a series of MOLART reports, that will summarise all research results obtained in the course of the project. Information about MOLART can be obtained from the project co-ordinator Prof. Dr. J.J. Boon, FOM-Institute for Atomic and Molecular Physics, Kruislaan 407 1098 SJ Amsterdam, The Netherlands.

The following publications resulted from research performed in the preparation of this PhD thesis:

Chapter 1

Odlyha, M., Boon, J. J., van den Brink, O. F., and Bacci, M., 'Environmental research for art conservation (ERA)', Journal of Thermal Analysis 49 (1997) 1571-1584.

Odlyha, M., Boon, J. J., van den Brink, O. F., and Bacci, M., 'ERA: Environmental Research for Art conservation', European Cultural Heritage Newsletter on Research 10 (June) (1997) 67-77.

Chapter 2

van den Brink, O. F., Eijkel, G. B., and Boon, J. J., 'Dosimetry of paintings: Determination of the degree of chemical change in museum exposed test paintings by mass spectrometry', Thermochimica Acta 365 (1-2) (2000) 1-23.

van den Brink, O. F., Peulvé, S., and Boon, J. J., 'Dosimetry of paintings: Chemical changes in test paintings as tools to assess the environmental stress in the museum environment' in SSCR Conference on Site effects: The impact of location on conservation treatments, ed. M.M. Wright and I.M.T. Player-Dahnsjö, The Scottish Society for Conservation and Restoration, Edinburgh, Dundee, Scotland (1998) 70-76.

van den Brink, O. F., Boon, J. J., and van der Hage, E. R. E., 'Dosimetry of Paintings: Molecular changes in paintings as a tool to determine the impact of environment on works of art.', European Cultural Heritage Newsletter on Research 10 (June) (1997) 142-144.

Chapter 3

van den Brink, O. F., Peulvé, S., and Boon, J. J., 'Chemical changes in test paintings measure the environmental impact on the museum collection.' in Art et Chimie, La Couleur, ed. J. Goupy and J.-P. Mohen, CNRS Editions, Paris (2000) 121-125.

Chapter 4

Odlyha, M., van den Brink, O. F., Boon, J. J., Bacci, M., and Cohen, N. S., 'Damage assessment of storage and display conditions for painted works of art', Journal of Thermal Analysis (2001). submitted

Chapter 6

van den Brink, O. F., Boon, J. J., O'Connor, P. B., Duursma, M. C., and Heeren, R. M. A., 'Matrix-assisted laser desorption/ionization Fourier transform mass spectrometric analysis of oxygenated triglycerides and phosphatidylcholines in egg tempera paint systems for environmental monitoring of museum conditions', Journal of Mass Spectrometry 36 (2001) 479-492.

van den Brink, O. F., O'Connor, P. B., Duursma, M. C., Heeren, R. M. A., Peulvé, S., and Boon, J. J., 'Analysis of oxygenated egg lipids in tempera paint by MALDI FT-ICR-MS(MS)' in 14th International Conference on Mass Spectrometry, ed. E.J. Karjalainen, A.E. Hesso, J.E. Jalonen, and U.P. Karjalainen, Advances in Mass Spectrometry, Vol. 14, Elsevier, Tampere, Finland (1997) POSTER C05 TUPO076.

van den Brink, O. F., O'Connor, P. B., Duursma, M. C., Peulvé, S., Heeren, R. M. A., and Boon, J. J., 'Analysis of Egg Lipids and Their Oxidation Products by MALDI-FTMS' in 45th ASMS Conference on Mass Spectrometry and Allied Topics, Palm Springs, CA, USA (1997) 1372.

Chapter 7

van den Brink, O. F., Duursma, M. C., Boon, J. J., and Heeren, R. M. A., 'An ESI-FTMSMS study of natural and photo-oxidized egg glycerolipids' in 48th ASMS Conference on Mass Spectrometry and Allied Topics, ed. A.B. Giordani, Elsevier, Long Beach, CA, USA (2000) 138-139.

van den Brink, O. F., Duursma, M. C., Boon, J. J., and Heeren, R. M. A., 'An ESI-FTMSMS Study of the Structure of Photo-oxidised Egg Glycerolipids.' in 15th International Conference on Mass Spectrometry, ed. E. Gelpi, Advances in Mass Spectrometry, Vol. 15, Elsevier, Barcelona, Spain (2000) in press.

Other publications that are related to this thesis

van den Brink, O. F., Duursma, M. C., Oonk, S., Eijkel, G. B., Boon, J. J., and Heeren, R. M. A., 'Probing changes in the lipid composition on the surface of laser treated artist paints by MALDI-MS.' in 49th ASMS Conference on Mass Spectrometry and Allied Topics, ed. A.B. Giordani, Elsevier, Chicago, IL, USA (2001) in press.

Odlyha, M., van den Brink, O. F., Boon, J. J., Bacci, M., and Cohen, N. S., 'Environmental Research for Art Conservation: a new risk assessment tool.' in 4th European Conference for Protection, Conservation and Enhancement of European Cultural Heritage, Strassbourg, France (2000) in press.

Odlyha, M., Cohen, N.S., Foster, G.M., Campana, R., Boon, J. J., van den Brink, O. F., Peulvé, S., Bacci, M., Picollo, M., and Porcinai, S., 'ERA, Environmental Research for Art Conservation' Final Report for the European Commission. University of London, Birkbeck College (London, U.K.), FOM Institute for Atomic and Molecular Physics (Amsterdam, NL) and Istituto di Ricerca sulle Onde Elettromagnetiche, CNR (Florence, IT), (1999) 210 + xc pp.

Peulvé, S., Boon, J. J., Duursma, M. C., van den Brink, O. F., O' Connor, P. B., and Heeren, R. M. A., 'Mass spectrometric studies of proteins in fresh egg and aged egg tempera paint films. Progress report I.' in 14th International Mass Spectrometry Conference, ed. E.J. Karjalainen, A.E. Hesso, J.E. Jalonen, and U.P. Karjalainen, Advances in Mass Spectrometry, Vol. 14, Elsevier, Tampere, Finland (1997) POSTER C02 WEPO051.

Boon, J. J., Peulvé, S. L., van den Brink, O. F., Duursma, M. C., and Rainford, D., 'Molecular aspects of mobile and stationary phases in ageing tempera and oil paint films' in Early Italian Painting Technique, ed. T. Bakkenist, R. Hoppenbrouwers, and H. Dubois, Limburg Conservation Institute, Maastricht, The Netherlands (1997) 32-47.

Glossary

AWG	arbitrary waveform generator
CID	collision-induced dissociation or decomposition
COP	cholesterol oxidation product
DA	discriminant analysis
DAG	diacylglycerol
DAPC	diacylphosphatidylcholine
DAPE	diacylphosphatidylethanolamine
DHB	2,5-dihydroxybenzoic acid
DT-FTMS	direct temperature-resolved Fourier transform mass spectrometry
DTMS	direct temperature-resolved mass spectrometry
EI	electron ionisation
ESI	electrospray ionisation
FA	fatty acid
FAB	fast-atom bombardment
FT	Fourier transform
FWHM	full width at half maximum
GC	gas chromatography
HP	high-performance
ICR	ion cyclotron resonance
IDOX	index for the degree of oxygenation
LAE	light ageing equivalent
LC	liquid chromatography
LDL	low density lipoprotein
MALDI	matrix-assisted laser desorption/ionisation
MCO	metal catalysed oxidation
MIKES	mass-analysed ion kinetic energy spectroscopy
MS	mass spectrometry
MSMS	tandem mass spectrometry
MT	mass thermogram
PL	phospholipid
SEC	size exclusion chromatography
SORI	sustained off-resonance irradiation
SWIFT	stored-waveform inverse Fourier transform
TAG	triacylglycerol
TBA	thiobarbituric acid
THF	tetrahydrofurane
TIC	total ion current
TLC	thin-layer chromatography

Contents

1. Introduction

This thesis reports research on the principle of paint-based dosimetry of museum conditions performed in the course of the EU supported ERA project (Environmental research for Art Conservation). The idea was tested to use the physico-chemical response of egg tempera paint to its environment as an indicator of the environmental stress. The first part of this chapter describes the rationale and approach of the research project. A variety of paint systems with different composition was prepared, cured and exposed under museum and laboratory conditions. These exposed paint systems play a central role in this thesis. A description of the preparation of the paints and their exposure conditions is therefore given in this chapter.

1.1 Rationale of the project

Painted works of art stored or displayed in museums and galleries are constantly subject to decay. The environment in the interior of a museum or historic building and the microclimate surrounding the object constitute a complex set of factors, which determines the nature and rate of decay. Such detrimental changes encompass not only discoloration of the varnish, but also discoloration of pigments and degradation of the binding medium. For example, Bacci *et al.* have observed a noticeable colour change in the "Predella della Trinità" by Luca Signorelli (1445-1523) on display in the Uffizi Gallery after a period of 66 months of regular exhibition to the public in the environmentally controlled Leonardo room [1]. Colour changes have also been observed in experimental paintings exposed in the National Gallery (London, UK) [2]. Important environmental factors are temperature, relative humidity, concentration of air pollutants, and light intensity and wavelength-distribution [3, 4]. Additional, less abundant but often much more harmful factors include vibration, insects and moulds, people and acts of God [4]. If the risk of damage on paintings were to be minimised, displaying them would be impossible and museums would lose part of their function. Cameron [4] describes this part of the museum's dilemma as follows: "People comfort is hazardous to works of art; one or the other must suffer." Hence, trade-offs have to be made. Depending on the materials present and provided the environment is understood, skilled and informed conservators

can to some extent retard the rate of deterioration of works of art. This can be achieved in a number of ways, for instance, by controlling physical environmental factors such as the temperature and relative humidity of the air. At great expense major museums direct much effort towards the standardisation of environmental conditions that surround works of art. In some cases new galleries or wings are thoroughly tested before use [5]. Maintaining a stable microclimate around a work of art, for instance, is probably the most effective method of protection, but widespread adoption of such methods will not occur until confidence is fully established and that will depend on a detailed understanding of the mechanisms of degradation due to environmental factors.

On the other hand not all art is well protected. Works of art are often stored in rooms with no climate control. Art on display in public buildings, historic buildings, palaces, churches and chapels is exposed to much larger environmental fluctuations. In particular where paintings are hung directly on external walls, large temperature and humidity fluctuations give rise to gradients, which affect the mechanical and chemical stability of the paint films. This may even lead to migration of organic constituents and cause blanching phenomena (for example in paintings by Stanley Spencer in the Sandham Chapel [6]). Such conditions require repeated interventions by trained conservators, which does not improve the condition and the overall stability of the works of art.

1.1.1 Model studies

In conservation science considerable attention is given to model studies on the effects of selected environmental factors on artists' materials. Hedley [7] has studied the effect of relative humidity on stress/strain response of genuine canvas samples of old paintings. Erhardt *et al.* [8] have investigated the effect of relative humidity changes on wooden panels and attempted to establish allowable relative humidity fluctuations. They have also determined expansion coefficients for typical layers of panel paintings, such as lead white oil paint, gesso and hide glue. This work has catalysed the development of thoughts on the issue of modelling painting behaviour and the establishment of new guidelines for museum conditions.

Due to the great interest of the paint industry, the colourfastness of dyes and pigments has been studied extensively. During the last decades, special devices have been used to expose paint systems to (very) high light intensities and /or specific weather conditions. Results obtained with such cabinets have contributed to the understanding of (some of) the variables which play a role in the fading of paintings [9]. More recently, devices were designed and constructed specifically to perform realistic light exposure model studies of materials used in

artefacts [10]. Saunders and Kirby have investigated light-induced damage to a variety of pigments [11]. In their study some pigments followed the reciprocity principle for light exposure, i.e. the degree of deterioration was determined by the product of exposure time and light intensity. In some cases however, the principle was not applicable. It must be noted that effects such as autocatalysis or the presence of an induction time may cause deviations from simple first order behaviour [12]. It was stated by Feller [12] that it is important that the degradation profile (kinetics of degradation) be understood when retarding of the degradation is an aim. To our knowledge apart from the efforts in the SCICULT project (partly published in [13]), no molecular model studies of light-induced deterioration of natural binding media have been carried out. Measurement of the light intensity can be relatively simple for artificially lit display areas. For side-lit interiors this is much more difficult. The intensity and wavelength distribution of the natural light is quite variable and depends on latitude, season, weather conditions and time of the day. Furthermore texture and reflectivity of the interior are important factors. As a result great variations in light intensity can occur within one room. Given this variation it is a very difficult task to predict the daylight dosages of objects in side-lit galleries [14], let alone to estimate the damage on those objects. However, given the fact that very high dosages (5% of annual recommendation) were measured after a single day of exposure in a side-lit gallery under sunny conditions [14], it is not surprising that great efforts are made to control the light intensity in galleries and in particular in historic buildings.

1.1.2 The chemical atmosphere

As early as 1850 the famous chemist and physicist Michael Faraday rang the alarm bell for the effects of sulphur dioxide on works of art, and suggested measures for the protection of paintings. In the 1960s attention was given again to the effects of air pollution on works of art. Holbrow [15] reviewed methods for the measurement of a variety of air pollutants and even reported results of exposure of fresh paint films to selected air pollutants at elevated levels. For example, sulphur dioxide was found to interfere with the drying process and lengthen the drying time of oil paint films, in extreme cases until 'infinity'. Unfortunately, very little attention was paid to the effects on mature paint films. In 1965 Thomson reviewed possible effects of a variety of air pollutants on antiquities [16]. He suggested that scientific conservation research be carried out to determine the relative importance of the reduction of concentrations of dirt and pollutants for various classes of objects. More recently Baer and Banks [17], and Brimblecombe [18] have drawn the attention of conservation science and

atmospheric scientists to the effects of air pollutants on museum objects. Not only did these authors discuss the potential effects of pollutants, such as nitrogen oxides and sulphur oxides, that are imported into the museum from outside, they also mention pollutants of typical indoor origin, such as formaldehyde from wood and wood composites, and other building materials. In showcases pollutants that originate from the cases or their exhibits are a major concern. Comparison by Baer [17] shows that many standards for levels of pollutants can be applied, but these are rather arbitrarily determined. The effects of air pollutants such as nitrogen oxides (NO_x and atmospheric nitric acid) [19, 20], sulphur oxides [21], peroxyacetyl nitrate [22] and ozone [23-26] on organic dyes have been studied extensively by Grosjean and Cass and co-workers and molecular changes have been identified mainly by mass spectrometric studies [27].

1.1.3 Monitoring of the environment

Monitoring of pollutants in the museum environment has received more and more attention since the 1980s. The internal environment of the Tate Gallery, for instance, has been studied extensively, and concentrations of nitrogen oxides and sulphur oxides in this museum have been determined using various methods [28]. Similar investigations have been carried out at the Victoria and Albert museum (London, UK) [29]. Hisham and Grosjean [30] have studied the indoor and outdoor levels of nitrogen dioxide, nitric acid, and peroxyacetyl nitrate in nine museums in Southern California. These studies clearly point to diurnal and seasonal variations in the levels of pollution. Variations in the values of relative humidity and temperature were investigated in a study of a museum microclimate in Padua by Camuffo [31]. The values were found to fluctuate considerably with season and the time of the day. Within the framework of the Uffizi Project [32] a comparative study of the air quality in two rooms of the Uffizi Gallery (Florence, Italy) has been carried out by Bernardi and Camuffo [33]. In their survey the temperature and relative humidity distributions were studied in detail and attention was given to particulate air pollution. Also within the Uffizi Project, De Santis *et al.* [34] have carried out monitoring of gaseous air pollutants, sulphur dioxide, nitric acid, nitrous acid and ozone. In this study, indoor and outdoor values were compared. At another site, this group investigated the relationship between indoor and outdoor levels of pollution [35] showing that the indoor levels of air pollution were greatly influenced by the magnitude of automotive traffic and by the weather conditions. Attention has also been paid to air pollution from indoor sources. At the V&A for instance, total volatile organic compound (TVOC) and formaldehyde concentrations were monitored in addition

[29]. The effectiveness of sealants to reduce VOC (formaldehyde, formic acid and acetic acid) emission from medium density fibreboard has been studied by Eremin and Wilthew [36]. A recent book by Camuffo [37] discusses in detail many physical factors that play a role in the micro-environments that surround objects of cultural heritage. It also deals with methods for monitoring of the microclimate.

The problem of dirt deposition on artefacts has been recognised since antiquity [38]. Dirt may originate from a variety of sources, and includes biological material from indoor or outdoor plants, soot from combustion, and fibres from visitor's clothes or cleaning activity. The visual quality of paintings can be affected by dirt deposition, or soiling. For instance, dark portions appear lighter due to surface scattering, and lighter portions can appear darker through absorption of light by the dust particles [39]. Recently Bellan *et al.* [40] determined the percentage surface coverage at which museum visitors can detect carbon black soiling of paintings. This percentage appeared to be higher than was previously thought. Apart from these visual effects, soiling may cause chemical effects, depending on the composition of the particles. It was determined that high acidity (or alkalinity) and in specific cases the iron content can have detrimental effects [38]. Scanning electron microscopy studies of paintings by Phenix and Burnstock [41] revealed that dirt may not only be present on the surface, but it may also be partially embedded in or even fully mixed with the surface coating of a painting. The mechanisms through which dirt deposition takes place are determined by factors such as size and texture of the particles. Camuffo [42] has discussed the particle deposition mechanisms that play a role in the soiling of murals, with a special focus on the temperature of the walls and the air. Murals differ from paintings in a few aspects. First of all, they are hung on a wall rather than part of it, so that they are more readily in the preferred state of thermal equilibrium with the ambient air. Secondly, they often have a different surface roughness. Nonetheless, the mechanisms that play an important role in the soiling of murals also apply to paintings, so that particle size, temperature gradients (in space) and density of the air must be considered important factors in the soiling of paintings too. Also the difference in polarity between surface and particle, and the relative humidity, which can increase the adhesion of the dirt particle by capillary condensation are important. The latter factor plays an important role at a relative humidity higher than 65% [41]. Hence it is not surprising that efforts are being made to keep dust away from paintings. These vary from the development of special framing methods to the placement of particle filters in the museum climate control installations. A very early example of efficient protection of paintings is an airtight frame designed by Simpson in 1892 [43]. As a matter of test one painting by Turner ("Venice") was placed in

the display case in the end of the last 19th century. Another painting by Turner (the seascape "Line Fishing off Hastings"), which was produced in the same period and had the same history as the first one was not placed in such a display case but exposed to the environment at the Victoria and Albert museum close to the one in the display case. In 1962 Bromelle [44] reported that "the picture (in the display case) appears to be in excellent condition without any of the yellowing or darkening which can often be seen in Turners of that period (c.1840)." At present a significant difference in the state of both paintings can be observed, which clearly indicates that the display case was very efficient in the protection of the painting [45].

1.1.4 Why paint-based dosimetry?

The internal environment of a building is subject to fluctuations. Hence, monitoring the quality of the museum environment by separate measurement of the individual factors that determine the museum environment at a particular point in time, however valuable, does not always yield a representative indication of the quality of the museum environment. Concentrations of indoor pollutants are often diluted with "fresh" air from outside the museum, which may cause them to drop below detectable (or alarming) levels, but does not take them away completely. Depending on their nature, such pollutants can still be detrimental due to cumulative effects.

Using dosimetry, factors that are not constant can be integrated over a longer period in time. Several dosimeters have been developed for specific purposes. Tennent and co-workers [46] developed an integrating dosimeter for ultraviolet light using the absorbance of a phenothiazine doped PVC-films, which increases proportionally with the dose of UV-light received by the foil due to transformation of the UV-sensitive phenothiazine. More recently, Leissner *et al.* [47-49] developed a dosimetric glass sensor that degrades as a function of the total experienced acidity during its exposure. Johansson *et al.* [50] developed a dosimetric system using metal strips to measure corrosivity in indoor environments.

Studies of the local museum environment mostly focus on a number of preselected factors, such as RH, temperature, light intensity and wavelength-distribution, or the monitoring of specific air pollutants, such as sulphur dioxide, nitrogen oxides and peroxyacetyl nitrate. A major disadvantage of separate measurements of environmental variables is that unexpected or exceptional factors can easily be overlooked. For example, during a routine conservation survey of the collection of the Herbert F. Johnson museum of Cornell University

an oily layer was discovered on many objects and display cases [51]. Mass spectrometric analysis of the material revealed that diethylaminoethanol (DEAE) had formed the oily layer. The volatile DEAE had been introduced into the museum environment by an open steam humidification system in which it was used as a corrosion inhibitor. Environmental monitoring by measurement of the concentrations of air pollutants can be compromised because some sources introduce a great variety of pollutants into the museum environment. Visitors, for instance, do not only change the relative humidity of the museum environment, they also change the chemical composition of the museum air as they release a wide range of organic compounds and inorganic gases [52].

A phenomenon that is often ignored in conservation science is that the effect of one factor may be greatly influenced by another. Some processes are inhibited by certain conditions, others are enhanced. There are factors which interact directly with each other to change the nature or reactivity of the museum environment and there are factors which are particularly harmful after some initial damage by another environmental factor has occurred on a painting. An example of the former is the effect of a combination of high relative humidity and NO_x or SO_2, which increases the acidity of the environment. As another example of interference of environmental factors, De Santis and Allegrini observed enhanced formation of sulphate (SO_4^{2-}) from sulphur dioxide (SO_2) by soot particles. This reaction strongly depends on the nature or the surface of the soot particles and is catalysed by the presence of nitrogen oxide (NO_2) and elevated relative humidity [53]. Under these latter conditions the potentially harmful nitrous acid (HONO), which forms very reactive hydroxyl radicals (OH·) upon photolysis by sunlight [54, 55] is also formed [53]. Carter *et al.* [56] found that the formation of hydroxyl radicals shows a linear dependence on light intensity and that it is further accelerated by increases in temperature and relative humidity. Clearly this latter example illustrates that the impact (reactivity) of the museum environment on works of art is made up of a complex combinations of the individual factors. Other examples include increased dirt adherence to paintings at elevated relative humidity [41], and enhanced photo-degradation at elevated relative humidity [57].

Fluctuations of temperature and relative humidity can play a role in two-step synergistic environmentally induced degradation processes, because they cause repeated shrinkage and expansion which ultimately leads to the formation of cracks. The material on the edges of the newly formed cracks is then exposed to the environment and can interact with light or air pollutants or can accumulate dust. If the cracks go deep into the painting they may expose underlying layers such as ground and preparatory layers. Such layers can be more sensitive to the micro-environment than the top layer(s). A calcium carbonate ($CaCO_3$) ground for instance can react to the more voluminous and moisture sensitive calcium

sulphate ($CaSO_4$) upon exposure to humidity and sulphur oxides resulting in a new source of stress from within the painting. The formation of calcium sulphate (gypsum) from calcium carbonate (chalk), often referred to as *fresco cancer* has been observed in frescoes and is caused by SO_x exposure [58]. Another possible example is the occurrence of blooming [6] (enforced by factors that accelerate hydrolytic processes), which changes the surface of a painting and makes it stickier and more sensitive to particle deposition.

These examples show that the effect of the environment on a work of art can not be considered simply as the integration of the effects of all the factors involved, but must be regarded as a complex more convoluted effect of various interacting factors. Therefore, monitoring the quality of the museum environment by separate measurement of the individual factors that constitute the museum environment, does not necessarily yield an accurate assessment of the damage done to the works of art on display. Moreover, most curators are less interested in the exact characterisation of the museum environment in terms of concentration of air pollutants, lighting conditions *et cetera* but rather in the question whether the museum environment implies potential danger for the museum collection, i.e. "Are the works of art really safe?".

1.2 Short description of the ERA project

Although the paintings themselves can be considered as dosimeters integrating all the effects of the environment, the deterioration of the physical and chemical condition of paintings can not be quantified easily. In the ERA project (project number EV5VCT94 0548 in the European Commission Environment Programme for the Conservation of Cultural Heritage) [59, 60], mock paintings take over this role and serve as dosimeters in which the compositional changes are related to environmental quality. Model paint systems have been prepared and exposed to extreme but controlled and well-defined environmental conditions in the laboratory. Mock paintings prepared with the same paint systems were also exposed to museum environments at selected *field sites*. Changes of the paints used in the mock paintings have been studied on the macroscopic, mesoscopic and molecular level by thermal and dynamic mechanical techniques (TGA, DMTA and DSC) [61-63], spectroscopic techniques (VIS and NIR) [64, 65] and mass spectrometric techniques [66-68]. The following subsections give details on the choice and preparation of the paint systems and their laboratory exposure. The field sites are described in a separate section. The section at the end of this

Chapter gives further information on the organisation of the ERA-project and places this thesis in the framework of the project.

1.3 Composition of the test systems based on egg tempera paint

1.3.1 The binding medium

Traditionally, paintings have been made with natural products, such drying oils, eggs, terpenoid resins, and natural glues. In the first stage of the development of a paint based dosimeter for museum conditions egg was selected as the binding medium, because it is the richest binding medium with respect to the variety of compounds and compound classes. The chemical composition of an average chicken egg as relevant to tempera painting is discussed in detail elsewhere [13, 69]. Eggs contain a large fraction of proteinaceous material. Proteins can undergo many alteration reactions, such as oxidation, β-elimination, alkylation and deamidation taking place on the amino acid residues, and cleavage of the peptide bonds. An overview of possible alteration reactions that proteinaceous materials can undergo is given by Boon *et al.* [13]. The second most abundant class is lipids, comprising cholesterol and glycerolipids, triglycerides and glycerophospholipids. These compounds can undergo oxidative reactions leading to a great variety of oxidation products depending on the degree of oxidative stress. Cholesterol for instance has many reactive sites, and many cholesterol alteration products are known in the literature [70-74]. Egg glycerolipids contain singly and multiply unsaturated fatty acid residues that all have their own reactivity towards oxidative stress. Depending on their degree of unsaturation, multiple oxygenation can occur, eventually leading to chain shortening [75]. Furthermore, triglycerides are sensitive to hydrolysis, ultimately leading to the formation of free fatty acids and glycerol.

Resin mastic was added to the egg binding medium for two reasons. First, it enhances the adhesive properties of the binding medium so that the paint adheres well to the relatively smooth surface of the inert Melinex® support. Secondly, it provides for another compound class that is not present in egg and it may provide potential marker molecules for processes that occur in terpenoid resins. Many components of mastic are known [76] and the ageing of triterpenoids has been studied at the FOM-institute in the framework of

MOLART, a multidisciplinary project on Molecular Aspects of Ageing in painted Art [77, 78]. A mixture of egg and resin has been used in Italian painting practice [79].

1.3.2 The pigments

Added to the binding medium were inorganic pigments containing a variety of metal ions, such as lead white (basic lead carbonate), azurite (basic copper carbonate), smalt (glass sintered with cobalt), lead chromate, sienna (a mixture of α-goethite, FeOOH, and α-haematite, Fe_2O_3), Naples yellow (lead antimonate), and vermilion (mercuric sulphide, from Kremer). Paint systems were also prepared that contained organic pigments that are known to be sensitive to photo-degradation and oxidation by air pollutants [21, 26]. These systems include indigo, curcumin and alizarin tempera. Azurite, smalt and vermilion were obtained from Kremer (Aichstetten, Germany), sienna and Naples yellow from Zecchi (Florence, Italy), and lead white and lead chromate from Aldrich (Steinheim, Germany). Alizarin and curcumin were from Acros (Geel, Belgium) and indigo was from Janssen (Geel Belgium).

1.3.3 Paint formulation and preparation of the test systems

The tempera binding medium was prepared by Roberto Belucci (restorer at the Opificio delle Pietre Dure, Florence, IT) following mostly the recipe reported in *Il libro dell'arte* by Cennino Cennini [80]. The yolk was separated from the white of an egg. The egg white was beaten so that a layer of foam formed on the liquid. After the egg white was left to stand overnight, the foam was separated from the liquid part of the egg white and discarded. The yolk was mixed with the remaining part of the egg white. To the egg were added three drops of apple cider vinegar and a solution of mastic in white spirit (Zecchi, Florence, IT), half the volume of the mixed egg. When pigmented tempera was prepared, the pigment was first ground with a few drops of water. Then the tempera binding medium was added, in some cases under addition of a few more drops of water to keep the paint easy to spread. The paint system was deposited on a sheet of Melinex® using a using a Byk Gardner (Geretsried, Germany) film applicator at 200 µm wet layer thickness. The paint was allowed to cure for a period of three months in the dark before it was subjected to artificial ageing.

1.3.4 Artificial light ageing of the test systems

Light ageing was performed in an ageing facility at the Tate Gallery (London). Samples were exposed in the light-box for 4, 8, 16, 32 and 64 days. The ageing facility used 6 Philips TLD94 58 Watt daylight rendering fluorescent tubes that were filtered with a Perspex VE ultraviolet filter which has a cut-on wavelength at about 400 nm. Tubes were changed regularly to maintain a constant sample illuminance of about 20 klx. Cooling fans maintained the temperature at 4-5°C above ambient, and 5-10% below ambient relative humidity. Effectively, this yielded average values of 28-29°C and 27-28% relative humidity when the ageing was carried out. Light intensity during the exposure of the tempera test systems (May–June 1996) was 18,000 lx. Potential interference of pollutants in these experiments cannot be excluded, although in retrospect the Tate Gallery has the best air quality.

1.3.5 Thermal ageing

Thermal ageing was also carried out at the Tate Gallery. The samples were placed in an oven that maintained the temperature at 60°C and relative humidity at 55%. No light was admitted into the oven. The samples were exposed for 7, 14 and 21 days.

1.3.6 Exposure to SO_2 and NO_x

Exposure to air pollutants was carried out at TNO (Delft, The Netherlands). The experimental set-up was used previously for the exposure of paper to air pollutants, and a detailed description is given by Havermans [81]. Samples mounted on A-4 size PMMA plates were placed in a gas chamber situated inside a climate chamber. During exposure the climate chamber was maintained the temperature at 23°C and relative humidity at 55%. Flows of SO_2, NO_x, and air were tuned continuously so that the overall concentrations of SO_2 and NO_x in the gas chamber were approximately 10 ppm and 20 ppm, respectively. Unlike light and thermal ageing, where samples were exposed for a range of times, the samples were exposed to NO_x/SO_2 for a single fixed period of 4 days. Effectively, the average concentrations of SO_2 and NO_x were 10.2 ppm and 16.7 ppm respectively during exposure.

1.4 Description of the field sites

Mock paintings were prepared that consisted of unexposed strips of the aforementioned formulations, mounted on a black background. **Figure 1** shows the design of these mock paintings. Identical dosimetric test systems, made according to this design, were simultaneously exposed at six selected sites for a period nine months, from mid December 1996 till the end of September 1997.
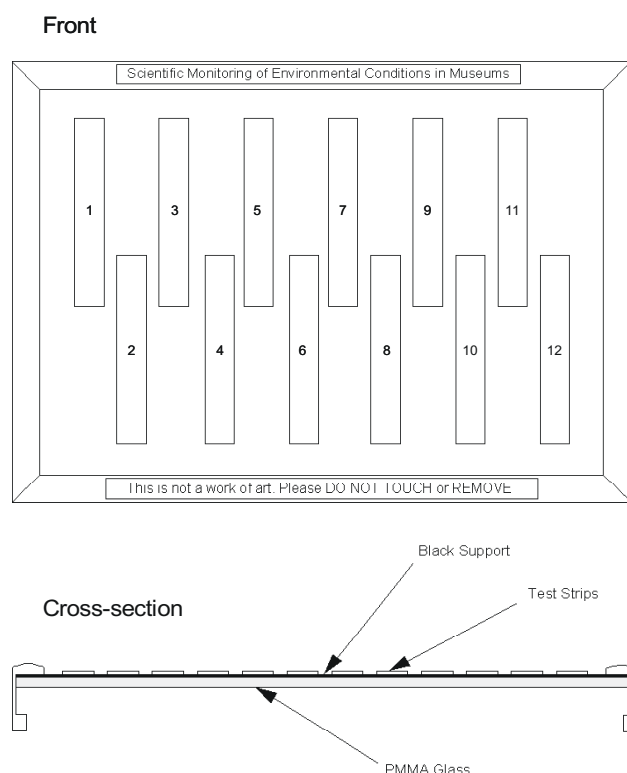
Figure 1. *Design of the mock painting with dosimetric test strips. The following paint systems were used: 1 unpigmented egg; 2 unpigmented egg + mastic; 3 lead white; 4 lead chromate; 5 curcumin; 6 sienna; 7 vermilion; 8 alizarin; 9 azurite; 10 smalt (Cobalt glass); 11 mastic resin and 12 Naples yellow (lead antimonate). Strips (65 x 9 mm) of the tempera paints on Melinex were mounted on a black support and framed.*

These included major art galleries where the indoor environment was controlled, such as the Nightwatch room of the Rijksmuseum in Amsterdam, the Clore Gallery (Tate Gallery) in London, and the Uffizi Gallery in Florence, and two additional sites where the environment was not controlled, viz. Sandham Memorial Chapel at Burghclere (National Trust, England) and El Alcázar in Segovia (Spain). A dosimeter was also placed in the storage facility "Depot

Oost" in the Rijksmuseum (**Figure 2**), where light levels are very low. An additional dosimeter served as a control and was stored at the FOM Institute for Atomic and Molecular Physics in an anti-corrosive bag (Preservation Equipment Ltd., Norfolk, UK) excluding oxygen and light.

The following subsections give a description of the field sites. For each of the field sites the exact location of the dosimeters in relation to the works of art on display is given, together with details of the light, temperature, RH, together with information on the environmental controls that are in place.

Figure 2 *Photograph of a test painting (in circle) on a storage rack in the Rijksmuseum Depot "Oost".*

1.4.1 El Alcázar in Segovia (ALC)

El Alcázar in Segovia is Spain's third most important monument and as such is a much visited site. The ERA dosimeter was exposed in the Cord Room. The dimensions of the room are 5.83m (h) x 10.60m (l) x 4.5m (w) and it has a stone floor and large windows.

During the exposure of the ERA dosimeters 417,461 people visited El Alcázar. There is no control or continuous monitoring of temperature and relative humidity in the Cord room. Data on the lighting, RH and temperature were obtained in the course of a number of visits during exposure of the ERA dosimeters. Some measurements were performed between 16th-23rd January 1997 and gave, in this unusually wet period, average values of 6.5°C and 84%.

Temperature and relative humidity values in spring were 17-23°C & 18-23% and in summer they were 24-28°C & 31-53%. Light levels were recorded each day during visits at about 1pm, with additional readings in the evenings before closing time. The lighting was unfiltered daylight and values at the site of the dosimeter varied from low levels of about 80 lx to close to 1000 lx. Blue wool standards indicated a total exposure of 450,000 lx h, which given the time of exposure, corresponds with 590 klx h/yr [82].

1.4.2 Rijksmuseum store room "Depot Oost" (RDO)

The depot "Oost" is located in the attic of the Rijksmuseum. Small glass windows in the long north wall of the room allow some daylight to enter. The room has concrete floors. The ERA dosimeter was placed in the middle of a rack for paintings, about 3m above the ground. There the dosimeter, like the paintings, can not be reached by direct sunlight, and light intensities are very low. Monitoring of UV and visible light intensity at the exact location of the dosimeter over a period of two days showed minimum and maximum light intensities of 2 and 12 lx at night and in the afternoon respectively, with UV light not being detected. The room is not connected to the central air-conditioning system, and RH is controlled by three "defensors" (mobile RH control units), although these devices are not always employed. Temperature is controlled by the central heating system. Relative humidity and temperature are monitored continuously (at 20 minute intervals). During the exposure of the ERA dosimeters, the average temperature was 22.7°C, with peaks of 29.2°C in August and 16.3°C on Christmas Day. Relative humidity varied between 28% at the end of December and 64% in mid May and the end of June 1997, with an average of 51.3%.

1.4.3 Rijksmuseum (RNW)

An ERA dosimeter was exposed in the Rijksmuseum, diagonally opposite the famous "Nightwatch" painting by Rembrandt, and in the upper left hand corner behind the painting "Corporaalschap van Kapitein Cornelis Bicker" by Joachim von Sandrart (1606-1688), Inv. no. 2117. During the nine months' exposure of the ERA dosimeter, the Rijksmuseum had 848,791 visitors, the majority of whom would have entered this room. The room has wooden floors, partly covered with a cotton carpet (11 x 5 m, near the Nightwatch painting), and is partially illuminated by daylight entering through milk glass in the roof. The daylight is dimmed and directed by cloth in order to obtain a pleasing illumination of the works of art on display. Additional light comes from daylight rendering artificial light sources on the ceiling of the room. Illumination by these lamps (installed in

November 1996) is regulated (dynamic range 10-100%) by the output of sensors in the roof of the room, thus assisting the daylight illumination under cloudy or dark conditions. Light levels at the ERA dosimeter were less than 100 lx and no UV radiation was detected.

The room is air conditioned by means of a central dual duct VAV (variable air volume) system that applies 70% air recirculation. The air inlet system uses EU-7 particle filters, but no chemical filtering is applied. Temperature and relative humidity are monitored at 8 minute intervals. The average temperature during the exposure was 20.5°C, with minimum and maximum values of 17.3°C, and 24.5°C, in March and August 1997, respectively. Average relative humidity was 53.4%. One relatively humid period was recorded (2 hours on 4th April 1997), when the RH was around 70%. The lowest RH (42%) was recorded on 23rd May 1997.

1.4.4 Sandham Memorial Chapel (SAC)

Sandham Memorial Chapel in Burghclere, Hampshire, contains a set of paintings by the British artist Stanley Spencer. During the period of exposure, about 8,200 people visited the chapel. The dosimeter was placed to the upper left of the painting "Sorting and Moving Kit-Bags" on the northeast facing wall. At this location the dosimeters, just like the painting, could be illuminated at a particular time of day by sunlight entering either one of the windows in the adjacent wall, provided that the Holland roller blinds were open, or through the main door, which opens directly to the external environment. Generally, the blinds are used to avoid high levels of illumination e.g. by direct sunlight. There is no total blackout when the Chapel is closed during the day, but also no electric light to supplement daylight on cloudy days. Under sunny conditions, this gave illumination levels of 33,000 lx. Cloudy weather with the blinds open yielded illumination levels of approx. 400 lx. Closing of the blinds under these conditions resulted in a significant reduction of the illuminance to values between 30 and 100 lx. Unfortunately, no data are available on the illuminance under sunny conditions with the blinds closed. Results on blue wool standards that were exposed in the Chapel alongside the tempera dosimeters indicate a total light exposure equivalent of 330 klx·h during the nine month exposure period [82]. Temperatures measured in the Chapel varied between 8.8°C in January and 21.1°C in July 1997. Values of relative humidity varied between 54% and 68%.

1.4.5 Tate Gallery (TAT)

The dosimeter at the Tate Gallery was exposed in the Clore Gallery (Room 103). This is a newly built extension, which was officially opened in 1987 and houses works of the 19th century British artist J. M. W. Turner. The number of visitors to the Clore Gallery during exposure of the dosimeter was estimated to be 190,000. Lighting is provided by a combination of low-UV fluorescent tubes and filtered daylight. During opening hours the illumination is at a constant level of 200 lx. The lighting is switched off when the museum is closed. The Clore Gallery is also air-conditioned (dual duct VAV), with controlled relative humidity and temperature, and 85% air recirculation. Temperature variations were small, between 19-22°C and relative humidity averaged 50%. The air that is brought in by the air-conditioning system is filtered through particle filters (65% against BS test Dust No1.), and through activated carbon filters (TR 70).

1.4.6 Uffizi Gallery (UFF)

The ERA dosimeter was located in Leonardo's room on a S-SW wall next to "The Baptism of Christ" (1472-1475, tempera on wood, Inv. 1890, No. 8358) by Andrea Verrocchio and Leonardo da Vinci and opposite the *predella* by Luca Signorelli on which colorimetric measurements have been performed [1].

More than one million people (1,044,350) visited the Uffizi during the nine months of exposure and it is likely that the majority of them visited the Leonardo's Room. The floor of the room is brickwork treated to prevent the production of dust with wear, and vacuum cleaners are used regularly for cleaning. Light at the location of the dosimeter comes from both artificial sources and from a central skylight through milk glass (there are no windows in the room). Levels are nearly constant, with values of 120-150 lx in the visible region and 500-700 $\mu W/m^2$ in the UV-A region, which is below recommended limits [3]. The environment in the room is controlled by air-conditioning. The inlet is equipped with polyester particle filters and is mounted to the room ceiling. Air is collected at the bottom of the room, with 67% of the air being recirculated. Dehumidification occurs by means of the air conditioning cooling system, whilst humidification is achieved with an ultrasound humidifier equipped with an inverse osmosis demineralisation device. Temperature and relative humidity are monitored continuously. During the period of exposure of the ERA dosimeters, the temperature varied between 13-20°C in December 1996, and 22-30°C in August 1997, while the RH oscillated between 30% and 60%, in winter and spring, and between 40% and 64% in summer. The average temperature was 22°C, and the average value for relative humidity was 49%.

1.4.7 Summary of environmental conditions of the field sites

Table 1 summarises the indoor environmental conditions of the sites where the ERA dosimeters were exposed.

Table 1 *Summary of the environmental data of the field sites.*

Site	RH (%)	T (°C)	Light intensity (lx)	UV intensity ($\mu W/m^2$)	Number of visitors	Glass sensor ΔR [exp time]
ALC	20-84	6.5-28	80-1000	7500 (UV-A)	417,461	0.036 [280 days]
RDO	28-64	16-29	2-12	0	Negligible	0.051 [189 days]
RNW	42-71	17-24.5	<100	0	848,791	0.059 [189 days]
SAC	54-68	8.8–21	30-600[I]	30 (UV)	8,200	0.034 [284 days]
TAT	40-60	19-22	<200	0	190,000	0.0155 [168 days]
UFF	30-60	13-30	120-150	500-700 (UV-A)	1,044,350	0.04 [179 days]

For each site the relative humidity, temperature, intensity of visible light, intensity of UV radiation (when available), and the number of visitors during the nine month period of exposure are listed. The table also shows the average ΔR values determined for the glass sensors and their exposure time at the field sites. The ΔR value is a measure of the overall corrosivity of the environment. The principle of monitoring with glass sensors has been described by Leissner *et al.* [49]. Additional data on pollutant gases are given in **Table 2**. Specific information regarding the rooms where the dosimeters were exposed (such as type of air-conditioning and filtration) is summarised in **Table 3**.

Table 2 *Concentrations of pollutant gases (ppb) at the field sites.*

Site	NO$_2$	SO$_2$	HNO$_3$	O$_3$
ALC	0-42 (O)	0	n.d.	0-33 (O)
RDO/RNW	35 (O)	2 (O)	n.d.	11 (O)
SAC	10-15 (O)	2-4 (O)	n.d.	n.d.
TAT	< 2 (I)	< 2 (I)	< 2 (I)	< 2 (I)
UFF	16-27 (I) 20-50 (O)[†]	0.4-2.1 (I) <6 (O)	0.04-0.27 (I)	1-15 (I) 5-50 (O)[†]
Conversion (1 ppb=)	1.9 µg/m^3	2.6 µg/m^3	2.6 µg/m^3	2.0 µg/m^3
[†]NO$_2$ levels highest in winter, O$_3$ levels highest in summer (I)= indoor value, (O) = outdoor value, n.d. = not determined				

Table 3 *Physical description of the field sites.*

Site	Climate control	Air filters	Room dimensions[†]	Floor type
ALC	None	None	10.6 x 4.5 x 5.8 {277}	Stone
RDO	Central heating and mobile RH control units	None	{578}	Concrete
RNW	Air conditioning	Particle filters	14.5 x 20 x 8 {2320}	Wood, carpet
SAC	Heating by radiators	None	9.4 x 5.2 x 7.9 {386}	Stone
TAT	Air conditioning	Particle and carbon filters	10 x 6 x 5 {300}	Wood
UFF	Air conditioning	Particle filters	11.6 x 11.3 x 7 {917}	Brick
[†] L x W x H (m) {volume (m^3)}				

1.5 The ERA-project and the scope of this thesis

As outlined in **Figure 3**, the development of a paint-based dosimeter for environmental conditions was pursued in two phases. Firstly, the concept was tested using artificial exposure, such as accelerated artificial light ageing, thermal ageing and exposure to high concentrations of air pollutants (NO_x and SO_2). The exposed test systems were analysed by the three partners in the project. In this stage analysis by ancillary techniques was also started. The results allowed identification of some of the ageing processes and facilitated interpretation of the data obtained from direct temperature-resolved mass spectrometry (DTMS). The results of the analysis of the laboratory exposed paint systems were used to decide on the duration of exposure at the field sites.
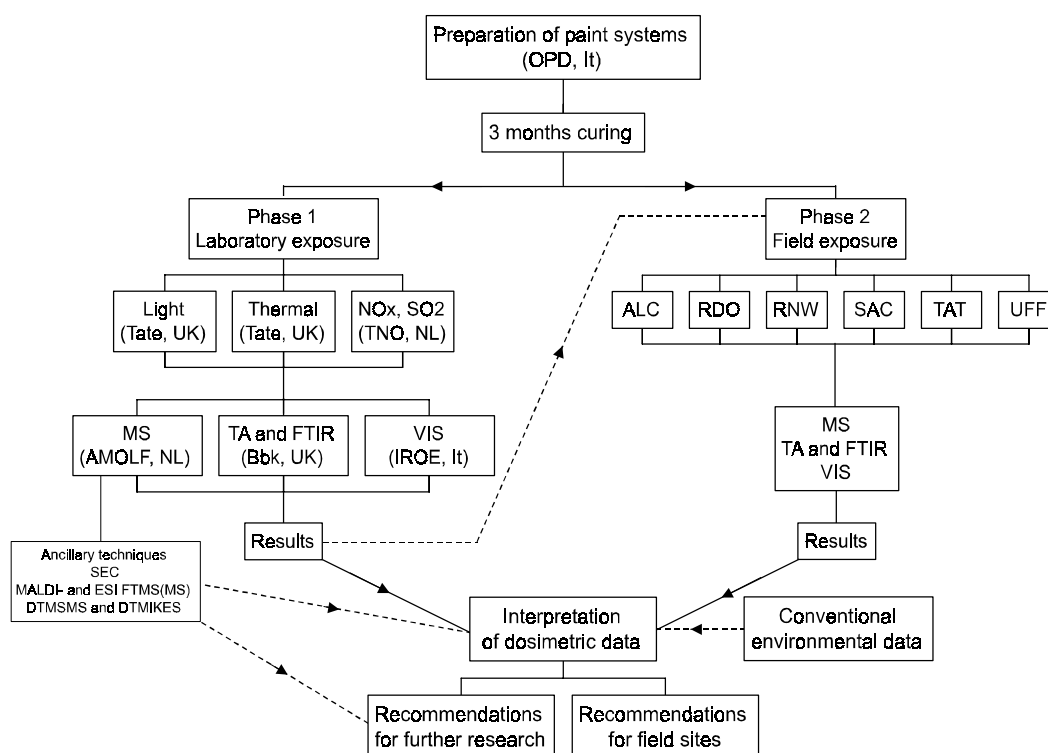
Figure 3 *Organisation of the ERA-project. OPD, Opificio delle Pietre Dure, Florence; Tate, Tate Gallery, London; TNO, Nederlandse organisatie voor Toegepast Natuurwetenschappelijk Onderzoek, Delft; Bbk, Birkbeck College London University; AMOLF, FOM Institute for Atomic and Molecular Physics; IROE, CNR Istituto di Ricerca sulle Onde Elettromagnetiche; MS, mass spectrometry; TA, thermoanalysis; FTIR, Fourier transform infrared spectroscopy; VIS, visible light spectroscopy.*

The mock paintings made from the tempera test systems were exposed for a period of nine months. After exposure, the mock paintings were analysed by the three partners of the project using the same analytical techniques and the results obtained were compared with those from the laboratory-exposed dosimeters. In the case of DTMS analysis, for instance, the set of light-aged samples served as a calibration set. Eventually, all dosimetric data obtained by each of the techniques were compared to the conventional environmental data on the field sites.

This thesis focuses on the mass spectrometric work carried out on paint samples taken from the dosimeters. It reports the work carried out at the FOM Institute for Atomic and Molecular Physics in the framework of the project. **Chapters 2 to 4** focus on paint-based dosimetry of the museum environment and the methodology applied to read out the dosimetric test systems. **Chapters 5 to 7** describe the investigation of the chemical changes in the tests systems in molecular detail. The results obtained allowed the identification of some of the ageing processes of the egg binding medium and facilitated interpretation of the DTMS data.

Chapter 2 describes the methodology that was applied to determine the degree of chemical change in the test systems by DTMS and discriminant analysis (DA). Chemical changes were observed by DTMS analysis of the laboratory-exposed dosimeters that could be correlated with the light ageing time using DA. **Chapter 2** also shows that the same methodology can be used to discriminate the various chemical processes in the paint-based dosimeters, such as those induced by light exposure and those induced by exposure to NO_x/SO_2.

The first part of **Chapter 3** describes the results of a test procedure that was developed to determine the efficacy of each of the test systems. The second part describes the results obtained by DTMS and DA of the laboratory-exposed and field-exposed dosimeters per test system. It is demonstrated that the chemical composition of the binding medium of a tempera paint is determined by its pigments. It is also found that the different test systems respond differently to the same environmental conditions.

An overall interpretation of the dosimetric results obtained by DTMS and DA of the field-exposed test systems is given in **Chapter 4**. This chapter also includes a report of a paint-based dosimetry survey that was carried out at nine sites in the Rijksmuseum (Amsterdam, The Netherlands).

The most important organic chemical changes observed in the test systems by DTMS were further investigated using ancillary techniques such as DTMSMS, size exclusion chromatography (SEC), matrix-assisted laser desorption/ionisation Fourier transform ion cyclotron resonance mass spectrometry (MALDI-FTMS),

and electrospray ionisation (ESI-) FTMSMS (see also **Figure 3**). This research was mainly performed on samples of the egg-only test system.

The degradation of cholesterol was studied by DTMSMS. The results reported in **Chapter 5** indicate that 7-ketocholesterol, 5,6-epoxycholestan-3-ol and cholestenediol are rapidly formed from cholesterol upon light ageing. The chances that cholesterol can be found intact in aged tempera paintings are minimal.

Chapter 6 reports the results obtained by MALDI-FTMS of solvent extracts of the laboratory-exposed egg-only test systems. Oxygenation and oxidative cleavage reactions of unsaturated fatty acid moieties were identified in the ageing of triacylglycerols and diacylphosphatidylcholines. SEC results also reported in this chapter show that cross-linking plays a role in the light ageing process.

ESI-FTMS(MS) was used to study the chemical changes in the glycerolipid fraction in more detail. It is demonstrated in **Chapter 7** that this technique can be used to monitor the degree of hydrolysis of triacylglycerols. This chapter also shows that tandem mass spectrometry with high resolution in broadband mode can be used to determine the fatty acid speciation of natural and oxidised triacylglycerols.

Recommendations for further development of paint-based dosimetry for environmental monitoring of museums are presented in **Chapter 8**.

References

1   Bacci, M., Picollo, M., Porcinai, S., and Radicati, B., 'Non-destructive spectrophotometry and colour measurements applied to the study of works of art', *TECHNE* **5** (1997) 28-33.

2   Bullock, L., 'Reflectance spectrophotometry for measurement of colour change', *National Gallery Technical Bulletin* **2** (1978) 49-55.

3   Thomson, G., *The Museum Environment*, Butterworth-Heinemann, Oxford (1995) 293 pp.

4   Cameron, D. F., 'Environmental control for an art museum: a theoretical solution to the design concept of a museum, incorporating environmental controls necessary to the protection of works of art', *The Canadian Architect* (1967) 62-69.

5   Saunders, D., 'The environment and lighting in the Sainsbury wing of the National Gallery' in *10th Triennial Meeting of the ICOM Committee for Conservation*, ed. J. Bridgland, Vol. 2, James & James, Washington, DC, USA (1993) 630-635.

6   Burnstock, A., Caldwell, M., and Odlyha, M., 'A technical examination of surface deterioration of Stanley Spencer's paintings at Sandham Memorial Chapel' in *11th Triennial Meeting of the ICOM Committee for Conservation*, ed. J. Bridgland, Vol. 1, James and James Ltd., London, UK, Edinburg, UK (1996) 231-238.

7   Hedley, G., 'Relative Humidity and the stress/strain response of canvas paintings: uniaxial measurements of naturally aged samples', *Studies in Conservation* **33** (1988) 133-148.

8   Erhardt, D., Mecklenburg, M. F., Tumosa, C. S., and McCormick-Goodhart, M., 'The Determination of Allowable RH Fluctuations', *WAAC Newsletter* **17** (1) (1995) 19-23.

9   Johnston-Feller, R. M., 'Reflections on the phenomenon of fading', *Journal of Coatings Technology* **58** (736) (1986) 33-50.

10   Bilz, M., and Grattan, D., 'The development of an apparatus for studying the effect of light exposure on museum materials' in *10th Triennial Meeting of the ICOM Committee for Conservation*, ed. J. Bridgland, James & James, Washington, DC, USA (1993) 559-565.

11   Saunders, D., and Kirby, J., 'Light-induced Damage: Investigating the reciprocity principle' in *11th Triennial Meeting of the ICOM Committee for Conservation*, ed. J. Bridgland, Vol. 1, James and James Ltd., London, UK, Edinburg, UK (1996) 87-90.

12   Feller, R. L., 'Aspects of chemical research in conservation: the deterioration process', *Journal of the American Institute for Conservation* **33** (1994) 91-99.

13   Boon, J. J., Peulvé, S. L., van den Brink, O. F., Duursma, M. C., and Rainford, D., 'Molecular aspects of mobile and stationary phases in ageing tempera and oil paint films' in *Early Italian Painting Technique*, ed. T. Bakkenist, R. Hoppenbrouwers, and H. Dubois, Limburg Conservation Institute, Maastricht, The Netherlands (1997) 32-47.

14   Cannon-Brookes, S., and Parry, M., 'Daylight dosage prediction for side-lit interiors in museum galleries and historic buildings.' in *11th Triennial Meeting of the ICOM Committee for Conservation*, ed. J. Bridgland, Vol. 1, James and James Ltd., London, UK, Edinburg, UK (1996) 19-26.

15   Holbrow, G. L., 'Atmospheric Pollution: Its measurement and some effects on paint', *Journal of the Oil and Colour Chemists' Association* **45** (1962) 701-718.

16   Thomson, G., 'Air Pollution - A Review for Conservation Chemists', *Studies in Conservation* **10** (1965) 147-168.

17   Baer, N. S., and Banks, P. N., 'Indoor Air Pollution: Effects on Cultural and Historic Materials', *The International Journal of Museum Management and Curatorship* **4** (1985) 9-20.

18   Brimblecombe, P., 'The Composition of Museum Atmospheres', *Atmospheric Environment* **24B** (1) (1990) 1-8.

19   Grosjean, D., Salmon, L. G., and Cass, G. R., 'Fading of Organic Artists' Colorants by Atmospheric Nitric Acid: Reaction Products and Mechanisms', *Environmental Science and Technology* **26** (5) (1992) 952-959.

20   Whitmore, P. M., and Cass, G. R., 'The fading of artists' colorants by exposure to atmospheric nitrogen dioxide', *Studies in Conservation* **34** (1989) 85-97.

21   Williams-II, E. L., Grosjean, E., and Grosjean, D., 'Exposure of Artists' Colorants to Sulfur Dioxide', *Journal of the American Institute for Conservation* **32** (1993) 291-310.

22   Williams-II, E. L., Grosjean, E., and Grosjean, D., 'Exposure of Artists' Colorants to Peroxyacetyl Nitrate', *Journal of the American Institute for Conservation* **32** (1993) 59-79.

23   Grosjean, D., Whitmore, P. M., Moor, C. P. D., Cass, G. R., and Druzik, J. R., 'Fading of Alizarin and Related Artists' Pigments by Atmospheric Ozone: Reaction Products and Mechanisms', *Environmental Science and Technology* **21** (7) (1987) 635-643.

24   Grosjean, D., Whitmore, P. M., Cass, G. R., and Druzik, J. R., 'Ozone Fading of Natural Organic Colorants: Mechanisms and Products of the Reaction of Ozone with Indigos', *Environmental Science and Technology* **22** (3) (1988) 292-298.

25   Grosjean, D., Whitmore, P. M., Moor, C. P. D., Cass, G. R., and Druzik, J. R., 'Ozone Fading of Organic Colorants: Products and Mechanism of the Reaction of Ozone with Curcumin', *Environmental Science and Technology* **22** (11) (1988) 1357-1361.

26   Shaver, C. L., Cass, G. R., and Druzik, J. R., 'Ozone and the Deterioration of Works of Art', *Environmental Science and Technology* **17** (12) (1983) 748-752.

27   Grosjean, D., Sensharma, D. K., and Cass, G. R., 'Fading of colorants by atmospheric pollutants: mass spectrometry studies', *The Science of the Total Environment* **152** (1994) 125-134.

28   Hackney, S., 'The Distribution of Gaseous Air Pollution within Museums', *Studies in Conservation* **29** (1984) 105-116.

29   Blades, N., 'Measuring pollution in the museum environment', *V & A Conservation Journal* (1995) 9-11.

30   Hisham, M. W. M., and Grosjean, D., 'Air Pollution in Southern California Museums: Indoor and Outdoor Levels of Nitrogen Dioxide, Peroxyacetyl Nitrate, Nitric Acid, and Chlorinated Hydrocarbons', *Environmental Science and Technology* **25** (5) (1991) 857-862.

31   Camuffo, D., and Bernardi, A., 'Study of the microclimate of the Hall of the Giants in the Carrara Palace in Padua', *Studies in Conservation* **40** (1995) 237-249.

32   Cappellini, V., *Uffizi Project*, Guinti, Prato, Italy (1993) 112 pp.

33   Bernardi, A., and Camuffo, D., 'Uffizi Galleries in Florence: a comparison between two different air conditioning systems', *Science and Technology for Cultural Heritage* **4** (2) (1995) 11-22.

34   De Santis, F., Di Palo, V., and Allegrini, I., 'Determination of some atmospheric pollutants inside a museum: relationship with the concentration outside.', *The Science of the Total Environment* **127** (1992) 211-223.

35   De Santis, F., Allegrini, I., Fazio, M. C., and Pasella, D., 'Characterization of indoor air quality in the church of San Luigi dei Francesi, Rome, Italy', *International Journal of Environmental Analytical Chemistry* **64** (1996) 71-81.

36   Eremin, K., and Wilthew, P., 'The effectiveness of barrier materials in reducing emissions of organic gases from fibreboard: Results of preliminary tests' in *11th Triennial Meeting of the ICOM Committee for Conservation*, ed. J. Bridgland, Vol. 1, James and James Ltd., London, UK, Edinburgh, UK (1996) 27-35.

37   Camuffo, D., *Microclimate for Cultural Heritage*, Vol. 23 Elsevier, Amsterdam, The Netherlands (1998) 416 pp.

38   Brimblecombe, P., 'Particulate material in air of art galleries' in *Dirt and Pictures Separated*, ed. S. Hackney, J. Townsend, and N. Eastaugh, The United Kingdom Institute of Conservation, London, Tate Gallery, London, UK (1990) 7-10.

39   Eastaugh, N., 'The visual effects of dirt on paintings' in *Dirt and Pictures Separated*, ed. S. Hackney, J. Townsend, and N. Eastaugh, The United Kingdom Institute of Conservation, London, Tate Gallery, London, UK (1990) 19-23.

40   Bellan, L. M., Salmon, L. G., and Cass, G. R., 'A study on the human ability to detect soot deposition onto works of art', *Environmental Science and Technology* **34** (2000) 1946-1952.

41   Phenix, A., and Burnstock, A., 'The deposition of dirt: A review of the literature, with scanning electron microscope studies of dirt on selected paintings' in *Dirt and Pictures Separated*, ed. S. Hackney, J. Townsend, and N. Eastaugh, The United Kingdom Institute of Conservation, London, Tate Gallery, London, UK (1990) 11-18.

42   Camuffo, D., 'Wall temperature and the soiling of murals', *Museum Management and Curatorship* **10** (1991) 373-383.

43   Simpson, W. S., An improved method or means of preserving oil paintings, water colour drawings, engravings, photographs, prints, and printed matter from atmospheric deterioration and from decay. *Patent* 6556. (1892) 3 pp. England.

44   Bromelle, N. S., and Harris, J. B., 'Museum Lighting Part 3. Aspects of the effect of light on deterioration', *The museum journal: Organ of the Museums Association* **62** (1962) 337-346.

45   Martin, G., 'Exchange rates in musuem cases - A standard?', *Oral communication at the "Indoor Air Quality" conference in Oxford, UK* (2000).

24

46   Tennent, N. H., Townsend, J. H., and Davis, A., 'A simple integrating dosimeter for ultraviolet light' in *IIC Washington Congress*, ed. N.S. Bromelle and G. Thomson,   The International Institute for Conservation of Historic Works of Art, London, UK, Washington (1982) 32-38.

47   Leissner, J., and Fuchs, D. R., 'Glass sensors: A European study to estimate the effectiveness of protective glazings at different cathedrals', *Central Cultural Fund Publication* **123** (1993) 264-274.

48   Pilz, M., and Leissner, J., 'Uberprufung von Auenschultzverglasungen historischer Glasfenster der Oppenheim Katharinenkirche und der Kathedrale von Tours mit Hilfe von Glassensoren' in *Conservation commune d'un patrimoine commun: 1er colloque du programme franco-allemand de recherche sur la conservation des monuments historiques*, Karlsruhe (1993) 291-298.

49   Leissner, J., Martin, G., Blades, N., and Redol, P., 'Assessment and monitoring the environment of cultural property', *European Cultural Heritage Newsletter on Research* **10** (Special issue) (1997) 5-49.

50   Johansson, E., *et al.*, 'Comparison of different methods for assessment of corrosivity in indoor environments', *European Cultural Heritage Newsletter on Research* **10** (Special issue) (1997) 92-94.

51   Volent, P., and Baer, N. S., 'Volatile Amines Used as Corrosion Inhibitors in Museum Humidification Systems', *The International Journal of Museum Management and Curatorship* **4** (1985) 359-364.

52   Wang, T. C., 'A study of bioeffluents in a college classroom', *ASHREA Transactions* **81** (1975) 32-44.

53   De Santis, F., 'Heterogeneous reactions of SO_2 and NO_2 on carbonaceous surfaces', *Atmospheric Environment* **26A** (16) (1992) 3061-3064.

54   Lammel, G., and Perner, D., 'The atmospheric aerosol as a source of nitrous acid in the polluted atmosphere', *Journal of Aerosol Science* **19** (7) (1988) 1199-1202.

55   Jenkin, M. E., Cox, R. A., and Williams, D. J., 'Laboratory studies of the kinetics of formation of the thermal reaction of nitrogen dioxide and water vapour', *Atmospheric Environment* **22** (3) (1988) 487-498.

56   Carter, W. P. L., Atkinson, R., Winter, A. M., and Pitts Jr., J. N., 'Experimental investigation of chamber-dependent radical sources', *International Journal of Chemical Kinetics* **14** (1982) 1071-1103.

57   Feller, R. L., *Accelerated Aging, Photochemical and Thermal Aspects*, Vol. 4   The Getty Conservation Institute, (1994) 275 pp.

58   Johnston, J., 'Science for art's sake', *Chemistry in Britain* (1992) 7-8.

59   Odlyha, M., Boon, J. J., van den Brink, O. F., and Bacci, M., 'ERA: Environmental Research for Art conservation', *European Cultural Heritage Newsletter on Research* **10** (Special issue) (1997) 67-77.

60   Odlyha, M., Boon, J. J., van den Brink, O. F., and Bacci, M., 'Environmental research for art conservation (ERA)', *Journal of Thermal Analysis* **49** (1997) 1571-1584.

61   Odlyha, M., Cohen, N. S., Campana, R., and Foster, G. M., 'Environmental Research for Art Conservation and Assessment of Indoor Condition Surrounding Cultural Objects' in *Art et Chimie, La Couleur*, ed. J. Goupy and J.-P. Mohen, CNRS Editions, Paris (2000) 163-168.

62   Odlyha, M., Cohen, N. S., and Foster, G. M., 'Dosimetry of Paintings: Determination of the degree of chemical change in museum exposed test paintings (smalt tempera) by thermal analysis.', *Thermochimica Acta* **365** (1-2) (2000) 35-44.

63   Odlyha, M., Cohen, N. S., Foster, G. M., and West, R. H., 'Dosimetry of paintings: Determination of the degree of chemical change in museum exposed test paintings (azurite tempera) by thermal analysis and spectroscopic analysis.', *Thermochimica Acta* **365** (1-2) (2000) 53-63.

64   Bacci, M., Picollo, M., Porcinai, S., and Radicati, B., 'Indoor environmental monitoring of colour changes of tempera-painted dosimeters' in *12th Triennial Meeting of the ICOM Committee for Conservation*, ed. J. Bridgland, Vol. 1, James & James, Lyon, France (1999) 3-7.

65   Bacci, M., Picollo, M., Porcinai, S., and Radicati, B., 'Tempera-painted dosimeters for environmental indoor monitoring: A spectroscopic and chemometric approach', *Environmental Science and Technology* **34** (13) (2000) 2859-2865.

66   van den Brink, O. F., Peulvé, S., and Boon, J. J., 'Dosimetry of paintings: Chemical changes in test paintings as tools to assess the environmental stress in the museum environment' in *SSCR Conference on Site effects: The impact of location on conservation treatments*, ed. M.M. Wright and I.M.T. Player-Dahnsjö, The Scottish Society for Conservation and Restoration, Edinburgh, Dundee, Scotland (1998) 70-76.

67   van den Brink, O. F., Peulvé, S., and Boon, J. J., 'Chemical changes in test paintings measure the environmental impact on the museum collection.' in *Art et Chimie, La Couleur*, ed. J. Goupy and J.-P. Mohen, CNRS Editions, Paris (2000) 121-125.

68   van den Brink, O. F., Eijkel, G. B., and Boon, J. J., 'Dosimetry of paintings: Determination of the degree of chemical change in museum exposed test paintings by mass spectrometry', *Thermochimica Acta* **365** (1-2) (2000) 1-23.

69   Phenix, A., 'The composition of eggs and egg tempera' in *Early Italian Painting Technique*, ed. T. Bakkenist, R. Hoppenbrouwers, and H. Dubois, Limburg Conservation Institute, Maastricht, The Netherlands (1997) 11-20.

70   Chicoye, E., Powrie, W. D., and Fennema, O., 'Photoxidation of Cholesterol in Spray-dried Egg Yolk Upon Irradaition', *Journal of Food Science* **33** (1968) 581-587.

71   Luby, J. M., Gray, J. J., Harte, B. R., and Ryan, T. C., 'Photooxidation of Cholesterol in Butter', *Journal of Food Science* **51** (4) (1986) 904-907.

72   Tsai, L.-S., and Hudson, C. A., 'Cholesterol Oxides in Commercial Dry Egg Products: Isolation and Identification', *Journal of Food Science* **49** (1984) 1245-1248.

73   Peng, S.-K., and Taylor, C. B., 'Cholesterol Autoxidation, Health and Arteriosclerosis', *Wld Rev. Nutr. Diet.* **44** (1984) 117-154.

74   Eriksson, C. E., 'Oxidation of Lipids in Food Systems' in *Autoxidation of Unsaturated Lipids*, ed. H.W.-S. Chan, Food Science and Technology, Academic Press, London (1987) 207-232.

75   Grosch, W., 'Reactions of Hydroperoxides - Products of Low Molecular Weight' in *Autoxidation of Unsaturated Lipids*, ed. H.W.-S. Chan, Food Science and Technology, Academic Press, London (1987) 95-140.

76   Mills, J. S., and White, R., *The Organic Chemistry of Museum Objects*, Butterworth-Heinemann Ltd., Oxford (1994) 206 pp.

77   van der Doelen, G. A., van den Berg, K. J., and Boon, J. J., 'Comparative chromatographic and mass spectrometric studies of triterpenoid varnishes: fresh material and aged samples from paintings', *Studies in Conservation* **43** (1998) 249-264.

78   van der Doelen, G. A., *Molecular studies of fresh and aged triterpenoid varnishes*, PhD Thesis, Universiteit van Amsterdam (1999).

79   Reinkowski-Häfner, E., 'Tempera: Zur Geschichte eines maltechnischen Begriffs', *Zeitschrift für Kunststechnologie und Konservierung* **8** (1994) 297-315.

80   Cennini, C. d. A., *Il Libro dell'Arte*, Dover, New York, USA. (1960) 142 pp.

81   Havermans, J. B. G. A., *Environmental influences on the deterioration of paper*, PhD Thesis, Technical University Delft (1995).

82   Bullock, L.,1998   Internal Report: National Trust, England.

2. Determination of the degree of chemical change in museum exposed test paintings by mass spectrometry and discriminant analysis

The main objective of a chemical investigation of the egg tempera dosimetric test systems is to find molecular markers for changes in the chemical composition that occur as a result of artificial ageing under controlled laboratory conditions and by exposure in the museum environment. A further objective is to produce an index that expresses the degree to which the chemical composition of a test system has changed as a result of its environmental exposure. This chapter describes the methodology that was developed to derive molecular information from the tempera dosimetric test systems and to quantify the results. The procedures are illustrated with relevant examples of direct temperature-resolved mass spectrometry (DTMS) data obtained on the test systems.

2.1 Introduction

The analytical methodology applied to obtain dosimetric results from the test systems is schematically shown in **Figure 1**. After exposure of a test system to the museum environment or to laboratory ageing conditions small samples are taken from a test system that can be processed directly when DTMS is applied. The DTMS methodology allows the analysis of particulate material on an analytical probe. Information is obtained on volatile matter *in vacuo* such as lipids, sterols and organic dyes at low analysis temperatures. Information of polymerised substances or materials with strong chemical bonds, for example metal-bonded organic networks, is obtained at higher temperatures. At the highest temperatures information on metals and inorganic salts is obtained. Thus, a DTMS analysis provides mass spectrometric information on a wide variety of compounds in one analytical run. A detailed description of the technique is given by Boon [1].

```
┌─────────────────────────────────────┐
│              Exposure                │
│     lab ageing and field conditons   │
└─────────────────────────────────────┘
                  │
┌─────────────────────────────────────┐
│              Sampling                │
└─────────────────────────────────────┘
                  │
┌─────────────────────────────────────┐
│            DTMS analysis             │
│            (in triplicate)           │
└─────────────────────────────────────┘
                  │
┌─────────────────────────────────────┐
│  Discriminant Analysis of DTMS results│
│        light ageing = calibration    │
└─────────────────────────────────────┘
                  │
┌─────────────────────────────────────┐
│               output                 │
│      (degree of chemical change )    │
└─────────────────────────────────────┘
```
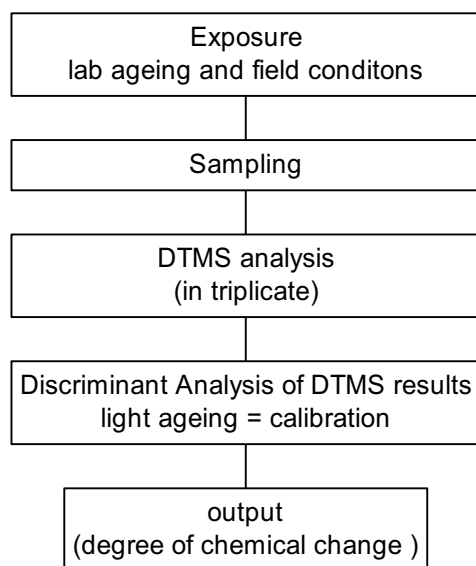
Figure 1 *Analytical methodology flow chart for evaluation of chemical changes using DTMS and DA.*

Analysis of the large number of test systems that were aged under the different conditions results in an enormous data set. For example, each DTMS run consists of 120 scans over a mass range from 20-1000 amu. Analyses were performed in triplicate. Samples of field-exposed dosimeters are compared with the control test system and the set of laboratory light-aged test systems. Hence, rigorous data reduction methodology must be applied to visualise and quantify the extent to which the dosimetric test system had changed chemically as a function of environmental exposure. As a first step in data reduction, the spectra obtained in the DTMS run were summed. Then, Discriminant Analysis (DA) was performed on the summation spectra to estimate analytical reproducibility and perform the data reduction. Using DA, field site data are mathematically compared with the light ageing data to derive a quantitative number on the environmental stress experienced.

2.2 Experimental

The tempera paints and mock paintings were prepared according to the method described in **Chapter 1**. The previous chapter also describes the laboratory exposure to light, temperature and air pollutants and gives a summary of the environmental conditions at the field sites where the mock paintings have been exposed.

2.2.1 Direct temperature-resolved mass spectrometry (DTMS)

Although the sensitivity of the DTMS method allows analysis of samples that are much smaller, for the analysis of the dosimetric test systems samples of approximately 1 mg were scraped off the Melinex support and homogenised into ethanol (~ 100 µl). The exact sample size and volume of the ethanol added varied with the composition of the tempera test system, i.e. the pigment-volume concentration. Aliquots of 1 µl of the sample suspension was deposited on the 0.1 mm diameter, platinum/rhodium (90:10) filament (Drijfhout, The Netherlands) of the DTMS probe. DTMS analysis was performed on a JEOL SX 102A double focusing mass spectrometer with B/E geometry. In the ion source of this instrument, the wire was resistively heated by ramping the current as a rate of 0.5 A/min. Using this ramp the temperature was linearly increased from ambient to approximately 800°C in two minutes. Desorbed and pyrolysed material was ionised by 16 eV electron impact ionisation. The mass spectrometer was scanned over a m/z range of 20-1000 using a 1 s cycle time. Samples were analysed in triplicate for discriminant analysis, and the spectra were summed over the TIC.

2.2.2 Discriminant Analysis (DA)

Mass spectra were numerically analysed by discriminant analysis (DA) with the FOMpyroMAP multivariate analysis programme, a modified version of the ARTHUR package from Infometrix Inc. (Seattle, USA; 1978 release) and with the FOM developed Matlab® (The Mathworks Inc., Natick, MA, USA) toolbox ChemomeTricks. DA, as applied here, is a double stage principle component analysis (PCA) technique [2].

There are a few requirements that have to be met in order to perform discriminant analysis successfully. Data on a test system must be available in at least duplicate before DA can be performed. In the present research, results of triplicate measurements were subjected to DA. Furthermore, the application of the DA to evaluate the chemical change in the dosimetric test systems requires that all samples be measured within a single day to minimise variance due to variance in the operation of the mass spectrometer.

2.3 Qualitative description of chemical changes in tempera test systems

Water, proteins and lipids are the main constituents of an egg. The chemical composition of an average chicken egg as relevant to tempera painting is discussed in detail elsewhere [3, 4]. Oxidised lipids, mastic and polymerised proteinaceous material are the components of aged tempera paint in our tempera test systems. Of these components, the lipid and mastic fraction is detected with greatest sensitivity by DTMS. Due to their polymeric nature, proteins are not detected as intact molecules, but are pyrolysed to fragments of lower molecular weight. The proteinaceous fraction is observed at lower sensitivity compared to the lipid components, because the yield from pyrolysis is relatively low compared to the more quantitative desorption of apolar substances.

2.3.1 Unpigmented tempera

Figure 2A shows the DTMS summation spectrum of the unpigmented tempera control sample. There are three important mass peak windows in which components of the binding medium are observed. Triglyceride mass peaks are present between m/z 830 and 900. The cluster between m/z 852 and 862 represents the triglycerides consisting of 55 C-atoms (C55-TGs), and the cluster at m/z 876-890 triglycerides consisting of 57 C-atoms (C57-TGs). Diglycerides and fragments of triglycerides (TGs) and phospholipids show mass peaks between m/z 540 and 640. In the range from m/z 350 to 500 mass peaks from mastic are detected together with peaks originating from cholesterol (m/z 368 and 386). In the lower mass range fragment ions from di- and triglycerides, ions from fatty acids and dicarboxylic acids, and ions from pyrolysis products of (pre)polymeric compounds are observed. The peaks at m/z 262 and m/z 264 e.g. originate from acylium ions that are formed as fragments of glycerolipids which contain linoleic and oleic acid residues, respectively. Peaks at m/z 262 and 264 are also observed in the spectra of free linoleic and oleic acid [5].

Figure 2B shows the DTMS spectrum of 64-day light-aged unpigmented tempera. Comparison with **Figure 2A** shows that linoleic (m/z 262) and oleic (m/z 264) acid residues are drastically depleted upon exposure to light, as indicated by the decrease of the relative intensities of the peaks. Linoleic acid residues decrease more than oleic acid residues. Increased intensities of peaks at m/z 84, m/z 98 and m/z 152 are ions indicative of dicarboxylic acids formed by
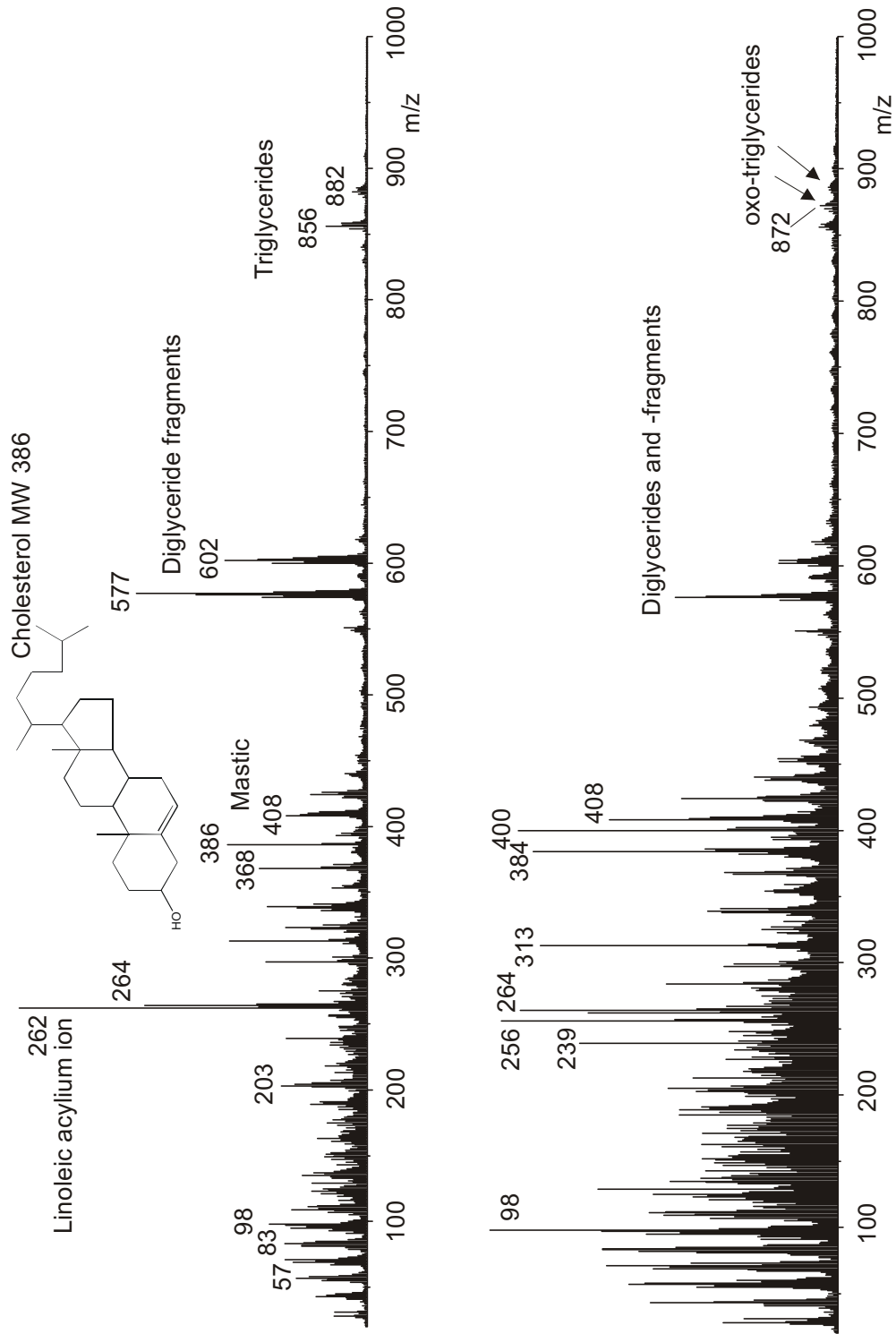
Figure 2 *DTMS summation spectra of unpigmented tempera control (A) and 64-day light-aged (B).*

oxidative cleavage of unsaturated fatty acid moieties. The unresolved peak pattern between m/z 100 and m/z 300, especially in the high temperature window of the data, is indicative of polymeric networks that break down upon pyrolysis. Free palmitic and stearic acid are formed upon ageing due to hydrolysis of glycerolipids, as indicated by an increase of the peaks at m/z 256 and m/z 284 respectively. Increased intensities of m/z 384, 400, and 402 relative to m/z 386 indicate oxidation of cholesterol to cholestenone (m/z 384), 7-ketocholesterol (m/z 400), and oxo-cholesterols (m/z 402). The formation of these compounds has been confirmed by GCMS analyses [4] and by DTMSMS studies (see **Chapter 5**)

Focusing on the relative intensities of the peaks at m/z 854, 856 and 858, a decrease can also be observed in m/z 854, the molecular ion of a fourfold unsaturated C55 triglyceride, and m/z 856, a triply unsaturated C55 triglyceride. This indicates that the degree of unsaturation determines the degree to which some of the triglycerides are depleted. Furthermore, in the triglyceride mass window of the light-aged sample, a cluster appears between m/z 860 and 875. The mass difference between the most abundant triglyceride peak in unaged tempera (m/z 856) and the most abundant peak in the light-aged sample (m/z 872), viz. 16 a.m.u., suggests that insertion of oxygen has taken place. The novel technique of matrix-assisted laser desorption/ionisation Fourier transform mass spectrometry (MALDI-FTMS) was applied to study the changes in the TGs in more detail [6, 7]. The high resolution of the MS data obtained by this technique allowed unequivocal determination of the elemental composition of triglyceride ageing products and unambiguously demonstrates that light ageing induces oxygenation of the unsaturated TGs (see also **Chapters 6 and 7**).

Table I summarises the attribution of the most important peaks in the DTMS spectra of fresh and aged unpigmented tempera. The first column shows the m/z value, the second the mass spectrometric interpretation and the third column shows the molecular origin of the compound or the compound class.

Most of the peaks in the table originate from the lipidic components of the binding medium, such as the glycerolipids, cholesterol and the mastic triterpenoids. It must be noted that apart from oxidation and hydrolysis, cross-linking plays a role in the ageing of the lipid fraction as well. This is evidenced by the size exclusion chromatography results shown in **Chapter 6**. The fragments of cross-linked glycerolipids appear at the same m/z values as the oxidation and hydrolysis products, e.g. m/z 98, 256 and 284. Peaks originating from the proteinaceous fraction of the egg also contribute to the DTMS summation spectrum but are present at relatively low intensities. This is due to the fact that the proteins are pyrolysed so that a great variety of pyrolysis products

Table 1 *Characteristic peaks in DTMS spectra.*

m/z	Interpretation	Compound class of origin	
84	Fragment of dicarboxylic acids	Glycero lipids	**aged**
98	Fragment of dicarboxylic acids	Glycero lipids	**aged**
99	Side chain fragment ion of 3-oxo-25,26,27-trinordammarano-24,20-lactone	Mastic TTP*	**aged**
109	Side chain fragment ion of hydroxydammerenone	Mastic TTP	
143	Side chain fragment ion of ocotillone	Mastic TTP	**aged**
152	C_9 dicarboxylic acid diacylium ion	Glycero lipids	**aged**
203	Pentacyclic triterpenoid fragment ion	Mastic TTP	
205	Pentacyclic triterpenoid fragment ion	Mastic TTP	
248	Fragment ion of oleanoic acid	Mastic TTP	
256	Palmitic acid	Glycero lipids	
262	Linoleic acid acylium ion	Glycero lipids	
264	Oleic acid acylium	Glycero lipids	
284	Stearic acid	Glycero lipids	
313	Palmitic acid monoglyceride fragment	Glycero lipids	
338, 339	Oleic acid monoglyceride fragment	Glycero lipids	
341	Stearic acid monoglyceride fragment	Glycero lipids	
368	Cholesterol – H_2O (Cholestadiene)	Sterols	
382	Cholestadienone	Sterols	**aged**
384	Cholestenone	Sterols	**aged**
386	Cholesterol	Sterols	
400	Hydroxycholestenone	Sterols	**aged**
402	Hydroxycholesterol	Sterols	**aged**
408	28-nor-olean-17-en-3-one	Mastic TTP	
414	3-oxo-25,26,27-trinordammarano-24,20-lactone	Mastic TTP	**aged**
426	Dammaradienol (3β-hydroxy-dammara-20,24-diene)	Mastic TTP	
439	Ursonic and oleanoic acid	Mastic TTP	
454	Ursonic and oleanoic acid	Mastic TTP	
468	Oxo- ursonic and oleanoic acid	Mastic TTP	
546-550	C_{35} diglyceryl ions (2 – 0 unsaturations)	Glycero lipids	
572-578	C_{37} diglyceryl ions (3 – 0 unsaturations)	Glycero lipids	
600-606	C_{39} diglyceryl ions	Glycero lipids	
852-862	C_{55} triglycerides (5 – 0 unsaturations)	Triglycerides	
866-876	Oxygenated C_{55} triglycerides	Triglycerides	**aged**
878-890	C_{57} triglycerides (6 – 0 unsaturations)	Triglycerides	
892-906	Oxygenated C_{57} triglycerides	Triglycerides	**aged**

*TTP = triterpenoids

is formed. Such products include side chain fragments and disubstituted diketopiperazines, pyrrolidindiones and diketopyrrolines [8]. An additional cause of the low intensity of the protein fragment peaks is that the pyrolysis products of proteinaceous material are less effectively ionised. Assignment of peaks based on unit mass is often very difficult because the peaks may originate from more than

one pyrolysis products and hence have different exact masses. O'Connor [9] has shown by high resolution DT-FTMS that at least 7 pyrolysis products of different elemental composition but identical nominal mass of 97 are formed upon pyrolysis of bovine serum albumin (MW 66kDa). Nonetheless, differences can be observed between the DTMS spectra of the proteinaceous fraction of the light-aged egg samples, when the lipid fraction has been removed with dicholomethane/ethanol. Pilot studies with DTMS-DA show trends with ageing. The main differences relate to the peaks from CO_2 and SO_2 released from oxidised functional groups. The complete interpretation of the changes indicated in the discriminant mass spectra of the proteinaceous fractions of the light-aged temperas is very complex and has not been studied further.

2.3.2 *Lead white pigmented tempera*

Figure 3A shows the DTMS spectrum of an unaged lead white pigmented test system. Due to the high pigment concentration, the peaks in this spectrum at m/z 206-208 (Pb) and m/z 44 (CO_2), which originate from the lead white pigment itself, are plotted off-scale. Comparison of the DTMS spectrum of the unaged lead white pigmented tempera with that of unaged unpigmented tempera shows that some alteration of unsaturated triglycerides has already taken place in the curing stage of the lead white tempera. Early metal catalysed oxidation reactions in the dark are evidenced by lower relative intensities of the peaks at m/z 854, 856, 262 and 264 and the presence of a small cluster at m/z 866-876. Oxidation of cholesterol is also taking place in the curing stage. Furthermore, in the unaged lead white tempera, free fatty acids such as palmitic acid (m/z 256) and stearic acid (m/z 284) are observed with higher relative abundance than in the unpigmented equivalent. This is interpreted as hydrolysis of glyceryl ester moieties in phospholipids and di- and triglycerides. The formation of free fatty acids is also observed in DSC results [10, 11] where a low temperature peak/shoulder develops upon light exposure. The spectrum of 64-day light-aged lead white test system (**Figure 3B**) indicates that light ageing leads to the formation of similar reaction products as observed in the corresponding light-aged unpigmented test systems, albeit at a higher reaction rate. This is deduced from the relative intensities of m/z 854, 856 and 858, which point to a lower degree of unsaturation in the di- and triglycerides for the light-aged lead white tempera (64 days) as compared to the unpigmented equivalent. Furthermore, the intensity of the cluster of peaks from oxygenated triglycerides (m/z 866-876) has increased.
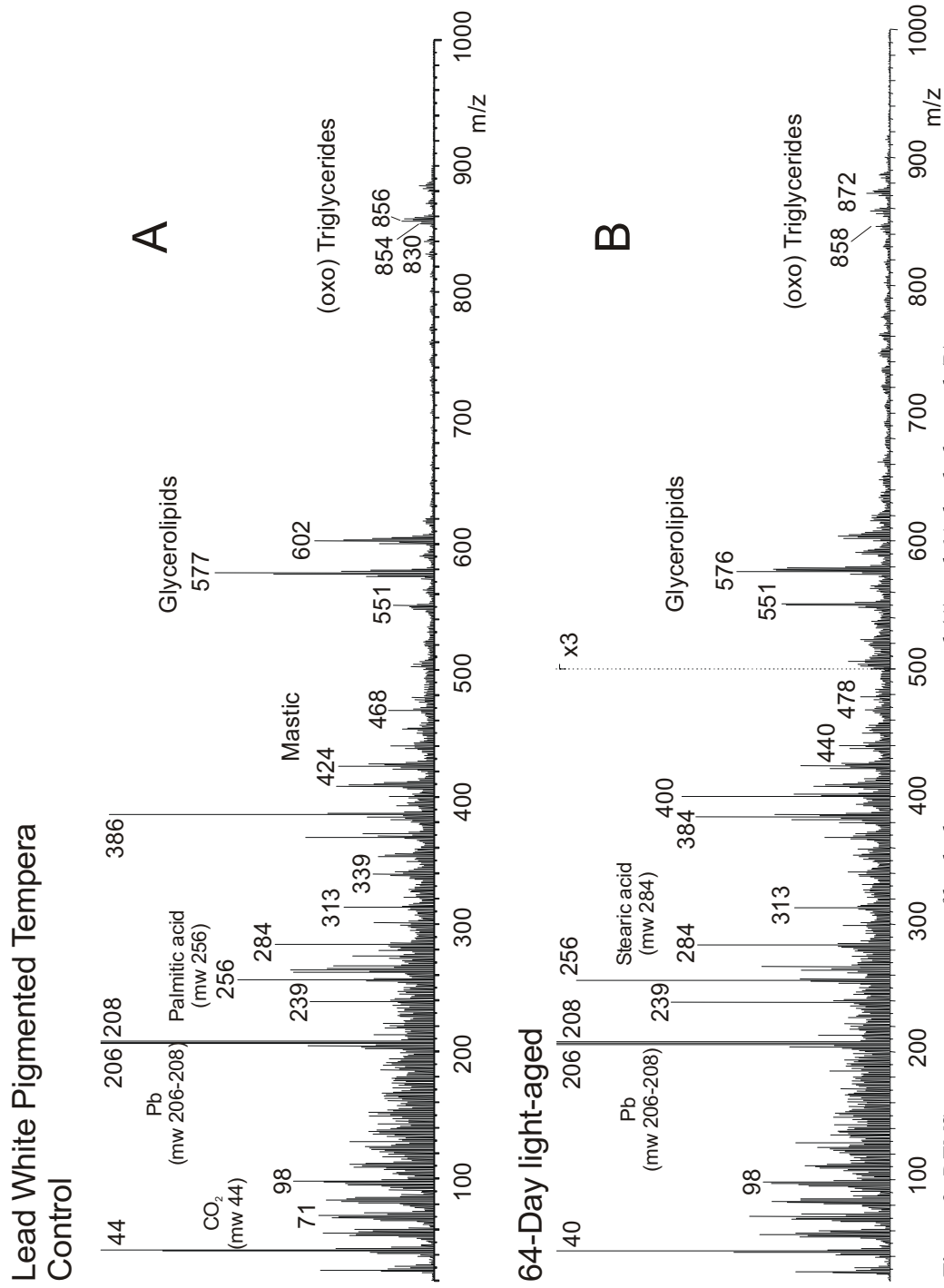
Figure 3 *DTMS summation spectra of lead white tempera control (A) and 64-day light-aged (B).*

2.3.3 *Azurite pigmented tempera*

The spectra of unaged and 64-day light-aged azurite pigmented test systems are shown in **Figure 4 A and B**. Azurite, a basic copper carbonate, decomposes and forms carbon dioxide at high temperature. The resulting m/z 44 dominates the spectra. Copper is not observed in the DTMS spectra of azurite tempera. Comparison of the spectrum of unaged azurite tempera with that of unaged unpigmented tempera strips shows that the effect of addition of azurite to the binding medium leads to severe changes in the curing stage. These changes are due to metal catalysed oxidation of the binding medium. Unlike lead white pigmented test systems, free fatty acids are not observed to a great extent in azurite test systems. Copper catalyses oxidation but does not affect the stability of the ester bonds in the triglycerides and phospholipids, to such a great extent as lead white. Comparison of the unaged with the 64-day light-aged azurite test system suggests that the lipid fraction of the paint undergoes only minor additional changes upon light ageing, such as further oxidation of cholesterol.

2.4 *Description of chemical changes in light-aged test systems by Discriminant Analysis*

The analytical results discussed above show that many processes in the test systems can be retrieved by DTMS. Since the DTMS spectra of the tempera dosimetric systems contain many mass peaks, quantification of the changes using peak ratios alone is insufficient. The multivariate technique of Discriminant Analysis (DA) was used to compare the spectra, determine the analytical reproducibility, and derive relevant sets of correlated mass peaks, which describe the changes quantitatively in the mathematical form of discriminant function scores.

      In the case of the DTMS and DA of a light ageing series of a tempera test system, an increase in the degree of chemical change with ageing time can be expected. **Figure 5** shows the result of DA of DTMS data from a light ageing series of unpigmented tempera strips. The abscissa represents the ageing time (days), while the ordinate represents the score on the first discriminant function. The spreading in the data is indicated with the grey band. This figure demonstrates that the light ageing of an unpigmented test system takes place very quickly in the first days of exposure. At longer exposure times the process proceeds at a much lower rate and the degree of chemical change appears to
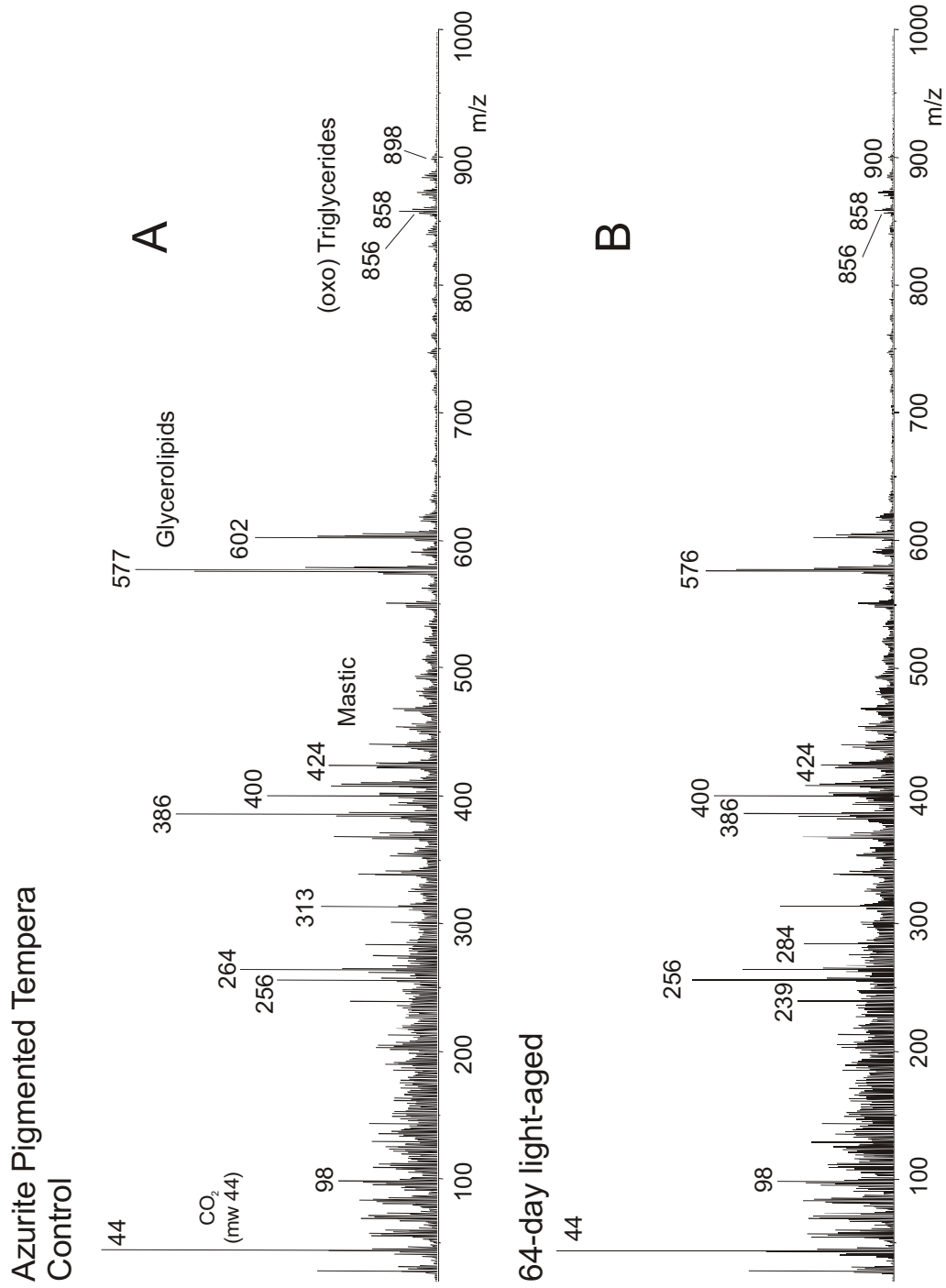
Figure 4 *DTMS summation spectra of azurite tempera control (A) and 64-day light-aged (B).*

plateau. These observations agree with classical kinetic considerations that predict that reaction rates decrease as time progresses due to diminishing concentrations of reactants. By performing an inverted standardisation procedure on the loadings of the m/z values of the discriminant functions so-called discriminant mass spectra can be derived, which indicate which m/z peaks increase or decrease as a function of the ageing time. In this way, discriminant function data can be interpreted chemically.
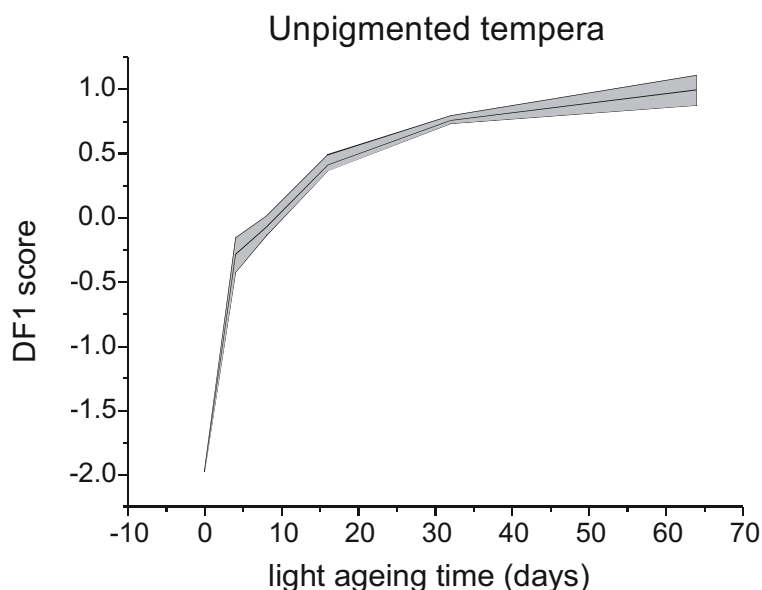
Figure 5 *Light ageing curve of unpigmented tempera obtained by DTMS and DA. The outer lines of the graph are the minimum and maximum, and the inner line is the average of three results.*

Figure 6A shows the first discriminant function (DF1) mass spectrum from the light ageing series of unpigmented tempera. Peaks in this figure that decrease in relative intensity upon exposure are plotted as negative peaks, whereas those that increase as a function of light exposure are positive peaks. The DF1 spectrum, therefore, indicates the following: a decrease in triglycerides with unsaturated bonds (m/z multiplets at 856 and 882); a decrease in mastic pentacyclic triterpenoids (m/z 454, 439, 426, 248, 203) [12]; a decrease in C18:2 and C18:1 fatty acyl moieties (m/z 262 and m/z 264) and a decrease in cholesterol (m/z 386 and 368). Light induced oxidation is exemplified by: an increase in oxidised triglycerides (872 and 898); high intensity peaks for oxidised cholesterol at m/z 400 and 384; and the appearance of mass peaks for palmitic acid (m/z 256), stearic acid (m/z 284), and azelaic acid (m/z 152 and 98).
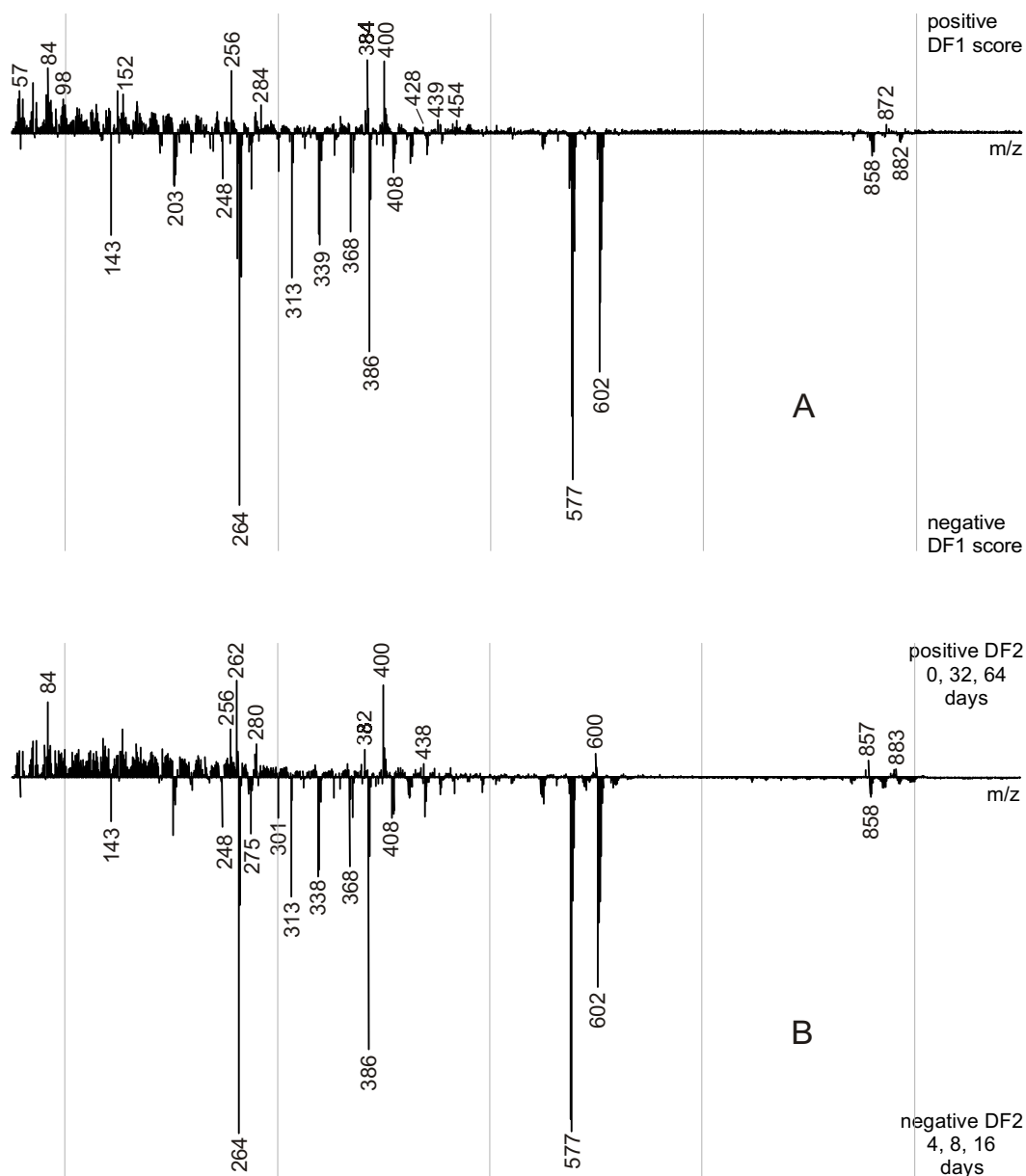
Figure 6 *First (A) and second (B) discriminant mass spectrum for light-aged unpigmented tempera.*

The DF2 spectrum is shown in **Figure 6B.** In this figure m/z 262 and m/z 264 appear on opposite sides of the spectrum. The scores of the different samples in the light ageing series on the second discriminant function (0, 32 and 64 days score positive while 4, 8, and 16 days score negative) indicate that the m/z 262 : m/z 264 ratio decreases in the first stage of light ageing, and increases again upon progressed light ageing (data not shown). This is explained as follows. Although the relative intensities in the DTMS summation spectrum of both m/z 262 and m/z 264 decrease, the m/z 262 initially decreases at a faster rate than the 264 so

that the m/z 262 : m/z 264 ratio decreases upon light ageing. At longer exposure times (32 and 64 days) the linoleic acid moieties are almost completely consumed, so that the oleic acid moieties are depleted at a higher rate and the m/z 262 : m/z 264 ratio increases again. The same line of reasoning applies for the peaks at m/z 600 and m/z 602. The phenomenon is not observed in the diacylglycerol cluster at m/z 572-580 because these C_{37} fragment ions contain the more saturated fatty acyl groups (see also **Chapter 6**) so that less linoleic acid moieties are present. Thus, these observations on **Figure 6B** are attributed to differences in reactivity of the oleic (m/z 264) and linoleic (m/z 262) acyl groups. Oleic acid and linoleic acid are reported to show significantly different autoxidation rates [13] and based the observations by Cho *et al.* [14] the same may be expected for photo-induced oxidation.

As many environmental factors interact in a museum environment, the changes in the chemical composition of a test system exposed in a museum cannot simply be seen as due to one process alone, but is an integration of a number of processes. The extent to which the processes have proceeded is a function of the different environmental factors. The presence of air pollutants such as nitrogen oxides and sulphur oxides in the museum atmosphere, for example, leads to oxidation of organic materials. Moreover, acidifying air pollutants in combination with high relative humidity accelerate hydrolytic processes, especially in the presence of higher temperatures.

The following example shows that different processes of chemical change can be identified in the tempera dosimetric test systems. In this case, the processes are determined by the pigments rather than by different environmental factors. DTMS data of the light ageing series of unpigmented, lead white pigmented and azurite pigmented test systems were subjected to discriminant analysis. Two different types of chemical reactions were detected.
Figure 7 shows plots of the data points obtained on the test systems as co-ordinates in the score map of the first discriminant function (DF-1) and the second discriminant function (DF-2). The geometric distance between the data points is a measure of the difference in chemical composition. Two ageing phenomena are observed and interpreted as due to (1) oxidation and to (2) hydrolysis of ester bonds in the glycerolipids and in the protein lipid network polymer [4]. DF1 (oxidation) separates unpigmented test systems from lead white and azurite pigmented ones. DF2 (ester bond hydrolysis) separates lead white pigmented from azurite pigmented tempera. The series of aged azurite pigmented tempera data points is less resolved because the most of the chemical changes had already taken place during the curing stage in the dark.
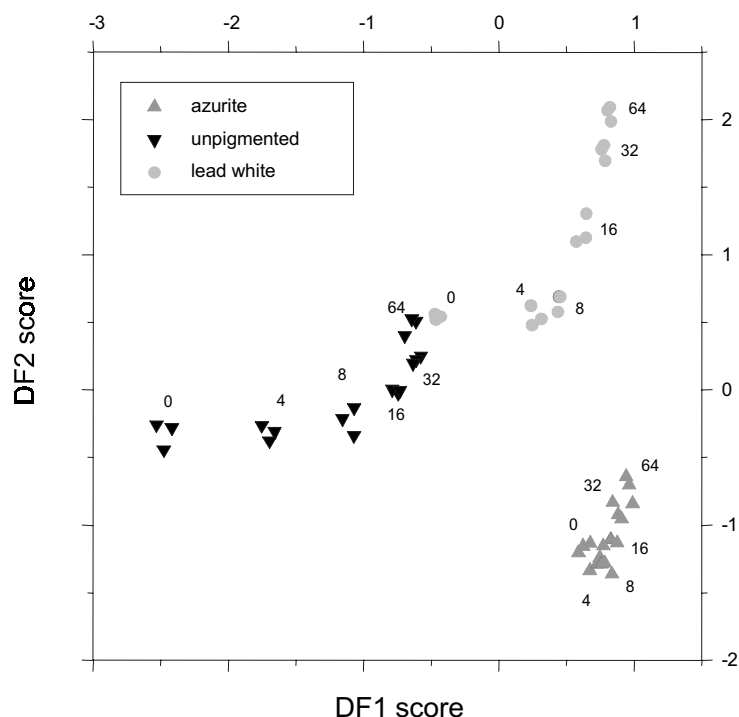
Figure 7 *Map of scores on the first two discriminant functions for light ageing series of unpigmented, lead white pigmented and azurite pigmented tempera.*

Figures 8 A and B show the corresponding discriminant mass spectra of the first (A) and the second (B) discriminant function. The first discriminant mass spectrum suggests that the process represented by the horizontal axis mainly involves oxidative processes, as indicated by m/z 386 (cholesterol) being plotted as reacting compound and m/z 384 and m/z 400 (cholesterol oxidation products) as ageing products. Oxidation is also indicated by the positions of intact TGs and oxidised TGs. The discriminant mass spectrum of the vertical axis shows di- and triglyceride peaks (m/z 570-620 and m/z 850-900) on the side of the reacting compounds and peaks at m/z 239, 256, 267, and 284 on the product side. This is interpreted as de-esterification of glycerolipids to form free fatty acids or fatty acid salts with the metal cations. Hence, the data shown in **Figure 7** indicate that hydrolysis of ester bonds is an important process during light ageing of lead white pigmented tempera. The map also indicates that the degree of oxidation of the binding medium of azurite pigmented tempera is very high, but that the degree of hydrolysis is relatively low compared to lead white pigmented systems.

These data clearly show that DTMS & DA can be used successfully to bring the different processes into focus that take place in the tempera dosimetric test systems. Hydrolytic and oxidative processes in the test systems induced by environmental factors are important tracers of the degradation processes. Tracing
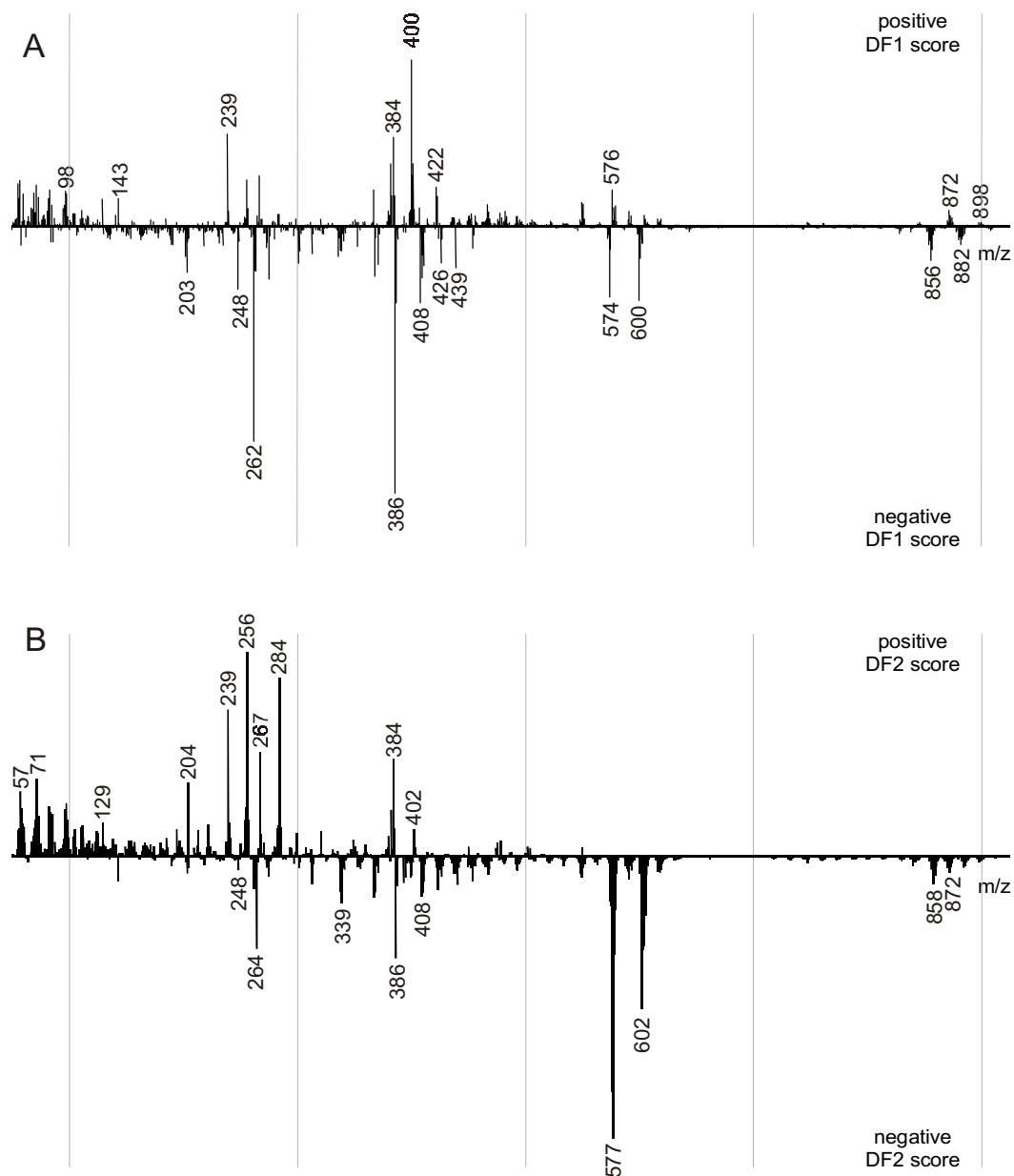
Figure 8 *First (A) and second (B) discriminant mass spectrum for light ageing series of unpigmented, lead white pigmented and azurite pigmented tempera.*

these phenomena in the field-exposed dosimetric test systems will give important indications on the quality of the exposure environment. A low severity environment should lead to chemical changes that correspond to only a few days of light ageing induced change under lab conditions. High severity environments on the other hand may lead to a degree of chemical change in the test systems considerably stronger than that seen in the 64-day light ageing experiments.

2.5 Effects on the chemistry of the test systems by exposure to NO$_x$ and SO$_2$.

In order to test the sensitivity of the dosimetric test systems to air pollutants, all tempera test systems prepared were subjected to a period of exposure lasting four days to evaluate the effects of exposure to NO$_x$ and SO$_2$. DTMS was used to investigate the chemical changes in the lipid marker compounds.
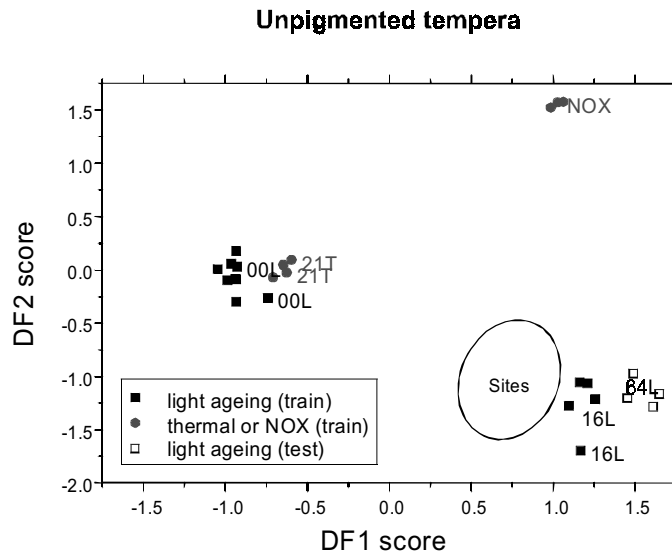
Figure 9 *Map of scores on the first two discriminant functions for light-aged (16L), thermally aged (21T) and NO$_x$/SO$_2$ exposed unpigmented tempera test systems.*

Figure 9 presents a discriminant function score map of a comparative study of controls, 21-day thermally aged, 16- and 64-day light-aged and NO$_x$/SO$_2$ exposed unpigmented tempera dosimetric test systems by DTMS. The study was designed to probe the data set for differences in effects of thermal ageing, light ageing and ageing due to noxious gases. The 16-day light-aged, 21-day thermally aged, the NO$_x$/SO$_2$ exposed and the control sample defined the training set. The 64-day light ageing results were used as test set. The geometric distance between controls (only curing) and 21 days thermal ageing is relatively small compared to the effect of light ageing. The conclusion can be drawn that thermal ageing effects (in the dark) on the lipids and mastic in the binder are small. The chemical effect of the noxious gases on the lipid fraction of the binding medium is similar to the effects of light ageing because triglycerides and sterols are oxidised. However, differences between the two conditions are detected in the second discriminant function (DF2). The mass spectral data in DF2 indicate that

45

the oxidation of sterols is less severe under NO_x/SO_2 conditions but that hydrolytic processes affecting the ester bond are more prominent. Incorporation of SO_2 in the form of sulphates or sulphonic acids is also evident from ions at m/z 64 which are due to pyrolytic elimination of SO_2 from the samples [15]. The presence of sulphates in the NO_x/SO_2 exposed unpigmented tempera test system was confirmed by FTIR spectroscopy [10]. Further comparative studies in the different tempera test systems have shown that NO_x/SO_2 effects are detected with good sensitivity in lead white, smalt, sienna and alizarin test systems.

2.6 DTMS studies of selected dosimetric test systems from the field sites

As mentioned in **Chapter 1**, mock test paintings were exposed at a selection of seven different sites, consisting of controlled (Tate, Rijksmuseum, Uffizi) and uncontrolled sites (Sandham Chapel and Alcázar). Control in this context means that the relative humidity and temperature are set by air conditioning systems. Furthermore, at controlled sites illuminance levels are such that the annual dose of illumination is below the generally accepted value of 650 klx·h for museum exposure of paintings [16]. At the uncontrolled sites the light levels are expected to exceed those values, and hence more drastic chemical changes in the test systems can be anticipated. On top of that, other environmental factors, such as variations in relative humidity, temperature and air pollution also contribute to the chemical changes in a test system. A detailed description of the field sites is given in **Chapter 1**.

The question was tested whether dosimetric test systems from field sites were similar to those subjected to the laboratory conditions of thermal ageing, light ageing or noxious gas exposure, respectively. The discriminant analysis with a training set consisting of the DTMS data of controls, thermally aged (21 days), NO_x/SO_2 and 16-day light ageing of the unpigmented tempera dosimeters shows that field site exposed dosimeters plot in the area of light-aged test systems of 8 to 16 days exposure. This implies that the chemistry at the field sites resembles mostly that of light ageing *(vide infra)*.

This observation was used to define a protocol for the comparison of field-exposed dosimeters. The DTMS data from the light ageing under laboratory conditions during 4, 8, 16, 32 and 64 days were used for calibration. Discriminant analysis was performed with the artificially light-aged dosimeters as

the training set in order to calculate a multivariate solution space in which the geometric position of the DTMS data of field-exposed dosimeters was interpolated (i.e., field site data were included as a test set). The following example illustrates the approach and discusses results on the field-exposed unpigmented tempera test systems. **Figure 10** shows the scores on the first discriminant function for the field-exposed unpigmented dosimeters. The light ageing data, the data from NO_x/SO_2 and from the control sample for field exposure (FOM, stored under dark and oxygen free conditions in a copper lined anticorrosive bag) are given for comparison. As might be expected, field-exposed test strips from the uncontrolled environments (the Alcàzar and Sandham Chapel) indicate a stronger chemical change than dosimeters exposed in the controlled museum environments. The result of the Rijksmuseum "Depot Oost" sample is remarkable because this dosimeter shows considerable chemical change, although it was exposed in the painting storage facility where light intensity is very low. It indicates that other factors than light intensity alone play an important role in environment-induced chemical processes.

Unpigmented tempera
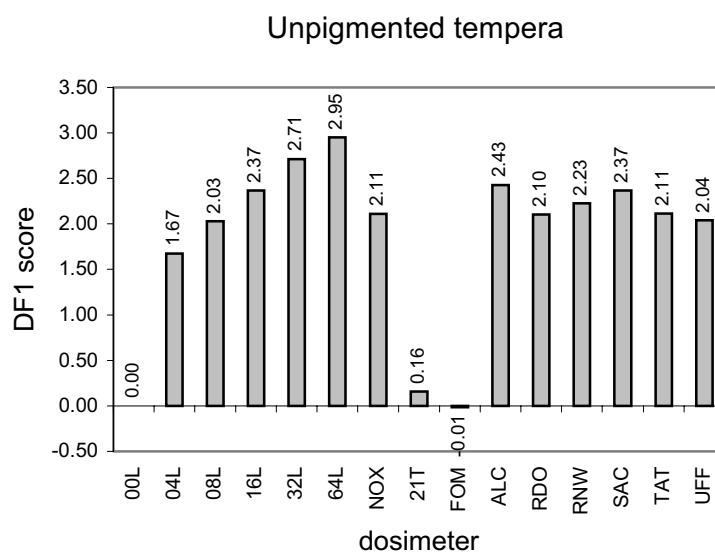
Figure 10 *Comparison of the scores on the first discriminant function (DF1) of laboratory-aged and field-exposed unpigmented tempera dosimeters. The light ageing series defined the training set for discriminant analysis. Discriminant scores are normalised so that the score of the control for light ageing (00L) is zero. Legend to field sites: FOM, control dosimeter stored under exclusion of oxygen; ALC, Alcázar; RDO, Rijksmuseum Depot "Oost"; RNW, Rijksmuseum Nightwatch; SAC, Sandham Chapel; TAT, Tate Gallery; and UFF, Uffizi.*

In the ideal situation the dosimetric test systems would be calibrated against all (combinations of) environmental factors. This, however, would require an extensive data set that would have been far too large for the explorative character of the ERA project. Therefore, the light ageing set was used for calibration of the degree of chemical change in the field-exposed dosimeters. This approach can only yield valid results if the chemical processes that take place during natural ageing at the field sites closely resemble those that take place during light ageing. Hence, it is important to compare the nature of the chemical change in the natural ageing process with that of the light ageing process. Discriminant analysis with both the light ageing and the field site DTMS data in the training set was used to determine whether the processes that occur during the light ageing differ substantially from those taking place during field exposure.

This was done for the unpigmented tempera dosimetric test systems. **Figure 11 A** shows the map of the scores on the first discriminant function plotted against those on the second discriminant direction. The relative significance of the discriminant functions indicated along the axes is 88 % (DF1) and 11 % (DF2). A deviation of the score on DF2 (the ordinate) is far less important than the score on DF1 (the abscissa). This demonstrates that field site exposure in the museums is expressed by the same molecular characteristics as the light ageing.

In the case of the lead white pigmented test systems, however, a difference is observed between the artificially light-aged and the majority of the field site exposed dosimeters. The map of the scores on the two first DFs for the lead white temperas is shown in **Figure 11B**. The DF1 separates the light-aged systems from the field-exposed systems, with the exception of the Tate Gallery exposed dosimeter. The discriminant mass spectrum shown in **Figure 12** indicates that chemically the differences are caused by hydrolysis of glycerolipids, producing free fatty acids (m/z 256 and 284) and lead soaps (m/z 239 and 267), and by the oxidation of cholesterol (m/z 386) to hydroxycholestenone (m/z 400) and oxo-cholesterol (m/z 402) in the field-exposed systems. Furthermore, the peak of the mastic derived ageing product 3-oxo-25,26,27-trinordamarano-24,20-lactone (m/z 414) and its main EI fragment peak (m/z 99) [17] are more abundantly present in the spectra of the field-exposed dosimeters.

The ranking order of the field sites according to environmental light ageing stress, shown in **Figure 10** for the lead white tempera test system, is not the same as in unpigmented dosimeters because the chemical changes induced by field exposure are not entirely comparable. The FOM control is classified as similar to the light ageing control. The dark storage room in the Rijksmuseum Depot (RDO) has again a relatively high stress score and is in this respect
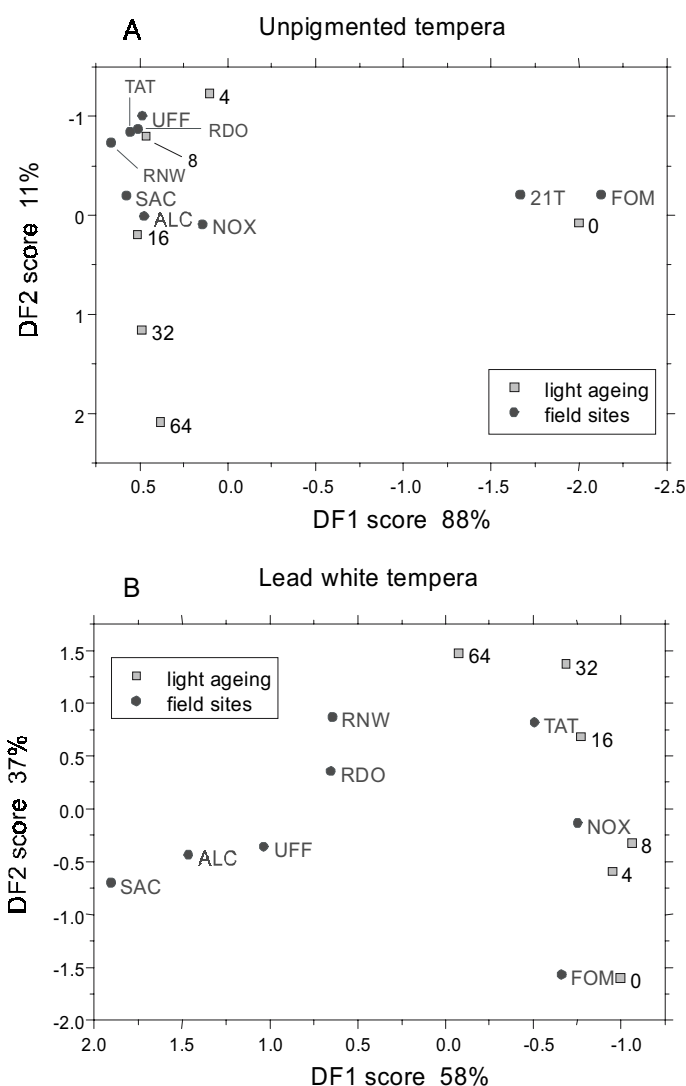
Figure 11 *Map of scores on the first two discriminant functions for light-aged and field-exposed unpigmented (A) and lead white tempera test systems (B). Both the light ageing results and the field exposure results were included in the training set.*

comparable to the unpigmented test system. This suggests that there is an unknown oxidising agent active in the dark, which contributes to a chemical change comparable to very strong light ageing. The lowest museum gallery stress value is found in the Tate Gallery dosimeter. The highest value is found for the Sandham Chapel, which is the site with the highest relative humidity. Comparison of the unpigmented and lead white tempera test systems of Uffizi Gallery suggests that the lead white test system detected an additional contribution to the environmental ageing stress in the Uffizi Gallery. Possible extra factors are the air pollution exposure, and the higher local temperatures. It

must be noted that, although the processes that take place during field ageing are not identical to those during light ageing, the ranking of the field sites presented in **Figure 10** is confirmed when the field site data alone are used as training set for DA.
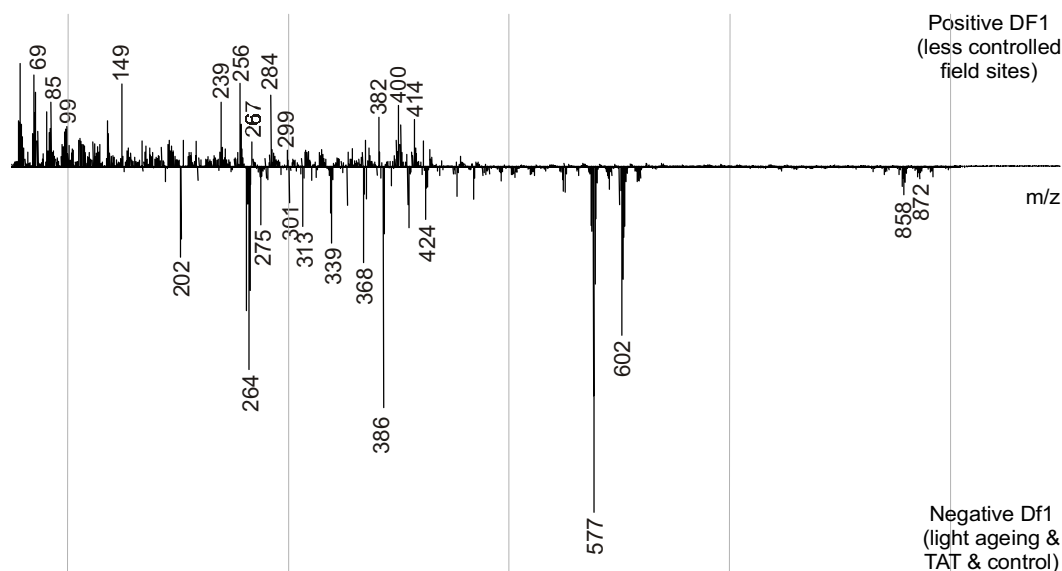
Figure 12 *First discriminant mass spectrum for the lead white tempera test systems. Both the light ageing results and the field exposure results were included in the training set.*

2.7 Extrapolation to museum exposure years

Referring to the dosimetric results obtained on the field-exposed unpigmented tempera dosimeters, it must be noted that even the "best" field sites, i.e. the ones with the smallest chemical change, show effects which are comparable with those observed upon eight days of artificial light ageing. This effect is even stronger in the case of the tempera systems with inorganic pigments (see **Chapter 3**). Using the reciprocity principle [18], this value of light exposure can be related to the number of years of exposure in a museum. The reciprocity principle states that the product of light intensity and exposure time determines the amount of damage to an object. Thus, eight days of artificial light ageing at 18 klx is 3.5 Mlx·h by reciprocity. This value exceeds the generally accepted annual dose of illumination of 650 klx·h [16] by more than a factor of 5.

The discrepancy between the actual effects of exposure to the museum environment observed and the theoretically expected value based on the reciprocity principle for light ageing may be explained in two different ways. Firstly, the assumption of the reciprocity is not valid because there are many factors that may affect the reciprocity principle, see [19]. The following factors may explain the relatively strong effects at lower light intensities. In several cases of radical initiated oxidative processes, the oxygen uptake is proportional to the square root of the light intensity. The depth of penetration of the light may vary when a layer of radiation absorbing material is formed on the surface. This factor becomes particularly relevant to the validity of the reciprocity principle when light intensities are so high that they allow two-photon processes to occur (very unlikely at 18,000 lx light intensity). Furthermore, the moisture content may affect the rates of light induced processes. In the present experiment moisture content may have played an important role; the artificial light ageing experiments were carried out at relatively low relative humidity (27-28%) and in many cases the relative humidity at the field sites was found to be much higher.

On the other hand, if the reciprocity principle is valid, the extreme effects cannot be explained when exposure to light is seen as the most important factor in ageing. Hence, the effects must originate from other factors that strongly contribute to the environmental stress (expressed as chemical change in the multivariate space) detected by the dosimeters. The composition (or reactivity) of the museum air may be such a factor. Dust is a potential factor as it may contain reactive pollutants or act as a nucleus for future deterioration. Gaseous air pollution, either diffusing into the museum from outside or originating from sources inside the museum, may strongly contribute to the deterioration processes. The results of the dosimeter that was exposed in the storage "Depot Oost" of the Rijksmuseum, where light intensity is very low, support the conjecture that light exposure is not the most important factor and that other factors must play an equally important role. One of these factors is NO_x/SO_2, which also contributes to the dosimeter's DTMS signature in almost the same way as the light ageing effects. NO_x is considered a component of air pollution that is very detrimental. Its action can be twofold. Firstly, it may increase the acidity of the environment by formation of nitric and nitrous acid. Secondly, it can oxidise organic materials that contain double bonds [20]. The action of nitrogen dioxide on polyunsaturated diacylphosphatidylcholines for instance has been studied by Balazy and co-workers [21]. Their results confirm the observation in this chapter that NO_x can cause oxidation of unsaturated lipids even in the absence of light.

2.8 Conclusions

The validity of the principle of paint-based dosimetry has been demonstrated. The degree of chemical change in the light-exposed tempera dosimetric test systems can be correlated with the duration of light exposure. The results of field exposure show that the chemical composition of the paints is changed by exposure in museums: significant differences are observed among dosimeters exposed in different field sites.

The effect observed upon exposure of the dosimeters to museum environments is more drastic than anticipated. This suggests that either the reciprocity principle of light ageing is not valid, or that the chemical composition of the museum atmosphere plays an even more important role than the exposure to light alone. Testing of the reciprocity principle for light ageing under *ceteris paribus* conditions is strongly recommended. The results of such a survey can contribute to the understanding of light-induced deterioration processes of paint systems.

Direct temperature-resolved mass spectrometry (DTMS) is a rapid and adequate method to determine the chemical composition (of primarily the lipid fraction) of tempera paint systems and changes therein. Discriminant analysis (DA) was successfully applied to quantify the difference between DTMS data obtained on dosimeters exposed under different environmental conditions. Moreover, DA can be used to distinguish and identify different processes that take place in the temperas as a result of exposure.

The chemical changes observed upon exposure of the unpigmented dosimeters to NO_x/SO_2 in the dark follow to a great extent the changes induced upon exposure to light. However, small chemical differences are observed. On the one hand cholesterol is less severely oxidised upon NO_x/SO_2 exposure. On the other hand hydrolysis of glycerolipids plays a more important role. Thermal ageing has a very small effect on the composition of the lipid fraction of the unpigmented tempera dosimeters.

Comparison of the chemical changes in the field-exposed dosimeters with those in the laboratory-exposed (light, temperature and NO_x/SO_2) dosimeters indicates that the processes taking place during field exposure resemble most those taking place during light ageing.

The light ageing series of the dosimeters was used successfully for calibration the degree of chemical change in the field-exposed unpigmented tempera dosimeters. The degree of chemical change is expressed as numbers (i.e. DF scores) that indicate the "environmental stress" detected by the dosimeters.

References

1   Boon, J. J., 'Analytical pyrolysis mass spectrometry: new vistas opened by temperature-resolved in-source PYMS', *International Journal of Mass Spectrometry and Ion Processes* **118/119** (1992) 755-787.

2   Hoogerbrugge, R., Willig, S. J., and Kistemaker, P. G., 'Discriminant Analysis by Double Stage Principal Component Analysis', *Analytical Chemistry* **55** (11) (1983) 1711-1712.

3   Phenix, A., 'The composition of eggs and egg tempera' in *Early Italian Painting Technique*, ed. T. Bakkenist, R. Hoppenbrouwers, and H. Dubois, Limburg Conservation Institute, Maastricht, The Netherlands (1997) 11-20.

4   Boon, J. J., Peulvé, S. L., van den Brink, O. F., Duursma, M. C., and Rainford, D., 'Molecular aspects of mobile and stationary phases in ageing tempera and oil paint films' in *Early Italian Painting Technique*, ed. T. Bakkenist, R. Hoppenbrouwers, and H. Dubois, Limburg Conservation Institute, Maastricht, The Netherlands (1997) 32-47.

5   Minor, E. C., Compositional heterogeneity within ocean POM: A study using flow cytometry and mass spectrometry, PhD Thesis, Massechusetts Institute of Technology (1998).

6   van den Brink, O. F., O'Connor, P. B., Duursma, M. C., Peulvé, S., Heeren, R. M. A., and Boon, J. J., 'Analysis of Egg Lipids and Their Oxidation Products by MALDI-FTMS' in *45th ASMS Conference on Mass Spectrometry and Allied Topics*, Palm Springs, CA, USA (1997) 1372.

7   van den Brink, O. F., Boon, J. J., O'Connor, P. B., Duursma, M. C., and Heeren, R. M. A., 'Matrix-assisted laser desorption/ionization Fourier transform mass spectrometric analysis of oxygenated triglycerides and phosphatidylcholines in egg tempera paint systems for environmental monitoring of museum conditions', *Journal of Mass Spectrometry* **36** (2001) 479-492.

8   Moldoveanu, S. C., *Analytical Pyrolysis of Natural Organic Polymers*, Vol. 20 Elsevier, Amsterdam (1998) 496 pp.

9   O'Connor, P. B., 'Direct temperature-resolved mass spectrometry of Albumin on a Fourier transform mass spectrometer.', *unpublished results* (1997).

10   Odlyha, M., Cohen, N. S., Foster, G. M., Campana, R., Boon, J.J., Van den Brink, O.F., Peulvé, S., Bacci, M., Picollo, M., and Porcinai, S., 'ERA, Environmental Research for Art Conservation' Final Report for the European Commission. University of London, Birkbeck College (London, U.K.), FOM Institute for Atomic and Molecular Physics (Amsterdam, NL) and Istituto di Ricerca sulle Onde Elettromagnetiche, CNR (Florence, IT), (1999) 210 + xc pp.

11   Odlyha, M., Cohen, N. S., Foster, G. M., and Campana, R., 'Environmental Research for Art Conservation and Assessment of Indoor Conditions Surrounding Cultural Objects', *Journal of Thermal Analysis and Calorimetry* **56** (1999) 1219-1232.

12   van der Doelen, G. A., *Molecular studies of fresh and aged triterpenoid varnishes*, PhD Thesis, Universiteit van Amsterdam (1999).

13   Frankel, E. N., *Lipid oxidation*, Vol. 10 The Oily Press, Dundee, Scotland (1998) 303 pp.

14   Cho, S.-Y., Miyashita, K., Miyazawa, T., Fujimoto, K., and Kaneda, T., 'Autoxidation of ethyl eicosapentaenoate and docosahexaenoate under light irradiation', *Nippon Suisan Gakkaishi* **53** (5) (1987) 813-817.

15   Van Loon, W. M. G. M., Boon, J. J., and De Groot, B., 'Quantitative analysis of sulfonic acid groups in macromolecular lignosulfonic acids and aquatic humic substnaces by temperature-resolved pyrolysis-mass spectrometry', *Environmental Science and Technology* **27** (1993) 2387-2396.

16   Thomson, G., *The Museum Environment*, Butterworth-Heinemann, Oxford (1995) 293 pp.

17   van der Doelen, G. A., van den Berg, K. J., and Boon, J. J., 'Comparative chromatographic and mass spectrometric studies of triterpenoid varnishes: fresh material and aged samples from paintings', *Studies in Conservation* **43** (1998) 249-264.

18   Saunders, D., and Kirby, J., 'Light-induced Damage: Investigating the reciprocity principle' in *11th Triennial Meeting of the ICOM Committee for Conservation*, ed. J. Bridgland, Vol. 1, James and James Ltd., London, UK, Edinburg, UK (1996) 87-90.

19   Feller, R. L., *Accelerated Aging, Photochemical and Thermal Aspects*, Vol. 4 The Getty Conservation Institute, (1994) 275 pp.

20   Gallon, A. A., and Pryor, W. A., 'The reaction of low levels of nitrogen dioxide with methyl linoleate in the presence and absence of oxygen', *Lipids* **29** (3) (1994) 171-176.

21   Jiang, H., Kruger, N., Lahiri, D. R., Wang, D., Vatèle, J.-M., and Balazy, M., 'Nitrogen dioxide induces cis-trans-isomerization of arachidonic acid within cellular phospholipids', *The Journal of Biological Chemistry* **274** (23) (1999) 16235-16241.

3. DTMS and DA of nine dosimetric test systems

This chapter describes the results of those dosimetric test systems that were exposed at the field sites and analysed using the methodology described in **Chapter 2**. The combination of DTMS and discriminant analysis (DA) was used successfully to express the degree of chemical change in exposed paint-based dosimeters as a number. The degree of chemical change is the overall result of a variety of chemical processes that take place during the exposure of the tempera test systems. These processes include hydrolysis of glycerolipids, oxidation of glycerolipids and cholesterol, changes in the proteins and polymerisation processes. The methodology presented in **Chapter 2** was illustrated with unpigmented, azurite and lead white tempera test systems. However, in the project a large variety of test systems was prepared, artificially aged, field-exposed and analysed. The quality of the dosimetric data obtained with the different test systems was found to vary greatly because the pigments in the various test systems have a strong influence on the outcome.

3.1 Introduction

The first part of this chapter discusses the efficacy of the dosimeters tested using four different criteria. The dosimetric results obtained with these test systems will be critically examined. Differences between light ageing effects and field ageing effects as assessed by discriminant analysis will be discussed shortly. Throughout this chapter the coding system given in **Table 1** will be used for the exposed dosimeters.

Table 1 *Coding system for laboratory-aged and field-exposed dosimeters.*

Code	Description	Code	Description
00L	Light ageing series, control	FOM	Stored at FOM (no oxygen)
04L	Light-aged, 4 days	ALC	Alcázar
08L	Light-aged, 8 days	RDO	Rijksmuseum Depot "Oost"
16L	Light-aged, 16 days	RNW	Rijksmuseum Nightwatch room
32L	Light-aged, 32 days	SAC	Sandham Memorial Chapel
64L	Light-aged, 64 days	TAT	Tate Gallery (Clore Gallery)
NOX	Exposed to NO_x and SO_2	UFF	Uffizi (Leonardo room)
21T	Thermally aged, 21 days		

3.2 Testing the efficacy of the dosimeters

3.2.1 Rationale

The DTMS data of the tempera paint systems are dominated by the lipid fraction of the binding medium. However, the quality of the dosimetric results that are derived from the chemical changes in this fraction is (partly) determined by the overall composition of the tempera dosimeter, including the pigments. Many of the pigments used in the paint systems also give peaks in DTMS spectra. In some cases these peaks are unwanted for the following two reasons. Firstly, pigment peaks may interfere with peaks from the binding medium that change upon ageing, so that information is lost by this interference (e.g. in the case of Naples yellow, *vide infra*). Bad reproducibility of the intensity of these pigment peaks can dominate relevant changes in the binding medium. Secondly, these peaks can dominate the spectrum when the pigment concentration in the paint is very high (e.g. in the case of the lead chromate paint system). In some cases the peak intensities exceed the upper detection limit of the mass spectrometer, so that they have to be removed from the spectra before DA (e.g. in the case of alizarin and lead white). These problems are all related to the method (DTMS followed by DA) used for the evaluation of the chemical changes in the dosimetric test systems.

Other factors that can affect the efficacy of the tempera dosimeters are directly related to the composition of the test systems. When the pigment concentration in the paint is high, the catalytic oxidation of the binding medium in the curing stage may be extreme so that subsequent changes upon exposure are

relatively small (e.g. in the case of smalt tempera). This affects the dynamic range of these test systems. Other systems display a poor reproducibility in the analytical stage, for instance, due to inhomogeneity of the paint films. Although large samples were taken for analysis (>100 – 1000 times the minimum quantity required for three analytical runs), this factor could play a role when course pigments are used or when the pigment to volume concentration of the paint layers is inhomogeneous.

Another complication is that the pigments, in particular the inorganic ones, influence the desorption and pyrolysis processes that take place during the DTMS analysis. This implies that the DTMS spectra are affected by the quantity of pigment present and hence are affected by inhomogeneity of the pigment volume concentration of the paint system and by differences in sample preparation. The latter was minimised by ensuring that a complete series of DTMS experiments on one test system was carried out by one operator only. If there are differences in sample preparation, they always develop gradually and are partly corrected for by the triplicate analysis. Moreover, if there is a significant change in the DTMS spectra that is due to time dependent effects (that take place over the period of analysis of a series, typically 6-10 hours) then this can be recognised immediately in the principle component analysis results that are generated first in the DA procedure. Such a trend was not observed in any of the data that underlie the results presented in this chapter. If random changes in the mass spectra occur, e.g. due to inhomogeneity of the pigment volume concentration or to minor random variations in sample preparation, then the paint system is considered to be less efficacious.

3.2.2 Description of the efficacy tests

The efficacy of the present generation of test systems in combination with the applied DTMS and DA methodology for evaluation of the quality of the museum environment was tested. Four tests were developed. The following describes the tests concisely and gives an overview of the results.

Test 1 Discriminatory power

The ratio of the between group variance and the within group variance (B/W ratio) is a measure of the significance of the chemical differences that are observed between predefined groups, and hence of the between group resolution when the combination of DTMS and DA is used to read out the test results. DA optimises the B/W ratio. The within group variance (W) is strongly affected by the reproducibility of the mass spectrometric data. The between group variance (B) reflects the difference between different exposed dosimeters of the same

initial composition. Comparison of the B/W ratios can give an insight into the discriminatory power (resolution) of the test systems. The discriminatory power of each of the test systems is given in the second column of **Table 2**. A high number indicates a good discriminatory power.

The B/W ratio can be determined when the results on the light ageing experiments are in the training set or when the results of field exposure are in the training set. Similarity of the ageing conditions at two or more field sites leads to similar degrees of chemical change and thus lowers the B/W value when the field site results define the training set in the discriminant analysis. In the case of the light ageing series obtained under laboratory condition, however, the different groups are well defined. Incidental overlap between two or more groups, and hence a low B/W, can only be interpreted as low discriminatory power. For this reason, the B/W values of the test systems are based solely on the light ageing data.

Test 2 Correlation of the degree of chemical change after light ageing

The degree of chemical change in the light-aged test systems is a function of the light intensity and the duration of the exposure. Hence, the degree of chemical change should increase with exposure time in the light ageing series. As the kinetics of the processes that take place during light exposure are not known, it is useless to test whether the response of the dosimeters follows linear or logarithmic trend with the light exposure time. The absence of local minima is taken as a criterion for the robustness of the test systems. The third column in **Table 2** indicates which test systems show a good trend with light ageing without a local minimum (+) and which ones do not (-).

Test 3 Consistency of the results

The consistency of the results obtained by DTMS and DA was tested by a "jack-knife" procedure. The next paragraph explains how a correlation coefficient is obtained from the data of the light ageing series. Briefly, this method tests whether the score of a data point from the ageing series on the first discriminant function changes when it is included in the test set instead of the training set. The value of this correlation coefficient for each test system is given in the fourth column of **Table 2**. A high correlation coefficient (1) indicates stability, and a low value (<0.9) indicates that the results are not consistent.

In the first step of the jack-knife procedure, the first sample in the light ageing set, i.e. the control sample, is excluded from the training set and included in the test set. Then in the second step, the result of this series, the score of the first sample included, is correlated with the results obtained when the complete

light ageing series is in the training set. This is repeated with the second sample of the light ageing series in the test set, the third and so forth. The correlation coefficients of the group averages obtained in each of the steps are averaged.

Although a jack-knife correlation is greatly influenced by the B/W, it gives additional information because it takes into account skewing effects that may be caused by high leverage points. This can be seen in the following example. Suppose that there is one data point in the training set for discriminant analysis that has a large influence on the direction of the correlated vectors in the discriminant space (for example when another process plays a role or a contaminant is present). Then, this point will have a different co-ordinate in the discriminant space and hence a different score on the first discriminant function when it is not in the training set but in the test set.

Test 4 Stability of the control

The similarity between the light ageing control (00L) and the control for field exposure (FOM) is used as an indication of the stability of the test systems. Note that the storage conditions of the 00L and the FOM samples were slightly different as the 00L sample was stored in a cryovial, whereas the FOM sample was stored under exclusion of oxygen in an anticorrosive bag (Corrosion Intercept, Preservation Equipment Ltd., Norfolk, England). A difference between the light ageing control and the field exposure control would indicate that the test system is sensitive to small differences in storage conditions or that differences in the chemical composition are caused by inhomogeneity in the paint. The stability of the control is calculated as the absolute value of the ratio of the degree of chemical change in the field exposure control (FOM) and the average degree of chemical change in the field-exposed dosimeters. The control of the light ageing series (00L) serves as a reference in all cases and hence its degree of chemical change is defined as zero. Thus, a small absolute value (~0) indicates a good stability and high absolute values (e.g. 0.5) indicate poor stability. The values obtained are given in the fifth column of **Table 2**.

3.2.3 Efficacy test results

Table 2 summarises the outcome of the tests that are described above. The last row in **Table 2** specifies for each of the tests the threshold above which the test is passed. Results in the table which imply failure of a test for a particular type of tempera are bold. If a tempera test system fails two or more tests it is considered not efficacious for read-out by DTMS/DA analysis. The table shows that very good results were obtained for the unpigmented tempera test system. In terms of stability of the control and the discriminatory power this test system ranks as best

and the jack-knife correlation coefficient (0.99) indicates a good consistency of the results. Very good values were also obtained for the egg-only test system.

In the case of the alizarin tempera high intensity pigment peaks had to be eliminated from the DTMS data before DA *(vide infra)*. As a result a good efficacy was found for this test system. The alizarin tempera shows a poor stability of the control. The origin of this effect is not fully understood. It must be taken as an indication that the unexposed dosimeters of this system are sensitive to differences in storage conditions. This was also observed for the curcumin tempera in combination with a lower discriminatory power. Hence, it must be concluded that this test system is less efficacious than the alizarin tempera. Although the low discriminatory power of the curcumin tempera test system may partly be due to contamination of some of the samples, it is largely attributed to the high concentration of the pigment, which produces a great variety of peaks at high intensity (*vide infra*).

Table 2 *Results of efficacy tests.*

Test system	Discriminatory power	Correlation	Consistency (correl coeff ± sd)		Stability of control
Unpigmented	200	+	0.99	± 0.01	0.0059
Egg	159	+	0.99991	± 0.00004	0.092
Alizarin	114	+	0.97	± 0.04	**0.20**
Curcumin	31	+	0.96	± 0.02	**0.11**
Lead white	**15**	+	0.96	± 0.04	0.0089
Sienna	192	+	0.993	± 0.007	0.0098
Smalt	78	+	**0.86**	**± 0.09**	0.082
Lead chromate	**5**	+	**0.8**	**± 0.2**	**0.18**
Naples Yellow	**21**	+/-	0.997	± 0.003	**0.27**
Tolerance	> 30	+	> 0.9		< 0.1

The pigment concentration in the lead white pigmented test system is relatively high (96%, as determined by TGA [1, 2]). Nonetheless, good results were obtained considering the efficacy tests of this system. Although the discriminatory power shows the low value of 15, it should be borne in mind that this value was determined on the basis of the data in the light ageing set. Because a chemical difference was detected between light ageing and field exposure, it is important to consider the discriminatory power on the basis of the data in the field ageing set. In that case, the higher value of 46 is found.

The efficacy test results for the other lead salt pigmented test systems, lead chromate and Naples yellow, are different. Although a local minimum was not observed in the Naples yellow tempera light ageing series, the degree of chemical change seems to plateau in the middle of the ageing curve. Furthermore, this test system shows a poor stability of the control. These results

indicate that the paint system is inhomogeneous and that the pigment to volume concentration is not constant. This was further supported by the low discriminatory power (B/W) and by visual inspection of the paint systems [1]. Lead chromate doesn't show a local minimum in the light ageing curve. The stability of the control and in particular the discriminatory power are poor. This is also attributed to inhomogeneity of the paint. Furthermore, the inorganic pigment in this paint system undergoes chemical processes (reduction) during the heating in the DTMS experiment, which may interfere with the desorption and chemical dissociation processes that occur during analysis of the paint system. Such processes are difficult to control because they depend on the spatial organisation of the sample material on the DTMS probe. This phenomenon is reflected in a poor consistency of the results.

The efficacy test results obtained on the sienna tempera compare well with those of the unpigmented test systems. The relatively low pigment content of this test system (67%, determined by TGA [1, 3]) in combination with the fact that there were no (interfering) pigment peaks observed in the mass spectra of this test system, contributes to the good efficacy.

The smalt tempera is found to be less efficacious. The test system scores lower in terms of discriminatory power and stability of the control, and the consistency value is the lowest of all test systems. There are two important factors which play a role here. Firstly, the smalt tempera system has a low medium content of approximately 10% [3] so that oxidative processes, due to the catalytic activity of the cobalt, are enhanced and saturation effects occur. The second factor is of practical nature. During the DTMS analysis glass (silicon dioxide) beads form on the filament of the DTMS probe, as the smalt melts when the filament reaches high temperatures. These glass beads affect the desorption process of the organic components and thus influence the mass spectra.

The efficacy test results of the present generation of dosimetric test systems show that the most reliable results are obtained for the unpigmented tests systems. The test results also show that a high pigment concentration does have some effect on the efficacy of the test systems but does not necessarily render them useless. It is recommended that for some test systems (e.g. smalt) a lower pigment concentration in the tempera paints should be used in future experiments. The lead chromate and Naples yellow pigmented temperas are regarded as not efficacious, but they can be improved by a better grinding and homogenisation of the paint (grain size and pigment to binder ratio). It must be stressed that, although differences in efficacy are observed among the test systems, the present test systems have nonetheless been very useful in the evaluation of the quality of the museum environment, as will be shown in the following sections.

3.3 Results obtained with the nine test systems

3.3.1 Unpigmented paint systems

Although the DTMS data that were obtained on the unpigmented tempera were already discussed in **Chapter 2**, they are briefly summarised in this chapter, along with the results obtained on the egg-only test system, in order to get a complete overview of all field-exposed strips that have been analysed. Furthermore, discussion and summary of these results facilitate the comparison with observations on other test systems.

Mass spectrometry

The mass spectrometric data of the unpigmented tempera originate predominantly from the lipid fraction of the paint. Experimentally the DTMS data is very straightforward, as no interference or domination of the mass spectrum by the pigment is observed. The following changes occur upon light ageing. Cholesterol is oxidised to ketocholesterol, hydroxycholesterol and epoxycholestanol (see **Chapter 5**). The glycerolipids are affected in several ways. Firstly, the unsaturated fatty acid residues are oxygenated, in extreme cases leading to the formation of oxidatively cleaved fatty acid residues (e.g. azelaic acid). **Figure 1** shows the DTMS sum spectrum of 64-day light-aged egg-only tempera.
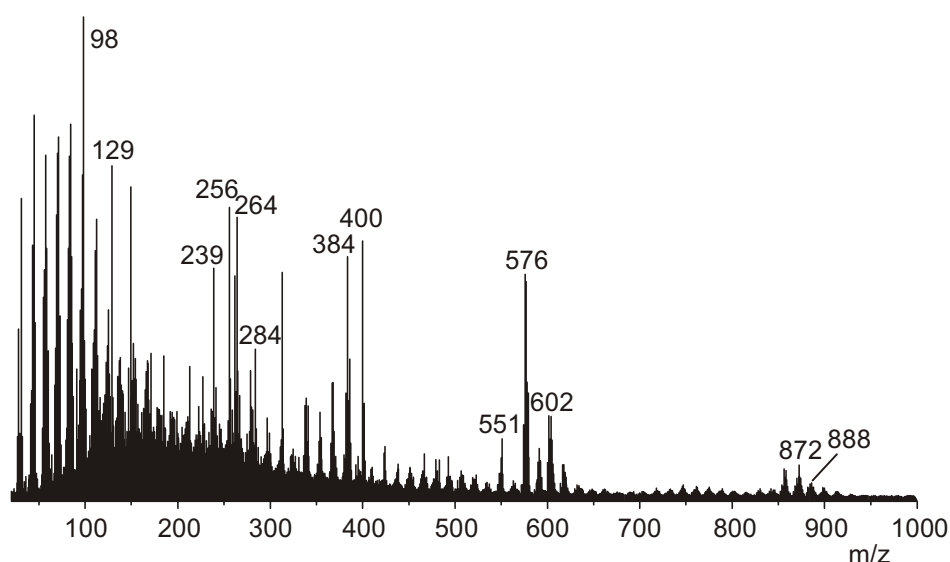

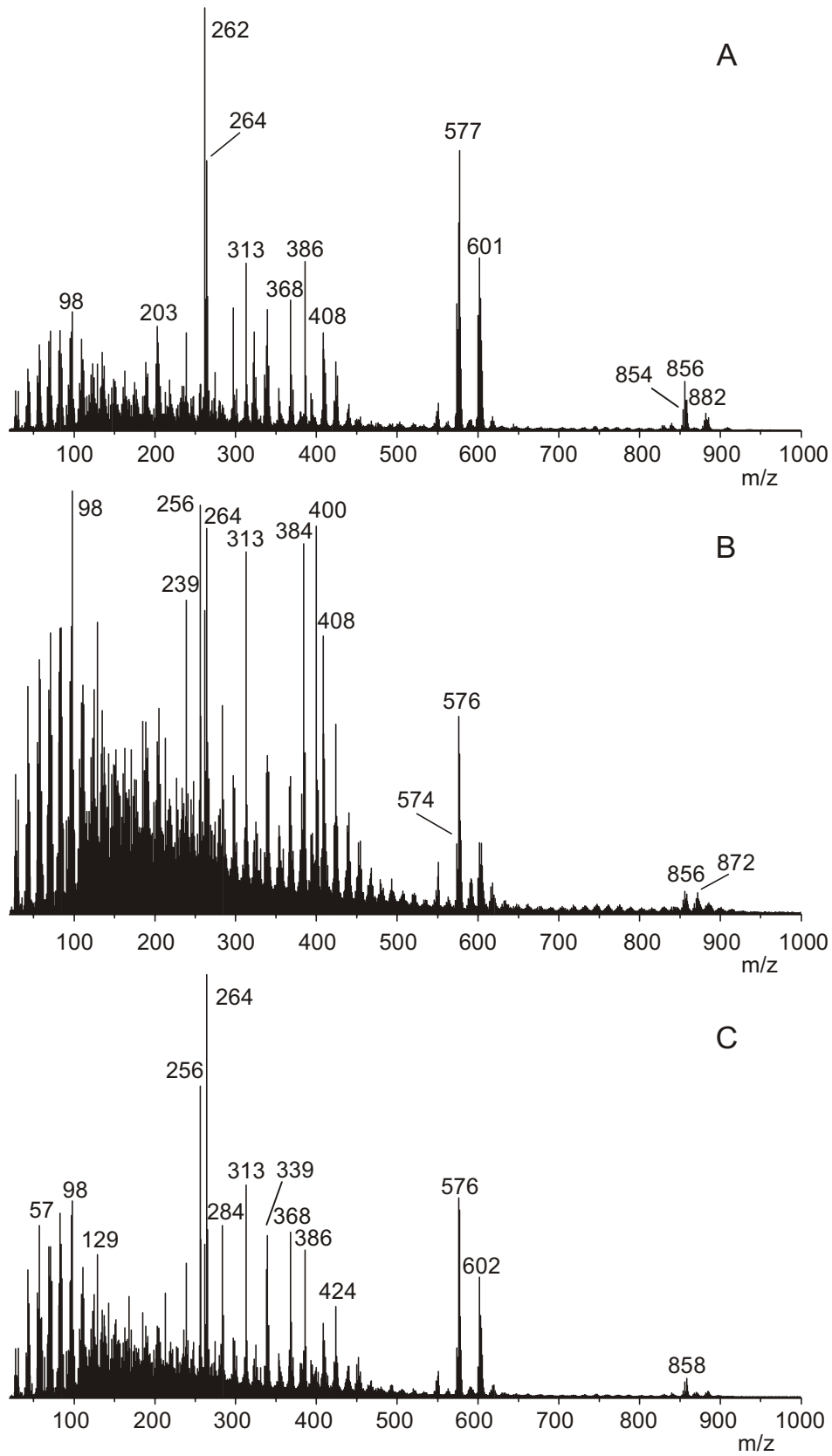**Figure 1** *DTMS summation spectrum of 64-day light-aged egg-only tempera.*

Figure 2 *DTMS summation spectra of the unexposed (A), the 64-day light-aged (B) and the NO_x/SO_2 exposed (C) unpigmented tempera.*

Comparison of this spectrum with that of the 64-day light-aged unpigmented tempera (**Figure 2B**) indicates that this latter reaction plays a more important role in the egg-only tempera than in the unpigmented tempera, as evidenced by the higher relative intensity of m/z 98 in the spectrum of the 64-day light-aged egg-only tempera. Secondly, cross-linking between the (oxygenated) glycerolipids takes place, leading to the formation of oligomers and high molecular weight polymers of glycerolipids. The oxidatively cleaved fatty acyl moieties are mainly present in this cross-linked material. Finally, the glycerolipids are hydrolysed and free fatty acids are formed. These changes are similar in the egg-only tempera and in the unpigmented (egg + mastic) tempera. The mastic fraction, which is present in the unpigmented tempera also changes upon light ageing. The changes involve mainly side chain oxidation [4, 5].

Exposure to NO_x/SO_2 for four days in the dark leads to similar processes as light ageing, but differences can be observed. The following paragraphs discuss these differences in more detail. **Figure 2** compares the DTMS sum spectra of the unexposed (A), the 64-day light-aged (B) and the NO_x/SO_2 exposed (C) unpigmented tempera. Similar reactions to those observed in the light ageing are observed in the dark upon exposure to air pollutants. Unsaturated fatty acylium ion peaks at m/z 262 and 264 are depleted and peaks originating from oxygenated TAGs emerge. Intact triglycerides are depleted due to oxidation, hydrolysis and cross-linking. The peaks at m/z 256 and 284 are observed at high relative intensity in the spectrum of the 64-day light-aged as well as in the spectrum of the NO_x/SO_2 exposed unpigmented tempera. These peaks may originate from the free fatty acids palmitic acid and stearic acid. They are also observed as fragment ions of phosphatidylcholines [6], cross-linked triglycerides [7] and metal salts of these fatty acids [7]. Comparison of the mass thermograms of these ions indicates that there is a difference in the contribution of the triglyceride consuming processes to the overall result. **Figure 3A** shows the mass thermograms (MT) of m/z 256 derived from the DTMS obtained on the unaged control of unpigmented tempera. The MT of m/z 854-860 is also shown as a reference for the desorption of triglycerides. The highest intensity of the m/z 256 is observed at scan number 60, approximately 10 scans later than the desorption of triglycerides. The m/z 256 ions that are formed between scan numbers 55 and 65 derive from the relatively polar and less volatile phosphatidylcholines. The MT of m/z 256 from the 64-day light-exposed sample, shown in **Figure 3B** has its apex at scan number 67. This difference in position of the apex, approximately 15 scans later than the desorption maximum of the triglycerides or 5 scans later than the desorption of the phospholipids, indicates that the m/z 256 mainly originates from cross-linked material rather than from phospholipids. The MT of m/z 256 further indicates that ions with this mass also desorb at low

temperatures (scan numbers 0-10), and hence that free fatty acids are also present in the 64-day light-aged sample. Comparison with the MT of m/z 256 from the NO_x/SO_2 exposed sample (**Figure 3C**) shows that the formation of free fatty acids is a much more important process in the NO_x/SO_2 induced deterioration of the unpigmented tempera.
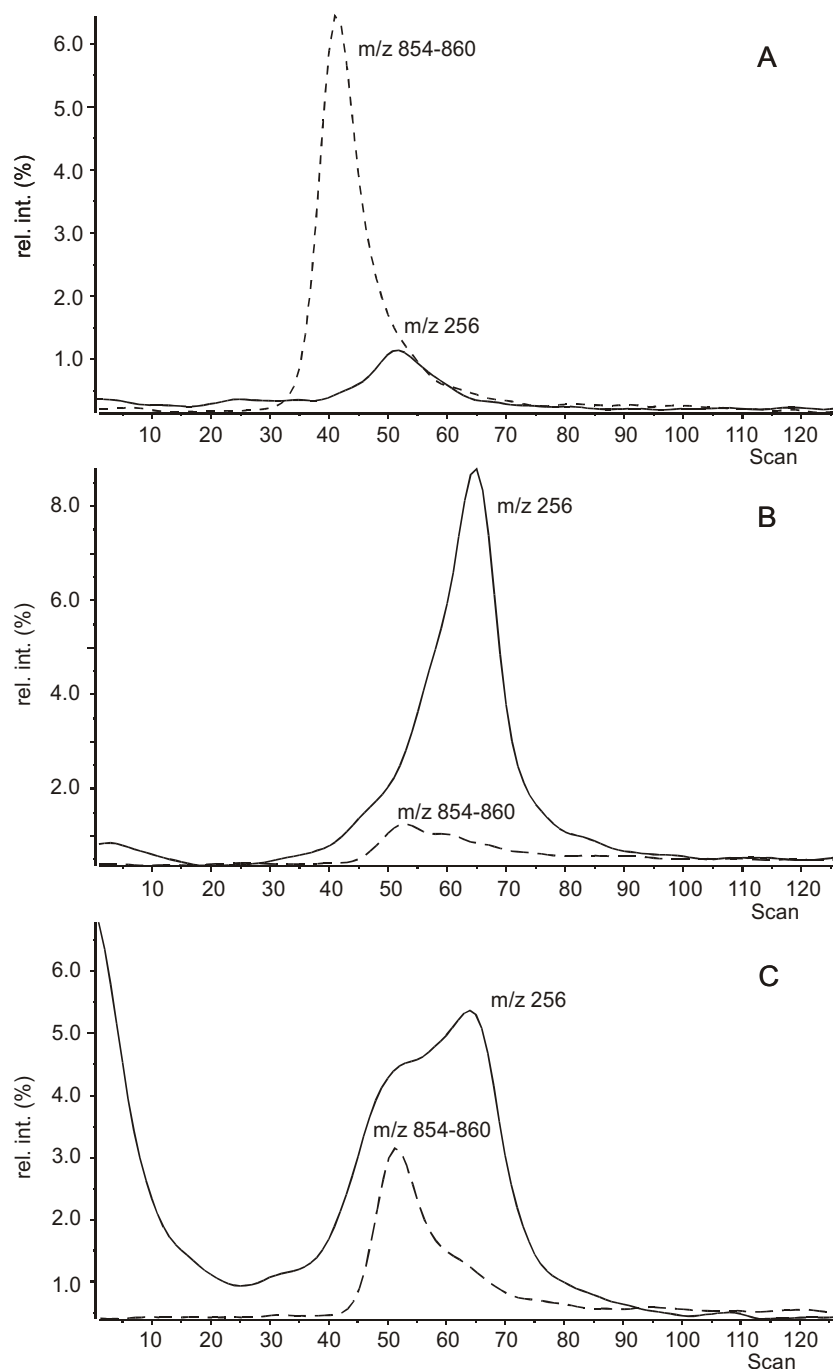

Figure 3 *Mass thermograms (MTs) of m/z 256 (solid lines) and m/z 854-860 (dashed line) derived from the DTMS obtained on the unaged control (A), 64-day light-exposed (B) and NO_x/SO_2 exposed (C) unpigmented tempera.*

Although a significant decrease in the intensity of the cholesterol peak is observed, the cholesterol oxidation products at m/z 384 and m/z 400 are not observed at high intensity in air pollutant exposed unpigmented tempera. Possibly air pollutant induced deterioration of cholesterol in unpigmented tempera involves a different mechanism and different products than deterioration under light ageing conditions. This effect is less pronounced in the case of the air pollutant exposed egg-only tempera (**Figure 4**), which shows peaks at m/z 384 and m/z 400, so that the overall change in this sample is more comparable to the light ageing process. Another difference between the effects of light exposure and exposure to NO_x/SO_2 is found in the high relative intensity of the m/z 368 peak in the DTMS spectrum of the NO_x/SO_2 exposed unpigmented and egg-only temperas. The MT of this peak indicates that this peak is formed in two events in the DTMS run. **Figure 5A** shows the MTs of m/z 368 (solid line) and m/z 386 (dashed line) derived from the DTMS data of the unaged control. The first peak in the MT of m/z 368 coincides with the desorption of cholesterol (m/z 386). The second peak emerges before the desorption of triglycerides. It is interpreted as the product (cholestadiene) of fragmentation of cholesterol ester molecular ions by loss of fatty acid neutral. Cholesterol esters are only present in very low quantities in fresh eggs [8], and their main constituents are cholesteryloleate (650 Da) and cholesterylpalmitate (624 Da) [9]. Their detection as cholestadiene fragments is probably relatively efficient. It must be noted that cholesterol, which only constitutes approximately 5 percent of the egg lipids [8], also produces very intense peaks in the spectra of egg temperas. The observation that a very small peak at m/z 650 is present in the spectra of the unpigmented tempera control sample, and that its MT shows a maximum that coincides with that of m/z 368 can only be taken as supportive indication but not as proof of the detection of cholesterol esters. Comparison of the MTs of m/z 368 derived from the 64-day light-aged (**Figure 5B**) and the NO_x/SO_2 exposed (**Figure 5C**) samples of unpigmented tempera, indicates that the unknown m/z 368 forming material present in the unpigmented tempera is depleted upon light ageing, but is less affected by the exposure to NO_x/SO_2. A similar observation was made for the egg-only tempera.

The DTMS spectrum of the NO_x/SO_2 exposed egg-only tempera (**Figure 4**) shows peaks at m/z 424, 450 and 452, which are not present in the spectra of the control and the light-aged samples. The MTs of these m/z values indicate that the material desorbs at temperatures (apex at scan numbers 28-30) below the desorption temperature of cholesterol (apex at scan number 37). The observation that these peaks are also present in the NO_x/SO_2 exposed samples of the other series suggests that they were taken up by the sample during the exposure.
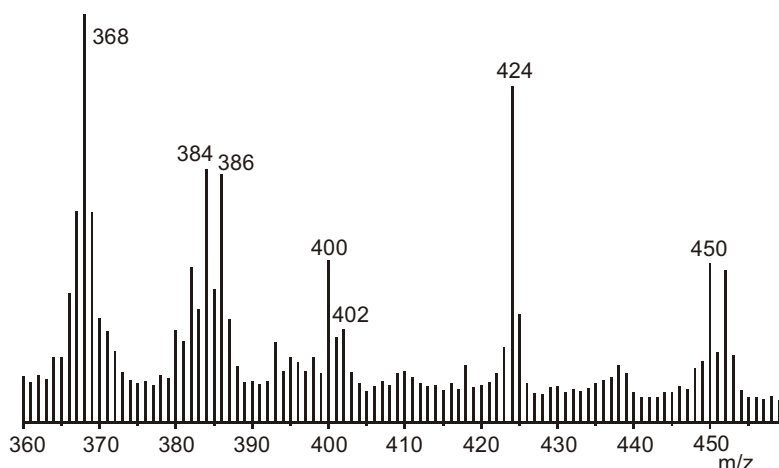
Figure 4 *Partial DTMS summation spectrum (m/z 360-460) of NO_x/SO_2 exposed egg-only tempera.*

Analysis of a control sample of NO_x/SO_2 exposed egg-only tempera, which was exposed to "clean" air in the gas exposure chamber also showed the peaks at m/z 424, 450 and 452 and an additional peak at m/z 448. The average spectrum of the window where the material desorbs in the DTMS run (scans 25 to 35) shows intense peaks at m/z 168 ($C_{12}H_{24}$), 257 ($C_{15}H_{31}COOH_2$), 264 (oleic acid acylium), 280 (linoleic acid) and 285 ($C_{17}H_{35}COOH_2$) and hence points to dodecylpalmitate (424Da), dodecylstearate (452Da) dodecyloleate (450Da) and dodecyllinoleate (448Da). Although the origin of these wax esters cannot be determined unambiguously, it is very likely that they have accumulated on the samples during exposure in the NO_x/SO_2 exposure facility.

One peak at m/z 64, which is strongly present in the spectra of air pollutant exposed samples of the egg-only and unpigmented tempera series is not significant in the DTMS spectrum of the light-aged samples. This peak is attributed to sulphur dioxide (SO_2) which forms during the DTMS run as a result of pyrolysis of the sample. The MT of m/z 64 from the NO_x/SO_2 exposed egg-only tempera sample shown in **Figure 6** (dotted line) indicates that SO_2 is formed at different stages in the DTMS run. The first peak in the MT appears where pyrolysis of the proteinaceous material occurs (scans 55-60). This peak is also present in the MT of the unaged control (solid line), albeit at very low intensity. The MT of the 64-day light-aged sample (dashed line) also shows this peak. In addition, it has two shoulders at higher scan numbers (between scan 60 and 75). These are likely to originate from proteinaceous material which has changed due to oxidation and cross-linking and thus become more thermally stable.

67
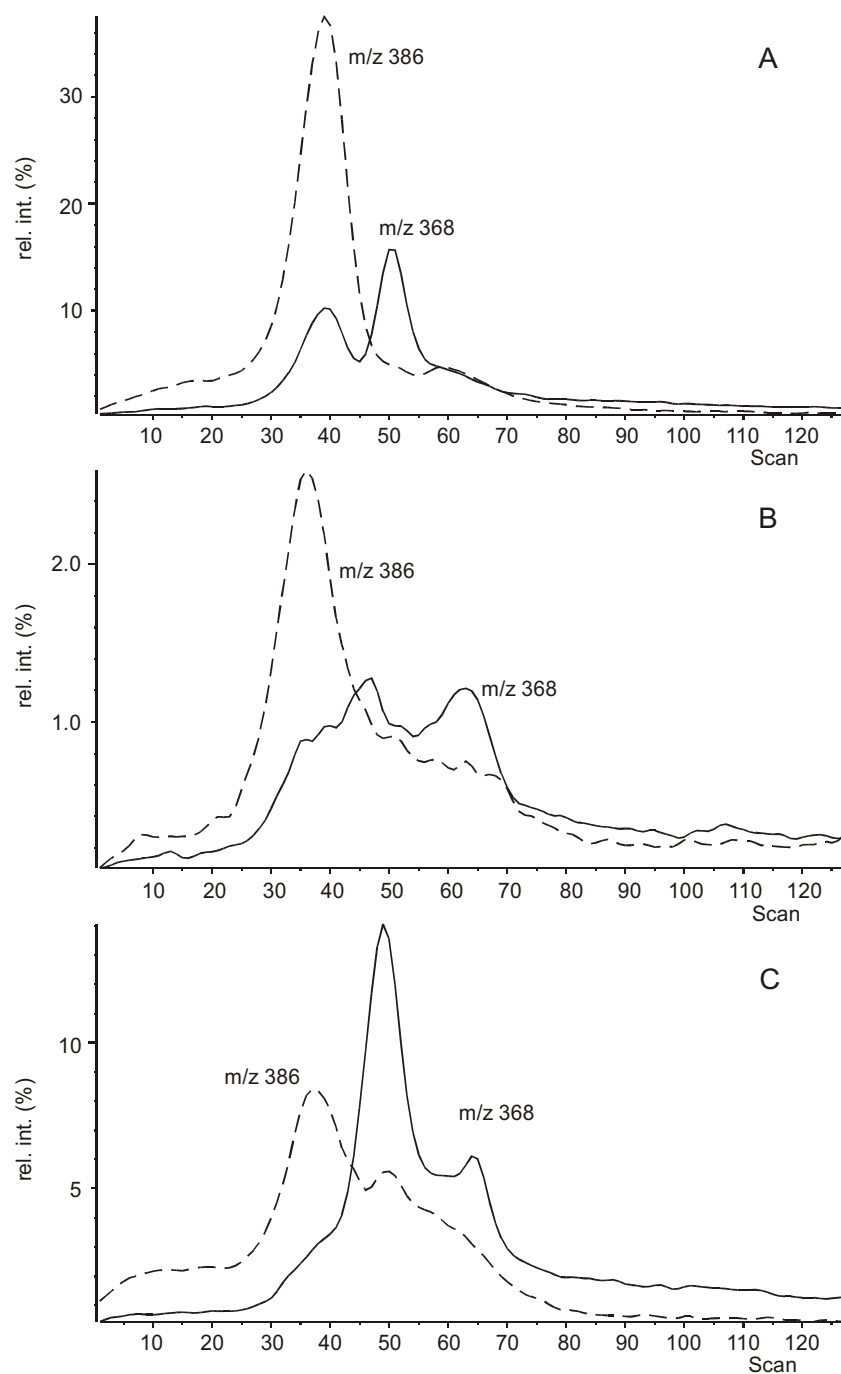
Figure 5 *MTs of m/z 368 (solid lines) and m/z 386 (dashed lines) derived from the DTMS data of the unaged control (A), 64-day light-aged (B), and NO_x /SO_2 exposed (C) of unpigmented tempera.*
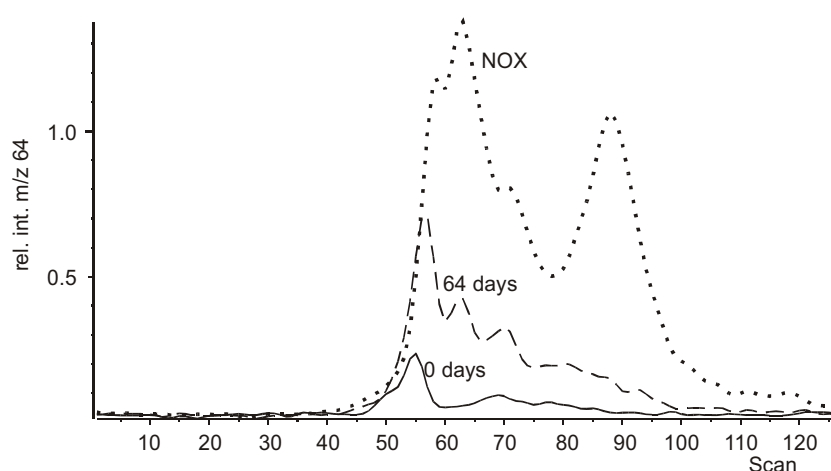
Figure 6 *MTs of m/z 64 from the control (solid line), 64-day light-aged (dashed line) and NO$_x$/SO$_2$ exposed (dotted line) egg-only tempera.*

The peak between scan 60 and 65 is the main peak in MT of m/z 64 from the NO$_x$/SO$_2$ exposed egg-only tempera, which indicates that the sulphur containing group of the proteins in the NO$_x$/SO$_2$ exposed sample are more severely affected than those in the 64-day light-exposed sample. The MT of m/z 64 of the NO$_x$/SO$_2$ exposed sample shows a local maximum between scan numbers 80 and 90, which is not observed in the MTs of the other samples. SO$_2$ that is desorbed at such high temperatures (scans 80 – 95) derives from inorganic sulphates [10]. De Santis [11] has found that SO$_2$ can react to sulphate on a surface such as active carbon and that the reaction is significantly accelerated when NO$_2$ is present. Another, tentative, explanation for the presence of inorganic sulphate is that it originates from progressed oxidation and subsequent elimination of sulphur containing side chains of proteins. Finally, the occurrence of m/z 64 peaks at the end of the DTMS run may be explained by the formation of thermally more stable (charred ?) proteinaceous material from oxidised proteins earlier in the DTMS run, that only decomposes at high temperatures under exclusive formation of SO$_2$.

Dosimetric results

As mentioned in **Chapter 2** the light ageing process in unpigmented tempera resembles the field ageing process, so that the light ageing series can be used for calibration. The same is true for the egg-only tempera series. **Figure 7** shows the scores of the unpigmented tempera dosimeters on the first discriminant function, with the light ageing set serving as calibration set. The field-exposed samples plot between 8 and 16 days of light ageing. The small relative difference between the scores could be wrongly interpreted as insignificant. It should be borne in

mind, however, that the discriminatory power of the data from the unpigmented tempera dosimeters is very high (200), so that the differences in degree of chemical change are related to differences in the quality of the museum environments at the exposure sites.
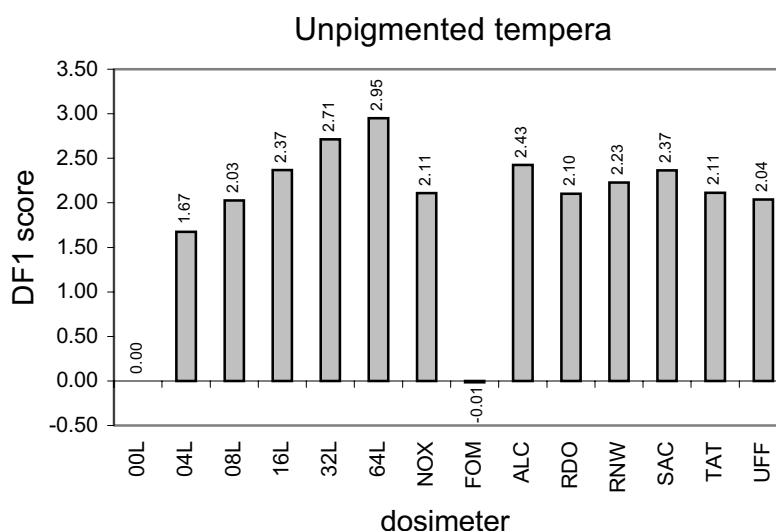
Figure 7 *Scores on the first discriminant function of laboratory-aged and field-exposed unpigmented tempera dosimeters.*

Rapid changes take place in the first 4 days of light ageing as can be observed from the relatively high score of sample 04L. This suggests that good results with the unpigmented tempera paint systems can also be obtained if a shorter ageing time is applied. Indeed an improved differentiation was obtained when the unpigmented tempera dosimeters were exposed for three months at nine different sites in the Rijksmuseum (Amsterdam, NL) (see **Chapter 4**). Numerically more resolving power between 4 and 64-day of light ageing was obtained when DA was carried out by exclusion of the control and using the light ageing set as the training set. The observation that the light ageing process in the first 4 days of artificial light ageing is chemically different from more progressed ageing is another reason to do this. In this way progressed ageing was used for calibration. The results of this approach [12] show that focusing on the more progressed ageing leads to the same results in terms of ranking sequence, but amplifies the differences among the sites. The B/W of the field exposure sites was increased by a factor of 1.8, when the control for light ageing was excluded from the training set.

Figure 8 shows the degree of chemical change in the field-exposed egg-only tempera test systems together with those of the laboratory-exposed samples. The low scores of the first two light-aged samples (04L and 08L) indicate that the ageing process develops slowly in the first stage of light ageing. Between 8 and 16 days of light ageing acceleration of the ageing process takes place and after 16 days the ageing process decelerates again. Discriminant mass spectra (not shown) indicate that in the first stage cholesterol oxidation is more important than glycerolipid oxidation. MALDI-FTMS results (see **Chapter 5**) confirm that glycerolipid oxidation becomes more predominant after 8 days of light ageing [13]. The NO_x/SO_2 exposed dosimeter scores higher than the field sites; the degree of chemical change is in the same range as 32L. This indicates that the test system is relatively sensitive indicator for these air pollutants. The field-exposed dosimeters all show scores that are comparable with that of 16 days of light ageing. There are no extreme differences observed between the field-exposed dosimeters. However, as the discriminatory power of the "egg-only" dosimeter is high, differences in degree of chemical change are highly significant. Possibly, a shorter exposure time would result in larger differences between the field site scores.
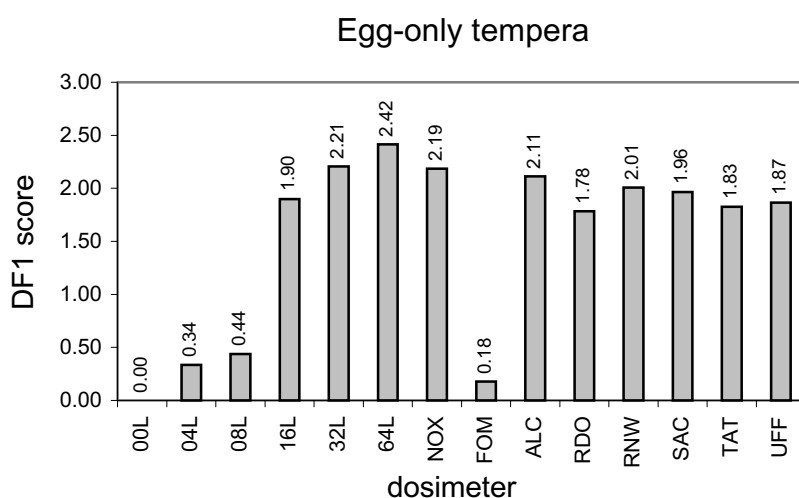
Figure 8 *Scores on the first discriminant function of laboratory-aged and field-exposed egg-only tempera dosimeters.*

3.3.2 Tempera with organic pigments

Mass spectrometry

Figure 9 shows the partial mass spectra (m/z 20-300) of the control (A) and 64-day light-aged (B) samples of alizarin tempera. The mass spectra of alizarin pigmented tempera show a very intense alizarin (1,2-dihydroxyanthraquinone) molecular ion peak at m/z 240. This is caused by two factors. Firstly, the paint is very strongly pigmented with alizarin. Second, the ionisation properties of the molecule are such that it preferentially forms molecular ions under (low-energy EI) DTMS conditions. The high intensity of the alizarin peak goes beyond the dynamic range of the mass spectrometer. Therefore, the m/z 240 peak was excluded from the alizarin tempera mass spectrometric data sets when they were subjected to discriminant analysis. The first isotope peak of alizarin at m/z 241 was not excluded and served as an indicator of alizarin.
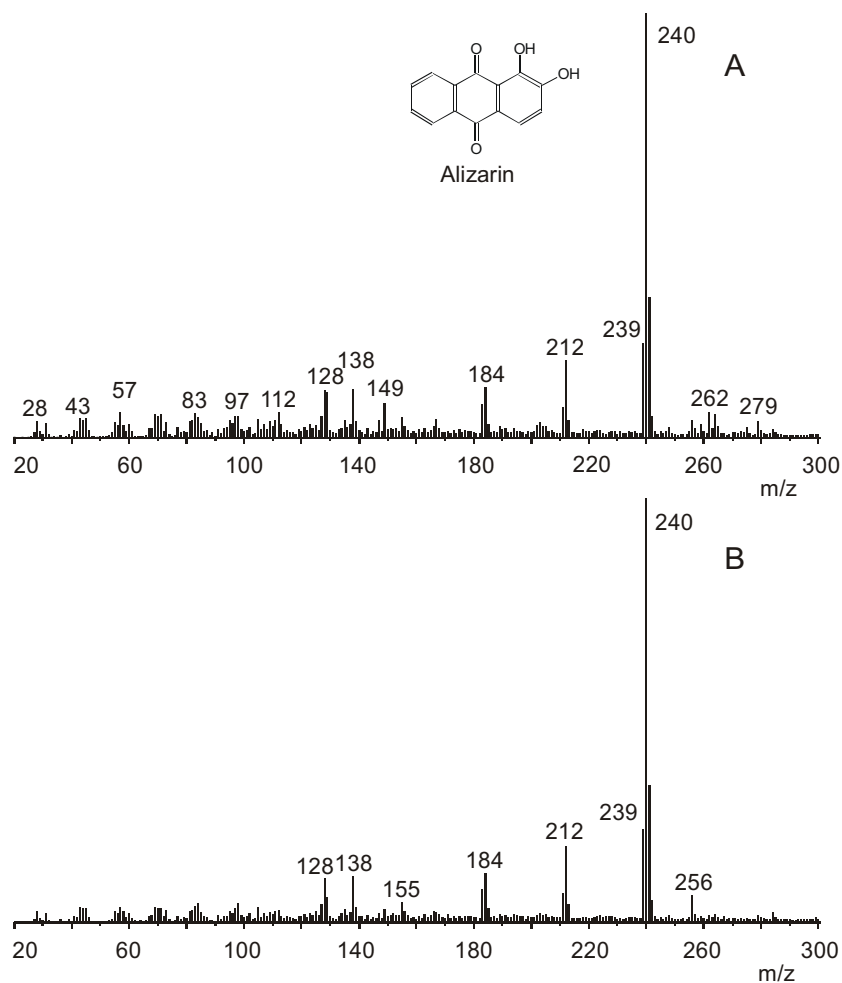
Figure 9 *Partial DTMS spectra (m/z 20-300) of the control (A) and 64-day light-aged (B) alizarin tempera.*
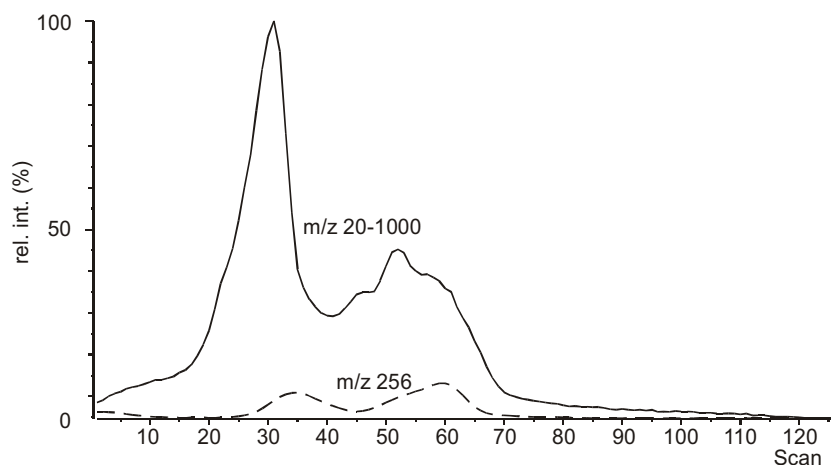
Figure 10 *TIC (solid line) and MT of m/z 256 (dashed line) of the 64-day light-aged alizarin tempera.*

The changes observed upon light ageing of the alizarin tempera are very similar to those observed in the unpigmented tempera. A peak at m/z 256 however appears to be significantly higher in the spectra of light-aged alizarin tempera than in the light-aged unpigmented tempera. Although this could be interpreted as the enhanced formation of palmitic acid by hydrolysis or the incorporation of palmitic acyl moieties in the cross-linked fraction, the peak at m/z 256 can also derive from oxygenation products of alizarin (probably trihydroxyanthraquinones). In order to check this hypothesis, the 64-day light-aged alizarin tempera sample was analysed by DTMS at a resolution sufficient to resolve the trihydroxyanthraquinone molecular ion (elemental composition $C_{14}H_8O_5$, exact mass 256.0366) from ions with elemental composition $C_{16}H_{32}O_2$ (exact mass 256.2397), i.e. palmitic acid. These experiments were carried out at 70eV ionisation voltage. **Figure 10** shows the TIC (desorption and pyrolysis profile, solid line) and the MT of m/z 256 (dashed line) of the 64-day light-aged alizarin tempera. **Figures 11A, 11B and 11C** show the partial mass spectra (m/z 255.5-256.5) derived from the desorption/pyrolysis windows of free fatty acids, alizarin, and cross-linked lipidic material, respectively. The figures clearly indicate that material with elemental composition $C_{14}H_8O_5$ is desorbed in the desorption window of alizarin and that material with the elemental composition of palmitic acid primarily forms in the desorption window of the free fatty acids and the pyrolysis window of cross-linked lipidic material.

The elemental composition of the material with molecular mass 256 that desorbs in the window of alizarin suggests that oxidation of alizarin takes place upon light ageing of the test systems. Purpurin (1,2,4-trihydroxyanthraquinone)
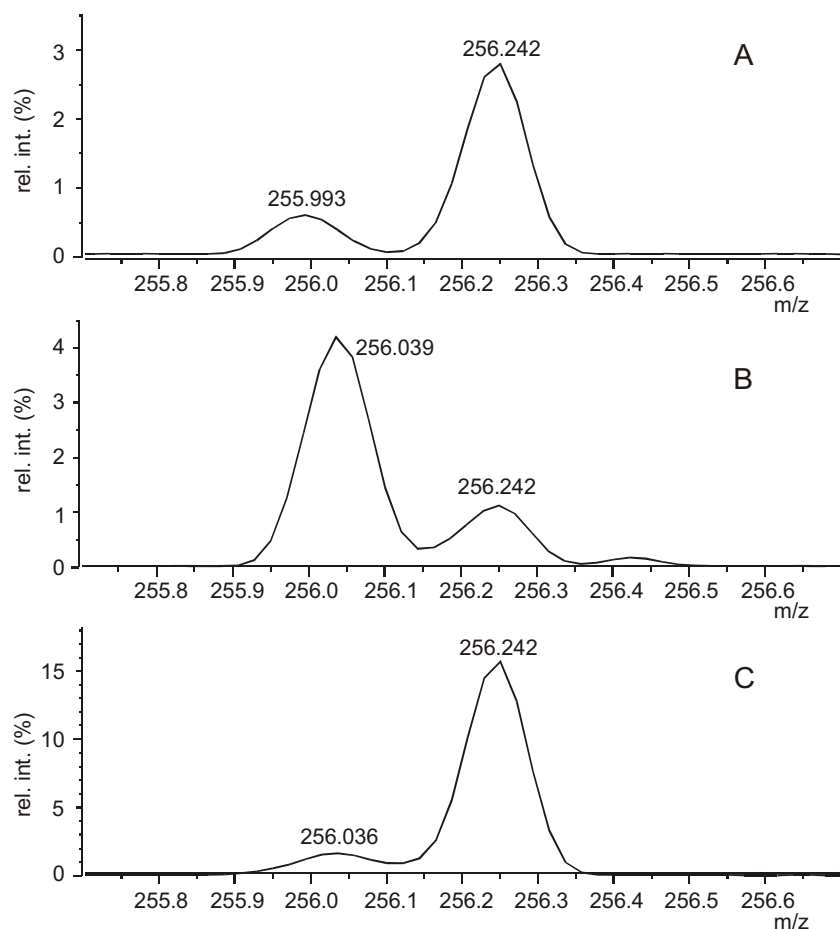
Figure 11 *Partial mass spectra (m/z 255.5-256.5) derived from the desorption / pyrolysis windows of free fatty acids (A), alizarin (B), and cross-linked lipidic material (C). The peak at m/z 255.993 in (A) originates from perfluorokerosine, which was allowed into the ion source during analysis for internal calibration purposes.*

and its isomers are known oxidation products of alizarin [14, 15]. In order to investigate whether purpurin was present in the 64-day light-aged test system, the structure of the ions at m/z 256 was investigated by collision-induced dissociation tandem MS experiments. **Figure 12A** shows the DT-MIKES spectrum of the m/z 256 peak in light-aged tempera 64 days. Comparison of this spectrum with the reference spectra of the m/z 256 peaks of palmitic acid (**Figure 12B**) and purpurin (**Figure 12C**) clearly shows that the spectrum in **Figure 12A** is not a linear combination of the spectra shown in **Figures 12B and C**. Combining the high-resolution DTMS and the DTMIKES results, it must be concluded that isomers of purpurin form in the alizarin tempera upon light ageing. Attempts to identify these oxidation products and to quantify their relative proportion in the light-aged alizarin temperas were not undertaken. It must be noted however that

the loading of m/z 241 on the first discriminant function indicates that the relative intensity of this alizarin peak in the DTMS spectra increases upon light ageing. This means that the alizarin is depleted at a slower rate than the most important components of the binding medium.
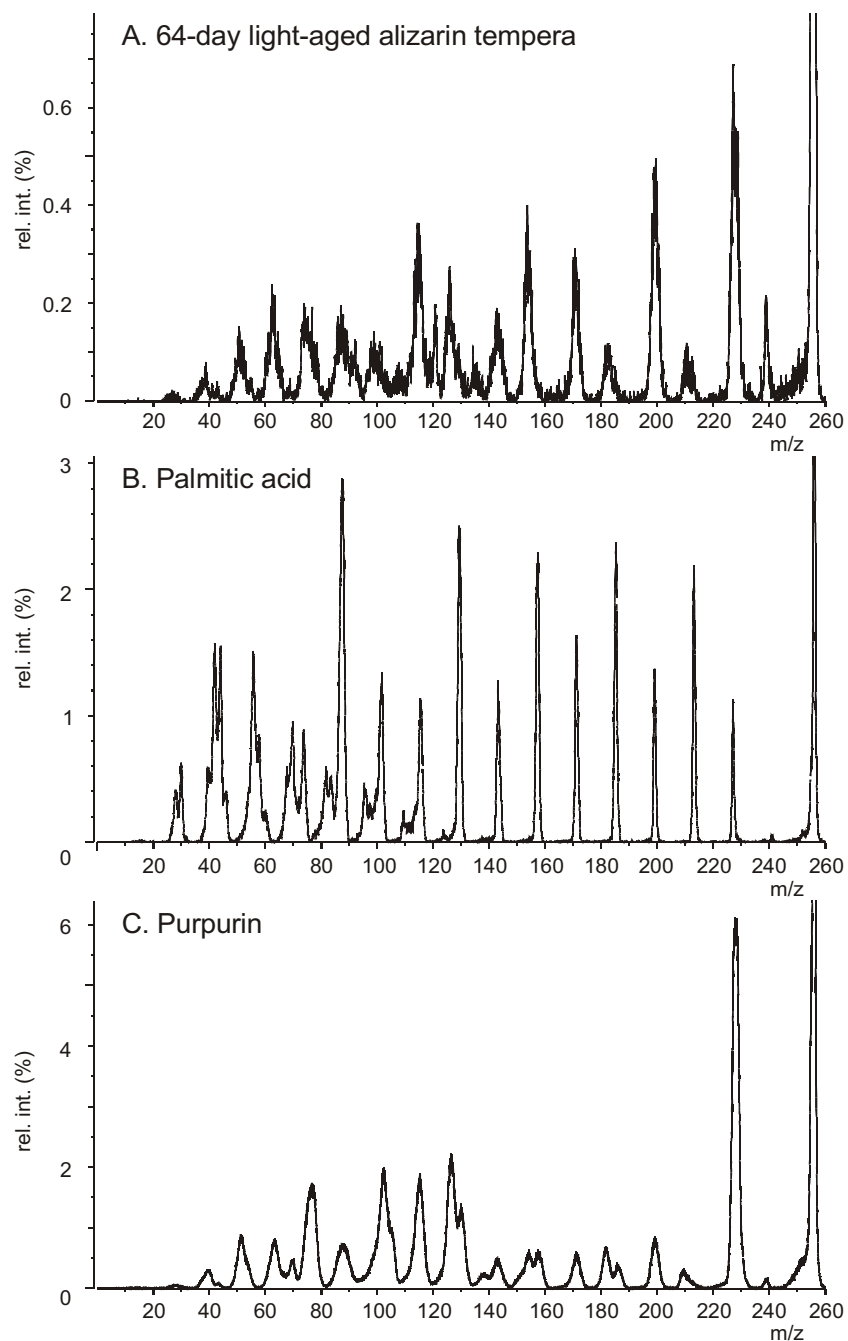
Figure 12 *DT-MIKES spectra of the m/z 256 peak in 64-day light-aged alizarin tempera (A), palmitic acid (B) and purpurin (C).*
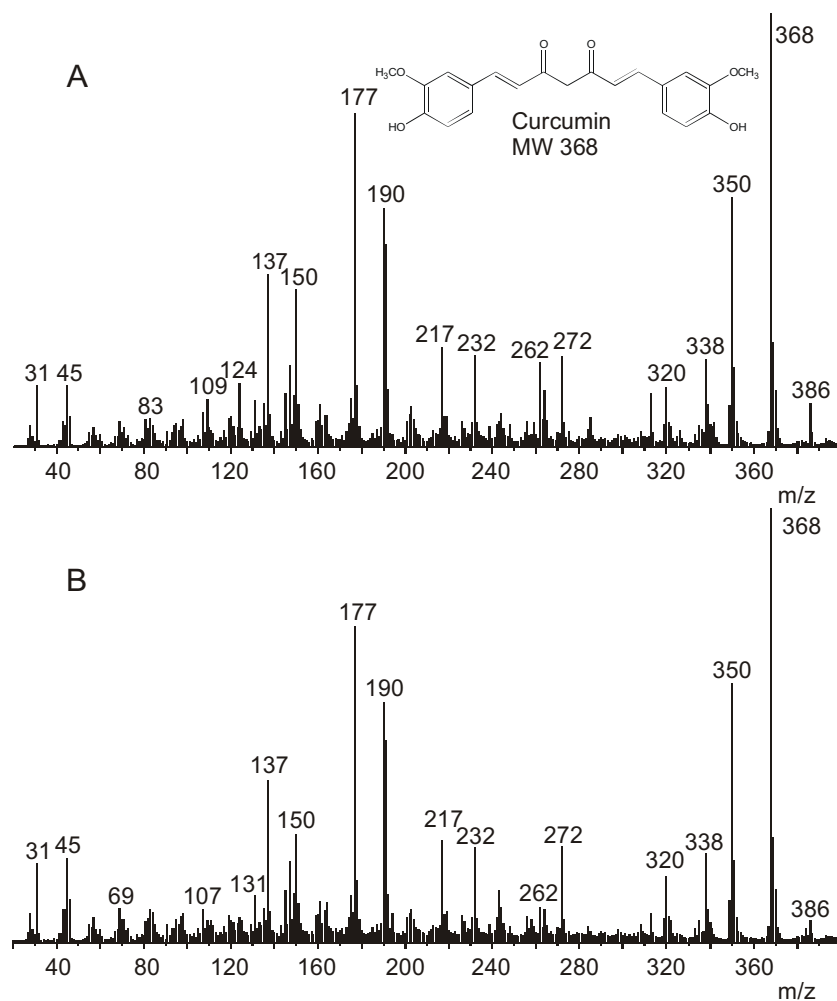
Figure 13 *Partial mass spectra (m/z 20-400) of curcumin tempera control (A) and 64-day light-aged (B).*

The partial mass spectra (m/z 20-400) of curcumin tempera control (A) and 64-day light-aged (B) are shown in **Figure 13**. Although curcumin tempera also contains a very high amount of pigment and the molecular ion peak of curcumin (m/z 368) is also the base peak in the mass spectra, the intensity of this peak was not so high (off-scale) that the peak had to be excluded form the data sets before DA. This is due to the lower stability of the curcumin molecular ion under the DTMS conditions. Many curcumin fragment peaks are present in the mass spectra and make identification of the changes in the mass window below m/z 368 a difficult task.

Light ageing of the curcumin tempera test system has some effect on the glycerolipids and cholesterol, albeit less so than in unpigmented tempera. Probably the pigment absorbs a large part of the light energy, so that photo-oxidation of the binding medium occurs to a lesser extent. From the mass spectra

it cannot be determined, at first hand, whether this absorption leads to breakdown of the curcumin itself. The high concentration of the pigment in the paint does not allow identification of breakdown products. Comparison of the partial mass spectra of the unaged control (**Figure 13A**) and the 64-day light-aged (**Figure 13B**) curcumin dosimeters indicates that several peaks become much less intense in the mass spectra of the light-aged material, viz. m/z 109, 124, 135 and 150. Later experiments, which were aimed at the reproduction of the spectra indicate that these peaks did not originate from the sample itself. They could be traced back to contamination with Kauri copal of one of the tools (probably a syringe) that were used for sample preparation before DTMS. Therefore, the following m/z values had to be excluded from the DTMS dataset before DA: m/z 94, 109, 110, 124, 125, 135, 136, 150, 151, 285, 286, 326, 327, 342, and 343.

The mass spectrum of air pollutant exposed alizarin tempera (data not shown) indicates oxidation of unsaturated glycerolipids. Cholesterol, however, was not transformed into the known oxidation products. The same effect was seen in the curcumin pigmented tempera. These observations are in agreement with those on the unpigmented tempera.

Dosimetric results

Discriminant analysis indicates that field ageing effects in alizarin tempera are comparable with light ageing effects. For the curcumin tempera the field ageing process was also found to primarily follow the light ageing process. It must be concluded that for both systems light ageing provides a good simulation of the field ageing process within this observational level.

Figure 14 shows the degree of chemical change in the laboratory-aged and in the field-exposed alizarin tempera dosimeters. It shows that in this system, like in the unpigmented tempera test system, the degree of chemical change is larger in the beginning of the light ageing series and then develops more slowly upon longer exposure. In many more respects, the test system is comparable with the unpigmented tempera test system. Both test systems are relatively insensitive to thermal ageing and display similar sensitivity toward exposure to air pollutants. Furthermore, the ranking of the field-exposed alizarin dosimeters is similar to that observed for the unpigmented tempera dosimeter, an exception being the ALC dosimeter. The position of the FOM control relative to the other samples (including the control for light ageing) suggests that the FOM control was conserved better than the control for light ageing. As stated in the experimental section, a difference between the light ageing control and the field exposure control would indicate that the test system is sensitive to small differences in storage conditions.

Alizarin and curcumin tempera
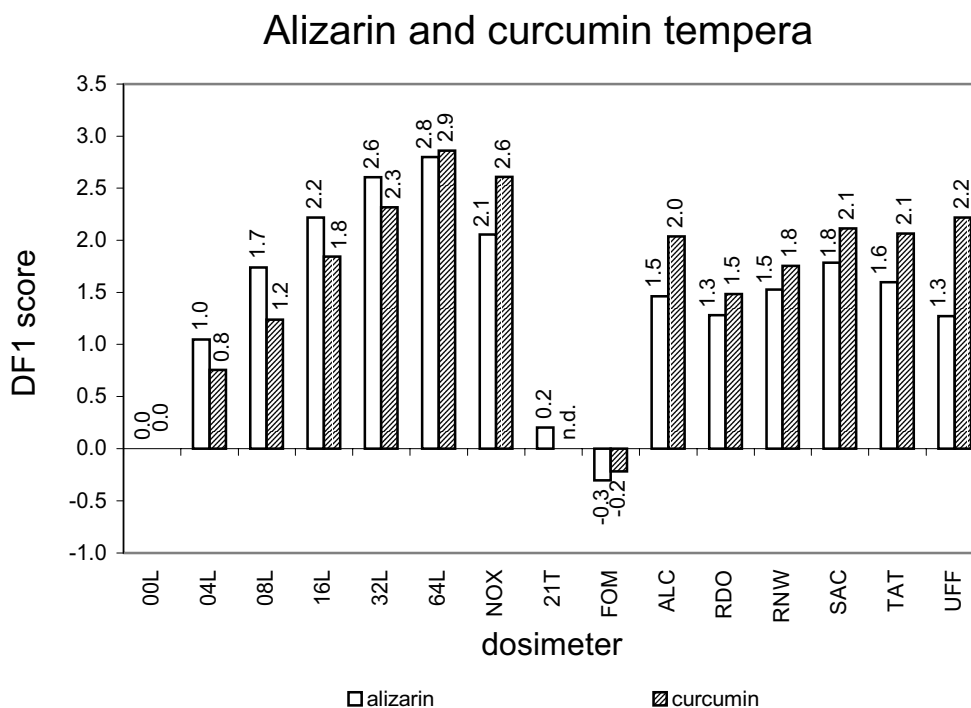
Figure 14 *Scores on the first discriminant function of laboratory-aged and field-exposed alizarin and curcumin tempera dosimeters.*

Comparison of the degree of chemical change of the laboratory-aged and field-exposed curcumin dosimeters (**Figure 14**) shows that the average light ageing equivalent of the sites is comparable with that observed for unpigmented tempera. The ranking of the sites differs considerably from the alizarin and the unpigmented tempera results. The relatively low score of the RDO site is the only similarity among the unpigmented and the organic pigmented tempera test systems. This is interpreted as an indication that these dosimeters are relatively sensitive to light as primary factor, because the RDO storage facility is a dark site. The dissimilarity with the alizarin and other test systems must then be taken as an indication that these systems are sensing different secondary factors. Clearly the current data set is too small (nor designed) to determine what these factors are. It should be noted that such differences in sensitivity might originate in the pigment's high reactivity towards reactive oxygen species such as ozone [16]. The recognised structural similarity of this pigment with coniferyl alcohol (1,7-bis(4-hydroxy-3-methoxyphenyl)-1,6-heptadiene-3,5-dione) [16], a monomeric unit of lignin, suggests that curcumin (4-(3-hydroxy-1-propenyl)-2-methoxyphenol) acts as a radical scavenger in a similar way as coniferyl alcohol

in the lignification of cell walls [17]. The relatively high light ageing equivalent of the NO_x/SO_2 exposed dosimeter is merely one of the potential differences in specific sensitivity. Hence, the explanation that the relatively high chemical change observed for UFF is caused by the high level of air pollutants at this site is a tentative one.

3.3.3 Tempera with lead containing pigments

Mass spectrometry

The mass spectra of the test systems that are pigmented with lead containing pigments show peaks at m/z 206-208. These originate from the lead that is formed and volatilised in the reductive regime at high temperature at the end of a DTMS run. Depending on the exact chemical composition of the pigment there are other pigment derived peaks present in the mass spectra. A carbon dioxide peak at m/z 44 for instance is present in mass spectra of lead white tempera. The Naples yellow pigment primarily consists of lead antimonate, $Pb_2Sb_2O_7$ [18]. Upon heating it disintegrates and is reduced to lead (observed as Pb), antimony (observed as Sb, Sb_2, Sb_3, and Sb_4), and a great variety of oxides of lead and antimony (such as SbO, SbO_2, PbO, Sb_2O_2, $PbSbO_2$, Sb_3O_4, $PbSb_2O_4$, Sb_4O_5 and Sb_4O_6). Thermal disintegration mainly takes place at higher temperatures in a DTMS run. This is illustrated by the total ion current of a sample of Naples yellow tempera shown in **Figure 15A**. The first peak in the total ion current (scan 30-70) mainly represents organic materials, which desorb or pyrolyse at lower temperatures. The second group of desorption peaks (scan 70-115) can be attributed to thermal reduction products of the pigment. This is illustrated as follows. Peaks for lead (m/z 206-208), lead oxides (m/z 222-224 and 424-428) and mixed lead and antimony oxides (m/z 578-585) dominate the total summation spectrum (scans 10-120) of the Naples yellow tempera control shown in **Figure 15B**. The DTMS spectrum of the same sample obtained after summation of scans 10-70 **(Figure 15C)** shows mainly information on the organic components of the tempera paint, as indicated by the high intensity of the peak at m/z 256 (palmitic acid moieities). The presence of peaks from Naples yellow in the DTMS spectra forms a problem for both interpretation of the spectra and evaluation of the DTMS results using the DA methodology for two reasons. Firstly, the intensity of the pigment peaks in the mass spectra (averaged over scan 10-120) is very high and not reproducible. This leads to great difficulties in discriminant analysis. Second, the great variety of compounds that are formed upon thermal disintegration of the Naples yellow pigment, and the broad isotopic distribution of
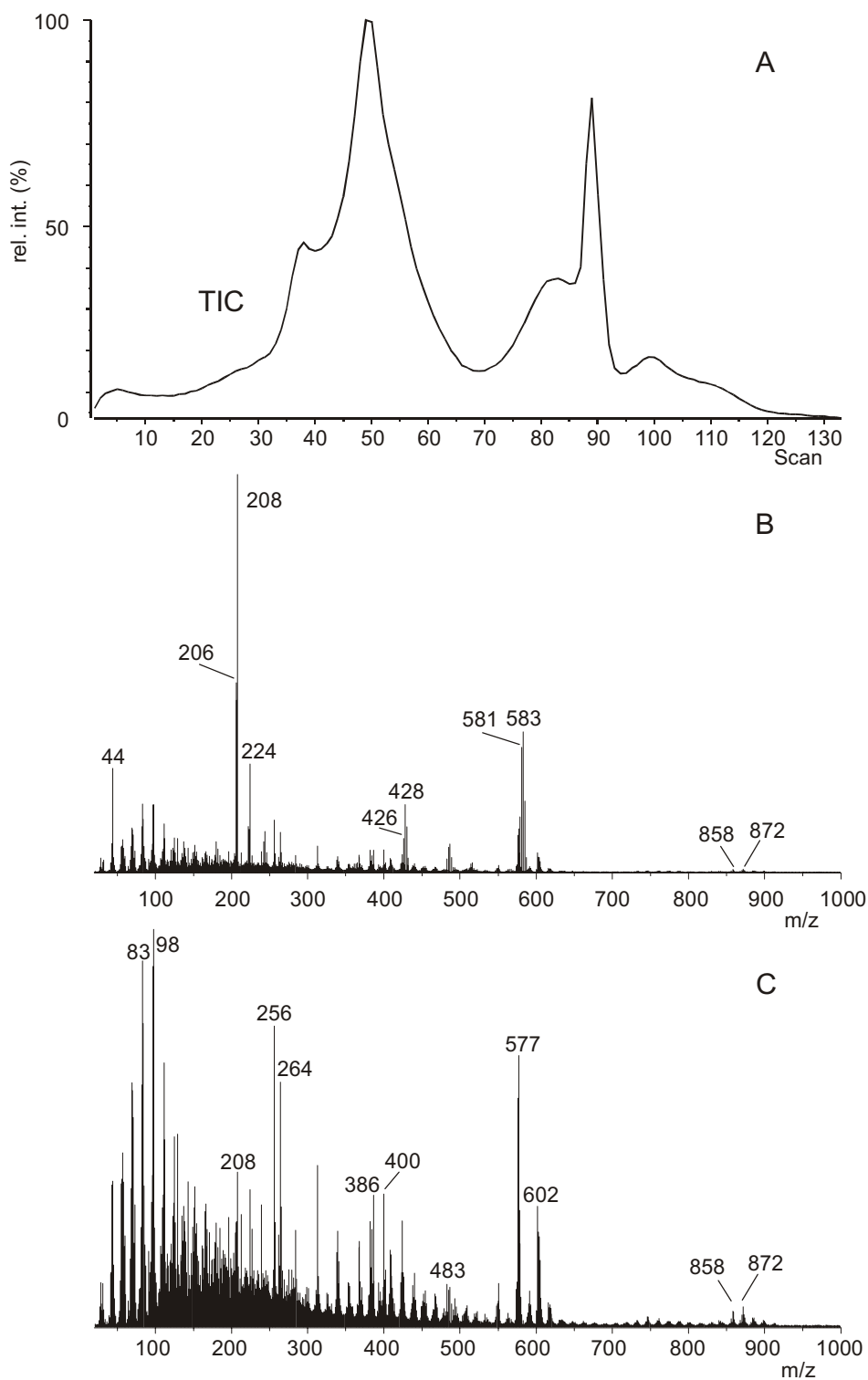
Figure 15 *Total ion current (TIC) of Naples yellow tempera control (A), DTMS spectra of the Naples yellow tempera control obtained after summation of scans 10-120 (B) and 10-70 (C).*

the elements involved, in particular Pb and Sb, leads to overlap with peaks that originate from the organic part of the paint. Less isobaric overlap at nominal mass was observed and no information on the lipid part was lost when scans 10-70 were summed instead of scans 10-120. Only elemental materials, viz. Sb, Pb, Sb_2, Sb_3, and Sb_4, that are formed upon reduction of the pigment appear (partly) below scan number 70. Therefore, for DA of Naples yellow DTMS results scans 10-70 were used.

Figure 16 compares the DTMS sum spectra of lead chromate tempera control (A) and 64-day light-aged (B). The mass spectra of lead chromate tempera are dominated by a great variety of pigment peaks, originating from lead, lead oxide and mixed lead chromium oxides. The binding medium peaks have relatively low intensities (< 10%). A similar approach as for the Naples yellow tempera spectra could not be used for the lead chromate tempera, because the majority of the pigment peaks also appear at low temperatures in the DTMS run.
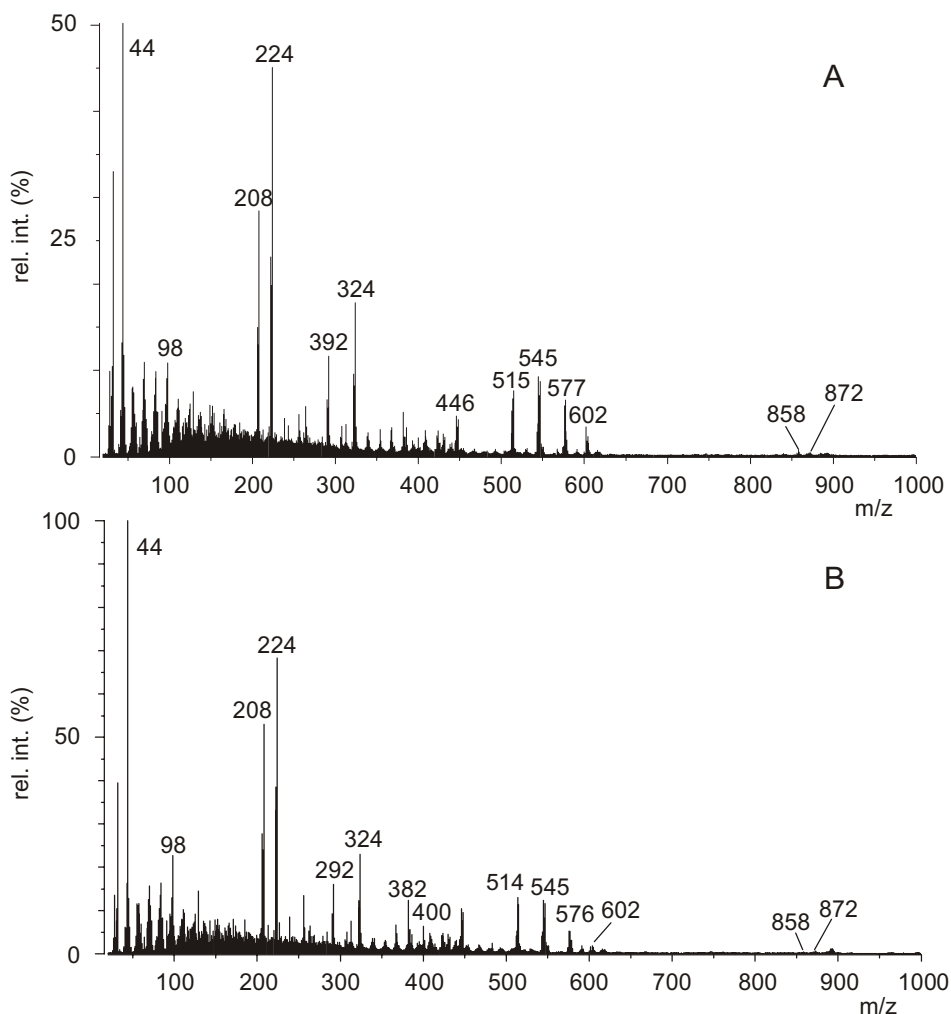
Figure 16 *DTMS summation spectra of lead chromate tempera control (A) and 64-day light-aged (B).*

For each of the lead salt pigmented temperas all mass peaks originating from the pigments were excluded from the mass spectrometric data set before DA. **Table 3** specifies and interprets these peaks. The first column gives the assignment of pigment peaks observed in the spectra. The second column specifies the ions that can be expected on the basis of the natural abundance of the isotopes of the elements. Contributions by ^{18}O are not taken into account due to its low natural abundance. Not all peaks in the second column were excluded from the data before DA, because the intensity of some pigment peaks was expected to be very low considering the theoretical isotope distribution. The peaks that were excluded are specified in the third column of the table. The fourth column indicates from which data set these peaks were excluded. From the lead white, Naples yellow and lead chromate tempera DTMS data sets 44, 18 and 152 peaks were excluded, respectively. It should be noted that deletion of the pigment peaks only partly corrects for inhomogeneities in the pigment concentration. Catalytic effects of the pigments on the chemical processes in the paint medium cannot be corrected by exclusion of the pigment peaks from the data sets before DA. Some peaks in this table overlap with mass peaks that contain information on the binding medium and therefore deletion of these peaks from the mass spectra leads to loss of information that is used for the determination of the degree of chemical change by DA.

The lead white pigment catalyses oxidative and hydrolytic processes in the binding medium, leading to a high degree of chemical change for the cured lead white pigmented film compared with a cured unpigmented tempera. This is observed to an even greater extent in the Naples yellow tempera. In the case of the lead chromate pigmented tempera the oxidative changes are the most extreme and the peaks of the cholesterol and glycerolipid oxidation products are more intense than those of the material from which they originate. Unaltered cholesterol (m/z 386) is still observed, however. Relative intensities in that mass window (m/z 384-396) indicate that contributions from $PbCr_2O_5$ to the intensity of the cholesterol peak are negligible. Light ageing of the lead salt pigmented temperas leads to further oxidation of the cholesterol and mastic components and depletion of the unsaturated glycerolipids. Also an increase in the intensity of the free unsaturated palmitic and stearic acid is observed. Despite the interference of the vast number of pigment peaks, these effects of light ageing can be identified in the lead chromate tempera paint system by comparison of the 64-day light-aged lead chromate tempera (**Figure 16B**) with its control (**Figure 16A**). Exposure to air pollutants appears to mainly affect the glycerolipids in the lead white paint by oxidation and hydrolysis and has a minor effect on the cholesterol. The Naples yellow tempera test system is relatively sensitive to the air pollutants

and here also the cholesterol is largely affected. Lead chromate tempera appears to be relatively insensitive to air pollution exposure.

Table 3 *Peaks excluded from the lead white, Naples yellow and lead chromate tempera DTMS data.*

Species	m/z *	Peaks excluded	Data set
Sb	121, 123	121, 123	N
Pb	204, 206-208	204, 206-208	N, C, W
PbO	220, 222-224	220, 222-224	C, W
Sb_2	242, 244, 246	242, 244, 246	N
PbCrO	270, 272-278	272-278	C
$PbCrO_2$	286, 288-294	288-294	C
$PbCrO_3$	302, 304-310	304-310	C
$PbCrO_4$	318, 320-326	320-326	C
Sb_3	363, 365, 367, 369	363, 365, 367, 369	N
$PbCr_2O_5$	384, 386, 388-396	388-395	C
Pb_2	408, 410-416	410-416	C
Pb_2O	424, 426-432	426-432	C
Pb_2O_2	440, 442-448	442-448	C, W
Sb_4	484, 486, 488, 490, 492	484, 486, 488, 490, 492	N
Pb_2CrO_3	506, 508, 510-518	510-518	C
Pb_2CrO_4	522, 524, 526-534	526-534	C
Pb_2CrO_5	538, 540, 542-550	542-550	C
$Pb_2Cr_2O_6$	606, 608, 610-620	610-618	C
Pb_3O_2	644, 646-656	648-656	C, W
Pb_3O_3	660, 662-672	664-672	C, W
Pb_3Cr_2O	728, 730, 732-748	736-746	C
$Pb_3Cr_2O_2$	744, 746, 748-764	752-762	C
Pb_4O_4	880, 882-896	886-896	C, W
* isotope (distributions) with negligible contributions not included N = Naples yellow; C = lead chromate; W = lead white			

Dosimetric results

As shown in **Chapter 2.6**, DA detects an important chemical difference between artificial light ageing and field exposure of the lead white tempera test system. This difference was attributed to sensitivity to relative humidity, caused by the presence of the hydroxyl group in the pigment. The results that were obtained with the light ageing series as calibration set are presented here, however, for consistency and because the ranking of the sites does not change when the field sites are used as the training set for DA. For the lead chromate and Naples yellow test systems the field ageing processes were found to be similar to the light ageing

processes, so that the light ageing series could be used for calibration. **Figure 17** shows the degree of chemical change in the lead white, lead chromate and Naples yellow test systems, respectively. The figure confirms the observations discussed above regarding the sensitivity of the test systems towards air pollutant exposure. In contrast to the lead white test system, the Naples yellow and the lead chromate test systems show relatively high scores for the FOM dosimeter. A possible explanation for this observation is that the binding medium is oxidised in a redox reaction with the pigment. It is known that Cr(VI) can be reduced to trivalent chromium by organic compounds. Possibly, Naples yellow plays a similar role in the oxidation of organic compounds, through reduction of Sb(V) to Sb(III). This would indicate that the oxidation of the binding medium during the storage of the field exposure control dosimeter in the anti-corrosive bag has progressed more than during storage in the cryovial used for the light ageing control. Although it can be argued that these paint systems are very sensitive dosimeters, it must be concluded that the stability of the controls of the lead chromate and Naples yellow tempera paint systems in the present study is poor. As stated in **Section 3.2**, this in combination with the low discriminatory power is taken as an indication that these systems (in the present composition) are less useful for the evaluation of the quality of the museum environment.
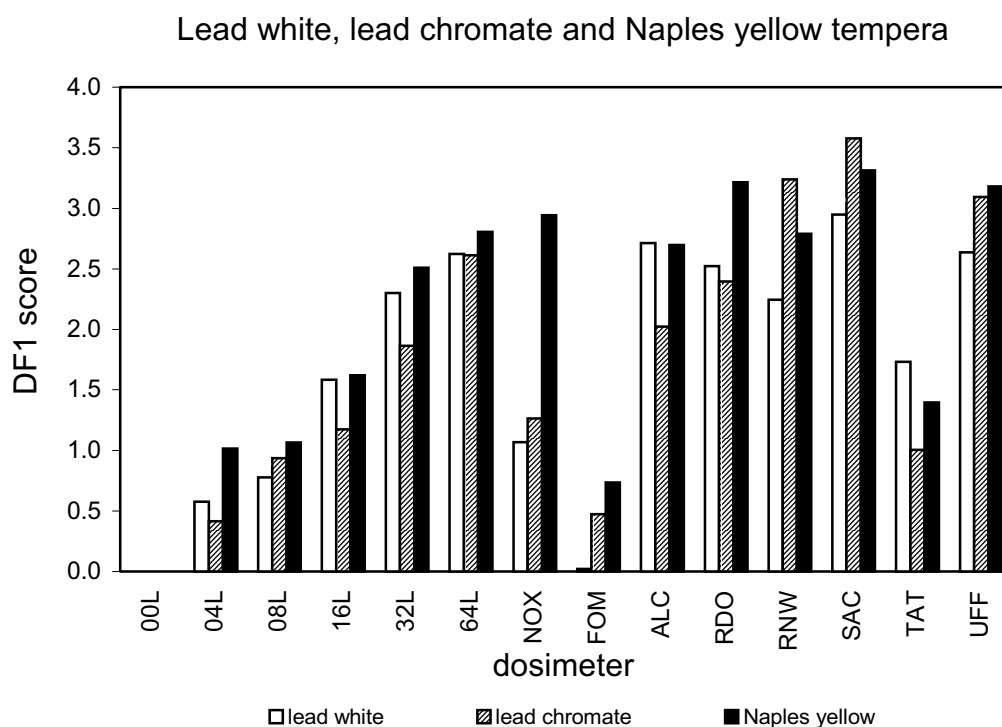
Figure 17 *Scores on the first discriminant function of laboratory-aged and field-exposed lead white, lead chromate and Naples yellow tempera dosimeters.*

The field site results obtained with the lead salt pigmented test systems have a few things in common. Firstly, they all show a light ageing equivalent of more than 64 days for the worst field sites. This is different from the observations on the unpigmented and organic pigmented dosimeters, and is attributed to a higher sensitivity towards (changes in) temperature and relative humidity. Possibly, the electrochemical activity of the chromate is also enhanced by these factors. This may serve as an explanation of the extremely high degrees of chemical change of the worst field sites on the lead chromate tempera test system, compared with that of the light-aged samples. A second common observation is that the degree of chemical change in the TAT exposed dosimeter is the lowest of all field sites for all three systems. As TAT is a very well controlled site regarding temperature and relative humidity, this observation supports the above conjecture on the sensitivity of the test systems towards temperature and relative humidity. Another possible cause of the relatively low score of the TAT dosimeter is that this site is the only one where the inlet air is filtered through carbon filters. The SAC dosimeter consistently shows the highest degree of chemical change of all field sites. It must be noted that care must be taken in drawing conclusions from the differences in degree of chemical change of the field-exposed lead chromate tempera dosimeters as the B/W for this system is very low (5). However, the results obtained with these three lead salt pigmented temperas clearly indicate that the systems display differences in the sensitivity towards specific environmental factors, such as temperature and relative humidity.

3.3.4 Sienna and smalt pigmented tempera

Mass Spectrometry

The DTMS sum spectra of sienna tempera control (A) and 64-day light-aged (B), and smalt tempera control (C) and 64-day light-aged (D) are shown in **Figure 18**. Unlike the lead containing pigments the sienna and smalt pigment give no important interfering peaks upon DTMS analysis. For sienna only a carbon dioxide peak is observed at m/z 44. It is not clear whether this peak originates from carbonate in the pigment or from the binding medium. The smalt shows no interference at all. As the smalt tempera has a low medium content a relatively large quantity of the paint must be coated on the DTMS filament. During the analysis the material is heated to such high temperatures that the glass of the pigment melts and forms a droplet that complicates the analytical process. The smalt was prepared according to traditional methods [19] using potash glass as a

base. SEM-EDX measurements of the smalt used in the tempera paint [1] indicated that silicon, potassium and cobalt are the main elements in the smalt pigment. It was determined by ICP-AES that the pigment contained 7% (w/w) potassium [20]. The presence of relatively large quantities of K in the pigment was confirmed by DTMS, as an intense signal of m/z 39 was observed at high temperatures at the end of the DTMS run.
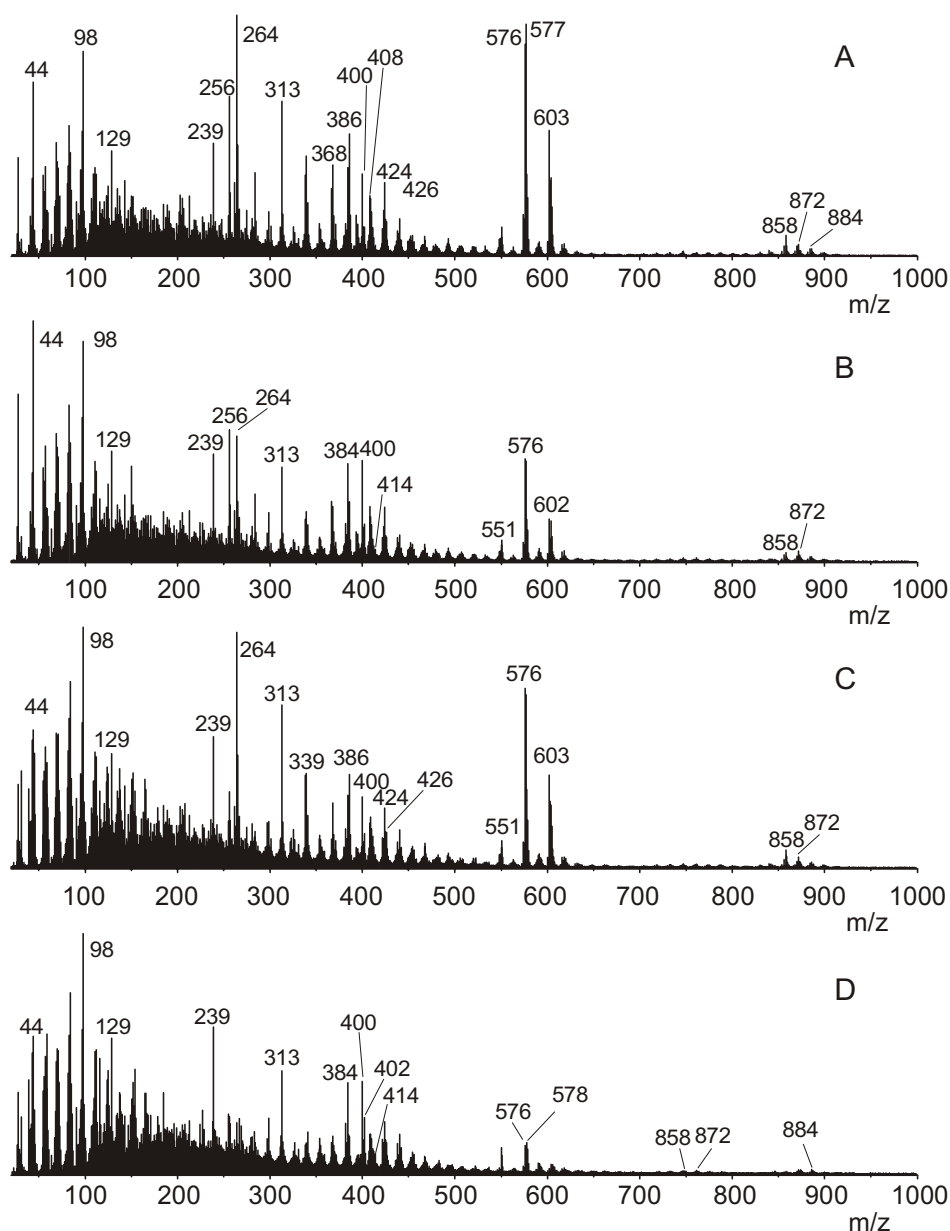
Figure 18 *DTMS summation spectra of sienna tempera control (A) and 64-day light-aged (B), and smalt tempera control (C) and 64-day light-aged (D).*

The mass spectra of unaged sienna and smalt pigmented temperas are well comparable with mass spectra of light-aged unpigmented tempera. Both pigmented temperas give rise to oxidation of the binding medium due to catalytic activity of the iron and cobalt [21] present in sienna and smalt respectively. Both pigmented temperas show almost complete depletion of linoleic acid residues. In the smalt tempera the degree of oxidation of the cholesterol is higher than in the sienna tempera.

Nonetheless, changes can still be observed upon light ageing. The spectra of the 64-day light-aged test systems show that light ageing further oxidises the oleic acid residues and cholesterol, as indicated by a decrease in the relative intensities of the peaks at m/z 264 and m/z 386, and an increase in the cholesterol oxidation products at m/z 384 and m/z 400. The spectra of light-aged sienna tempera indicate that hydrolysis also plays a role in this paint. In both temperas the mastic fraction is further oxidised upon light ageing, as indicated by an increase in the intensity of m/z 414 (marker for 3-oxo-25,26,27-trisnordammarano-24,20-lactone) and m/z 99 (marker for side-chain oxidation of mastic components) and a decrease in the intensity of m/z 408 (28-nor-oleane-17-en-3-one) and m/z 426 (dammaradienol).

Exposure of the sienna tempera to air pollutants leads to progressed depletion of the unsaturated fatty acid residues, to a greater extent than 64-day light ageing. Furthermore, the mass spectrum suggests preferential formation of the cholesterol oxidation products detected at m/z 382 m/z 400. These results promise that the sienna tempera dosimeter is a good indicator of air pollution related damage. The effects on the smalt tempera are less drastic than 64-day light ageing. In contrast to what happens upon exposure of unpigmented tempera to air pollutants, the usual cholesterol oxidation products are formed in smalt pigmented tempera under these conditions. An intense peak is observed at m/z 64 (SO_2). The MT of m/z 64 derived from the analysis of NO_x/SO_2 exposed smalt tempera is shown in **Figure 19**. The figure shows that SO_2 is mainly formed at high temperature at the end of the DTMS run. Hence, it originates from inorganic sulphate formed upon chemical reaction with the pigment.

Dosimetric results

As pointed out in **section 3.2.1**, the smalt tempera displays a poor efficacy, due to its low medium content and behaviour of the pigment during DTMS analysis. The sienna tempera, with a much higher medium content, was found to be very efficacious, i.e. comparable with the unpigmented systems.
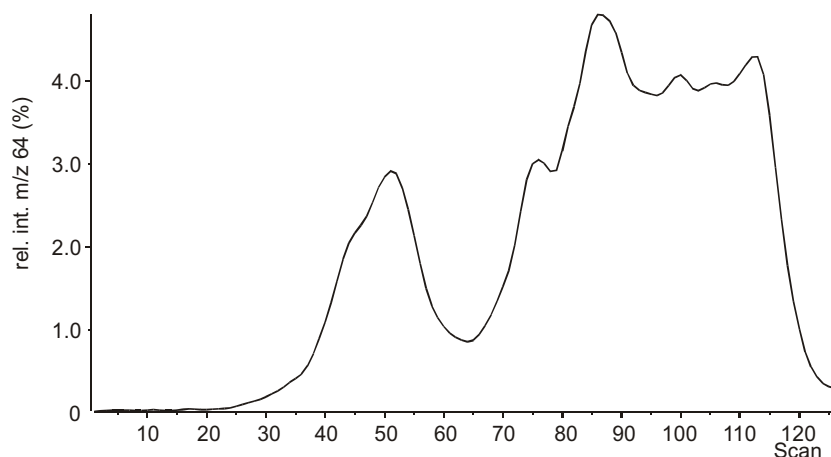
Figure 19 *MT of m/z 64 derived from the DTMS data of NO$_x$/SO$_2$ exposed smalt tempera.*

For the sienna tempera only the second and less important discriminant function (DF-2) discriminates between the light-aged and (most of) the field-exposed dosimeters. The discriminant mass spectrum of DF-2 indicates that hydrolysis of glycerolipids is more important in natural ageing than in the artificial light ageing. This may have been caused by the higher relative humidity during the field exposure. Possibly, the presence of the basic hydroxyl group in the sienna pigment (a mixture of α-goethite, FeOOH, and α-haematite, Fe$_2$O$_3$) plays a role in the acceleration of the hydrolytic processes at higher relative humidity. As the first discriminant function is more important than the second, it is concluded that calibration against the light ageing series is a valid approach. For the smalt tempera no difference was observed between laboratory ageing and field exposure effects.

The degree of chemical change (score on DF-1) for each of the exposed sienna tempera dosimetric test systems is shown in **Figure 20**. The figure confirms the high sensitivity of the test system towards air pollutant exposure. The degree of chemical change of the 21-day thermally aged (21T) dosimeter is higher than that of the 4-day light-aged dosimeter (which shows a small chemical change). This suggests that thermal ageing has a small but extant effect on the chemical composition of the test system and that this effect (partly) compares with light ageing. Thermal ageing for a longer period must be carried out to confirm this.

The Tate Gallery dosimeter shows the smallest chemical change of the field sites and compares with 16 days of light ageing. All other field-exposed dosimeters show a light ageing equivalent of more than 64 days. Thus, the average light ageing equivalent of the field-exposed sienna dosimeters is higher

than for the other tempera test systems. This indicates that other factors than light are very important in the natural ageing process of the sienna tempera test system. The fact that the UFF dosimeter shows the highest change suggests that the air quality in the Uffizi Gallery largely contributes to the ageing process. The conventional data in **Chapter 1** suggest that this is partly caused by the large number of visitors of the relatively small room. In addition, temperature effects may be a cause of the high degree of chemical change in the UFF dosimeter.
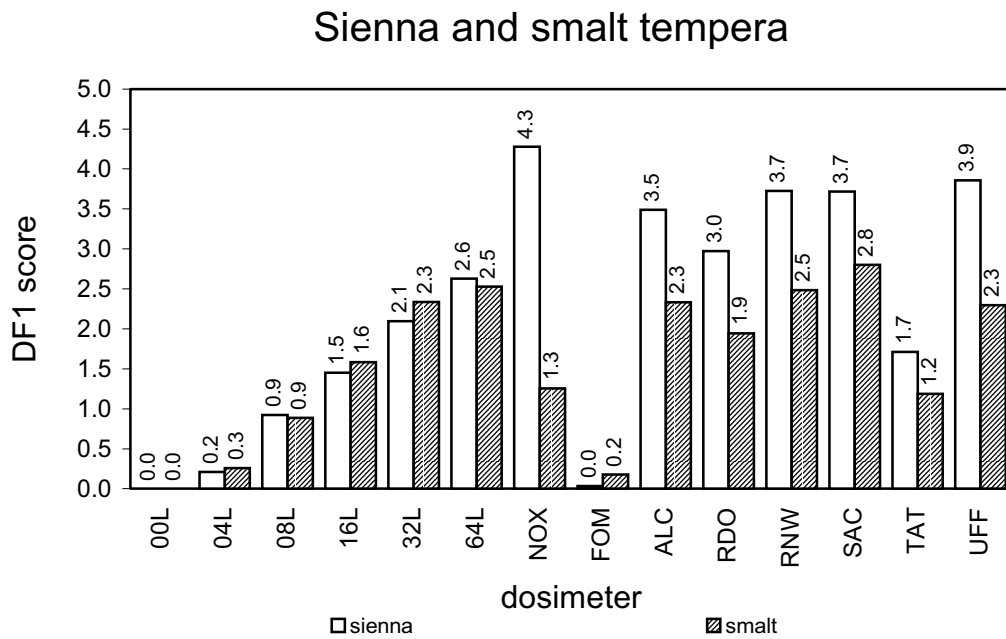
Figure 20 *Scores on the first discriminant function of laboratory-aged and field-exposed sienna and smalt tempera dosimeters.*

The degree of chemical change in the smalt tempera test system is shown in **Figure 20**. Although the discriminatory power (B/W) determined for the light ageing calibration set had a high value of 78, the spread in the scores of the field-exposed dosimeters within each group indicates that the discriminatory power (7) for that set is significantly lower. Hence, conclusions can only be drawn with care. Nonetheless, it is safe to conclude that the exposure in the Tate Gallery once more leads to the smallest chemical change.

3.4 Conclusions and recommendations

The analytical methodology of DTMS followed by DA described in **Chapter 2** was successfully applied to determine the degree of chemical change in the other test systems that were exposed at the field sites.

Although the mass spectra of the pigmented temperas all show peaks that originate from the binding medium, they all differ significantly. This is due to a few effects. In some cases extra peaks that originate from the pigment are observed. These include molecular ions such as those observed for alizarin tempera, or additional fragment peaks, such as observed in the mass spectra of the curcumin tempera. Inorganic pigments can produce metal and metal oxide derived peaks in the DTMS spectra upon pyrolysis. This was observed for the lead white, lead chromate and Naples yellow pigmented temperas. Another cause of difference among mass spectra of different pigmented temperas is catalytic activity of the pigments on the autoxidation of the binding medium in the preparation and curing of the tempera. This leads to differences in degree of oxidation and degree of hydrolysis among the cured unexposed temperas. Partly as a result of these differences in starting point, the various tempera test systems show their specific response to the same environmental conditions.

For each of the tempera paints a correlation between the degree of chemical change and the light ageing time is found. In general, no local minima are observed. Only in the case of the Naples yellow tempera test system the ageing curve shows a local plateau at 8 days of light ageing. Most test systems are insensitive to thermal ageing, only the sienna dosimeter upon 21 days ageing at 60°C shows a small response that is comparable with 4 to 8 days of light ageing. The relative response of the test systems to the air pollutants NO_x and SO_2 differs greatly per test system. The less sensitive tempera paints show a degree of chemical change that is comparable with 8 days of light ageing. The sienna tempera is extremely sensitive, and the degree of chemical change upon air pollutant exposure greatly exceeds that of the 64-day light-aged dosimeter. Moreover, for various test systems the processes that occur upon air pollutant exposure are different from the light-induced changes, and molecular markers can be identified for exposure to NO_x/SO_2 (e.g. m/z 64 or different behaviour of cholesterol).

Mass thermograms (MTs) of peaks in the DTMS spectra provide information on the origin of the ions detected and are as such of great value for the interpretation of the DTMS sum spectra and discriminant mass spectra.

The ancillary use of Direct Temperature-resolved MIKES of peaks in the DTMS spectra of tempera test systems facilitates the interpretation of the DTMS

spectra. MIKES results have shown that the peak at m/z 256 in the DTMS spectra of light-aged alizarin tempera originates from palmitic acid and trihydroxyanthraquinone (oxidation product of alizarin).

The efficacy of the test systems in combination with the applied DTMS and DA methodology for evaluation of the quality of the museum environment was tested. The efficacy test results of the dosimetric test systems show that best results are obtained for the unpigmented tests systems. These test results also show that the high pigment concentrations of the alizarin, curcumin, lead white, sienna and smalt dosimeters have a small negative effect on the efficacy of these test systems but they remain reliable. The lead chromate and Naples yellow pigmented dosimeters give poor test results and fail the efficacy test. The homogeneity of the latter paint systems might be improved by reduction of the pigment grain size and a higher medium concentration. In general an increase in the medium content is assumed to further improve the efficacy of the test systems.

The unpigmented tempera dosimeter is very valuable, in the first place because it responds in a different way compared to the pigmented tempera dosimeters and in the second place because it has a high discriminatory power (indicated by the B/W ratio). Due to the absence of catalytic activity in the curing stage of the unpigmented tempera, the paint is relatively fresh before exposure. Furthermore, light ageing results indicate that this system undergoes significant changes in the early stage of exposure. Hence, it has the potential to be used effectively with shorter museum exposure times. This also applies to the egg-only and alizarin temperas. Results of field exposure of the unpigmented test systems for a shorter period are described in the **next chapter**.

The pigments determine the test system's chemical response to the environmental conditions. As a result, each pigmented test system gives a specific dosimetric result. The comparison of the dosimetric results will be the subject of the **next chapter**.

References

1   Odlyha, M., Cohen, N. S., Foster, G. M., Campana, R., Boon, J.J., Van den Brink, O.F., Peulvé, S., Bacci, M., Picollo, M., and Porcinai, S., 'ERA, Environmental Research for Art Conservation' Final Report for the European Commission. University of London, Birkbeck College (London, U.K.), FOM Institute for Atomic and Molecular Physics (Amsterdam, NL) and Istituto di Ricerca sulle Onde Elettromagnetiche, CNR (Florence, IT), (1999) 210 + xc pp.

2 Cohen, N. S., Odlyha, M., and Campana, R., 'Dosimetry of Paintings: Determination of the degree of chemical change in museum exposed test paintings (lead white tempera) by thermal analysis and infrared spectroscopy.', *Thermochimica Acta* **365** (1-2) (2000) 45-52.

3 Odlyha, M., Cohen, N. S., and Foster, G. M., 'Dosimetry of Paintings: Determination of the degree of chemical change in museum exposed test paintings (smalt tempera) by thermal analysis.', *Thermochimica Acta* **365** (1-2) (2000) 35-44.

4 Boon, J. J., and van der Doelen, G. A., 'Advances in the current understanding of aged dammar and mastic varnishes on the molecular level' in *Varnish - Aesthetics - History*, AdR - Schriftenreihe zur Restaurierung und Grabungstechnik, Herzog Anton Ulrich-Museum und die Arbeitsgemeinschaft der Restauratoren, Braunsweich (1999) 92-103.

5 van der Doelen, G. A., van den Berg, K. J., and Boon, J. J., 'Comparative chromatographic and mass spectrometric studies of triterpenoid varnishes: fresh material and aged samples from paintings', *Studies in Conservation* **43** (1998) 249-264.

6 van den Brink, O. F., 'DTMS of (aged) egg phosphatidylcholines', *unpublished results* (1999).

7 van den Berg, J. D. J., *Analytical Chemical Studies on Traditional Oil Paint*, PhD Thesis, University of Amsterdam (2002, in preparation).

8 Kuksis, A., 'Yolk lipids', *Biochimica et Biophysica Acta* **1124** (1992) 205-222.

9 Noble, R. C., and Moore, J. H., 'Studies on the lipid metabolism of the chick embryo', *Canadian Journal of Biochemistry* **42** (1964) 1729-1741.

10 Van Loon, W. M. G. M., Boon, J. J., and De Groot, B., 'Quantitative analysis of sulfonic acid groups in macromolecular lignosulfonic acids and aquatic humic substnaces by temperature-resolved pyrolysis-mass spectrometry', *Environmental Science and Technology* **27** (1993) 2387-2396.

11 De Santis, F., 'Heterogeneous reactions of SO_2 and NO_2 on carbonaceous surfaces', *Atmospheric Environment* **26A** (16) (1992) 3061-3064.

12 van den Brink, O. F., Peulvé, S., and Boon, J. J., 'Dosimetry of paintings: Chemical changes in test paintings as tools to assess the environmental stress in the museum environment' in *SSCR Conference on Site effects: The impact of location on conservation treatments*, ed. M.M. Wright and I.M.T. Player-Dahnsjö, The Scottish Society for Conservation and Restoration, Edinburgh, Dundee, Scotland (1998) 70-76.

13 van den Brink, O. F., Boon, J. J., O'Connor, P. B., Duursma, M. C., and Heeren, R. M. A., 'Matrix-assisted laser desorption/ionization Fourier transform mass spectrometric analysis of oxygenated triglycerides and phosphatidylcholines in egg tempera paint systems for environmental monitoring of museum conditions', *Journal of Mass Spectrometry* **36** (2001) 479-492.

14   Grosjean, D., Salmon, L. G., and Cass, G. R., 'Fading of Organic Artists' Colorants by Atmospheric Nitric Acid: Reaction Products and Mechanisms', *Environmental Science and Technology* **26** (5) (1992) 952-959.

15   Grosjean, D., Sensharma, D. K., and Cass, G. R., 'Fading of colorants by atmospheric pollutants: mass spectrometry studies', *The Science of the Total Environment* **152** (1994) 125-134.

16   Grosjean, D., Whitmore, P. M., Moor, C. P. D., Cass, G. R., and Druzik, J. R., 'Ozone Fading of Organic Colorants: Products and Mechanism of the Reaction of Ozone with Curcumin', *Environmental Science and Technology* **22** (11) (1988) 1357-1361.

17   Higuchi, T., 'Biosynthesis of lignin' in *Biosynthesis and Biodegradation of Wood Components*, ed. T. Higuchi, Academic Press, Tokyo (1985) 141-160.

18   Wainwright, I. M., Taylor, J. M., and Harley, R. D., 'Lead Antimonate Yellow' in *Artists' Pigments A Handbook of their History and Characteristics*, ed. R.L. Feller, Artists' Pigments, Vol. 1, National Gallery of Art, Washington (1986) 219-254.

19   Mühlethaler, B., and Thissen, J., 'Smalt' in *Artists' Pigments*, ed. A. Roy, Vol. 2, National Gallery of Art and Oxford University Press, Washington (1993) 113-130.

20   Genuit, W.,1996   ICP-AES and ICP-MS of smalt pigments. Amsterdam: Shell Research and Technology Center Amsterdam.

21   Pokorný, J., 'Major Factors Affecting the Autoxidation of Lipids' in *Autoxidation of Unsaturated Lipids*, ed. H.W.-S. Chan, Food Science and Technology, Academic Press, London (1987) 140-206.

4. Dosimetry of the environment in various museums: Interpretation of the results of the field studies

In the **previous chapter** the results of paint-based dosimetry obtained on nine paint systems exposed at five different sites in Europe were presented. The results were shown as bar graphs and shortly discussed. This chapter presents the results in a different way, viz. as ranking of the sites. This allows comparison of the sites and the identification of test systems that show similarities in their response. In a survey performed at nine different sites in the Rijksmuseum (Amsterdam, NL), paint-based dosimeters were exposed for a shorter period than in the European survey. The results of the survey at the Rijksmuseum are reported in section 3 of this chapter. The conclusions of the two surveys are summarised in the fourth section of this chapter.

4.1 Introduction

4.1.1 The nature of the chemical changes observed in paint-based dosimeters

The lipid fraction of the egg tempera binding medium, that consist of egg triglycerides and cholesterol, and triterpenoids from mastic is detected with greatest sensitivity by DTMS. The proteinaceous fraction of the egg is observed as fragments that result from pyrolysis of the proteinaceous macromolecules. DTMS indicates that the inorganic pigments catalyse the oxidation of the lipid fraction as early as the curing stage. Oxidation products are not observed in the cured unpigmented and organic pigmented test systems. Upon light ageing chemical changes in the lipid fraction of the tempera binding medium are observed. An important process is the oxidation of (poly)unsaturated fatty acid residues in glycerolipids. Hydrolysis of the glycerolipids takes place upon light ageing of the unpigmented tempera. Chemically, enhancement of hydrolytic

processes can be related to a higher moisture content and/or higher temperatures. Test systems with inorganic pigments are more sensitive to the effect of relative humidity due to their ability to bind water by direct interaction with the pigment. A process generally observed upon ageing is the oxidation of cholesterol to 7-ketocholesterol, and oxo-cholesterol. The triterpenoids in the mastic fraction undergo specific side-chain oxidation processes upon light exposure.

Exposure to NO_x and SO_2 in the dark for four days leads to similar alteration processes in the lipid fraction, although in some cases differences are observed. Hydrolytic processes, for instance, are more prominent under NO_x/SO_2 conditions; cholesterol on the other hand is less severely oxidised. Furthermore, in some cases NO_x/SO_2 exposure leads to the formation of sulphates or sulphonic acids. On the other hand, in most cases thermal ageing in the dark for up to 21 days does not result in significant changes of the mass spectra.

The degree of chemical change in the light-exposed tempera dosimetric test systems correlates well with the duration of light exposure. The results of field exposure show that the chemical composition of the paint is changed by exposure in museums: significant differences in chemical composition are observed among test systems exposed in different field sites.

The processes that are observed upon field exposure of the test systems are most similar to those occurring upon light ageing, and hence the light ageing sample series was used for calibration of the degree of chemical change. Only in the case of lead white tempera, discriminant analysis detects that the chemical changes occurring upon field exposure differ significantly from those observed upon light ageing. Although the difference is observed in the first discriminant function, this does not lead to a difference in the classification of the field sites. In some other inorganic pigmented test systems the field-exposed dosimeters are distinguished from the light ageing series by the less significant second discriminant function. Enhanced hydrolysis has been identified as one of the reasons that the field exposure processes differ from those occurring during light ageing.

4.1.2 Quantification of the chemical changes in the paint-based dosimeters

The tempera light ageing series were used successfully to calibrate the degree of chemical change in the field-exposed tempera dosimeters. As the light ageing set was used for calibration, the degree of chemical change in the thermally aged test systems and the NO_x/SO_2 exposed test systems can also be expressed in terms of

light ageing equivalents (LAE). In general the thermally aged test systems show a negligible light ageing equivalent, except for the sienna tempera, which displays a low light ageing equivalent of less than 8 days. The test systems are more changed upon exposure to NO_x/SO_2, showing LAEs between a minimum of less than 8 days for lead white and much more than 64 days in the case of sienna. On the basis of the LAEs of the NO_x/SO_2 exposed dosimeters the different test systems can be grouped as follows:

> low sensitivity to NO_x/SO_2 (LAE < 16 days):
> > lead white, alizarin, and smalt
> medium sensitivity to NO_x/SO_2 (16 < LAE < 32 days):
> > unpigmented, lead chromate, and egg only
> high sensitivity to NO_x/SO_2 (LAE > 32 days):
> > curcumin, Naples yellow, and sienna (extremely)

4.2 Paint-based dosimetry at five European museums

4.2.1 Summary of the dosimetric results

In the **previous chapter** average (n=3) values of the degree of chemical change were presented, and the significance of differences in degree of chemical change was shortly discussed in terms of discriminatory power of the dosimetric results. As the nature of the chemical change in the test systems differs from test system to test system, direct comparison of the degree of chemical change (score on the first discriminant function) is not useful. Therefore, in this summary the ranking order of the exposure sites is given per test system. The presentation of the ranking order takes into account the significance of the difference in degree of chemical change. Sites are given the same rank when the ranges of scores of triplicate measurements partly overlap. Such overlap can be caused by either a low discriminatory power of the dosimeter or a high degree of similarity in chemical composition of the test system after exposure in the sites.

Table 1 summarises the ranking results that have been obtained with each of the field-exposed tempera dosimeters. The ranking position of a site is given as a number between one (least chemical change) and six (largest chemical change). In the case of overlap more than one rank number is given. For

comparison, the degree of chemical change of the 64-day light-aged sample is given in the second column of the table. In order to provide an indication of the sensitivity of a test system towards NO_x/SO_2 exposure, the degree of chemical change in the dosimeter that was exposed to these gasses is expressed as LAE and shown in the third column of the table. In some cases the degree of chemical change in a field-exposed dosimeter or in a NO_x/SO_2 exposed dosimeter exceeded that of the 64-day light-aged dosimeter. These cases are highlighted as bold in **Table 1**.

Table 1 *Ranking of the exposure sites based on the dosimetric results obtained by DTMS.*

Test system	64L dcc[*]	NOX LAE[†] (dcc)	ALC rank (dcc)	RDO rank (dcc)	RNW rank (dcc)	SAC rank (dcc)	TAT rank (dcc)	UFF rank (dcc)
Egg-only	2.4	32 (2.19)	6 (2.11)	1 (1.78)	5 (2.01)	4 (1.96)	2 (1.83)	3 (1.87)
Unpigmented	2.95	>16 (2.11)	6 (2.43)	2=3 (2.10)	4 (2.23)	5 (2.37)	2=3 (2.11)	1 (2.04)
Alizarin	2.8	<16 (2.1)	3 (1.5)	1=2 (1.3)	4 (1.5)	6 (1.8)	5 (1.6)	1=2 (1.3)
Curcumin	2.9	<64 (2.6)	3=4=5 (2.0)	1 (1.5)	2 (1.8)	3=4=5 (2.1)	3=4=5 (2.1)	6 (2.2)
Lead white	2.6	>8 (1.1)	**4=5** **(2.7)**	3 (2.5)	2 (2.2)	**6** **(2.9)**	1 (1.7)	4=5 (2.6)
Sienna	2.6	**>>64** **(4.3)**	**3** **(3.5)**	**2** **(3.0)**	**4=5** **(3.7)**	**4=5** **(3.7)**	1 (1.7)	**6** **(3.9)**
Smalt	2.5	<16 (1.3)	3=4=5 (2.3)	2 (1.9)	3=4=5 (2.5)	**6** **(2.8)**	1 (1.2)	3=4=5 (2.3)
Lead chromate	2.6	>16 (1.3)	2=3 (2.0)	2=3 (2.4)	**4=5=6** **(3.2)**	**4=5=6** **(3.6)**	1 (1.0)	**4=5=6** **(3.1)**
Naples yellow	2.8	**>64** **(2.9)**	2=3 (2.7)	**4=5=6** **(3.2)**	2=3 (2.8)	**4=5=6** **(3.3)**	1 (1.4)	**4=5=6** **(3.2)**
[*] dcc = degree of chemical change (A.U.); [†] LAE = light ageing equivalent (days) **bold** = value exceeds that of the 64-day light-aged dosimeter.								

4.2.2 Interpretation of the dosimetric ranking results

The dosimetric results obtained with the field-exposed dosimeters can be divided into two groups. The first group is those of the unpigmented and organic pigmented temperas, of which the field-exposed dosimeters all show degrees of chemical change that fall within the light ageing calibration set. The second

group is that of the inorganic pigment temperas, where the dosimeters exposed at the "worst" sites show degrees of chemical change, which exceed the dynamic range of the light ageing calibration set (i.e. the degree of chemical change in the 64-day light-aged sample).

A few general observations can be made that apply to each of the exposed test systems. Firstly, the degree of chemical change observed in the dosimeters that were exposed at the Rijksmuseum Depot "Oost" strongly suggests that environmental factors other than light contribute to chemical changes in the dosimeters that were exposed at this site. The high ΔR value of the RDO exposed glass sensor, which measures the corrosion of glass (**Chapter 1, Table 1**), supports the hypothesis that the air quality induces the chemical change in the Depot "Oost" dosimeters. Further investigation is necessary to determine which factor at the Rijksmuseum leads to these severe changes in the chemical composition of the test systems. The RDO was also included as one of the sites in the 3-months survey at the Rijksmuseum (*vide infra*). Second, there is a general observation that the dosimeters exposed at the uncontrolled environments of the Alcázar and Sandham Chapel classify among those with the largest chemical change. Clearly, many factors are present in these uncontrolled environments that may lead to accelerated degradation. Firstly, the relative humidity and temperature fluctuate strongly. Then, the light intensity is not in agreement with museum standards and, possibly more importantly, the intensity of UV light may be considerably higher than in the controlled museum sites.

The dosimeters of the unpigmented and organic pigmented temperas that have been exposed in the Depot "Oost" of the Rijksmuseum all rank among those with the lowest degree of chemical change compared with the dosimeters of the same test systems that were exposed at the other field sites. This is probably due to the fact that the Depot is a dark site. Thus the results suggest that light intensity is an additional important factor in the deterioration of the unpigmented and organic pigmented test systems.

The observation on the inorganic pigmented temperas that the degree of chemical change in the dosimeters exposed at the "worst" sites exceed the light ageing calibration set immediately addresses the question of the validity of the reciprocity principle for light ageing. Often, in the inorganic pigmented systems, hydrolysis is identified as an important component of the light ageing process. In some of the test systems enhanced hydrolysis has been identified as one of the reasons that the field exposure processes differ from those occurring during light ageing. Chemically, enhancement of hydrolytic processes can be related to a higher moisture content and/or higher temperatures. Test systems with inorganic pigments are more sensitive to the effect of relative humidity due to their ability to bind water by direct interaction with the pigment.

The consistent observation on the field-exposed inorganic pigment temperas that the Tate Gallery dosimeter classifies as the one with the smallest degree of chemical change confirms the above line of reasoning. As shown in **Chapter 1**, the Tate Gallery (Clore Gallery) is the best-controlled site regarding temperature and relative humidity. Not only the average humidity during exposure but also the fluctuations in relative humidity and temperature are thought by repeated expansion and shrinkage to influence the craquelure formation and hence accessibility of the paint for reactive species. SEM results [1] showed that crack formation plays a role in the tempera test systems. Light intensities in the Rijksmuseum Nightwatch room and the Uffizi Gallery are equal to or lower than those in the Tate Gallery. However, they have less well controlled relative humidity and temperature. This may explain the higher degree of chemical change in the RNW and UFF exposed dosimeters. Another cause of the difference observed may be that the Tate Gallery is the only site where the inlet air for the air conditioning system is filtered through carbon filters to remove air pollutants. Furthermore, the number of visitors in the Clore Gallery (Tate Gallery) is considerably lower than in the Uffizi Gallery and the Rijksmuseum Nightwatch room. Supporting evidence that the air quality plays an important role in the deterioration of the dosimeters comes from the comparison of the results obtained on the respective field-exposed inorganic dosimeters. The number of field-exposed dosimeters which score a light ageing equivalent of more than 64 days varies strongly among the inorganic pigmented test systems. In fact the number of sites that have an LAE higher than 64 days seems to correlate with the sensitivity of the test system towards NO_x/SO_2. In the case of the test systems which show a low sensitivity to NO_x/SO_2, viz. the lead white and smalt temperas, the number of field-exposed dosimeters that have an LAE of more than 64 days is small compared to the sensitive Naples yellow and sienna temperas. Clearly, further research and comparison of dosimetric results with conventional environmental data is necessary to resolve this question. The following section presents results of a survey at nine sites in the Rijksmuseum, which included an attempt to address the effect of the museum air quality on the dosimeters.

4.3 Paint-based dosimetry at nine sites in the Rijksmuseum

4.3.1 Introduction

The rationale behind a survey of nine different sites at the Rijksmuseum was twofold. First, as discussed above, the results of the field study at the five European sites indicated that the degree of chemical change in the dosimeters exposed in the Rijksmuseum was much higher than expected. The staff of the Rijksmuseum suggested as explanation that the climate in some rooms in the museum, viz. the older part of the building, could be of worse quality than the air in the newer part of the building. Hence, a new survey was planned at the request of Dr. A. Wallert and H. Kat of the Rijksmuseum Conservation Department. In this survey sensors were exposed in the older as well as in the newer part of the museum. Secondly, as the effects of nine months' exposure were already severe, shorter exposure of the mock paintings was thought to be advantageous and could lead to enhancement of the differences in degree of chemical change among the sites. Therefore, the dosimetric mock paintings in the new survey were exposed for a period of 3 months (97 days).

4.3.2 Description of the exposure sites and monitor design

The nine exposure sites in the Rijksmuseum are described in **Box 1**. At two of the sites, i.e. the Library and the Nightwatch room, two mock paintings were exposed, one unshielded and one shielded from the light, in order to assess the effect of the air composition.

The exposed mock paintings consisted of 4 dosimetric test strips of egg tempera paint on Melinex, of which one was unpigmented, another one was pigmented with alizarin, and two were pigmented with the inorganic pigments azurite and lead chromate. The strips were cut from the same batch of tempera paint as the ones used for the first field study, and hence had identical composition. Their dimensions were 9 x 25 mm (azurite and unpigmented) and 9 x 35 mm (lead chromate and alizarin). They were attached to the same black polymer support material as used in the first set of test systems. Selection of the temperas was based on availability of spare material that was not consumed in laboratory testing and field exposure. **Figure 1** shows one of the mock paintings exposed in the study collection of the Rijksmuseum.

Box 1 *Description of the nine exposure sites in the Rijksmuseum.*

1. Office Dr. Arie Wallert in "Villa" (OVI), no air, dosimeter placed in window sill facing outside.

2. "Villadepot" (RDV), rack 315, independent air-conditioning, RH and T controlled, very low light intensity, (dark)

3. Depot "Oost" (RDO), in old building, rack 235, same site as in previous exposure, controlled by defensors light intensity very low (2-12 lux)

4. Depot "Zuid" (RDZ), in newer South wing, rack 515, independent air-conditioning RH & T control, very low light intensity (dark)

5. Study room (STU), old building, next to Tüchlein by Pordenone, central air-conditioning, big room, artificial light (UV filtered TLs).

6. Library (Lib), in old building, upper walkway. One dosimeter exposed to the light (Lib L) and one shielded from the light (Lib D). No air-conditioning, combined artificial and daylight.

7. Department Textilia (TEX), in newer South wing, Gallery of hats, behind painting of Mrs.Jannink-Veraguth. Fully controlled RH & T, moderate museum lighting.

8. Nightwatch room (NW), old building, behind painting by Sandrart, same site as in previous exposure. One dosimeter exposed to the light (NW L) and one shielded from the light (NW D). Central air-conditioning, controlled RH and T, normal museum lighting intensity.

9. Room 205, old building (205), horizontally placed above a painting by Van Heemskerk. The light intensity is higher than in the Nightwatch room.

4.3.3 Results

After exposure, the unpigmented tempera test strips were analysed according to the methodology described in **Chapter 2**. **Figure 2** shows the results obtained for the unpigmented tempera dosimeters. The degree of chemical change in the 16-day light-aged unpigmented tempera sample is also shown in this figure for reference. The difference in degree of chemical change between the NW L and the RDO exposed dosimeter in this assay is larger than in the assay with 9 months' exposure time. This supports the notion in **Chapter 3** that a better discrimination can be obtained with the unpigmented tempera test system when shorter exposure times are used. The results clearly indicate that there is a large
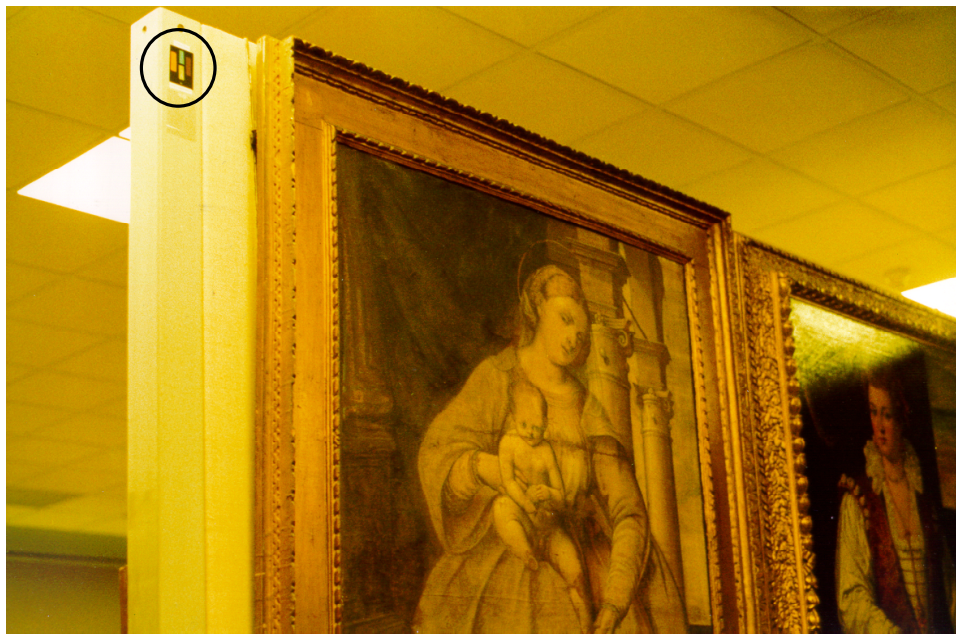
Figure 1 *Exposure of a test system in the Rijksmuseum study room close to a Tüchlein by G.A. Pordenone. The circle indicates the dosimeter.*

difference in quality among the depots. Exposure in the Villa depot (RDV) leads to largest chemical change observed for the depots, and the Depot Zuid (RDZ) leads to the lowest degree of chemical change.

Differences between dosimeters that have been exposed in the exhibition rooms are less pronounced. The dosimeter exposed in the department Textilia (TEX), which is located in the newer South wing of the building shows the smallest degree of chemical change. Together with the result obtained on the RDZ dosimeter, this is interpreted as an indication that there is a difference in the quality of the museum conditions between the older part of the building and the South wing. The dosimeter exposed in room 205 shows the largest degree of chemical change of dosimeters exposed in exhibition rooms. This may be caused by the fact that the dosimeter was placed horizontally. Visual inspection of the dosimeter by microscopy revealed that it had collected dust on the surface. The dust may have acted as a catalyst of the deterioration processes and thus may have led to the high degree of chemical change.

The degree of chemical change observed in the dark exposed dosimeters from the Nightwatch room (NW L) and the Library (Lib L) is very small. This indicates that either the activation by light plays a decisive role in the ageing processes or that the design of the box for light shielding hampers the free flow of air and hence understates the influence of the air quality on the chemical composition of the test system. Additional experiments are required to resolve this matter.

Unpigmented tempera
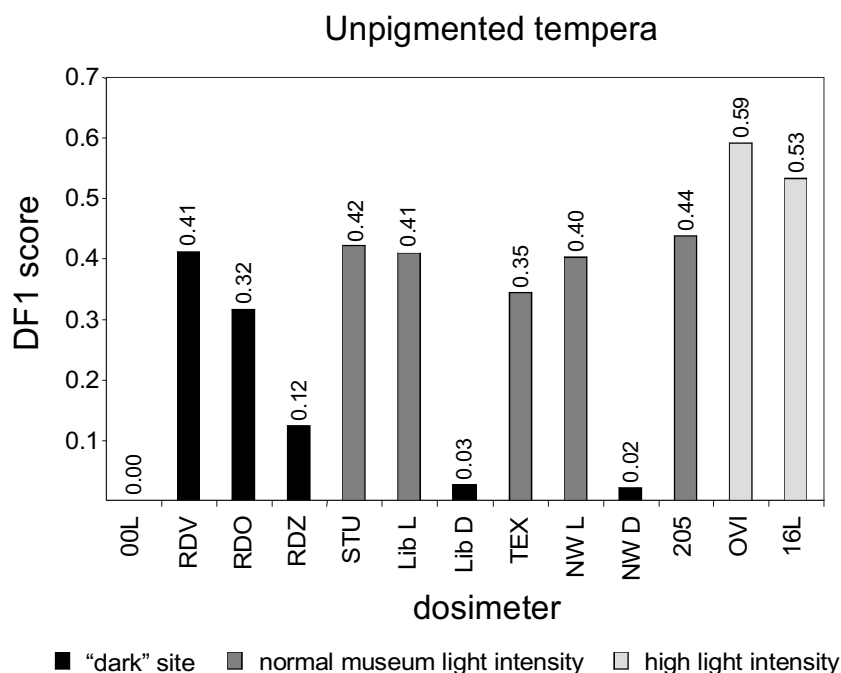
Figure 2 *Scores on the first discriminant function for unpigmented tempera dosimeters exposed in the field study at the Rijksmuseum.*

As expected the sensor exposed in the uncontrolled Villa office (OVI) shows the highest degree of chemical change. It plots higher than the 16-day light-aged unpigmented tempera. There are many factors that can explain this high score. First, the light intensity in the windowsill can be very high on sunny days and the sensor may even be exposed to direct sunlight through glass. Hence, the high UV intensity may also have lead to extreme ageing in this test system. In addition, the relative humidity and temperature in the room are not controlled.

4.4 Conclusions of the two dosimetric field studies

4.4.1 European survey

The controlled museum environments have less affected the chemical composition of lipid components of the egg tempera dosimetric test systems compared with the uncontrolled museum environments.

The Tate Gallery exposure site, which has the best-controlled relative humidity and temperature and uses carbon filters for the inlet of the air-

conditioning system, shows the smallest degree of chemical change in the inorganic pigmented temperas.

There are strong indications that the air quality plays an important role in the environmentally induced chemical change in the paint-based dosimeters.

The test systems that do not contain inorganic pigments, viz. alizarin, curcumin, unpigmented and egg-only tempera, display a higher relative sensitivity to light (dosage) than the inorganic-pigmented temperas.

4.4.2 Rijksmuseum survey

Exposure of unpigmented tempera paint-based dosimeters for a shorter period than in the first field study also results in a good differentiation among the exposure sites. Moreover, the difference between the two sites that were also included in the first field study were enhanced upon reduction of the exposure period. Given the high degree of chemical change in the inorganic pigmented dosimeters that were exposed for nine months in the first field study, it is expected that short-term exposure of these test systems will also give good results.

The results obtained in the survey confirm the notion of a difference in the quality of the museum environment between the older part of the Rijksmuseum and the newer South wing.

Reference

1   Odlyha, M., Cohen, N. S., Foster, G. M., Campana, R., Boon, J.J., Van den Brink, O.F., Peulvé, S., Bacci, M., Picollo, M., and Porcinai, S., 'ERA, Environmental Research for Art Conservation' Final Report for the European Commission. University of London, Birkbeck College (London, U.K.), FOM Institute for Atomic and Molecular Physics (Amsterdam, NL) and Istituto di Ricerca sulle Onde Elettromagnetiche, CNR (Florence, IT), (1999) 210 + xc pp.

5. Cholesterol oxidation products in light-aged egg tempera

Cholesterol constitutes about 5% of the lipid fraction of eggs. The question whether cholesterol is a stable compound in egg tempera dosimeters is addressed in this chapter. Earlier, we have indicated in **Chapter 2** that cholesterol oxidises in egg tempera paint under the conditions of light exposure, which makes it an important marker for dosimetry. Further evidence is provided here to support the assignments of characteristic mass peaks to specific cholesterol oxidation products (COPs). The idea that cholesterol might be a marker for egg tempera paint [1] is challenged.

5.1 Introduction

The oxidation of cholesterol in the human body has been studied extensively in relation to atherosclerosis and cancer. A great variety of tens of COPs has been identified in an even greater number of different materials [2, 3]. These include compounds that are formed in the very early stage of oxidation (cholesterol hydroperoxides) as well as more stable oxidation products. A strongly preferred position for the autoxidation of cholesterol is the 7-position (see Scheme 1 for the numbering of the carbon atoms in cholesterol). The initiation of the autoxidation reaction involves the formation of a carbon-centred allylic C-7 radical, which reacts with molecular oxygen and subsequently abstracts a hydrogen, leading to the formation of 7-hydroperoxycholesterol. This compound can then react to 3-hydroxycholest-5-en-7-one and cholest-5-ene-3,7-diol, which are known as the major autoxidation products of cholesterol. Other positions in cholesterol which are sensitive to oxidation include C-20 and C-25.

The (classical) methodology for the determination of COPs in complex matrices involves extraction followed by thin-layer chromatography (TLC) or derivatisation and gas chromatography (GC). Although exposure to alkaline conditions of the samples before analysis leads to breakdown and hence to a lower recovery of some of the COPs [4-6], saponification has been performed by some researchers to also assess the oxidation of cholesteryl esters. Luby *et al.* [7]

for instance have used TLC for the separation of cholesterol and COPs in saponified butter extracts. Nam *et al.* [8] have determined a variety of COPs in raw meat using trimethylsilyl derivatisation and GC. Efforts are also made to devise a methodology for rapid and economical analysis of COPs in blood using TLC without as well as in combination with silylation [9].

The presence of COPs in eggs and egg products has been investigated by a number of groups since the 1960s. A review article about the analysis and the biological effects of sterol oxides in foodstuffs has appeared in 1983 [10]. The COPs identified in spray-dried or air-exposed egg yolk the aforementioned major products as well as cholestane-3,5,6-triol, and 5,6-epoxycholestan-3-ol [6, 11]. The latter is reported to derive from cholesterol by reaction with 7-hydroperoxycholesterol or with the hydroxyl radical (OH•) [2]. Some researchers have investigated the prerequisites for the formation of epoxy-cholestanols during spray-drying [12]. Lai *et al.* [13] have identified the presence of NO_x as an important factor in the rapid formation of COPs in gas-fired spray-driers. Tsai and Hudson [5] used high-performance liquid chromatography (HPLC) for the isolation of epoxy-cholestanols from egg powders. In their research MS, NMR and IR spectroscopy were used for identification of the compounds.

Employing extraction, liquid chromatography pre-separation and derivatisation GC, Van de Bovenkamp *et al.* [4] have determined the presence of 7-hydroxycholesterol, 7-keto-cholesterol and 5,6-epoxy-cholesterol at the sub-µg/g-level in fresh egg yolk. Yang and Chen [14] have used TLC and derivatisation-GC for the determination of COPs in a selection of Chinese egg products. They found that between 1 and 2% of the cholesterol was transformed to 7-β-hydroxycholesterol and 20-hydroxycholesterol by various methods of processing of the eggs.

Kim and Nawar [15] have shown that the rates of cholesterol oxidation in model systems that contain different triacylglycerols vary strongly and that interpretation of the observations is very difficult. It is not the purpose of this chapter to resolve issues of reaction mechanisms and kinetics of cholesterol oxidation in the egg tempera binding medium. Instead, it is our intention to identify marker peaks indicative for cholesterol oxidation products traced by the DTMS-DA methodology. The possibilities for assignment of the marker peaks will be discussed first. Experimental data from DTMSMS of standards and egg tempera paint will be presented subsequently. The spectra will be compared and discussed in the light of mass spectral data on sterols reported in the literature.

5.2 Experimental

5.2.1 Egg tempera samples

For the MSMS and derivatisation experiments on light-aged egg-only tempera a sample of the unexposed egg-only tempera on Melinex (prepared as described in **Chapter 1**) was exposed to elevated levels of visible light in the MOLART light ageing facility at the Limburg Conservation Institute (SRAL) in Maastricht, The Netherlands. The ageing facility uses 12 Philips TLD-36W/96 fluorescent daylight tubes to illuminate a surface of 1.2 m^2. The resulting light intensity during the 21 days' exposure of the egg-only tempera sample was 10,200 lx. Perspex (PMMA) filters were used to absorb most of the already low intensities of UV radiation produced by the fluorescent lights. Because the light ageing facility is placed in an air-conditioned room, the temperature and relative humidity could be maintained constant at values of 22°C and 40-44%, respectively.

5.2.2 Reference compounds

Cholesta-4,6-diene-3-one, 5-cholesten-3-one, 5-cholesten-3β-ol (cholesterol), 5-cholesten-3β-ol-7-one, 5β,6β-epoxycholestan-3β-ol, and 5-cholestene-3β,7β-diol were obtained from Sigma-Aldrich Chemie (Steinheim, Germany).

5.2.3 Trimethylsilyl derivatisation

A dichloromethane : ethanol (7:3, v/v) extract of 21-day light-aged egg material were evaporated to dryness in GC auto-injector vials. To the dried extract were added 50 µl per mg sample (weight before extraction) of bis(trimethylsilyl)trifluoroacetamide, containing 1% trimethylchlorosilane (Fluka, Zwijndrecht, The Netherlands) and 50 µl per mg sample (weight before extraction) of pyridine. The reaction vials were flushed with dry nitrogen and placed in an oven at 65°C for 60 minutes. After a subsequent cooling period, the solvent was removed under a gentle stream of dry nitrogen and the residue was redissolved in dichloromethane.

5.2.4 DTMS(MS)

Direct Temperature-resolved Mass Spectrometry (DTMS) was performed as described in the experimental section of **Chapter 2**. DTMSMS experiments were performed on a JEOL JMS-SX/SX 102A four-sector instrument of B/E-B/E geometry (which was kindly made available by Prof. Dr. A.R.J. Heck of the Bijvoet-Institute of Utrecht University before it was acquired by the FOM-Institute for Atomic and Molecular Physics). Ions produced in the ion source with a kinetic energy of 8kV were selected by MS1 (first two sectors of the instrument). They were thus passed through the collision cell, which was at ground potential. Helium was used as collision gas. The gas pressure was set to produce a precursor ion signal intensity of 90% of the initial signal intensity on MS2 (no collision gas). As a result, the pressure in the collision cell was 3.5×10^{-3} mbar.

5.3 Results and Discussion

5.3.1 DTMS analysis

Discriminant analysis of the spectra of the light ageing series of the egg temperas (results shown in **Chapters 2 and 3**) indicated which peaks in the mass spectra of the tempera paints increased and which decreased upon light ageing. The peak at m/z 386 was found to decrease upon light ageing. Peaks in the mass window around cholesterol (i.e. m/z 350-450) that increase in intensity upon light ageing are likely to be alteration (oxidation) products of cholesterol. These include m/z 402 (oxocholesterol), 400 (hydroxycholestenone), 384 (cholestenone) and 382 (dehydration product of hydroxycholestenone). The mass thermograms (MTs) of m/z 384, 386, 400 and 402, derived from the DTMS data of 64-day light-aged egg-only tempera are compared in **Figure 1.** The first peak in the MTs of m/z 384, 400 and 402 (scan number 34) occurs at a higher scan number than that of cholesterol (scan number 30). This is attributed to the higher polarity of the COPs, which causes them to desorb at higher temperatures. At even higher temperatures in the DTMS run other, more abundant and less volatile, material desorbs and pyrolyses, leading to an increase in the signal intensity over a wide mass range. This explains the peaks in the MTs at higher temperatures. It must be noted the low-temperature peaks in the MTs appear in a desorption window
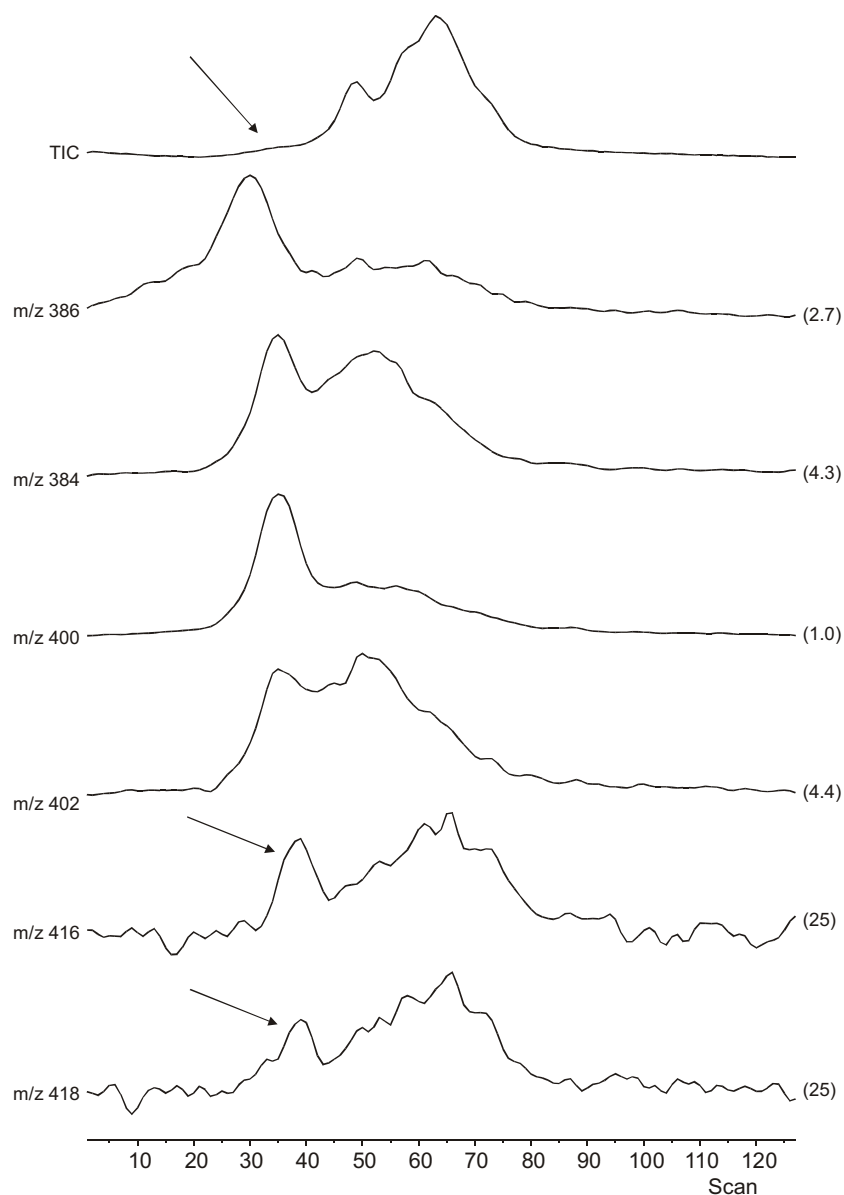
Figure 1 *TIC and MTs of m/z 386, 384, 400, 402, 416 and 418 derived from the DTMS data of 64-day light-aged egg-only tempera. The MTs are normalised to the maximum intensity of m/z 400; the normalisation factors are given in parentheses.*

where the total signal intensity is less than 20% of the maximum (as indicated by the arrow on the total ion current (TIC) trace). **Figure 2** shows the summation mass spectrum of 64-day light-aged egg-only tempera over the desorption window of cholesterol (scans 25-40). This spectrum shows high intensities of the peaks m/z 384, 386 and 400. The peaks labelled with "G" derive from glycerolipids (for assignment see **Chapter 2, Table 1**). The label "BG" indicates a peak that originates from background signal (chemical noise).

Table 1 summarises the possibly cholesterol-related peaks in **Figure 2** and gives their assignment. This table only specifies assignments that seem likely on the basis of the literature on cholesterol oxidation in egg yolk, or in exceptional cases on the basis of pathways of progressed oxidation of egg-yolk COPs. Hydroperoxides are not included in the table, given their presumed short life-time in their chemical matrix and the instability of their molecular ions under EI conditions. A specified (in parentheses) example of the structure of the ion [16] or molecule (A- and B-rings only) mentioned in the second column of **Table 1** is given in the third column of the table. As an aid for the interpretation of the table **Scheme 1** shows the numbering of the cholesterol skeleton.
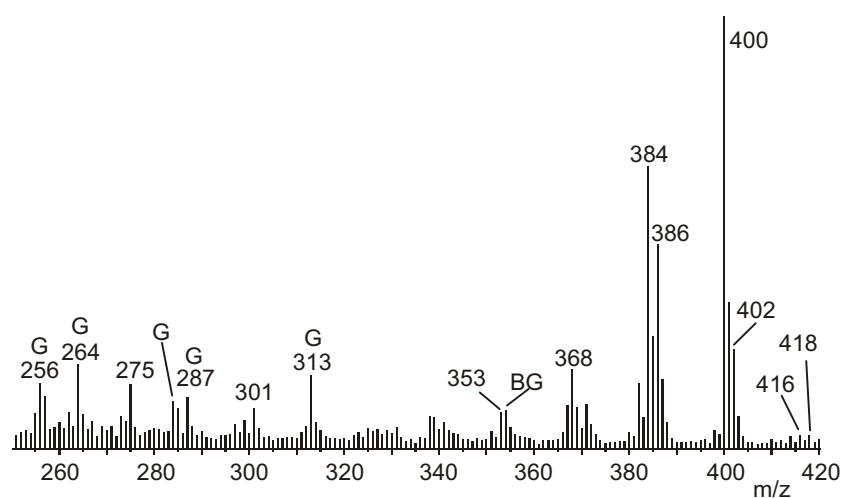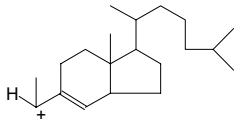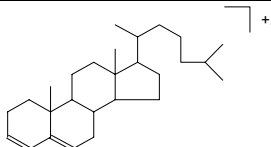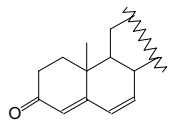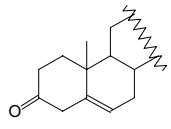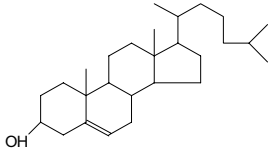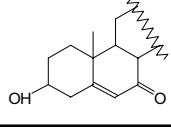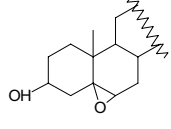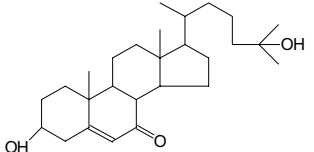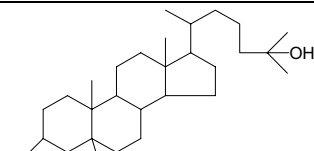
Figure 2 *Partial (m/z 250-420) summation mass spectrum of the cholesterol desorption window (scans 25-40) for 64-day light-aged egg-only tempera. Peaks labelled with G derive from glycerolipids; BG from background (chemical noise).*

The first three peaks listed most probably derive from cholesterol and are assigned as EI fragmentation products. The same applies for the peak at m/z 368, although there are two other possible sources, viz. cholestadiene and a fragment due to loss of a fatty acid neutral from a cholesterol ester molecular ion. The latter is discussed in **Chapter 3**. Cholestadiene is not classified as a COP, but rather as a dehydration or pyrolysis product of cholesterol [2]. DTMS analysis of free cholesterol indicated that the pyrolytic formation of cholestadiene from cholesterol is minimal during the DTMS experiment. Catalytic dehydration in the presence of large amounts of inorganic paint substances, however, cannot be excluded.

Table 1 *Assignment of intense peaks in the summation mass spectrum of the cholesterol desorption window of light-aged tempera.*

m/z	Compound/fragment	Structure of compound / fragment
275	$M^{+\bullet}$-$C_7H_{11}O^\bullet$ (C1-7) from cholesterol	
301	$M^{+\bullet}$-$C_6H_{13}^\bullet$ (C22-27) from cholesterol	
353	$M^{+\bullet}$-(H_2O + $CH_3^\bullet$) from cholesterol	
368	$M^{+\bullet}$-H_2O from cholesterol $M^{+\bullet}$-FA from cholesterylester	
371	$M^{+\bullet}$-$CH_3^\bullet$ from cholesterol	
382	cholestadienone $M^{+\bullet}$-H_2O from cholest-5-en-3-ol-7-one	(cholesta-4,6-dien-3-one)
384	cholestenone $M^{+\bullet}$-H2O from cholest-5-en-diols $M^{+\bullet}$-H2O from 5,6-epoxy-cholestan-3-ol	(cholest-5-en-3-one)
386	Cholesterol (cholest-5-en-3-ol)	
400	3-hydroxycholest-5-en-7-one (7-hydroxycholest-5-en-3-one) $M^{+\bullet}$-H_2O from m/z 418	(cholest-5-en-3-ol-7-one)
402	5,6-epoxy-cholestan-3-ol cholest-5-en-3,7-diol cholest-5-ene-3,20-diol cholest-5-ene-3,25-diol ($M^{+\bullet}$-H_2O from cholestane-3,5,6-triol)	(5,6-epoxy-cholestan-3-ol)
416	3,25-dihydroxycholest-5-en-7-one	
418	5,6-epoxycholestan-3,25-diol 5-cholesten-3,7,25-triol	(5,6-epoxycholestan-3,25-diol)
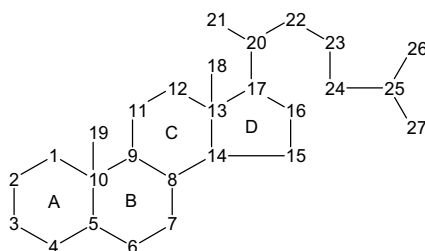
Scheme 1 *Numbering of C-atoms in the cholesterol skeleton.*

On the basis of molecular mass cholestadienone is a suggestion for the peak at m/z 382. Smith [2] has suggested three pathways for the oxidative formation of cholesta-4,6-dien-3-one from cholesterol. One of these involves successive oxidation, isomerisation and dehydration of cholest-5-en-3,7-diol. Another is based on reaction of cholest-5-en-3-one with singlet oxygen ($^1O_2$), and suggests 5-hydroperoxycholest-6-en-3-one as an intermediate. Experiments by Chicoye [6] have indicated that cholest-5-en-3-ol-7-one is transformed to cholesta-3,5-dien-7-one under conditions of saponification (81°C in KOH solution). Thus, in the case of the lead white tempera, the basicity of the lead hydroxy carbonate pigment ($Pb_2(OH)_2CO_3$) may account for the high intensity of the m/z 382 peak in the DTMS spectra of light-aged lead white tempera (see **Chapter 3**). In relation to this it must be remarked that m/z 400 is the highest peak in the cholesterol mass window of the DTMS spectra of lipid extracts of light-aged lead white tempera (data not shown). This indicates that transformation of ketocholesterol to cholestadienone takes place in the desorption process on the DTMS probe.

The peak at m/z 384 may derive from the molecular ion of 5-cholesten-3-one, which can be formed from cholesterol upon reaction with $^3O_2$ [2]. As mentioned before, 3-hydroxycholest-5-en-7-one is another well-known (abundant) COP. Attribution of the peak at m/z 400 to this compound is therefore plausible. The possibililty of a minor contribution from 7-hydroxycholest-5-en-3-one is not excluded as this is one of the structures involved in the aforementioned pathway for the formation of cholesta-4,6-dien-3-one from cholest-5-en-3,7-diol.

Two of the COPs mentioned in the introduction have a molecular weight of 402 Da, viz. 5,6-epoxy-cholestan-3-ol and cholest-5-en-3,7-diol. Clearly, other cholestendiols may also be responsible for the peak at m/z 402. Cholest-5-ene-3,20-diol and cholest-5-ene-3,25-diol have been detected in egg products [17].

If the possibility of multiple oxygenation of cholesterol is taken into account, COPs with molecular weights between 414 and 420Da can be expected. Therefore, extra attention was paid to these masses in **Figure 2**. As a result two of the peaks in this mass window could be tentatively assigned to COPs on the basis of their MTs, viz. m/z 416 and 418. The MTs of these peaks are also shown

in **Figure 1.** The shift of the local maximum of these MTs (marked with arrows) with respect to the maximum of the MTs of m/z 400 and 384 is again attributed to the higher polarity of these compounds as a result of their higher degree of oxygenation. The MTs of the other peaks between m/z 414 and 420 (data not shown) do not show a local maximum in the desorption window of cholesterol. Based on the extensive literature on the oxidation of cholesterol, progressed oxidation can occur. The two most-preferred sites on the sterol skeleton for progressed oxidation are the 7- and the 25-position. Thus, 5,6-epoxycholestan-3,25-diol and 5-cholesten-3,7,25-triol are suggested as the most probable COPs for m/z 418 and 3,25-dihydroxycholest-5-en-7-one for m/z 416. The formation of the latter two products by autoxidation of 5-cholesten-3,25-diol has been suggested by Smith [18]. Similarly, autoxidation of the well-known COP 5-cholesten-3-ol-7-one at the 25-position was suggested to explain the formation of 3,25-dihydroxycholest-5-en-7-one.

As indicated in **Table 1**, loss of water from molecular radical cations is also part of the attribution of the peaks in **Figure 2**. Thus, water loss from the $M^{+\bullet}$ of ketocholesterols can contribute to the intensity of the peak at m/z 382. It must be noted however that the relative intensity of m/z 382 in the 16eV DTMS spectrum of cholest-5-en-3-ol-7-one is less than 20% of the base peak ($M^{+\bullet}$). In the 16eV DTMS spectrum of cholest-5-en-3,7-diol, the $M^{+\bullet}$-H_2O peak (m/z 384) is the base-peak and the molecular ion (m/z 402) shows a relative intensity of 15% (data not shown). It must be assumed that the spectra of other cholestenediols will also show a significant peak at m/z 384. 5,6-Epoxycholestan-3-ol produces $M^{+\bullet}$-H_2O ions at a relative intensity of 20% of the molecular ion (base-peak) and hence will also contribute to the signal intensity at m/z 384.

The ion at m/z 402, in turn, can partly originate from water loss of a COP with molecular weight 420. Cholestane-3,5,6-triol, which is known as a hydration product of 5,6-epoxy-cholestan-3-ol [2] and has been detected in an 8-year old egg yolk sample [17]. Water loss from the molecular ion of this compound is highly probable due to the presence of three hydroxyl groups and may even explain the absence of a peak at m/z 420 in **Figure 2**. Hence, the presence of small quantities of the compound in the light-aged tempera sample cannot be excluded. Because **Figure 2** indicates the presence of COPs with a molecular weight of 418Da, which probably contain more than one hydroxyl-group, fragmentation of the molecular ions of these compounds by loss of water may also partly account for the m/z 400 peak.

5.3.2 DTMSMS of COPs

Although it is evident that m/z 386 originates from cholesterol, it was subjected to DTMSMS analysis as a (matter of) test for the DTMSMS methodology. **Figure 3A** shows the DTMSMS spectrum of peak m/z 386 from sample of 21-day light-aged egg-only tempera. Comparison with the 70 eV electron impact ionisation spectrum of cholesterol (**Figure 3B**) indicates that peak m/z 386 in the DTMS spectra of egg-only tempera can indeed be attributed to cholesterol. Characteristic peaks for the fragmentation of cholesterol are observed in both spectra. These include peaks at m/z 371 ($M^{+\bullet} - CH_3^{\bullet}$), m/z 368 ($M^{+\bullet} - H_2O$), m/z 353 ($M^{+\bullet} - CH_3^{\bullet} - H_2O$), m/z 301 (loss of C22-27), m/z 275 (loss of C1-7) [16, 19], m/z 273 (loss of C20-27 +H), m/z 231 (loss of C16-17+C20-27+H) and m/z 213 (loss of C16-17+C20-27+H+H_2O).
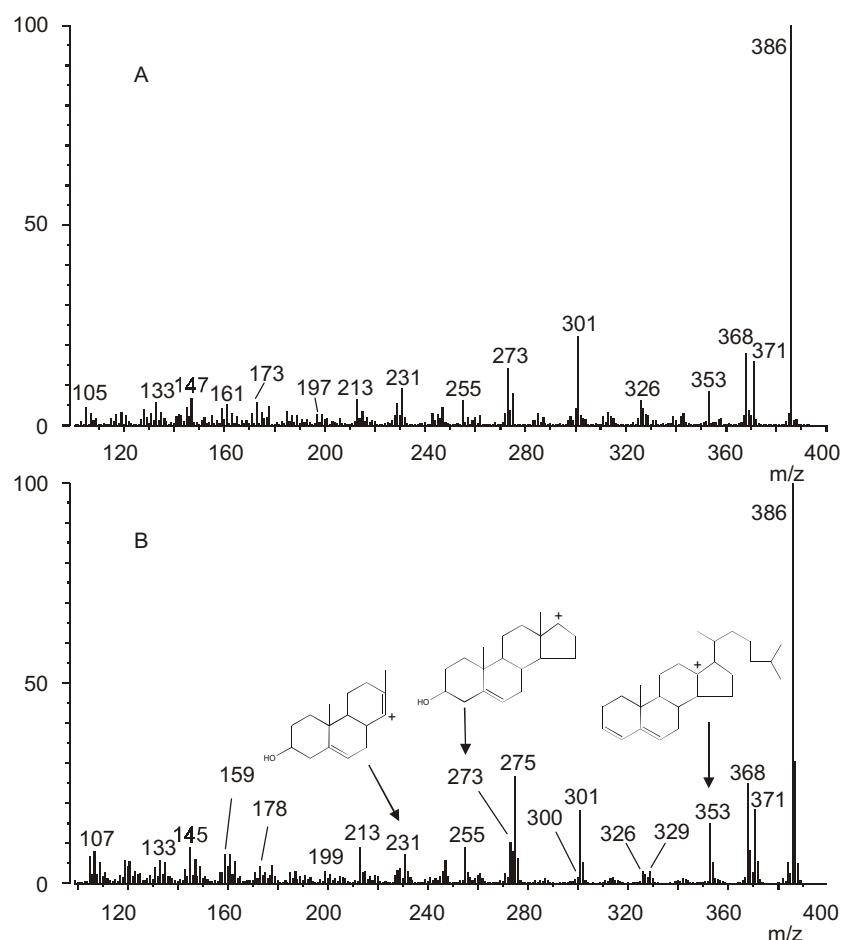
Figure 3 *DTMSMS spectrum of peak m/z 386 from 21-day light-aged egg-only tempera (A) and DTMS spectrum (EI, 70 eV) of cholesterol (B).*

Figure 4A shows the DTMSMS spectrum of the m/z 400 peak from light-aged (21 days at 10,000 lx) egg-only tempera. Comparison of this spectrum with the DTMSMS spectrum of a 5-cholesten-3-ol-7-one standard (**Figure 4B**) shows great similarities. M/z 385 and m/z 382 are attributed to loss of a methyl radical and a water molecule, respectively. The peak at m/z 367 is the combined result of these two fragmentations. Fragmentation at the side chain (bond C17-20) leads to the formation of m/z 287 by loss of a $C_8H_{17}{}^{\bullet}$ radical. The peak at m/z 205 derives from a rearrangement fragmentation in the C-ring, that breaks the bonds C8-14 and C12-13 and involves the transfer of one hydrogen. The same fragmentation combined with the loss of water results in m/z 187. Each of these peaks in the MSMS spectrum of the standard compound is also present in **Figure 4A**. A few peaks in the DTMSMS spectrum of m/z 400 from the light-aged egg-only sample do not appear in the spectrum of the standard compound (e.g. 297 and 315). This suggests that other components must be present in the light-aged tempera, which form ions of m/z 400. Possibly fragment ions with m/z 400 that result from water
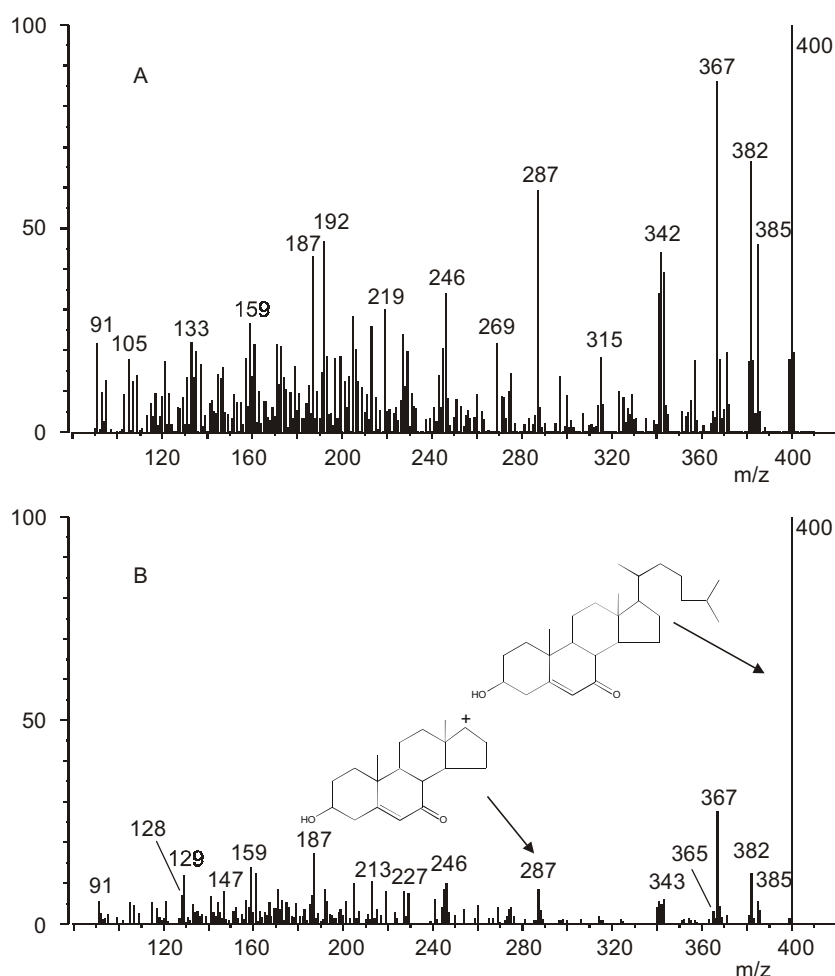
Figure 4 *DTMSMS spectra of peak m/z 400 from 21-day light-aged egg-only tempera (A) and 3-hydroxycholest-5-en-7-one (B).*

loss of COPs with molecular weight 418 Da contribute to the peak. Differences in internal energy of the ions may account for differences in relative intensities of important peaks in the mass spectra. The presence of a peak at m/z 192 in the 70eV EI spectrum of 5-cholesten-3-ol-7-one confirms this notion.
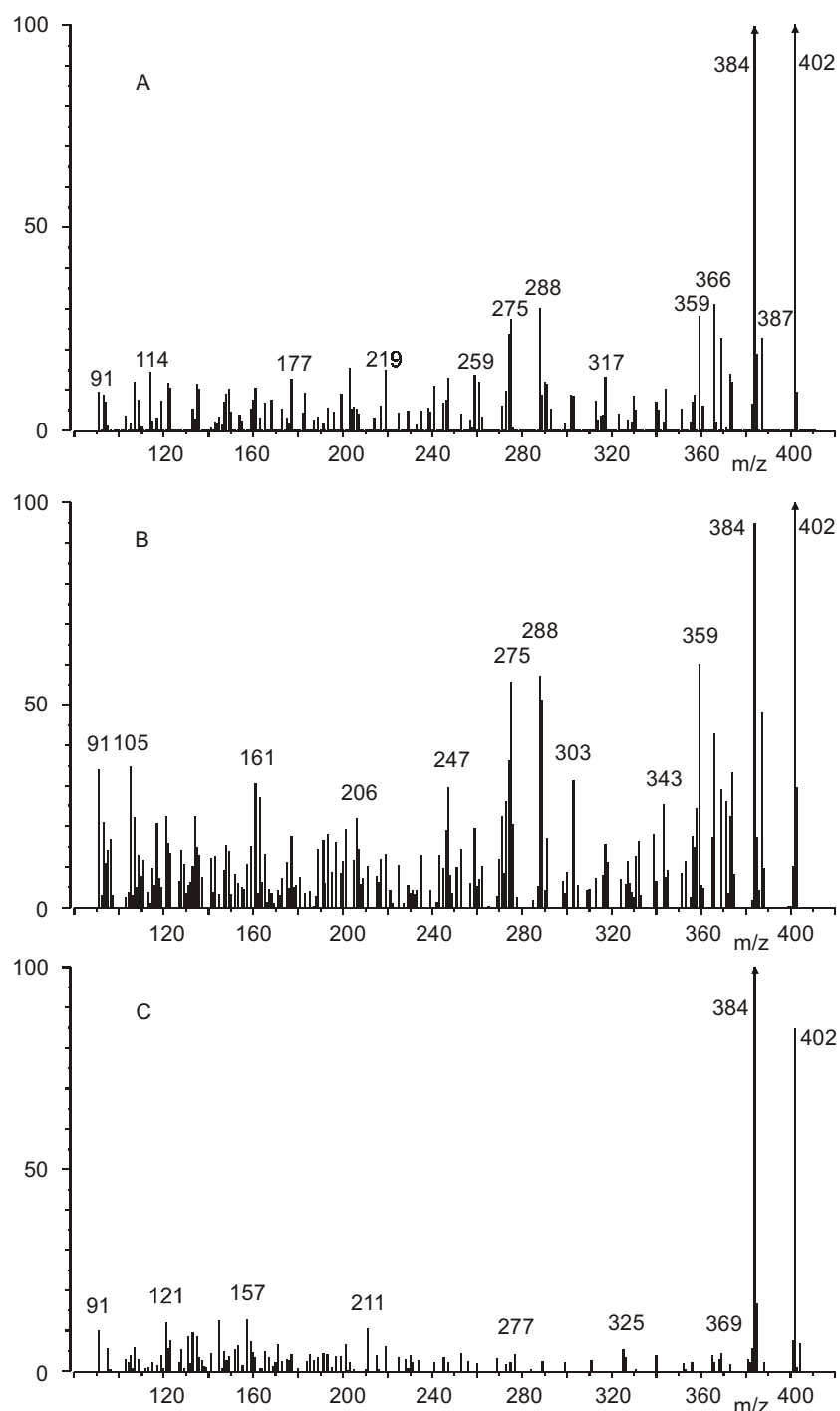
Figure 5 *DTMSMS spectra of peak m/z 402 from 21-day light-aged egg-only tempera (A), 5,6-epoxy-cholestan-3-ol (B) and cholest-5-en-3,7-diol (C).*

The DTMSMS spectrum of peak m/z 402 from the light-aged egg-only tempera sample (21 days) shown in **Figure 5A** closely resembles that of the molecular ion of 5,6-epoxy-cholestan-3-ol shown in **Figure 5B**. Differences between the spectra may derive from a variety of factors. First of all there may be a minor difference in internal energy of the precursor ions. Then, Tsai *et al.* [5] have shown that configurational differences in the structure of 5,6-epoxy-cholestan-3-ol are expressed in the mass spectra. Although discrimination between the two epimers is not possible on the basis of the spectra presented, 5,6-epoxy-cholestan-3-ol is positively identified in the light-aged egg-only tempera. It must be remarked that the 5β,6β-epoxide is thermodynamically more stable than the 5α,6α-epoxide and this is used to explain the higher relative abundance of the β-epoxide [13]. 5,6-Epoxycholesterols are formed upon reaction of cholesterol with active oxygen species such as singlet oxygen ($^1O_2$) and hydroperoxide [18]. The high abundance of 5,6-epoxycholesterols may thus be explained by interaction between cholesterol and hydroperoxide functionalities of (oxidised) egg glycerolipids. As mentioned earlier 5-cholesten-3,7-diol is another likely candidate to (partly) account for the peak m/z 402. The DTMSMS spectrum of the molecular ion of this compound is shown in **Figure 5C**. The lack of specificity of the DTMSMS spectrum and the strong contribution of 5,6-epoxy-cholestan-3-ol to the spectrum in **Figure 5A** do not allow a partial attribution of the peak at m/z 402 to 5-cholesten-3,7-diol. Recall, however that cholest-5-en-3,7-diol shows a relatively small molecular ion peak m/z 402 under 16eV EI conditions. Therefore, the cholest-5-en-3,7-diol will mainly contribute to the intensity at m/z 384.

The MSMS peaks from m/z 384 in the spectra of 5-cholesten-3-one ($M^{+\bullet}$), 5-cholesten-3,7-diol and 5,6-epoxy-cholestan-3-ol (both $M^{+\bullet} - H_2O$) did not allow the unambiguous identification of the structure of the precursor ion.

The question of the identity of the presence of cholestenediols was also investigated by DTMS analysis of trimethylsilyl (TMS) derivatised standards and samples. DTMS analysis of silylated COPs, such as 5-cholesten-3-ol-7-one, 5-cholesten-3-one and 5,6-epoxy-cholestan-3-ol, indicated that epoxy- and keto-functionalities are not silylated. The spectrum of TMS derivatised cholest-5-en-3,7-diol showed a molecular ion at m/z 546 and a base peak at m/z 456, indicating that the loss of trimethylsilanol ($HOSi(CH_3)_3$) is an important feature in the spectra of silylated cholestenediols. The observation of a peak at m/z 546 and an intense peak at m/z 456 in the partial (cholesterol desorption window) DTMS spectrum of the silylated extract of 21-day light-aged egg-only tempera (data not shown) indicate the presence of COPs with two hydroxyl functionalities on a cholestene skeleton in the light-aged sample. Furthermore, in a similar way, the

observation of peaks at m/z 472 and 474 in the same spectrum confirmed the presence of hydroxycholestenone (probably cholest-5-en-3-ol-7-one) and 5,6-epoxy-cholestan-3-ol in the 21-day light-aged egg-only tempera sample.

5.4 Concluding remarks

The results presented show that DTMSMS and the combined use of DTMS with trimethylsilyl derivatisation are useful tools for the characterisation of molecular changes in light-aged egg tempera samples.   Using DTMSMS, 5,6-epoxycholestan-3-ol and 3-hydroxycholest-5-en-7-one were positively identified in light-aged egg tempera binding medium. The former compound is likely to have been formed as a result of interaction between peroxidised glycerolipids and cholesterol. DTMS of trimethylsilyl derivatised light-aged egg-only tempera allowed the identification of cholestenediol. Hence the assignment of cholesterol-related m/z peaks in **Chapter 2** is confirmed and refined. The markers identified are useful in tempera paint-based dosimetry.

As the oxidation of cholesterol develops early in the life-time of egg tempera paint and is accelerated by the presence of inorganic pigments, cholesterol itself is not a good marker for egg as binding medium in paintings. Alternatively, cholesterol oxidation products may be better markers, provided that they survive in the course of time.

References

1   Mills, J. S., and White, R., *The Organic Chemistry of Museum Objects*,   Butterworth-Heinemann Ltd., Oxford (1994) 206 pp.

2   Smith, L. L., *Cholesterol Autoxidation*, Plenum Press, New York (1981) 674 + xviii pp.

3   Smith, L. L., 'Review of progress in sterol oxidations: 1987-1995', *Lipids* **31** (5) (1996) 453-487.

4   van de Bovenkamp, P., Kosmeijer-Schuil, T. G., and Katan, M. B., 'Quantification of oxysterols in Dutch foods: Egg products and mixed diets', *Lipids* **23** (11) (1988) 1079-1085.

5   Tsai, L.-S., and Hudson, C. A., 'Cholesterol Oxides in Commercial Dry Egg Products: Isolation and Identification', *Journal of Food Science* **49** (1984) 1245-1248.

6   Chicoye, E., Powrie, W. D., and Fennema, O., 'Photoxidation of Cholesterol in Spray-dried Egg Yolk Upon Irradaition', *Journal of Food Science* **33** (1968) 581-587.

7   Luby, J. M., Gray, J. J., Harte, B. R., and Ryan, T. C., 'Photooxidation of Cholesterol in Butter', *Journal of Food Science* **51** (4) (1986) 904-907.

8   Nam, K. C., Du, M., Jo, C., and Ahn, D. U., 'Cholesterol oxidation products in irradiated raw meat with different packaging and storage time', *Meat Science* **58** (2001) 431-435.

9   Janoszka, B., Wielkoszynski, T., Tyrpien, K., Dobosz, C., and Bodzek, P., 'Analysis of oxygenated cholesterol derivatives by planar chromatography', *Journal of Planar Chromatography* **13** (November/December) (2000) 437-442.

10   Finocchiaro, E. T., and Richardson, T., 'Sterol oxides in foodstuffs: A review', *Journal of Food Protection* **46** (10) (1983) 917-925.

11   Ahn, D. U., Lee, J. I., Jo, C., and Sell, J. L., 'Analysis of cholesterol oxides in egg yolk and turkey meat.', *Poultry Science* **78** (1999) 1060-1064.

12   Morgan, J. N., and Armstrong, D. J., 'Formation of cholesterol-5,6-epoxides during spray-drying of egg yolk.', *Journal of Food Science* **52** (5) (1987) 1224-1227.

13   Lai, S.-M., Gray, I., Buckley, D. J., and Kelly, P. M., 'Influence of free radicals and other factors on formation of cholesterol oxidation products in spray-dried whole egg.', *Journal of Agricultural and Food Chemistry* **43** (1995) 1127-1131.

14   Yang, S. C., and Chen, K. H., 'The oxidation of cholesterol in the yolk selective traditional chinese egg products', *Poultry Science: Official journal of the Poultry (Science) Association* **80** (2001) 370-375.

15   Kim, S. K., and Nawar, W. W., 'Oxidative interactions of cholesterol with triacylglycerols', *The Journal of the American Oil Chemists' Society* **68** (12) (1991) 931-934.

16   Zaretskii, Z. e. V., *Mass spectrometry of steroids*, John Wiley and Sons, New York (1976) 182 + xi pp.

17   Nourooz-Zadeh, J., and Appelqvist, L.-Å., 'Cholesterol oxides in Swedish foods and food ingredients: Fresh eggs and dehydrated egg products.', *Journal of Food Science* **52** (1) (1987) 57-62, 67.

18   Smith, L. L., Teng, J. I., Lin, Y. Y., Seitz, P. K., and McGehee, M. F., 'Sterol metabolism-XLVII. Oxidized sterol esters in human tissues', *Journal of Steroid Biochemistry* **14** (1981) 889-900.

19   Knights, B. A., 'Identification of plant sterols using combined GLC/Mass Spectrometry', *Journal of Gas Chromatography* **5** (1967) 273-282.

6. MALDI-FTMS analysis of oxygenated tri- glycerides and phosphatidylcholines in egg tempera paint dosimeters

Previous chapters discussed results that were obtained by direct temperature resolved mass spectrometric analysis of egg tempera test systems. This technique highlights the chemical changes in the lipidic part of the tempera binding medium. Changes in the mastic triterpenoids, egg cholesterol and triacylglycerols were observed. Changes observed in the triacylglycerol mass window pointed at addition of oxygen to unsaturated triacylglycerols. Phospholipids, although abundantly present in egg were not detected by DTMS. The present chapter reports analyses that were carried out to further investigate the changes in triacylglycerols and diacylphosphatidylcholines in light-aged and pollutant-exposed egg-only tempera. Furthermore, the effect of the addition of inorganic pigments to the fresh binding medium is assessed.

6.1 Introduction

Since the glycerolipids mainly contain unsaturated fatty acids they are prone to oxidation. The oxidation of phosphatidylcholines has been studied extensively by Barclay [1]. Chan broadly reviewed the autoxidation of unsaturated lipids [2]. In a more recent book Frankel gives a systematic overview of the processes in lipid oxidation [3]. His book also discusses methods for the determination of the extent of oxidation. Several essays have been developed to determine the state of oxidation of unsaturated lipids. The thiobarbituric acid (TBA) assay for instance focuses on TBA reactive substances, such as malonic dialdehyde [4], whereas the HPLC/iron thiocyanate assay quantifies the abundance of phospholipid hydroperoxides [5]. Murphy and Harrison [6] have reviewed the analysis of phospholipids by FAB-MS. In more recent work FAB-MS was used for the analysis of intermediate products of lipid oxidation in phosphatidylcholine liposomes [7]. Research by Harvey *et al.* [8] and by Marto *et al.* [9] showed that phospholipids can also be easily analysed by matrix-assisted laser

desorption/ionisation Fourier transform mass spectrometry (MALDI-FTMS). Triglycerides have been studied widely using a great variety of ionization techniques. In the most recent research ESI [10], laser desorption [11] and MALDI [12, 13] have successfully been applied to generate pseudomolecular ions with great efficiency.

In principle ESI is a softer ionization technique than MALDI, and hence forms molecular ions more efficiently without loss due to fragmentation. However, as was pointed out by Duffin *et al.* [14], the ionization efficiency is greatly influenced by the analyte polarity. Therefore, in this comparative study we use MALDI-FTMS for rapid and simultaneous analysis of diacylphosphatidylcholines and triacylglycerols.

6.2 Experimental

6.2.1 Materials and sample preparation

The preparation of the egg-only tempera samples subjected to MALDI-FTMS analysis is described in **Chapter 1**. The light ageing series (0, 4, 8, 16, 32 and 64 days), the NO_x/SO_2 exposed sample and the 21-day thermally aged sample of the egg-only tempera test system were analysed. In addition the unexposed azurite (basic copper carbonate) and lead white (basic lead carbonate) were analysed.

Direct temperature-resolved mass spectrometry (DTMS) was performed as described in the experimental section of **Chapter 2**.

6.2.2 Matrix-assisted laser desorption/ionisation Fourier transform ion cyclotron resonance mass spectrometry (MALDI-FTMS)

Samples were scraped off the Melinex support, extracted with dichloromethane/ethanol (2:1), and centrifuged. A drop of the supernatant was applied on the MALDI probe, which had been coated with a layer of 2,5-dihydroxybenzoic acid (DHB, Aldrich, Steinheim, Germany). FTMS analysis was performed on a modified Bruker Spectrospin (Fällanden, Switzerland) APEX 7.0e FT-ICR-MS instrument with an Infinity™ Cell and a home-built external ion source for CI, EI, FAB, ESI and MALDI [15]. For MALDI a 600 ps laser pulse

(337nm, 0.48 mJ) from a Photon Technology PL2300 (London, Ontario, Canada) nitrogen laser was used to desorb and ionise the analytes from the probe inside the ion source of the FTMS instrument. The laser light impinging on the probe under a 45° angle produced a 4.5 mm^2 spot. Ions were trapped in the ICR-cell using a 900 μs trapping delay (p2). Spectra were acquired in broadband mode (128k datapoints). Data of 100 shots were summed to obtain the spectra presented.

6.2.3 High performance size exclusion chromatography (HPSEC)

Samples were homogenised in tetrahydrofurane (HPLC grade, Fluka, Buchs, Switzerland) and centrifuged. 100 μl of the supernatant was injected into an Applied Biosystems 480 injector module. The sample was separated on a Polymer Laboratories 10^3 Å (300 x 7.5 mm i.d., 5 μm particle size) HPSEC column, using a 1 ml/min flow of THF from an Applied Biosystems 400 solvent delivery system. Detection of eluted components was performed by a LDC/Milton Roy SM 4000 programmable wavelength UV detector, using 240nm UV-light. Data acquisition was accomplished using a PC with Chrompack Maestro HPLC software (version 2.3 for Windows). Polystyrene standards (Polymer Laboratories, Zeist, The Netherlands) were used to calibrate the HPSEC separation.

6.3 Results and discussion

6.3.1 Direct temperature-resolved mass spectrometry

The results obtained on unexposed and light-aged egg-only tempera by direct temperature-resolved mass spectrometry (DTMS) on a sector instrument (see **Chapter 3**) indicated changes in the triacylglycerols (TAGs) [16-18]. **Figure 1** shows the DTMS spectra from m/z 500 to m/z 950 of unaged egg-only tempera stored in the dark (A) and exposed to light for 16 days (B). The clusters of peaks at m/z 820-910 originate from TAGs. Peaks at m/z 540-620 are diglycerides and fragments from TAGs and phospholipids. In the spectrum of the light-aged sample new clusters of peaks appear at masses roughly 16 mass units higher than the TAG peaks. Although oxygenation of TAGs seems evident, the exact nature of the changes cannot be identified on the basis of these DTMS results.

Moreover, phospholipids (PLs) although abundantly present in egg [19] cannot be identified in the DTMS spectra, due to the extensive fragmentation of PLs under EI conditions resulting in mass spectrometric overlap with fragments of TAGs in the diglyceride region of the mass spectrum. Phospholipids can be detected by chemical ionisation DTMS on a sector instrument, but in that case still high-resolution experiments would be required for the identification of the products of the ageing processes. Hence, MALDI-FTMS was selected for the simultaneous investigation of the degree of oxygenation of triglycerides and phospholipids.
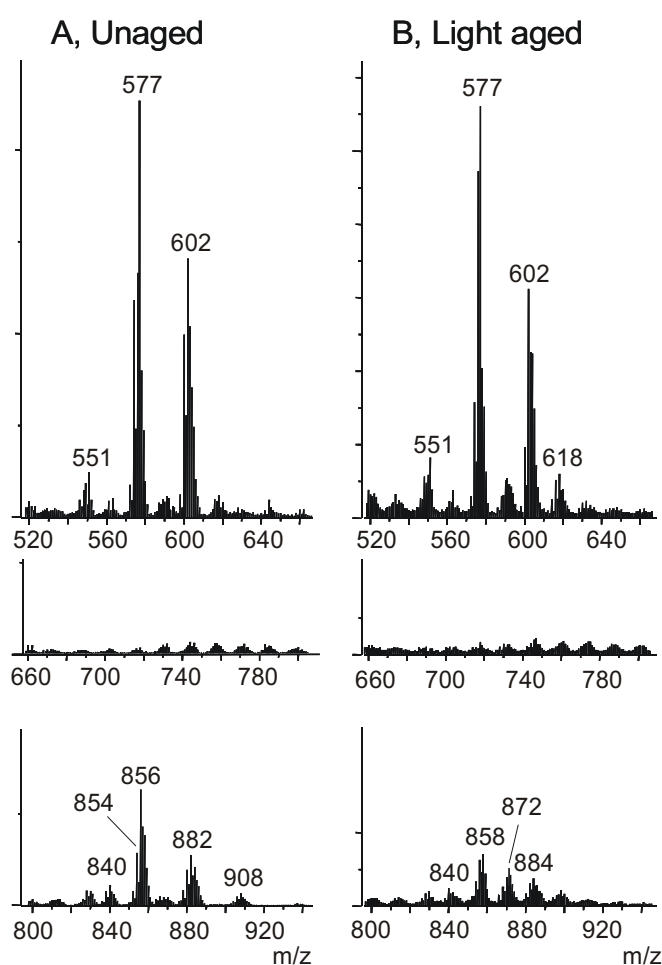
Figure 1 *Comparison of DTMS spectra of control (A) and 16-day light-aged (B) egg-only tempera samples.*

6.3.2 *MALDI-FTMS of the unaged egg-only tempera*

Figure 2 shows the MALDI-FTMS spectrum of the DCM:EtOH extract of the control egg-only tempera sample. Here sodium cationised molecular ions of both triacylglycerols and phosphatidylcholines (DAPCs) are observed. The triacylglycerols are observed between m/z 850 and 910, the DAPCs between m/z

720 and 820. Diglyceride peaks, observed between *m/z* 560 and 660 (data not shown), originate from hydrolysed TAGs and PLs, which are present as such in the sample, and from fragments due to loss of fatty acids from TAG pseudomolecular ions and loss of phosphate groups from PLs.

In the triacylglycerol mass window, primarily three clusters of peaks are observed: 1) C53-TAGs, 2) C55-TAGs, and 3) C57-TAGs. The peak at *m/z* 881, for example, corresponds to a sodium cationised C55-TAG with three unsaturations (TAG55:3). **Table 1** compares the molecular distribution of triacylglycerols as determined from the mass spectra with values found in the literature [19]. The table shows that TAGs reported to be present in egg in low relative abundance (< 1%) are not detected in our experiments. Furthermore, compared with the literature, the more unsaturated TAGs are observed in the MALDI-FTMS spectra with higher relative abundance. Thus far, it is not clear whether this is due to the original composition of the egg which is known to be affected by the diet of the chicken, or due to mass spectrometric effects such as enhanced ion formation from unsaturated TAGs in the MALDI process. Another, less likely, explanation would be that the sample preparation in the method used by Kuksis, which is rather lengthy compared to the sample preparation used here, had caused degradation of unsaturated TAGs before their measurement.
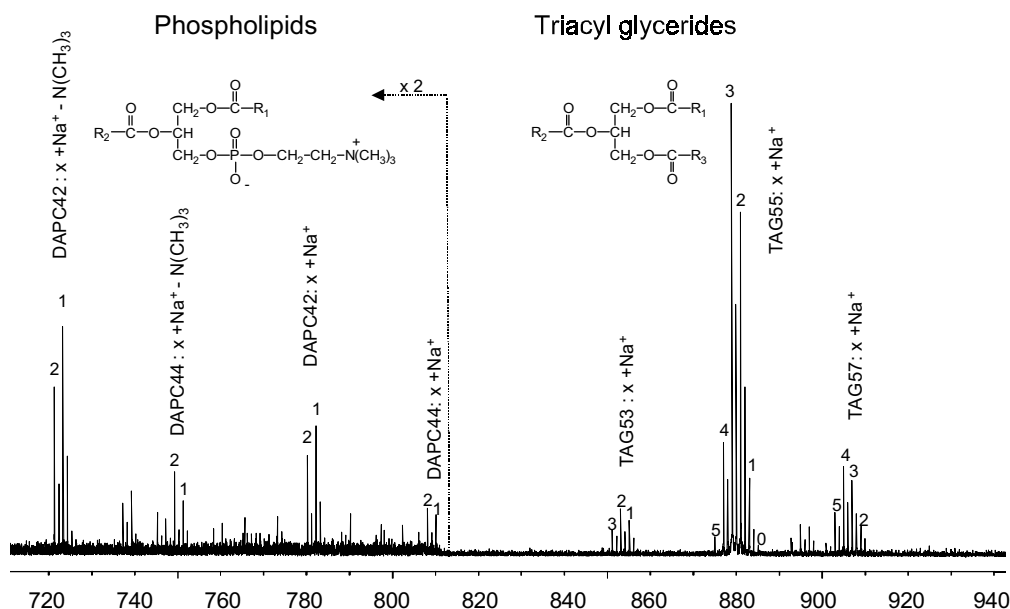
Figure 2 *MALDI-FTMS spectrum of unaged egg-only tempera sample. Numbers above peaks indicate the degree of unsaturation of the diacylphosphatidylcholine (DAPC) or triacylglycerol (TAG).*

Table 1 *Experimental abundance of egg triacylglycerols determined by MALDI-FTMS compared with literature values.*

Com-pound	Principal composition [19]	Rel. abundance in literature (%) [19]	Rel. ab. (%) By MALDI-FTMS	+ O	+ 2O	+3O	+4O
C51:0	16:0-16:0-16:0	0.1	n.d.				
C51:1	16:0-18:1-14:0	0.6	n.d.				
C51:2	14:0-18:1-16:1	0.4	n.d.				
C53:0	16:0-18:0-16:0	0.3	n.d.				
C53:1	16:0-18:1-16:0	5.7	2.6				
C53:2	18:0-16:1-16:1	3.5	3.4	32,64			
C53:3	16:0-18:2-16:1	1.1	2.2	16			
C53:4	14:0-18:2-18:2 (0.15) 16:1-18:2-16:1 (0.15)	0.3	n.d.				
C55:0	16:0-18:0-18:0	0.2	n.d.				
C55:1	16:0-18:1-18:0	9.5	4.9	32,64			
C55:2	16:0-18:1-18:1	33.0	24.3	4-64	16-64	16-64	16-64
C55:3	16:0-18:2-18:1	21.3	33.9	4-64	4-64	16-64	16-64
C55:4	16:1-18:2-18:1 (3.8) 16:0-18:2-18:2 (2.9)	6.7	9.1	4-64	16-64	16-64	16-64
C55:5	????	n.d	0.9		16,32		
C57:0	18:0-18:0-18:0	< 0.1	n.d.				
C57:1	18:0-18:1-18:0	0.3	n.d.				
C57:2	18:0-18:1-18:1	1.9	1.5	16			
C57:3	18:1-18:1-18:1	5.9	5.6	8-64	16-64		
C57:4	18:1-18:2-18:1	7.0	6.7	8-32	16-64	16	
C57:5	18:1-18:2-18:2	1.0	3.6	8	64		
C57:6	18:2-18:2-18:2	1.0	1.1				

The MALDI-FTMS spectrum of the unaged egg-only tempera sample also shows C42-DAPCs and C44-DAPCs. For comparison and identification the MALDI-FTMS spectrum of egg yolk DAPCs (Sigma, St Louis MO, USA) is shown in **Figure 3**. Both the reference spectrum and the spectrum of the unaged egg-only tempera sample show sodiated and protonated molecular ions of DAPCs, albeit in different ratios. Furthermore, the FTMS spectra of the reference material and the unaged egg-only tempera sample indicate loss of trimethylamine from sodium cationised DAPCs leading to $[M-59+Na]^+$ ions. This observation and interpretation agree with a publication by Marto [9] and corrections thereof [20]. Potassium cationised DAPCs were observed at low relative abundances in the unaged egg-only tempera sample only. These peaks were identified by their exact masses.
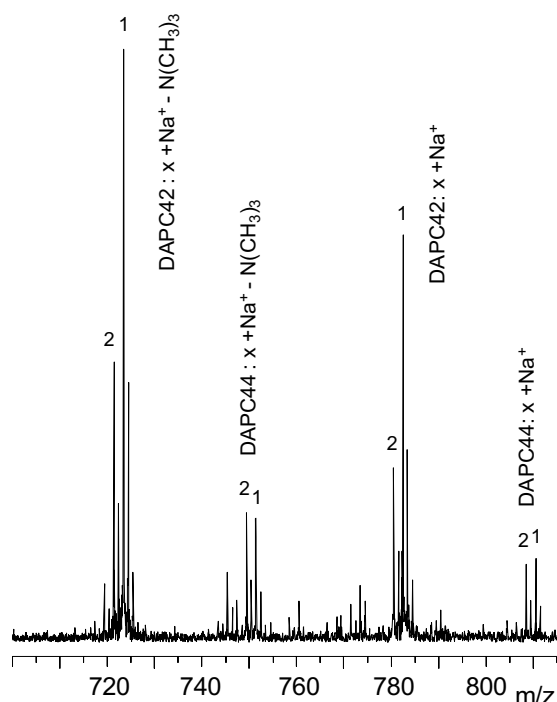
Figure 3 *MALDI-FTMS spectrum of chicken egg diacylphosphatidylcholines.*

Diacylphosphatidylethanolamines (DAPEs), although found to contribute up to 24 % of the PL fraction in egg yolk [19], are not observed in our data. Analysis of commercially available phosphatidylethanolamine extracted from egg (data not shown) showed that this compound class can be detected by MALDI-FTMS as [M+Na]$^+$ and [M-H+2Na]$^+$ pseudomolecular ions. Egg yolk DAPEs mainly consist of arachidonic acid residues (C20:4) which oxidise quickly upon exposure to air. In the first stage of oxidation of arachidonoyl phospholipids one to three oxygen atoms are introduced, resulting in hydroxy, 1,3-cyclic diol and thromboxane structures [21]. More progressed oxidation leads to formation of a variety of chain-shortened products [22]. The arachidonic acid containing DAPEs were observed unaltered in the MALDI-FTMS spectrum of commercially available DAPEs isolated from chicken egg yolk; oxidation products were not observed (data not shown). This proves that our sample preparation method for MALDI-FTMS does not lead to oxidation of the polyunsaturated fatty acyl chains. We could rule out charge competition processes between DAPE and DAPC in the MALDI ion production as explanation of the absence of DAPEs in the spectra, using MALDI-TOF-MS experiments with a mixture of palmitoyl-oleoyl-glycerophosphocholine and of palmitoyl-oleoyl-glycerophosphoethanol-amine (both species were observed; data not shown). Hence the absence of DAPEs in the spectra must be caused by the chemical behaviour of these substances in the paint samples rather than by experimental factors, and further study is necessary to resolve this issue.

Table 2 *Experimental abundance of egg diacylphosphatidylcholines determined by MALDI- FTMS compared with literature values.*

Compound	Experimental relative abundance (%)	Relative abundance (%) in the literature [19]
PC-C42:1	40.3	41.2
PC-C42:2	33.6	24.5
PC-C44:1	9.8	10.6
PC-C44:2	14.8	15.3
PC-C44:3	1.5	2.1
PC-C44:4	n.d.	2.7
PC-C46:4	n.d.	3.6
n.d. = not detected		

Table 2 compares the relative abundance of DAPCs observed by FTMS of the unexposed egg-only tempera sample with those determined by Kuksis [19]. This table only includes species that have been observed by Kuksis with a relative abundance higher than 2%. These compounds account for 93% of all egg DAPCs. The table shows that the relative abundances determined by MALDI-FTMS are very similar to those observed by other workers, although some difference is observed for the doubly unsaturated C42-DAPCs. Another difference with respect to our data is that fourfold unsaturated C44-DAPCs and C46-DAPCs were not detected in our MALDI-FTMS, but have been observed by Kuksis with 2.7% and 3.6% abundance respectively.

6.3.3 Changes in the TAGs upon light ageing

Figure 4 compares the FTMS spectra in the triacylglycerol mass window (m/z 870 – 950) for all light-aged samples. The figure shows that two major changes occur upon light ageing. First, within each cluster the intensities of the more unsaturated TAGs decrease relative to the less unsaturated TAGs. The average number of unsaturations per TAG, based on an assumed equal response factors of all TAGs for MALDI-FTMS, decreases from 2.8 in the unaged egg-only tempera sample to 1.7 in the 64-day light-aged sample. Second, clusters of peaks are introduced at approximately 16 a.m.u. higher than the depleted peaks. The average exact mass difference between the peaks formed and the peaks depleted, 15.994 +/- 0.006 a.m.u., agrees exactly with the exact mass of oxygen (15.9949). This unambiguously proves that light ageing leads to oxygenation of the TAGs. SORI-CAD [23] and resonant excitation CAD experiments [24, 25] on singly oxygenated TAGs formed upon light ageing showed which one of the three fatty acid had undergone oxygenation (see also **Chapter 7**).
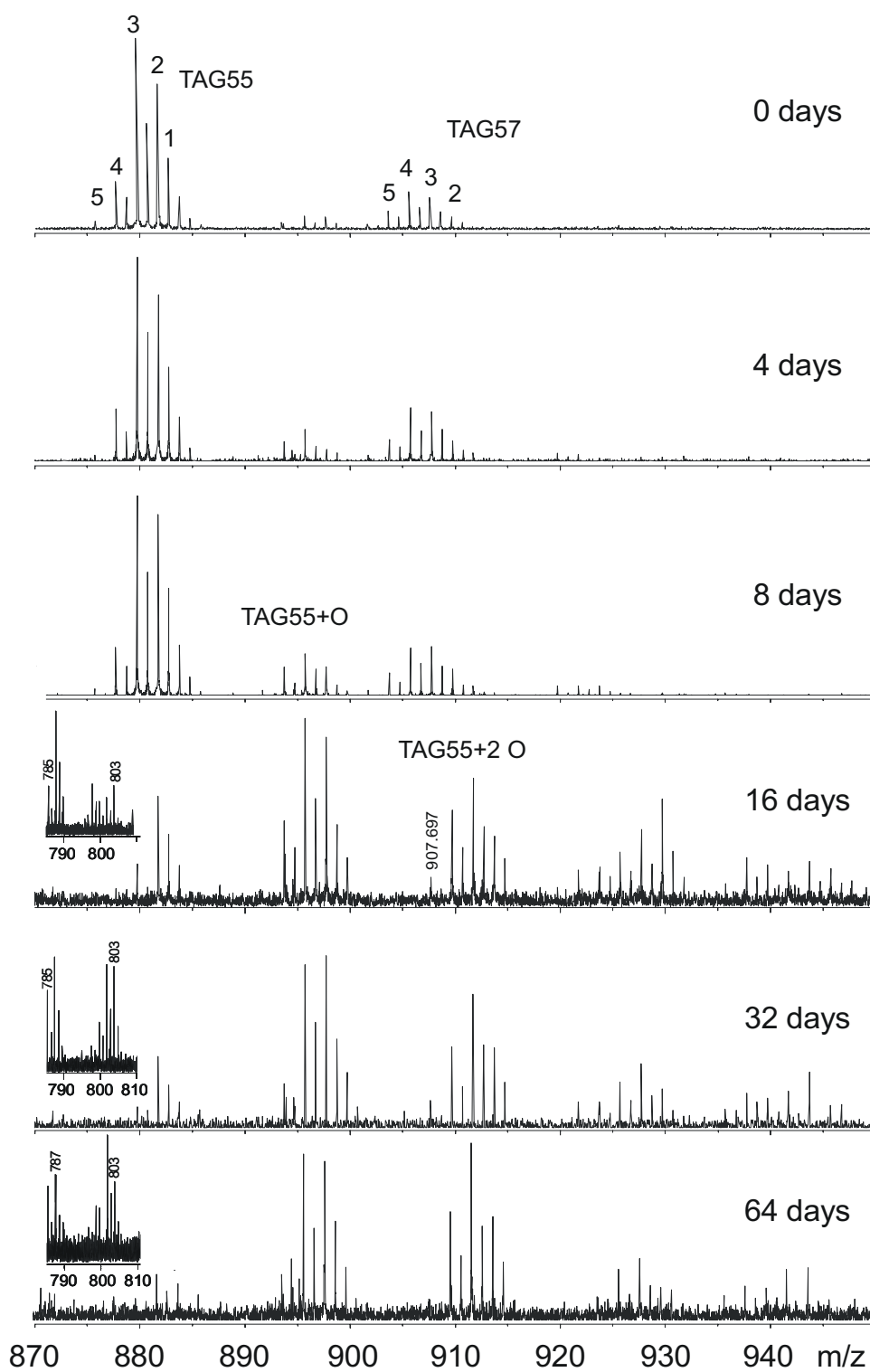
Figure 4 *Comparison of triacylglycerol mass ranges in MALDI-FTMS spectra egg-only tempera samples light-aged for 0, 4, 8, 16, 32, and 64 days.*

Another significant difference between the MALDI-FTMS spectra of light-exposed and unexposed egg-only tempera is the emergence of peaks in the ranges *m/z* 910-915 and m/z 935-940, which indicates multiple oxygenation of C55-TAGs and C57-TAGs. Introduction of up to four oxygen atoms is observed in the light-aged samples. The average degree of unsaturation of all intact TAGs in the unaged material is 2.81. The degree of unsaturation of the sum of the oxidised and unoxidised material does not change upon light ageing, and its average over all light ageing samples with ageing times between 0 and 64 days is 2.83 ± 0.03. This implies that the net result of light ageing is the introduction of oxygen without addition or abstraction of hydrogen and suggests that structures like hydroxides, epoxides, hydroperoxides, and epidioxides are forming predominantly upon ageing. The results in the last three columns of **Table 1**, in particular the observation of triply and fourfold oxygenated TAG55:2 and fourfold oxygenated TAG55:3, indicate that at least in some cases more than one oxygen is introduced per double bond. This suggests that hydroperoxide, epidioxide, hydroxy epoxide or diol functionalities form upon oxidation of the unsaturated fatty acid moieties. Such structures have been observed in autoxidation studies of unsaturated fatty acid methyl esters [3] and trilinoleoylglycerol [26]. Theoretically it can also indicate that oxygenation may lead to a decrease in the degree of unsaturation. As the degree of unsaturation is conserved such a process should be compensated by the formation of unsaturated oxygen containing functional groups, such as a keto functionality by loss of water from a hydroperoxy group.

Based on its exact mass, the peak at m/z 907.697 in the spectrum of the 16-day light-aged egg-only tempera sample is attributed to doubly oxygenated TAG55 with elemental composition $C_{55}H_{96}O_8$ (exact mass 907.700), rather than to TAG57:3 (exact mass 907.773). This example shows that the resolution (mass accuracy) of the FTMS data allows a precise determination of the degree of oxygenation of TAGs.

The total intensity (based on peak height) of the unreacted TAGs was determined and the same was done for the singly, doubly, three and fourfold oxygenated TAGs. Normalisation of each mass spectrum was carried out by summation of the intensity (height) of all oxidised and unreacted TAGs. Intensities of the nominal mass peak (all ^{12}C) and the first isotope peak ($^{13}C_1$) were summed; contributions of second isotope peaks ($^{13}C_2$) of compounds 2 amu lighter than the peak of interest were neglected because of their small contribution. The relative intensities of the unreacted, singly and multiply oxygenated compounds were used to calculate the index for the degree of oxygenation of the TAGs using the following formula:

$$\text{IDOX}_{\text{TAG}} = \sum_{n=1}^{4} n * I_n$$

in which IDOX_{TAG} is the degree of oxygenation; n is the number of oxygen atoms introduced to the TAG; and I_n is the total relative intensity of the all n-fold oxygenated TAGs after normalisation.

Figure 5 plots IDOX_{TAG} as a function of the exposure time. The figure suggests that the degree of oxygenation slowly develops in the first 8 days of light ageing, and plateaus after 16 days. **Figure 6** plots the relative abundances of the unaffected TAGs and the oxygenated TAGs as a function of the exposure time, and gives a more detailed view of the oxygenation processes. The curve of the unreacted TAGs in this figure indicates that the relative abundance of the unreacted TAGs decreases rapidly as the ageing time increases. Furthermore, the intensity of singly oxygenated species appears to plateau after 16 days of light ageing, indicating that the rate of formation and depletion of this species have equilibrated. The curves of the multiply oxygenated species indicate that multiple oxygenation mainly happens after single oxygenation. After 16 (or 32) days of light ageing the relative concentrations of triply and quadruply oxygenated species also appear to plateau, indicating that these species are not only formed, but also depleted during light ageing.
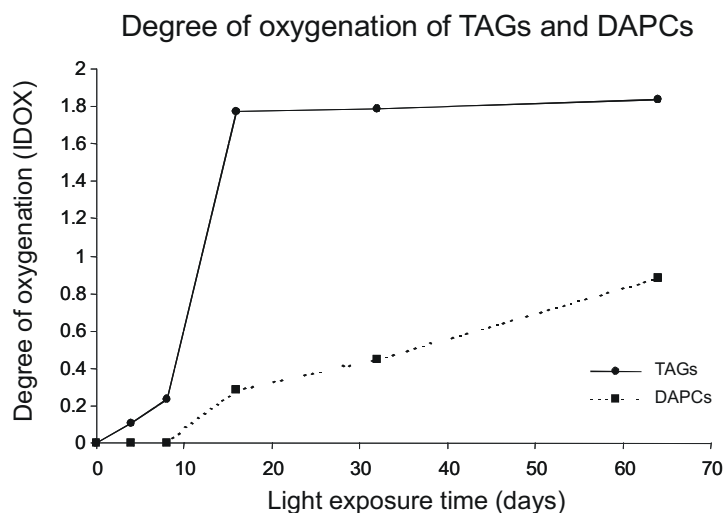
Figure 5 *Degree of oxygenation of triacylglycerols (solid line) and diacylphosphatidylcholines (dotted line) as function of light ageing time.*

Number of oxygen atoms introduced in TAGs
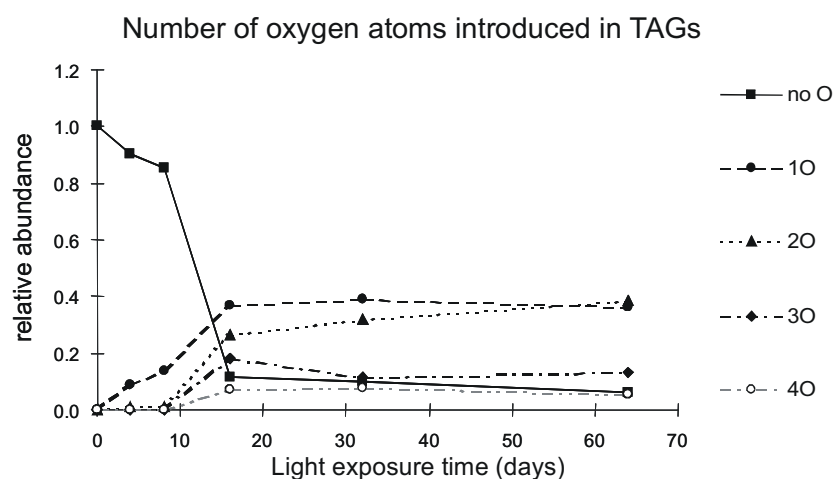
Figure 6 *Relative abundance of unreacted and oxygenated triacylglycerols as function of light ageing time.*

Table 3 *Effect of light ageing time on the relative abundance of unreacted, oxygenated and chain shortened triacylglycerols.*

Light exposure time	Unreacted TAGs	Oxygenated TAGs	Oxidative cleavage products
0	1.00	0.00	0.00
4	0.90	0.10	0.00
8	0.82	0.14	0.04
16	0.10	0.78	0.12
32	0.08	0.70	0.22
64	0.05	0.76	0.19

The literature suggests oxidative cleavage of the fatty acid chain as a result of progressed oxidation [27]. In the FTMS spectra of 16-, 32- and 64-day light-aged egg-only tempera (**Figure 4**) peaks are observed at m/z 789.615, 787.602, and 785.588. The exact m/z of these peaks agree with the elemental compositions $C_{46}H_{86}O_8Na$ (789.621), $C_{46}H_{84}O_8Na$ (787.606), and $C_{46}H_{82}O_8Na$ (785.590) respectively, and suggest a net addition of two oxygen atoms and chain shortening by a C9 unit of unsaturated C55-TAGs. The presence of oxidatively cleaved TAGs is further evidenced by fragment peaks at m/z 505 and m/z 533 (not shown) due to loss of one of the C_{16} or C_{18} fatty acid chains from the pseudo-molecular ions of the oxidatively cleaved species. In the 16-, 32- and 64-day light-aged samples (**Figure 4**) peaks have also been observed at m/z 799.570, 801.587 and 803.606. Their exact masses agree with the elemental compositions $C_{46}H_{80}O_9Na$ (799.569), $C_{46}H_{82}O_9Na$ (801.585) and $C_{46}H_{84}O_9Na$ (803.601) , suggesting either progressed oxidation of oxidatively cleaved TAGs or oxidative

cleavage of TAGs with two oxidised fatty acid chains. **Table 3** shows the relative abundances of unreacted TAGs, oxygenated TAGs and oxidative cleavage products in the light-aged samples. These data clearly show that oxidative cleavage follows a similar trend as the oxygenation of TAGs.

Another process that consumes oxygenated TAGs is cross-linking [28-30]. To verify whether cross-linking plays a role in the light ageing of egg, control and aged samples were extracted with THF and analysed by SEC. **Figure 7** compares the SEC chromatograms of the control, 4-, 16-, and 64-day light-aged egg-only tempera samples. The figure clearly shows that cross-linking plays an important role in the light ageing of egg, and hence may be seen as one of the possible causes of depletion of oxygenated TAGs. Furthermore, TAGs are affected by hydrolysis leading to the formation of diglycerides. In fact, this is thought to be a major cause of the decrease in the signal to noise ratio of the TAGs upon light ageing. Hydrolysis reactions have been further confirmed by data on light-aged egg yolk tempera paints studies by extractive silylation and GCMS [31] and by ESI-FTMS (see **Chapter 7**).
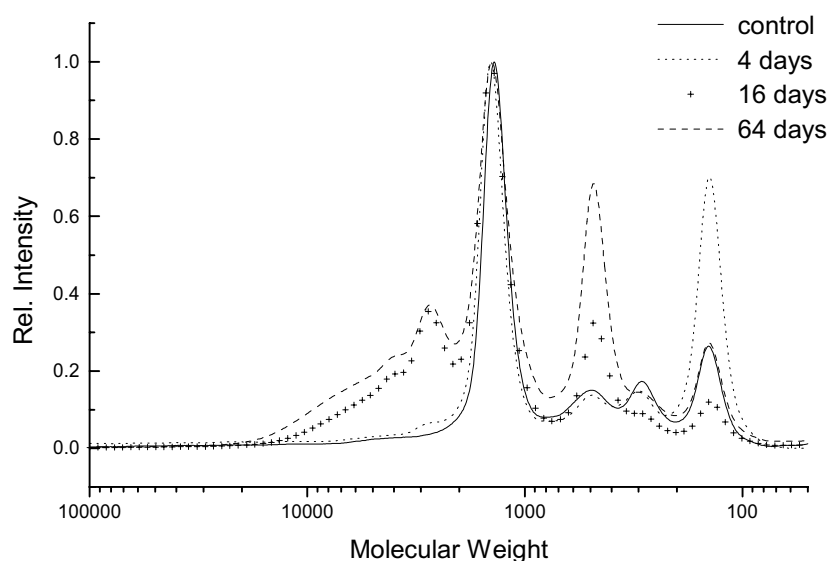
Figure 7 *HPSEC chromatograms of unaged and light-aged egg samples (0, 4, 16, and 64 days). Calibration against polystyrene.*

Figure 8 compares the effects of thermal ageing (A) and exposure to air pollutants (B). Thermal ageing (21 days at 60°C) appears to have no effect on the TAGs, as no significant change of the FTMS spectrum in the TAG mass range is observed (see also **Figure 4** for comparison). The calculated degree of oxygenation is zero. Exposure to NO_x and SO_2 (10 ppm, 17 ppm) for four days,
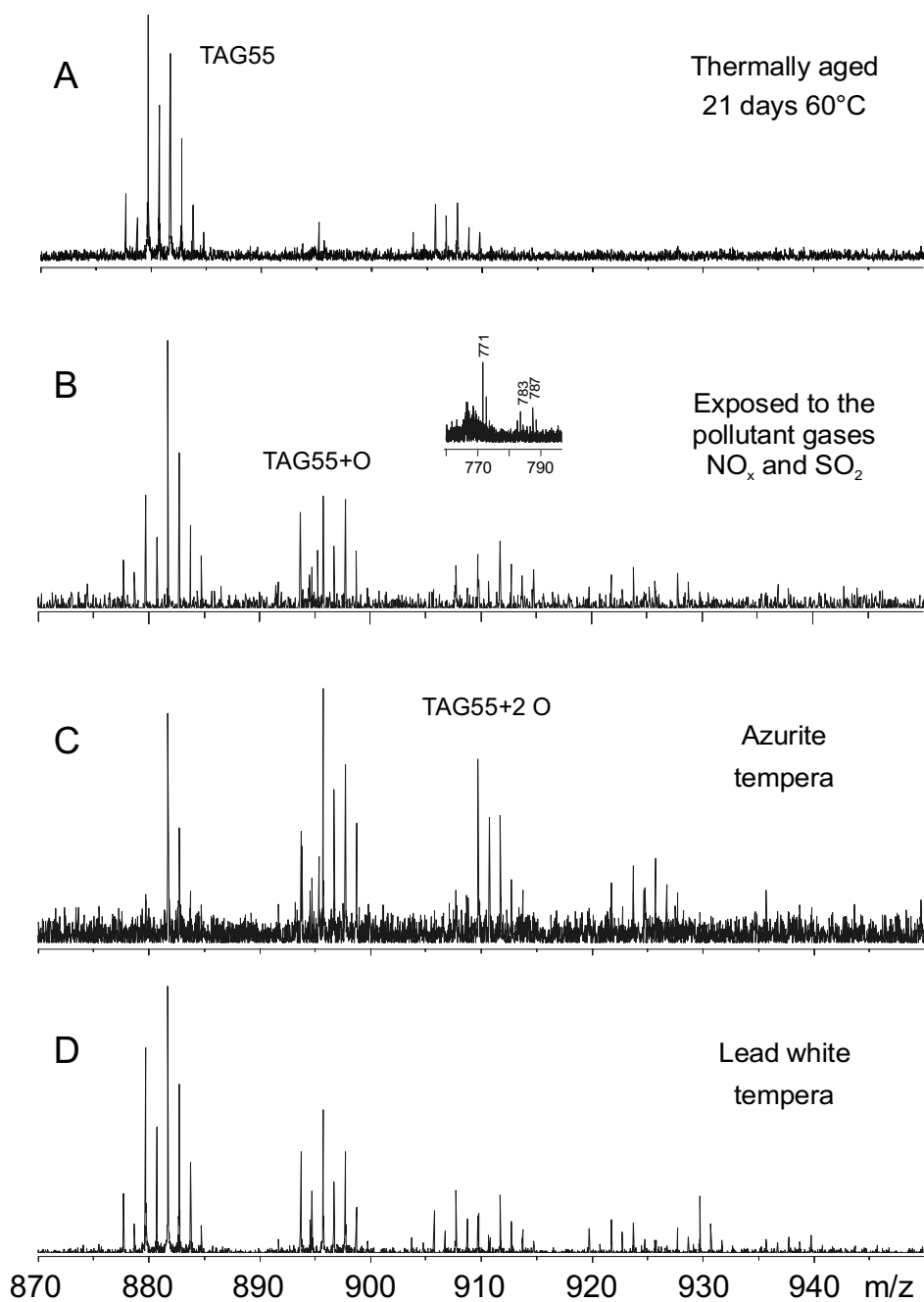
Figure 8 *TAG range of the MALDI-FTMS spectra of thermally aged (A) and air pollutant [NO$_x$, SO$_2$] exposed (B) egg, and azurite (C) and lead white (D) pigmented tempera.*

also in the dark, appears to greatly enhance oxygenation. The FTMS spectrum shows extensive oxygenation and depletion of unsaturated TAGs. The degree of oxygenation, calculated by the aforementioned method is 0.87. The spectrum also shows the oxidative cleavage product at m/z 787.601 (inset). More products of oxidative cleavage are observed at m/z 771.611 and 783.565 corresponding to

the masses of doubly and fourfold unsaturated oxygenated C46-TAGs with elemental compositions $C_{46}H_{84}O_7Na$ (771.611) and $C_{46}H_{80}O_8Na$ (783.575) respectively. These peaks were not observed in the FTMS spectra of light-aged egg-only tempera samples. Further research is required to determine whether these products are unique and can be used as markers for exposure to NO_x and SO_2. Gallon and Pryor [32] have determined that NO_2 addition products are formed when methyl linoleate is exposed to NO_2 in the absence of oxygen. In the presence of oxygen (air), as was the case with the exposure of the tempera test systems to NO_x/SO_2, hydroperoxides are observed as primary oxidation products.

The presence of metal salts as inorganic pigments in tempera paint may lead to metal catalysed oxidation (MCO) of unsaturated lipids. MCO of unsaturated lipids has been studied extensively [33]. The effects of a variety of pigments on the chemistry of linseed oil has been studied by Rasti and Scott [34]. These workers also observed a catalytic effect of the copper containing pigment verdigris on oxidative reactions in the drying of linseed oil [35]. It has been stated by others that different pigments variously affect oxidative degradation in egg tempera paint [36, 37]. Extractive silylation GCMS experiments carried out in our group [31] indicate that the presence of inorganic pigments strongly influences the chemical composition of the egg tempera binding medium. Additions of inorganic pigments to the egg and mastic binding medium of our tempera paint systems appear to greatly enhance oxidation. **Figures 8C and 8D** show this phenomenon in unexposed azurite and lead white temperas respectively. As a control experiment, a mixture of egg and mastic that had been coated on Melinex and stored in the dark along with the pigmented paints was analysed by MALDI-FTMS. No significant difference between the resulting spectrum and the spectrum of the unaged egg-only tempera sample was observed. This indicates that the oxidation can only be explained by the presence of the pigments. The degree of oxygenation of the lead white pigmented sample was 0.84. The azurite pigmented sample shows an even higher degree of oxygenation (1.42) and complete depletion of polyunsaturated TAGs. These results are confirmed by DTMS analysis of the same systems [31, 38, 39] (see also **Chapter 3**). The observation that copper catalyses the autoxidation of unsaturated TAGs to a greater extent than lead is in agreement with the literature [33].

6.3.4 Changes in the DAPCs upon light ageing

Figure 9 compares the phospholipid m/z ranges (m/z 700 – 830) of the mass spectra of unexposed and 8-, 32- and 64-day light-aged egg-only tempera samples. Three changes are clearly observed in this comparison. Firstly as in the light ageing of the TAGs, the more unsaturated DAPCs are preferentially

depleted. This can be seen by comparing the peak ratio of doubly unsaturated DAPCs to singly unsaturated DAPCs during light ageing. The average degree of unsaturation of the DAPCs decreases from 1.5 for the unaged sample to 1 for the 64-day light-aged sample. Secondly, the signal to noise ratio decreases greatly upon light ageing due to hydrolysis [31]. Thirdly, new peaks appear at *m/z* 737 and 739. The mass difference between these peaks and the depleted peaks agrees with the exact mass of an oxygen atom, thus again indicating oxygenation of the DAPCs. Given their exact masses, the peaks at m/z 737.443 and 739.461 in the spectrum of the 8-day light-aged sample were identified as the potassiated $[M+K-N(CH_3)_3]^+$ ions. Unlike the observations in the oxidation of TAGs, products of multiple oxidation of phospholipids are not observed in the samples that were exposed for longer times (16, 32, 64 days). This may be explained by the lower degree of unsaturation of the phospholipid fraction as compared with the TAGs, resulting in a lower reactivity in oxidative environments. However, Porter and coworkers [40] observed introduction of hydroperoxide groups into palmitoyl-linoleoyl- glycerophosphocholines (24.5% of egg DAPC) after 16 hours of exposure to air at room temperature. Hydroperoxides were also found upon reaction with HO• radicals in solution [7]. This suggests that the presence of other materials in the egg causes transformation of hydroperoxides. Indeed, cysteine residues in proteinaceous materials are known to reduce lipid hydroperoxides to hydroxides [33]. The appearance of singly oxygenated DAPCs could also point to intermolecular oxygen transfer from hydroperoxides to form epoxides and hydroxides observed in lipid monolayers [41]. This would imply that phospholipids could interact with each other in the dried tempera paint film, for instance, in intact low-density lipoprotein (LDL). In related experiments [42] we have found evidence that LDLs are still intact in the unaged unpigmented tempera material.

The development of the relative abundance of oxygenated DAPCs as a function of the ageing time is shown in **Figure 5**. The oxygenation only starts after 8 days of light ageing and develops more gradually than the oxygenation of TAGs. Again this is interpreted as due to the lower degree of unsaturation of DAPCs as compared to TAGs in egg. Fukuzawa *et al.* [43] observed that the rate of peroxidation of egg DAPC liposomes, measured as oxygen consumption, increased drastically after a lag-period. The length of this lag-period was found to depend on the concentration of DAPC hydroperoxides endogenously present in the liposomes. Longer lag-times were observed when less endogenous hydroperoxide was present. Such autocatalytic processes may also explain the observed delay in oxygenation of the DAPC fraction in our systems.

138
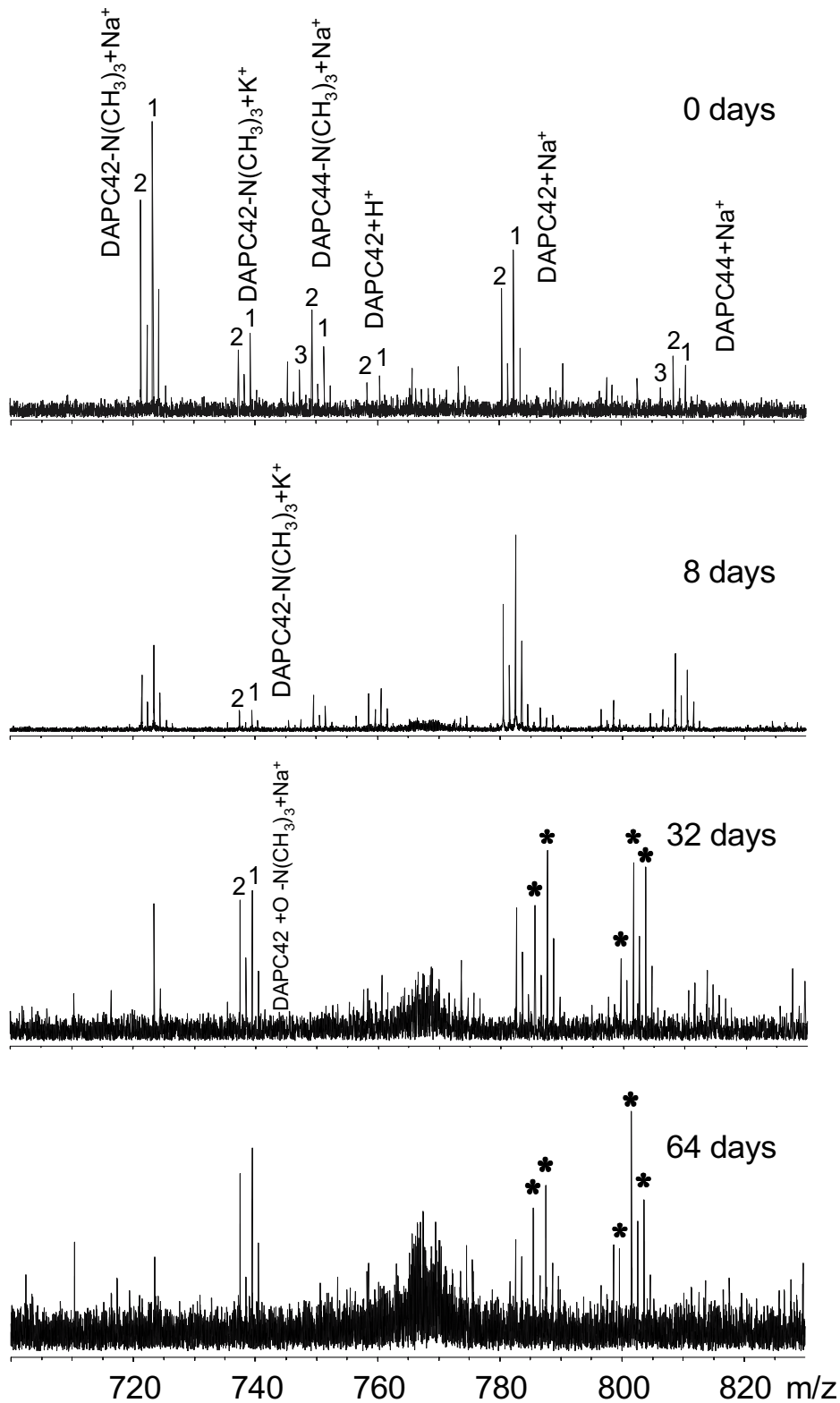
Figure 9 *DAPC range of the MALDI-FTMS spectra of unaged, and 8-, 32- and 64-day light-aged egg. Peaks marked with * originate from oxidative cleavage products of triacylglycerols.*

Figure 10 shows the DAPC range of FTMS spectra of the thermally aged egg-only tempera sample (A), the lead white pigmented sample (B), and the azurite pigmented tempera (C). The spectrum of the thermally aged sample closely resembles that of the unaged egg-only tempera sample. This is in agreement with the observations in the TAG range. The spectrum of the sample that had been exposed to SO_2 and NO_x is not included here because it shows almost no contribution from peaks of DAPC origin. The high acidity in the paint film as a consequence of the exposure may have caused hydrolysis of the DAPCs.

The DAPCs in the lead white pigmented sample show oxygenation as indicated by the peaks at m/z 737, 739, 796 and 798. Furthermore, the peaks observed at m/z 735.452 and 794.527 have exact masses corresponding to the oxygenated $[(DAPC42:3+O)+Na-N(CH_3)_3]^+$ (735.457) and $[(DAPC42:3+O)+Na]^+$ (794.531) respectively. This suggests that specific oxidation products are formed in the presence of a pigment. The DAPC-range of the FTMS spectrum of the azurite pigmented tempera is more complicated. In addition to protonated, sodium cationised DAPCs and fragments thereof also the copper cationised singly unsaturated DAPC42:1 was identified at m/z 822-825. The singly unsaturated DAPC44:1 was observed at low intensity at 850 and 852 (data not shown). The absence of peaks from doubly unsaturated DAPCs indicates that the DAPC fraction has undergone vast chemical changes due to the presence of the azurite pigment. In addition to the singly oxygenated DAPCs that were observed in the spectrum of the lead white tempera, the azurite tempera spectrum shows high intensities of protonated singly oxygenated C42-DAPCs (m/z 772-775) and peaks from doubly oxygenated DAPCs (m/z 810-813). These latter peaks were assigned on the basis of their exact mass and presence of peaks due to the characteristic loss of trimethylamine from the sodium cationised molecules. The inset shows that the peaks at m/z 810 and 811 consist of doublets. The heavier and less intense peaks of the doublets originate from the sodium cationised singly unsaturated DAPC44:1. Although based on the exact mass the peaks at m/z 814.557 and m/z 816.572 could be interpreted as $[(DAPC42:1+2O)+Na]^+$ (814.557) and $[(DAPC42:0+2O)+Na]^+$ (816.573), these peaks were attributed to $[(DAPC44:4+2O)+H]^+$ (814.559) and $[(DAPC44:3+2O)+H]^+$ (816.575) because fragment peaks due to loss of $N(CH_3)_3$ were not observed. In a similar way it was determined that the high relative intensity of the peak at m/z 798.560 is caused by the combination of $[(DAPC42:1+O)+Na]^+$ (exact mass 798.563) and $[(DAPC44:4+O)+H]^+$ (exact mass 798.565).
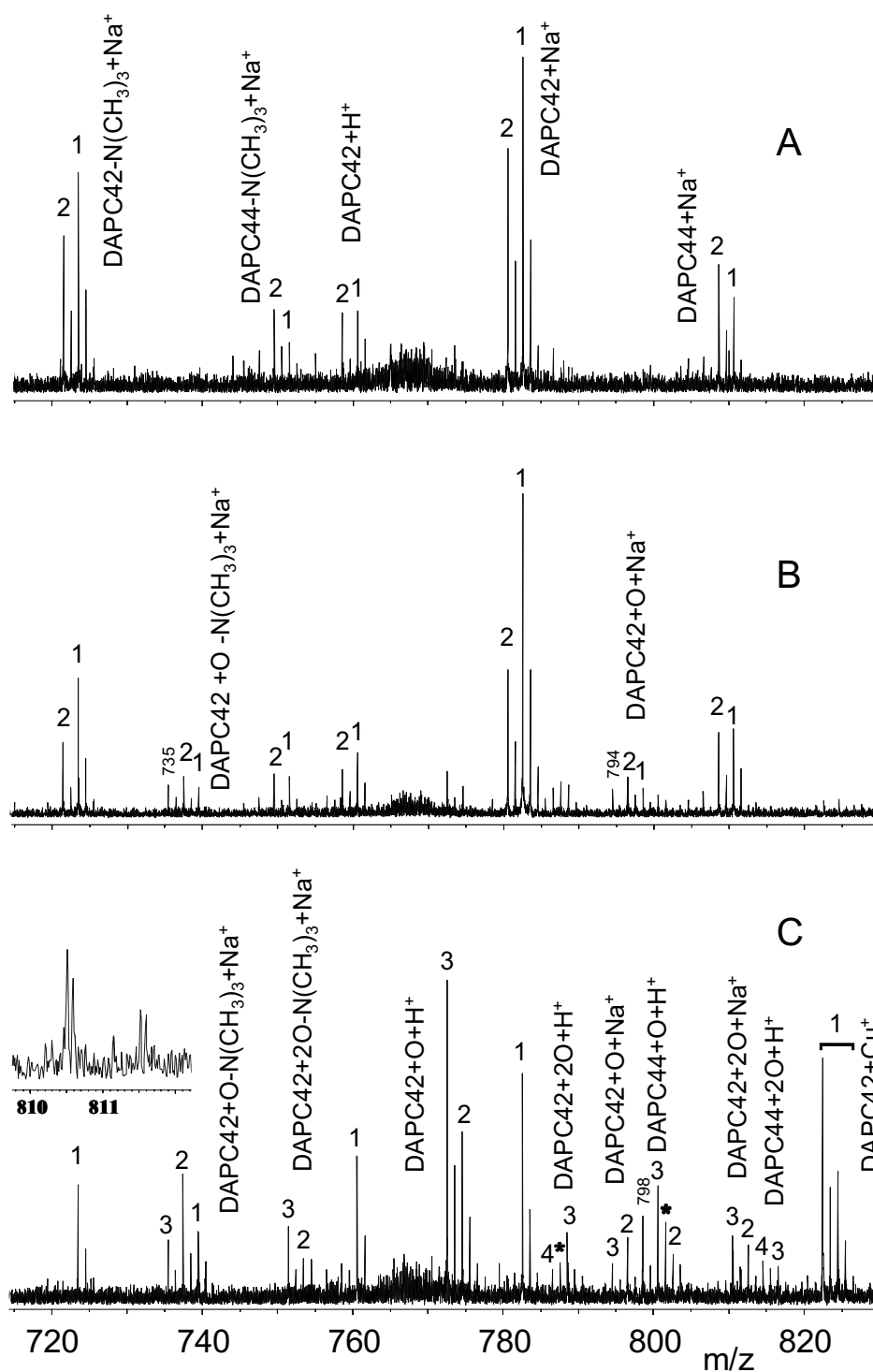
Figure 10 *DAPC range of the MALDI-FTMS spectra of thermally aged egg (A), lead white pigmented tempera (B), and azurite pigmented tempera (C). Peaks marked with * originate from or have contributions from oxidative cleavage products of triacylglycerols.*

6.3.5 *Implications for paintings and paint-based dosimetry*

The results presented here unequivocally show that oxidative changes occur in the egg tempera binding medium when exposed to visible light. The rates with which a glycerolipid in the egg-only tempera is oxygenated depends on its structure. The DAPC fraction is found to be oxidised at a slower initial rate than the TAGs. The number of unsaturations in the compound determines the rate of oxygenation. Progressed oxidation leads to multiple insertions of oxygen and is accompanied by oxidative cleavage reactions and the formation of THF extractable cross-linked material. Lipid oxidation products, unlike the native glycerolipids, are very reactive towards amine moieties in the proteinaceous fraction of the egg. This type of lipid protein interaction plays an important role in the anhydrous conditions in the dry paint film [31]. The increased reactivity of the lipid fraction towards the proteinaceous components in egg tempera paint leads to changes in the size and nature of the polymeric network. Hence, exposure to light as a consequence of the very function of a painting leads to important changes in the overall composition of the egg tempera binding medium. The high $IDOX_{TAG}$ of the sample exposed to NO_x and SO_2 in the dark implies that air pollution can be an important factor in the quality of the museum environment and the effects that it has on the art objects.

The observation that the inorganic pigments lead white and azurite, when present in egg tempera paint, catalyse the oxidation of their binding medium in the early stage of the drying of the film strongly suggests that the organic chemical composition of a paint is influenced by its pigments. Based on the observation that pigments can, by catalytic action, change the chemistry of the binding medium, it must be expected that temperas with different pigments respond differently to environmental conditions. Thus the MALDI-FTMS results obtained on the pigmented temperas suggest that a variety of paint systems should be exposed for successful environmental monitoring using paint-based dosimeters. In fact dosimetry of the museum environment in six different sites using pigmented temperas has shown that there is a pigment dependent difference in chemical response to the environmental conditions [17, 18] (see **Chapter 3**).

In view of the potential for detailed analysis, the question can be posed whether MALDI-FTMS should be used instead of DTMS (EI) for the evaluation of chemical changes in tempera paint based dosimeters. The main advantage of DTMS is its multi-component analytical potential. It allows, in one analytical run, the evaluation of changes in a greater variety of compound classes than glycerolipids alone. Besides changes in the glycerolipids, DTMS also detects changes in the cholesterol, and the formation of cross-linked material is also reflected in the DTMS spectra [16-18] (see **Chapters 2 and 3**). MALDI-FTMS

as applied here, on the other hand, allows the investigation of changes in the TAGs and DAPCs. The latter are not observed as molecular ions in the DTMS runs. Changes in the glycerolipids can be studied in much more detail, due to this specificity and the high resolution of the FTMS data. Hence, MALDI-FTMS is a good technique for supportive, ancillary identification of chemical changes observed by fingerprinting DTMS.

Although the degree of unsaturation of TAGs is found not to change upon oxygenation and the number of possible functional groups introduced into the fatty acyl chains can be limited to relatively few, detailed kinetic information on the rates of oxygenation of fatty acyl chains with different degrees of unsaturation cannot yet be derived from the present data. Investigation of the structure of oxidation products should contribute to the understanding of the reactions that take place during photo-oxidation of the egg tempera binding medium. ESI-FTMSMS work reported in **Chapter 7** is aimed at determination of the fatty acyl side chain on which the oxidation has taken place and work in progress is aimed at determination of the functional groups that are formed upon oxygenation.

6.3.6 Other applications of the methodology

The oxidation of lipids also plays a role in a variety of diseases, including atherosclerosis. Oxidative cleavage products of phospholipids can even act as inflammatory mediators [44]. Progressed oxidation of unsaturated lipids in food leads to the formation of off-flavour volatile compounds [3]. The present MALDI-FTMS method also can be used as for rapid direct screening of the oxygenation of TAGs and DAPCs in biochemical and food samples. The simple sample preparation for MALDI-FTMS makes this analytical method very suitable for determination of the degree of oxygenation of lipids in complex matrices. The high resolution of the mass spectrometric data allows determination of the number of oxygen atoms taken up by a TAG or DAPC molecule and hence expression of the oxygen uptake by these glycerolipids as the degree of oxygenation irrespective of the functional groups introduced upon oxygenation.

6.4 Conclusions

MALDI-FTMS is a rapid and sensitive method for the simultaneous analysis of TAGs and DAPCs and their oxidation products in a complex mixture such as egg. DHB is a suitable matrix for these compounds, mainly producing sodiated molecular ions and characteristic fragment ions.

The high mass accuracy (mass difference accuracy) of the FTMS data is used to determine the elemental composition of TAG and DAPC oxidation products. Indications were found for products of oxidative cleavage of triacylglycerols.

Triglycerides and diacylphosphatidylcholines are sensitive to light-induced oxidation as an increasing function of the degree of unsaturation. The results obtained on the light ageing series confirm the notion that oxygenation of glycerolipids plays an important role in the light ageing of tempera test systems. Moreover, the trend observed by MALDI-FTMS of the egg glycerolipids compares very well with that observed by DTMS and DA of the whole test system. The results provide a scientific basis for the use of test paintings as environmental monitors.

Exposure of egg glycerolipids to high concentrations of SO_2 and NO_x in the dark results in extensive oxidation. These observations suggest that the combination of exposure to light and sulphur oxides and nitrogen oxides imposes considerable oxidative stress on unsaturated glycerolipids.

The presence of basic lead carbonate and basic copper carbonate, which are common pigments in traditional egg tempera paint, leads to extensive oxidation of egg glycerolipids in the curing stage of an egg tempera paint.

References

1   Barclay, L. R. C., '1992 Syntex Award Lecture "Model biomembranes: quantitative studies of peroxidation, antioxidant action, partitioning, and oxidative stress"', *Can. J. Chem.* **71** (1993) 1-16.

2   Chan, H. W.-S., *Autoxidation of Unsaturated Lipids*, Academic Press, London (1987) 296 +x pp.

3   Frankel, E. N., *Lipid oxidation*, Vol. 10 The Oily Press, Dundee, Scotland (1998) 303 pp.

4   Corliss, G. A., and Dugan, L. R., 'Phospholipid oxidation in emulsions', *Lipids* **5** (1970) 846-853.

5   Mullertz, A., Schmedes, A., and Hølmer, G., 'Separation and detection of phospholipid hydroperoxides in the low nanomolar range by high performance liquid chromatography/ironthiocyanate assay', *Lipids* **25** (7) (1990) 415-418.

6   Murphy, R. C., and Harrison, K. A., 'Fats atom bombardment mass spectrometry of phospolipids', *Mass Spectrometry Reviews* **13** (1994) 57-75.

7   Facino, R. M., Carini, M., Aldini, G., and Colombo, L., 'Characterization of the intermediate products of lipid peroxidation in phosphatidylcholine liposomes by fast-atom bombardment mass spectrometry techniques', *Rapid Communications in Mass Spectrometry* **10** (1996) 1148-1152.

8   Harvey, D. J., 'Matrix-assisted Laser Desorption/Ionisation Mass Spectrometry of Phospholipids', *Journal of Mass Spectrometry* **30** (1995) 1333-1346.

9   Marto, J. A., White, F. M., Seldomridge, S., and Marshall, A. G., 'Structural characterization of phospholipids by matrix assisted laser desorption/ionization Fourier transform ion cyclotron resonance mass spectrometry', *Analytical Chemistry* **67** (1995) 3979-3984.

10   Cheng, C., Gross, M. L., and Pittenauer, E., 'Complete stuctural elucidation of triacylglycerols by tandem sector mass spectrometry', *Analytical Chemistry* **70** (1998) 4417-4426.

11   Simonsick Jr., W. J., and Ross III, C. W., 'The characterization of novel dispersants, fluorinated surfactants, and modified natural oils by laser desorption Fourier transform ion cyclotron mass spectrometry (LD-FTICR-MS)', *International Journal of Mass Spectrometry and Ion Processes* **157-158** (1996) 379-390.

12   Zöllner, P., Schmid, E. R., and Allmaier, G., 'K$_4$[Fe(CN)$_6$]/Glycerol- A new liquid matrix system for matrix-assisted laser desorption/ionization mass spectrometry of hydrophobic compounds', *Rapid Communications in Mass Spectrometry* **10** (1996) 1287-1282.

13   Asbury, G. R., Al-Saad, K., Siems, W. F., Hannan, R. M., and Hill Jr, H. H., 'Analysis of Triacylglycerols and Whole Oils by Matrix-Assisted Laser Desorption/Ionization Time of Flight Mass Spectrometry', *Journal of the American Society for Mass Spectrometry* **10** (1999) 983-991.

14   Duffin, K. L., Henion, J. D., and Shieh, J. J., 'Electrospray and Tandem Mass Spectrometric Characterization of Acylglycerol Mixtures That Are Dissolved in Nonpolar Solvents', *Analytical Chemistry* **63** (1991) 1781-1788.

15   Heeren, R. M. A., and Boon, J. J., 'Rapid microscale analyses with an external ion source Fourier transform ion cyclotron resonance mass spectrometer', *International Journal of Mass Spectrometry and Ion Processes* **157/158** (1996) 391-403.

16   van den Brink, O. F., Peulvé, S., and Boon, J. J., 'Dosimetry of paintings: Chemical changes in test paintings as tools to assess the environmental stress in the museum environment' in *SSCR Conference on Site effects: The impact of location on conservation treatments*, ed. M.M. Wright and I.M.T. Player-Dahnsjö, The Scottish Society for Conservation and Restoration, Edinburgh, Dundee, Scotland (1998) 70-76.

17   van den Brink, O. F., Peulvé, S., and Boon, J. J., 'Chemical changes in test paintings measure the environmental impact on the museum collection.' in *Art et Chimie, La Couleur*, ed. J. Goupy and J.-P. Mohen, CNRS Editions, Paris (2000) 121-125.

18   van den Brink, O. F., Eijkel, G. B., and Boon, J. J., 'Dosimetry of paintings: Determination of the degree of chemical change in museum exposed test paintings by mass spectrometry', *Thermochimica Acta* **365** (1-2) (2000) 1-23.

19   Kuksis, A., 'Yolk lipids', *Biochimica et Biophysica Acta* **1124** (1992) 205-222.

20   Marto, J. A., Correction of paper "Structural Characterization of phospholipids by matrix assisted laser desorption/ionization fourier transform ion cyclotron resonance mass spectrometry" (1997) personal communication.

21   Murphy, R. C., and Harrison, K. A., 'Isoeicosanoids: mass spectromerty of free radical oxidation products derived from arachidonoyl phospholipids' in *Mass Spectrometry in the Biological Sciences*, ed. A.L. Burlingame and S.A. Carr, Humana Press, Totowa, NJ, USA (1996) 451-476.

22   Kayganich-Harrison, K. A., and Murphy, R. C., 'Characterization of chain-shortened oxidized glycerophosphocholine lipids using fast atom bombardment and tandem mass spectrometry', *Analytical Biochemistry* **221** (1994) 16-24.

23   van den Brink, O. F., O'Connor, P. B., Duursma, M. C., Heeren, R. M. A., Peulvé, S., and Boon, J. J., 'Analysis of oxygenated egg lipids in tempera paint by MALDI FT-ICR-MS(MS)' in *14th International Conference on Mass Spectrometry*, ed. E.J. Karjalainen, A.E. Hesso, J.E. Jalonen, and U.P. Karjalainen, Advances in Mass Spectrometry, Vol. 14, Elsevier, Tampere, Finland (1997) POSTER C05 TUPO076.

24   van den Brink, O. F., Duursma, M. C., Boon, J. J., and Heeren, R. M. A., 'An ESI-FTMSMS Study of the Structure of Photo-oxidised Egg Glycerolipids.' in *15th International Conference on Mass Spectrometry*, ed. E. Gelpi, Advances in Mass Spectrometry, Vol. 15, Elsevier, Barcelona, Spain (2000) in press.

25   van den Brink, O. F., Duursma, M. C., Boon, J. J., and Heeren, R. M. A., 'An ESI-FTMSMS study of natural and photo-oxidized egg glycerolipids' in *48th ASMS Conference on Mass Spectrometry and Allied Topics*, ed. A.B. Giordani, Elsevier, Long Beach, CA, USA (2000) 138-139.

26   Neff, W. E., Frankel, E. N., and Miyashita, K., 'Autoxidation of polyunsaturated triacylglycerols. I. Trilinoleoylglycerol', *Lipids* **25** (1990) 33-39.

27   Grosch, W., 'Reactions of Hydroperoxides - Products of Low Molecular Weight' in *Autoxidation of Unsaturated Lipids*, ed. H.W.-S. Chan, Food Science and Technology, Academic Press, London (1987) 95-140.

28   Muizebelt, W. J., and Nielen, M. W. F., 'Oxidative crosslinking of unsaturated fatty acids studied with mass spectrometry', *Journal of Mass Spectrometry* **31** (1996) 545-554.

29   Muizebelt, W. J., Hubert, J. C., and Venderbosch, R. A. M., 'Mechanistic study of drying of alkyd resins using ethyl linoleate as a model substance', *Progress in Organic Coatings* **24** (1994) 263-279.

30   Gardner, H. W., 'Reactions of Hydroperoxides - Products of High Molecular Weight' in *Autoxidation of Unsaturated Lipids*, ed. H.W.-S. Chan, Food Science and Technology, Academic Press, London (1987) 51-94.

31   Boon, J. J., Peulvé, S. L., van den Brink, O. F., Duursma, M. C., and Rainford, D., 'Molecular aspects of mobile and stationary phases in ageing tempera and oil paint films' in *Early Italian Painting Technique*, ed. T. Bakkenist, R. Hoppenbrouwers, and H. Dubois, Limburg Conservation Institute, Maastricht, The Netherlands (1997) 32-47.

32   Gallon, A. A., and Pryor, W. A., 'The reaction of low levels of nitrogen dioxide with methyl linoleate in the presence and absence of oxygen', *Lipids* **29** (3) (1994) 171-176.

33   Pokorný, J., 'Major Factors Affecting the Autoxidation of Lipids' in *Autoxidation of Unsaturated Lipids*, ed. H.W.-S. Chan, Food Science and Technology, Academic Press, London (1987) 140-206.

34   Rasti, F., and Scott, G., 'The effects of some common pigments on the photo-oxidation of linseed oil-based paint media', *Studies in Conservation* **25** (1980) 145-156.

35   Rasti, F., and Scott, G., 'Mechanisms of antioxidant action: the role of copper salts in the photostabilisation of paint media', *European Polymer Journal* **16** (1980) 1153-1158.

36   Phenix, A., 'The composition of eggs and egg tempera' in *Early Italian Painting Technique*, ed. T. Bakkenist, R. Hoppenbrouwers, and H. Dubois, Limburg Conservation Institute, Maastricht, The Netherlands (1997) 11-20.

37   Khandekar, N., Phenix, A., and Sharp, J., 'Pilot study into the effects of solvents on artificially aged egg tempera films', *The Conservator* **18** (1994) 62-72.

38   Odlyha, M., Cohen, N. S., Foster, G. M., Campana, R., Boon, J.J., Van den Brink, O.F., Peulvé, S., Bacci, M., Picollo, M., and Porcinai, S., 'ERA, Environmental Research for Art Conservation' Final Report for the European Commission. University of London, Birkbeck College (London, U.K.), FOM Institute for Atomic and Molecular Physics (Amsterdam, NL) and Istituto di Ricerca sulle Onde Elettromagnetiche, CNR (Florence, IT), (1999) 210 + xc pp.

39   Odlyha, M., Boon, J. J., van den Brink, O. F., and Bacci, M., 'Environmental research for art conservation (ERA)', *Journal of Thermal Analysis* **49** (1997) 1571-1584.

40   Porter, N. A., Wolf, R. A., and Weenen, H., 'The free radical oxidation of polyunsaturated lecithins', *Lipids* **15** (1981) 163-170.

41   O'Brien, R. J., 'Oxidation of Lipids in Biological Membranes and Intracellular Consequences' in *Autoxidation of Unsaturated Lipids*, ed. H.W.-S. Chan, Food Science and Technology, Academic Press, London (1987) 233-280.

42   Peulvé, S., Boon, J. J., Duursma, M. C., van den Brink, O. F., O' Connor, P. B., and Heeren, R. M. A., 'Mass spectrometric studies of proteins in fresh egg and aged egg tempera paint films. Progress report I.' in *14th International Mass Spectrometry Conference*, ed. E.J. Karjalainen, A.E. Hesso, J.E. Jalonen, and U.P. Karjalainen, Advances in Mass Spectrometry, Vol. 14, Elsevier, Tampere, Finland (1997) POSTER C02 WEPO051.

43   Fukuzawa, K., Iemura, M., and Tokumura, A., 'Lipid peroxidation in egg phosphatidylcholine liposomes: comparative studies on the induction systems Fe^{2+}/ascorbate and Fe^{3+}-chelates/xanthine oxidase', *Biol Pharm. Bull.* **19** (5) (1996) 665-671.

44   Zimmerman, G. A., Prescott, S. M., and McIntyre, T. M., 'Oxidatively fragmented phospholipids as inflammatory mediators: The dark side of polyunsaturated lipids', *The Journal of Nutrition* **125** (1995) 1661S-1665S.

7. Electrospray ionisation FT-ICR-MS(MS) of light-aged egg glycerolipids

Comparative MALDI-FT-ICR-MS data on light-induced oxidation of egg glycerolipids in paint systems reported in the previous chapter were used to quantify the degree of oxygenation of egg glycerolipids in a series of light-aged egg tempera paint systems. Electrospray ionisation FT-ICR-MSMS is now applied for a more detailed study of the changes in the egg glycerolipids.

ESI-FTMS of a mixture of egg glycerolipids extracted from unexposed and light-aged egg-only tempera samples was carried out with great ease using ammonium acetate to facilitate the production of positively charged ions. As a result diacylglycerols, triacylglycerols, diacylphosphatidylcholines and lysophosphatidylcholines were detected and their oxygenation products were identified in the extracts of the light-aged egg samples. In addition a variety of oxidative cleavage products of triacylglycerols and diacylphosphatidylcholines were identified in the light-aged sample.

ESI-FTMSMS studies of fresh and light-aged glycerolipids could be carried out with great ease, because of the efficiency and relative stability of the ion production. Resonant excitation CID-MSMS of molecules observed in the fresh egg glycerolipids reveals their fatty acid speciation, and the data can even be used to determine the position of the fatty acid residues on the glycerol backbone. The high mass resolution of the FTMSMS data is indispensable for the interpretation of the MSMS spectra of such complex mixtures as oxidised egg glycerolipids. MSMS data of the oxygenated triglycerides indicate which of the fatty acyl moieties have been oxidised. This provides particularly interesting information when multiply oxygenated glycerolipids are studied. Not only the more sensitive doubly unsaturated fatty acyl moieties are oxidised but also the less sensitive singly unsaturated fatty acyl groups. This chapter furthermore presents the successful application of ESI-FTMS(MS) to identify hydroxyl and hydroperoxyl groups by analysis of trimethylsilyl derivatised extracts of light-aged egg-only tempera samples.

7.1 Introduction

A comprehensive overview of the methodology of triglyceride analysis is presented in a series of books on lipids methodology edited by Christie [7-11]. The fatty acid speciation of natural oils is usually investigated by gas chromatography – mass spectrometric (GCMS) analysis of the transesterified fatty acid moieties of the triacylglycerols (TAGs). This method must be preceded by separation of the different TAGs, e.g. on the basis of the number of unsaturations by TLC, in order to study the triacylglycerol (TAG) composition of oils. Thin-layer chromatography is often applied for the analysis of phosphatidylcholines and phosphatidylethanolamines [1]. Since the 1980s liquid chromatography was more often used for the separation of phospholipids. Singleton and Pattee [2], for instance, used HPLC for the separation of peanut oil TAGs and analysed the fractions by GC or electron impact MS. Rezanka *et al.* [3] utilised GC, HPLC and DCI-MS in a comparative study on the quantitative analysis of plant oils and concluded that the combination of these techniques made qualitative and quantitative analysis of plant oils feasible. With the aim to determine the elution factors of TAG oxidation products, Sjövall *et al.* [4] used ESI-MS for the identification of (synthesised) TAG oxidation products, such as hydroperoxides, hydroxides, epoxides and core aldehydes that were separated by HPLC. The same technique (LC-ESI-MS) proved very useful for the analysis of mixtures of phospholipids [5] or oxidised phosphatidylcholine [6].

FTMS and FTMSMS of glycerolipids has already been demonstrated in combination with MALDI as ionisation technique [12-14]. The aim of the research presented in this chapter is to investigate the fatty acid speciation of native and oxygenated TAGs by ESI-FTMSMS. The efficiency of the ion production by ESI was considered to be an advantage for high resolution MSMS studies. Earlier, Duffin *et al.* [15] applied ESI-MSMS for the characterisation of mixtures of native TAGs. Cheng and Gross [16] have demonstrated that complete structural elucidation of natural *non-oxygenated* TAGs can be accomplished by (ESI)-MSMS on a four sector instrument at a resolving power of approximately 1000. Complete structural elucidation or even determination of the fatty acid speciation of *oxygenated* TAGs is much more complicated because there is isobaric overlap (on unit mass) of native TAGs with doubly oxygenated TAGs (see also **Chapter 6**). Hence, either pre-separation or the high mass resolution of an FTMS is necessary to resolve these isobars.

The first part of this chapter (**section 7.3**) presents results of direct ESI-FTMS analysis of mixtures of glycerolipids and discusses the advantages of the method. The second part (**section 7.4**) reports the exploratory use of ESI-

FTMSMS to derive information on the fatty acid speciation of natural and oxygenated TAGs from unexposed and light-aged egg samples. Oxygenation introduces a great variety of oxygen containing functional groups that cannot be identified by (low energy) CID-MSMS. In order to identify the presence of hydroxyl or hydroperoxyl functionalities on the oxygenated fatty acyl moieties, ESI-FTMSMS was carried out on a trimethylsilyl derivatised sample of light-aged egg-only tempera. Trimethylsilyl derivatised oxygenated TAGs were efficiently ionised by ESI, which was a prerequisite for the success of that approach. Secondly, the fragmentation of derivatised oxygenated TAG pseudo-molecular ions must produce structurally significant ions (e.g. DAG fragments) from the TAGs. The results of the direct ESI-FTMS and some data on ESI-FTMSMS of trimethylsilyl derivatised extracts of light-aged egg-only tempera samples are presented in the third part of this chapter (**section 7.5**).

7.2 Experimental

7.2.1 Materials and sample preparation

The preparation of the egg samples analysed by ESI-FTMS is described in **Chapter 1**. Two different samples were used, viz. the unexposed control sample of egg on Melinex and the 16-day light-aged sample of egg-only tempera. These samples had been stored in polypropylene cryovials from HCI (Hedel, The Netherlands) at room temperature for approximately four years after their preparation.

For the MSMS experiments on derivatised and underivatised oxidised egg a sample of the unexposed egg (prepared as described in **Chapter 1**) was exposed to elevated levels of visible light in the MOLART light ageing facility at the Limburg Conservation Institute (SRAL) in Maastricht, The Netherlands. The ageing facility uses 12 Philips TLD-36W/96 fluorescent daylight tubes to illuminate a surface of 1.2 m^2. The resulting light intensity during the 21 days' exposure of the egg sample was 10,200 lx. Perspex (PMMA) filters were used to absorb most of the already low intensities of UV radiation produced by the fluorescent lights. Because the light ageing facility is placed in an air-conditioned room, the temperature and relative humidity could be maintained at constant values of 22°C and 40-44%, respectively.

α-Palmitoyl-β,γ-distearoylglycerol, α-palmitoyl-β-oleoyl-γ-stearoylglycerol and α-palmitoyl-β-oleoyl-γ-linoleoylglycerol was obtained from Sigma-Aldrich Chemie (Steinheim, Germany). Fresh free-range eggs (approximately 1 day old) were obtained from Frank Langedijk's chicken farm in Hoorn (The Netherlands).

To extract the glycerolipids from an egg-only tempera sample, an aliquot was separated from its Melinex support and extracted with approximately 800 times its weight in dichloromethane : ethanol (7:3, v/v). Before analysis equal volumes of the extract were mixed with a 20 mM solution of ammonium (or sodium) acetate in dichloromethane : ethanol (7:3, v/v).

7.2.2 Trimethylsilane (TMS) derivatisation

Dichloromethane:ethanol extracts of 16-day light-aged or 21-day light-aged egg-only tempera were subjected to TMS derivatisation according to the procedure specified in the experimental section of **Chapter 5**. After derivatisation and evaporation to dryness, the samples were redissolved in dichloromethane : ethanol (7:3, v/v) (the volume equal to the original volume of the extract). To prepare samples for ESI-FTMS(MS) analysis, a volume of the supernatant was mixed with an equal volume of a 20 mM solution of ammonium (or sodium) acetate in dichloromethane : ethanol (7:3, v/v).

7.2.3 ESI-FTMS

FTMS analysis was performed on a modified Bruker Spectrospin (Fällanden, Switzerland) APEX 7.0e (7 Tesla) FT-ICR-MS instrument with a home-built external ion source for CI, EI, FAB, MALDI and ESI [17] and a home-built open ICR-cell [18]. Electrospray ionisation on the five-stage differentially pumped instrument was largely carried out as described by Koster *et al.* [19] and by Heeren [20]. For ESI, a 50 μm i.d. New Objective Pico Tip™ nanospray needle (Cambridge, MA, USA) with an 8 μm tip and golden coating was filled with extract of the egg-only tempera sample. It is placed at a distance of 2-3 mm from the heated desolvation capillary (20 cm x 0.75 mm i.d., from Alltech, Deerfield, IL, USA) which was kept at a potential of 100 V. Positively charged droplets were emitted from the spray needle by application of a 1300 V potential on the needle. The capillary into which the charged droplets were sprayed was located inside a ceramic tube bound with a tungsten wire through which a 1.8 A current was passed to keep the stainless steel capillary at a temperature of 170°C. The end of the capillary (nozzle) was at a distance of approximately 5 mm from a 1.0 mm diameter copper skimmer surrounded by a 25 mm diameter tube lens. The

nozzle-skimmer potential applied in the experiments had a low value of typically 25 V, in order to limit nozzle-skimmer activation. As a result excess neutrals were removed from the beam exiting the capillary. The pressure in this first pumping stage was approximately 1 mbar. The second pumping stage (p = ~10^{-5} mbar) contained an RF-only quadrupole that was kept at a potential of 25 V so that the ions were stored in the quadrupole until the potential was decreased to allow the ions to enter the ICR-cell. Thus, the quadrupole potential was only low during the trapping event. On their way to the ICR-cell the ions passed another tube lens and an acceleration region where they were accelerated to 3000 V in order to prevent radial ejection by the magnetic field of the 7 T superconductive magnet containing the ICR-cell. The ions were decelerated to 1 eV before they entered the cell in which they were trapped. The trapping event was constituted by a low (0 V) potential on the source-proximal trapping electrodes of the cell, which were on 1 V under normal conditions.

During the trapping event Ar gas was allowed (pulsed) into the ICR-cell (p= 4 x 10^{-6} mbar, measured just outside the ICR-cell) to assist the trapping of the kinetic energy of the ions by collisional cooling. After a delay of 5 seconds to pump away the Ar gas and restore the pressure in the ICR-cell to its normal value of 10^{-9} mbar the ions were excited (250kHz bandwidth, lower m/z limit 429) and detected. The pressure difference between the exit of the quadrupole and the ICR-cell was bridged by three additional pumping stages. Acquisition and processing of the 128 k transients was performed by the Bruker XMASS software. The spectra presented in this chapter are the result of the summation of 50 scans (unless stated otherwise).

7.2.4 ESI-FTMSMS

ESI-FTMS(MS) experiments were performed on the same instrument. However, small adjustments were made to the operation of the electrospray. Instead of a nanospray needle, a 0.25 mm i.d. spray needle was used to create the electrospray. The spray needle was fed with analyte solution from a syringe driven by a Harvard model 55-1111 syringe pump (Kent, UK) at a flow rate of 0.1 ml/h. A potential of 3000 V was applied to the needle for the generation of positively charged droplets.

After trapping of the electrospray ions in the ICR-cell, a tailored excitation waveform was applied to eject all the ions from the cell except the ions with the m/z of interest. This was accomplished using the FOM designed and built Arbitrary Waveform Generator (AWG). The design and performance of the FOM AWG are described by Van Rooij [21]. Calculation of the excitation waveform and operation of the AWG were performed using our in-house

developed ICR-AWG dedicated software. In order to facilitate the interpretation of the MSMS spectra both the mono-isotopic peak (all-^{12}C) and the first isotope peak (^{13}C$_1$) were selected when samples of light-aged egg-only tempera were analysed.

After selection, the ions were resonantly excited and collided with Ar gas (p=3.6 x 10^{-6} mbar). The resulting fragment ions were excited (1MHz excitation bandwidth; lower m/z limit 110) and detected using the normal Bruker detection sequence described above. The results of 10 experimental sequences were summed to generate the spectra presented (unless stated otherwise).

7.3 ESI-FTMS of light-exposed and unexposed egg samples

7.3.1 7.3.1 Unexposed egg

The ESI-FTMS spectrum of the extract of the unexposed egg sample is shown in **Figure 1**. The mass window between m/z 750 and 1000 shows triacylglycerols and diacylphosphatidylcholines. Because ammonium acetate was used for cationisation of the glycerolipids, triacylglycerols are detected as ammonium cationised molecules ([M+NH$_4$]$^+$) and phosphatidylcholines are detected as protonated molecules ([M+H]$^+$). Fragments of phosphatidylcholine pseudo-molecular ions formed by loss of trimethylamine that were observed in the MALDI spectra of the same egg sample [22] (see **Chapter 6**) are not seen in the ESI spectra, because the internal energy deposition is less under ESI conditions. Although the ESI spectrum shows peaks at masses higher than m/z 1200, this part of the mass spectra is not discussed here because it is unclear whether these peaks are due to cluster formation of lipids during the ionisation process or originate from other dichloromethane/ethanol extractable material such as polymerised glycerolipids. This mass window will be subject of future investigations. Peaks in the spectrum are identified on the basis of exact mass, tolerating a difference between the measured m/z and the exact mass of a glycerolipid of ± 0.005 amu. The presence of the first isotope peak (one ^{13}C per molecule) was an additional prerequisite for identification.

The first three columns of **Table 1** list the compounds identified in the FTMS spectrum of the unexposed egg-only tempera sample. Columns 4 through 10 do the same for the FTMS spectra of the underivatised and the derivatised 16-day light-aged egg-only tempera (*vide infra*). Here we focus on the data obtained

on the unexposed egg-only tempera sample (i.e. columns 1 through 3). The compounds identified are grouped according to lipid class (specified in bold). Within each group the compounds are ordered according to their increasing carbon number. The number of C-atoms per molecule is given in the first column. The second column gives the degree of unsaturation. The number of oxygen atoms that are not part of an ester bond or of a phospho-group in the molecule is given in the third column. In the partial spectrum shown in **Figure 1A** a greater variety of triacylglycerols (TAGs) can be identified compared to the MALDI-FTMS approach. TAGs with 51 C-atoms, for instance, that were not observed by MALDI of the same sample [22] are observed at low abundance in the ESI spectra. Furthermore, TAGs with 59 or 61 C atoms and 3 to 7 unsaturations show pseudo-molecular ions at m/z 922-932 and m/z 950-958. These TAGs have not been reported in the literature on the glycerolipid composition of hen's eggs [23]. The fact that these TAGs are observed here can be attributed to the high sensitivity of ESI-FTMS or to a peculiarity of the eggs used in our experiments. As the same peaks were also observed in fresh eggs (data not shown), it is concluded that the detection is due to the high sensitivity of ESI-FTMS.

Compared to the MALDI results, ESI also detects a greater variety of diacyl phosphatidylcholines (DAPCs). DAPCs with 46 carbons and 4 to 6 unsaturations and DAPCs with 48 carbons with 4 to 7 unsaturations are only observed in the ESI mass spectrum. As these species only contain two fatty acyl chains, the number of unsaturations per fatty acyl chain must be high. According to Kuksis [23] the highly unsaturated fatty acyl moieties arachidonoyl (20:4), docosatetraenoyl (22:4), docosapentaenoyl (22:5) and docosahexaenoyl (22:6) are present in these DAPCs. These fatty acids are known to be very prone to oxidation. Their detection implies that the conditions under which the samples have been stored for four years after their preparation (cryovials under ambient conditions) have been very efficient in the protection against oxidative processes. The fact that a greater variety of glycerolipids is detected in the ESI-FTMS spectra compared to the MALDI spectra is attributed to the higher sensitivity of the ESI-FTMS set-up. This is a combined effect of the use of the open cell and the application of quadrupolar accumulation of electrospray ions before FTMS detection. An additional effect may be that the ESI process generates ions more efficiently than the MALDI process.

The relative intensities within the clusters of peaks of TAGs and DAPCs observed in the ESI are similar to those observed in the MALDI spectra (**Chapter 6 Figure 2**). The relative intensities of the TAG and DAPC clusters themselves cannot be compared due to differences in ionisation efficiency in the ESI process [15] and due to the time of flight effect in the external MALDI-FTMS [17, 24].
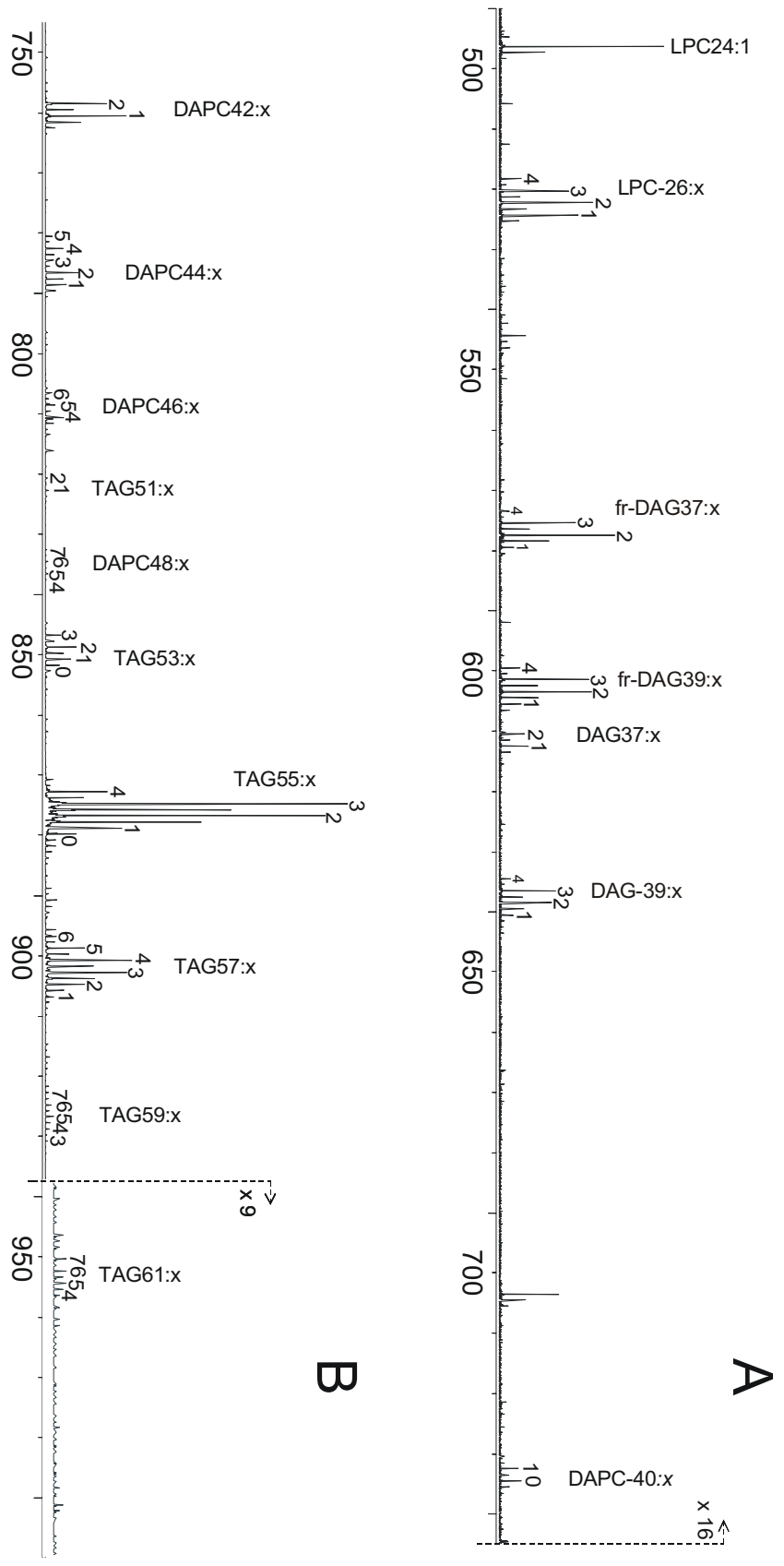
Figure 1 *FTMS spectrum of unexposed egg-only tempera: (A) the triacylglycerol and diacylphosphatidylcholine mass window (m/z 490-750) and (B) the diglyceride mass window (m/z 750-1000). The spectrum presented is the result of summation of 25 single scan spectra.*

Next to the most abundant clusters in **Figure 1** at m/z 888-896 (TAG55) and m/z 912-920 (TAG57), at a distance of approximately 16 amu, peak clusters are observed at low relative intensity. Similar observations were made by Duffin *et al.* [15] on a mixture of unknown lipids. Although the mass resolution of their measurements was not sufficient to discriminate between a TAG-n:x (n C atoms and x unsaturations) and a TAG-(n-1):(x+1)+O (Δm/z = 0.0364) it was concluded without further verification by Duffin *et al.* that such peaks originate from TAGs containing fatty acyl groups with an odd number of carbons. They do not mention the possibility that the more sensitive unsaturated TAGs in their samples could be oxidised. The mass accuracy of the FTMS data obtained on our unexposed egg-only dosimeters allows identification of low intensity clusters at m/z 888-896 and m/z 912-920. The peaks are identified as single oxygenation products of the most abundant TAGs (viz. TAG55 and TAG57).

The mass window between m/z 490 and 650 (**Figure 1B**) shows peaks that can be attributed to diacylglycerols (DAGs) present in the sample and to diacylglycerol fragment ions derived from TAGs and DAPCs due to nozzle-skimmer activation in the ESI ion source. The DAG fragment ions are observed as protonated species and are formed from ammonium cationised TAGs by neutral loss of a fatty acid plus ammonia or from protonated DAPCs by neutral loss of the phosphocholine group ($HPO_4(CH_2)_2N(CH_3)_3$). Clearly, native DAGs originally present in the sample can be discriminated from DAG fragments because they contain one more oxygen atom (from the hydroxyl functionality on the sn-1 or sn-2 position of the glycerol) and two more hydrogen atoms. The discrimination between native DAGs and DAG fragments on the basis of the cationic adduct (H^+ or NH_4^+) can be advantageous in the interpretation of spectra of oxidised egg-only tempera samples (*vide infra*).

Although lysophosphatidylcholines are reported to constitute a total of less than 1% of the glycerophospholipid fraction in egg yolk [23], they are clearly observed in the ESI-FTMS spectrum (m/z 496 and m/z 518-524). The LPCs represent approximately 1.4% of the total intensity of the spectrum. LPC peaks were observed in the ESI-FTMS spectrum of fresh eggs and represented approximately 0.8% of the total intensity. This difference in intensity of the LPCs can be due to biological variability in the LPC content of eggs or to hydrolysis during preparation (mixing and spreading on Melinex) and storage of the egg-only tempera. The latter may also explain the observation of DAGs in the untreated egg sample, because DAGs are not reported as constituents of fresh eggs. The observation that the DAPCs and LPCs are protonated in the ESI process and DAGs and TAGs are ammoniated, suggests that cationisation takes place on the phosphocholine group of these glycerophospholipids instead of on the ester group(s).

Table 1 *Overview of compounds identified in the FTMS spectra of unexposed and 16-day light-aged egg-only tempera.*

Diglyceride fragments [TAG+NH$_4$-(FA+NH$_3$)]$^+$

Control			16-day light-aged			16-day light-aged silylated			
#C	#uns	# O	#C	#uns	# O	#C	#uns	# O	TMS
37	0-3		37	1, 2					
			37	2	1				
39	1-4		39	1-3					
			39	3	1				

Diacylglycerols [DAG+NH$_4$]$^+$

Control			16-day light-aged			16-day light-aged silylated			
#C	#uns	# O	#C	#uns	# O	#C	#uns	# O	TMS
37	1, 2		37	1		37	1		1
			37	1, 2	1	37	2	1	1
						37	1, 2	1	2
39	1-4		39	1, 2		39	1, 2		1
			39	1-3	1	39	2, 3	1	1
			39	3	2				

Lysophosphatidylcholines [LPC+H]$^+$

Control			16-day light-aged			16-day light-aged silylated			
#C	#uns	# O	#C	#uns	# O	#C	#uns	# O	TMS
24	1		24	1		24	1		1
26	1-4		26	1-4		26	1, 2		1
			26	2, 3	1				

Diacylglycerophosphocholines [DAPC+H]$^+$

Control			16-day light-aged			16-day light-aged silylated			
#C	#uns	# O	#C	#uns	# O	#C	#uns	# O	TMS
			31	1	2[b]				
			32	1	2[b]				
			33	1	2[b]				
			35	1,2,4	2[b]				
			36	2	3[b]				
40[b]	0-2		40	0, 1					
42	1, 2		42	1, 2					
42	2	1	42	1-3	1	42	1	1	1
			42	1-3	2[b]				
44[b]	1-5		44	1, 2		44	1		
			44	1-4	1[b]				
46[b]	4-6								
48[b]	4[a]–7[a]								

[a] compound not reported in the literature [23]. [b] cluster contains compound(s) not detected by MALDI-FTMS [22] (specified for DAPCs and TAGs only) [c] compound that indicates cross-linking.

Table 1 *(Continued).*

Triacylglycerols [TAG+NH₄]⁺ (oxidative cleavage products)

Control			16-day light-aged			16-day light-aged silylated			
#C	#uns	# O	#C	#uns	# O	#C	#uns	# O	TMS
			46	1-3	2	46	1, 2	2	
			46	2-4	3	46	2-3 3	3	0 1
			47	2, 3	2 [b]				
			48	2, 3	1 [b]				
			48	1-3	2 [b]				
			48	2-4	3 [b]				
			49	3-4	4 [b]				

Triacylglycerols [TAG+NH₄]⁺

Control			16-day light-aged			16-day light-aged silylated			
#C	#uns	# O	#C	#uns	# O	#C	#uns	# O	TMS
51	0-2		51	0, 1					
53	1-4		53	0-2		53	1, 2		
			53	1-3	1 [b]	53	2, 3 1, 2	1	0 1
55	0-4		55	0-3		55	1-3		
55	2-4	1	55	1-4	1	55	1-4 2, 3	1	0 1
			55	1-5	2 [b]	55	3-5 2-4 2, 3	2	0 1 2
			55	1-5	3 [b]	55	2, 3 2, 3 2, 3	3	1 2 3
			55	1-4	4 [b]	55	3, 4 2, 3 2	4	2 3 4
			55	2-4	5 [b]				
			55	2-4	6 [b]				
57	1-6		57	1-3		57	1-3		
57	3-5	1	57	2-4	1	57	2-4	1	
			57	2-5	2 [b]	57	2-4 2, 3	2	1 2
			57	2-5	3 [b]	57	3, 4 2, 3	3	2 3
			57	2-5	4 [b]	57	3 3	4	3 4
			57	3-5	5 [b]				
59 [a,b]	3-7								
			60	1-3	2 [b,c]				
61 [a,b]	4-7								
			61	2, 3	2 [b,c]				

159

7.3.2 Light-exposed egg

Figure 2A shows the TAG and DAPC mass window (m/z 750 – 1000) of the ESI-FTMS spectrum of 16-day light-aged egg-only tempera. In this spectrum a greater variety of TAG and DAPC oxidation products is observed than when MALDI was used [22]. In the MALDI spectra presented in the **previous chapter** up to fourfold oxygenation of TAGs was observed. The ESI-FTMS data show up to sixfold oxygenation of TAGs. Furthermore, a greater variety of oxidative cleavage products of TAGs appear in the mass window between m/z 780 and 830. At m/z 794 a quartet of peaks is detected (see inset) in which the peaks are separated by 0.036 amu. This mass difference agrees with the exchange of one oxygen (15.995) against one CH_2 group plus H_2 (16.031). Thus, the quartet was assigned as follows: m/z 794.582, $[(TAG45:5+4O)+NH_4]^+$ (exact mass 794.578); m/z 794.615, $[(TAG46:4+3O)+NH_4]^+$ (794.614); m/z 794.652, $[(TAG47:3+2O)+NH_4]^+$ (794.650); m/z 794.690, $[(TAG48:2+O)+NH_4]^+$ (794.687). Note that the identification of the first peak of this quartet is tentative, because its first isotope peak shows a very low intensity (s/n ~ 1.3). Similar multiplets are observed at m/z 796 and 812.

As mentioned above, intact DAGs present in the sample can be discriminated from DAG fragments of oxygenated TAGs and DAPCs on the basis of the cation. This is particularly relevant for the light-aged sample because here also TAG+O are abundantly present and these can also fragment by loss of a fatty acid. If the DAG fragments could not be identified on the basis of the cation, e.g. when sodium is used for cationisation, a $[(TAG55:x+O)+Na-16:0]^+$ fragment ion would overlap with a genuine $[DAG39:(x+1)+Na]^+$ ion. **Figure 2B** shows the lower mass window (m/z 490-750) of the ESI-FTMS spectrum of 16-day light-aged egg. DAGs are observed at m/z 612-613 (DAG37:1) and m/z 638-641 (DAG39:1 and DAG39:2). Fragments of singly oxygenated TAGs (and DAPCs) are observed at m/z 591-592 (fr-DAG37:2+O) and m/z 617-618 (fr-DAG39:3+O).

Other compound classes observed in **Figure 2** include LPCs (m/z 490-530), oxygenated LPCs (m/z 536-539), singly oxygenated DAGs (m/z 620-660), a doubly oxygenated DAG39:3 (m/z 668-669), oxygenated DAPCs (m/z 770-810) and oxidative cleavage products of DAPCs (m/z 630-730). Columns three to six in **Table 1** list of the components that are identified in the 16-day light-aged sample. Specific details are discussed in the next section.

Figure 2 *FTMS spectrum of 16-day light-aged egg-only tempera: (A) the triacylglycerol and diacylphosphatidylcholine mass window (m/z 750–1000) and (B) the diglyceride mass window (m/z 490–750). Doublets are marked with *. The inset shows a quartet of peaks at m/z 794. Twenty-five spectra were summed.*

7.3.3 *Chemical interpretation of the molecular changes observed upon light exposure*

The vast majority of the oxidative cleavage products contain between 46 and 49 carbon atoms. The TAG46 and TAG48 are the most abundant oxidative cleavage products. This suggests that oxidative cleavage occurs primarily by loss of C_9 moieties from the TAG55 and TAG57 and to a lesser extent by loss of C_8 moieties. Thermal decomposition studies of fatty ester peroxides by Frankel *et al.* [25] have identified methyl-9-oxononanoate as the major thermal decomposition product of peroxidised methyl linolenate (9,16-dihydroperoxy-octadecatrienoate). The decomposition schemes proposed by these authors suggest that oxidative cleavage (decomposition) takes place mainly at the site of peroxidation, involving simultaneous cleavage of the O—OH bond and the R'C—C(OOH)R bond on the aliphatic side of the acid group. It must be noted, however, that Frankel also found other decomposition products. Not surprising perhaps because the temperature at which decomposition was forced in their experiments was 200°C. As the light-aged samples analysed in the present study have not been heated but stored at ambient temperatures, it is plausible that decomposition is only taking place slowly. The results obtained on the light-aged egg samples indicate that peroxide functionalities have been present mainly on the C9 and C10 positions. This is also the most frequently occurring position of a double bond in the unexposed native/natural samples as oleic acid, linoleic acid and linolenic acid all have a double bond on the C9 position. According to Frankel [26] the main primary photo-oxidation products of oleic acid (9-octadecenoic acid) are 10-hydroperoxy-9-trans-octadecenoate and 9-hydroperoxy-10-trans-octadecenoate. Autoxidation is reported to lead to a greater variety of processes. Therefore, the current results are taken as an indication that the oxidation of the exposed sample is mainly caused by photo-oxidation.

In many cases oxidised TAGs are observed in which the number of oxygen atoms exceeds the number of unsaturations (e.g. TAG55:2+4O). Hence, it must be concluded that functionalities such as hydroperoxides, epidioxides, diols, and triols are present in the oxidised samples. Hydroperoxide is very probable because it is very often reported in the literature [26, 27] as primary oxidation product and as such it is a well-known precursor of oxidative cleavage products [25]. Diols and triols are reported to occur as breakdown products of linoleic acid hydroperoxides [26, 28]. Hydroperoxy-epidioxides are only reported as progressed oxidation products of linolenate [26]. Linolenic acid moieties are present at low abundance in egg yolk [23]. Thus, based on the literature, hydroxy-epidioxide must be expected to be a rare functional group in the light-exposed egg.

Condensation reactions are also taking place upon light ageing of the egg-only tempera. The peaks at m/z 978.870 and m/z 976.854 for instance are attributed to [(TAG60:2+2O)+NH$_4$]$^+$ (exact mass 978.870) and [(TAG60:3+2O)+NH$_4$]$^+$ (exact mass 976.854) respectively. The peaks at m/z 990 and 992 are attributed to [(TAG61:3+2O)+NH$_4$]$^+$ and [(TAG61:2+2O)+NH$_4$]$^+$. Although the latter two compounds may result from double oxygenation of the TAGs-61, they are seen as indications for condensation reactions because the degree of unsaturation does not match with that of the TAG61:x in the unexposed sample (x=4-7). They are likely to originate from addition of C$_6$ molecules to TAG55:x (most abundant TAGs).

Doubly oxygenated DAPC42:x+2O (x=1-3) that were not detected in the 16-day light-aged sample by MALDI are now observed in the ESI-FTMS spectrum. It is a very small fraction however, so that the remark in **Chapter 6** made on the fate of phospholipid primary oxidation products remains valid. The highly unsaturated DAPC46 and DAPC48 are not detected anymore in the light-exposed sample. Primary oxygenation products of these very sensitive compounds are not observed either. Cho *et al.* [29] have found that the primary photo-oxidation products of fatty acids with more than three double bonds are relatively unstable. Their photo-oxidation studies have indicated that oligomeric material is formed. Cross-linking plays a role in the photo-oxidation of egg-only tempera as demonstrated in **Chapter 6**.

It is also very likely, and this was also considered by Cho *et al.*, that these DAPCs have undergone chain shortening in advanced stages of oxidation. Oxidative cleavage products of DAPCs are observed in the mass window m/z 630-700 in **Figure 2B**. An additional DAPC36:2+3O ([(DAPC36:2+3O)+H]$^+$; exact mass: 722.460) is observed at m/z 722.457. The oxidative cleavage products of DAPCs are also known as core aldehydes or platelet activating factor (PAF)-like phospholipids as reported by Zimmerman *et al.* [30]. The most intense peak of the oxidatively cleaved DAPCs is the [(DAPC33:1+2O)+H]$^+$ (exact mass: 666.434), observed at m/z 666.434. This compound is likely to mainly derive from DAPC42:x, the most abundant DAPCs in fresh egg, by loss of a C$_9$ chain and net uptake of two oxygen atoms. Tanaka *et al.* [31] who identified PAF-like phosphatidylcholines in peroxidised egg yolk PC, observed mainly hydroxide and carboxylic acid functionalities on the fatty acyl chain where cleavage had taken place. Aldehyde and (oxygen free) hydrogen terminated chains were also observed. The α-position in egg yolk DAPC is often occupied by a saturated fatty acyl chain [23] that is not sensitive to oxidation. The β-position of the DAPC42 is occupied by an oleoyl or linoleoyl chain. Hence, the

literature suggests that the oxidative cleavage of DAPCs observed in the spectrum presented here contain acid functionalities.

Compared with the spectrum of the unaged egg, **Figure 2B** shows a higher intensity ratio of the DAGs and DAG fragment ions. This clearly indicates that the relative abundance of diglycerides has increased upon light exposure. Analysis of the egg systems by other techniques such as DTMS [32, 33] (see also **Chapter 3**) and differential scanning calorimetry [32] confirm that hydrolysis is one of the processes that take place upon light ageing of the egg systems.

Changes in the LPC fraction are evidenced by a decrease in the degree of unsaturation of the LPCs and the formation of oxidation products such as LPC26:3+O ([(LPC26:3+O)+H]$^+$, exact mass 536.336) and LPC26:2+O ([(LPC26:2+O)+H]$^+$, exact mass 538.350) observed at m/z 536.336 and m/z 538.352. Because LPCs are detected as protonated molecules discrimination between LPCs and fragments of oxygenated DAPCs formed by loss of a fatty acid is not possible. Recall, however, that the most important fragmentation pathway of DAPC pseudomolecular ions is neutral loss of trimethylamine (N(CH$_3$)$_3$) or loss of the phosphocholine group [14, 34]. DAPC fragment ions due to loss of trimethylamine are not observed in the spectrum. Moreover, the intensity of the DAG fragments is lower than that of the LPCs. Therefore, the increased relative intensity of the LPCs in the ESI-FTMS spectrum of light-aged egg is seen as an indication that light ageing of the egg systems results in hydrolysis of the DAPCs.

7.4 *Part B: CID-MSMS of TAGs and selected peaks in the ESI-FTMS spectra*

7.4.1 *7.4.1 MSMS of TAG standards*

The fragmentation behaviour of triglycerides was first studied using two commercially available TAGs, viz. α-palmitoyl-β-oleoyl-γ-stearoylglycerol and α-palmitoyl-β-oleoyl-γ-linoleoylglycerol. **Figure 3** shows the CID-MSMS spectrum of the ammonium adduct of the former compound ([TAG55:1+NH$_4$]$^+$; m/z 878.817). Note that this MSMS spectrum and the ones shown hereafter have a lower mass resolution (approx. 12,000 FWHM) than the spectra shown in **Figures 1 and 2**, because a broader detection bandwidth was used in order to also

detect the low mass fragments (down to m/z 110). In **Figure 3**, one fragment at m/z 861.646 originates from loss of ammonia, $[M+NH_4-NH_3]^+$. The main fragments observed are formed by loss of fatty acid (FA) neutrals plus ammonia $[M+NH_4-(FA+NH_3)]^+$. Thus, the peaks at m/z 605.477 and m/z 577.454 originate from loss of palmitic acid plus ammonia (exact mass 273.267) and stearic acid plus ammonia (exact mass 301.298) respectively. The relative intensity of the peak due to loss of ammonia plus oleic acid (exact mass: 299.282) from the β-position (m/z 579.468) is approximately half of that of the other two diglyceride fragments (sn-1:sn-2:sn-3 = 0.40:0.21:0.40). In order to be able to use the relative abundance of the DAG fragments for the determination of the position of the fatty acyl chains on the triglyceride backbone of a TAG, two requirements have to be met. Firstly, the intensity ratio of the fragments must be independent of the collision energy, over the energy range that corresponds with 0 to 100% of the survival yield of the parent ion. Second, the intensity ratio must be independent of length and degree of unsaturation of the fatty acyl chains.

Figure 3 *CAD-MSMS spectrum of ammonium-cationised α-palmitoyl-β-oleoyl-γ-stearoylglycerol (m/z 878). Resonant excitation time: 150 μs; kinetic collision energy: 130 eV. Three spectra were summed.*

The first criterion was tested by fragmentation of the TAG55:1 at several collision energies. In these experiments mono-isotopic selection of the parent ion was performed before MSMS in order to facilitate the determination of the fragment peak ratios. The resulting energy-resolved fragmentation diagram of the $[TAG55:1 +NH_4]^+$ parent ion is shown in **Figure 4.** Loss of only ammonia $([M+NH_4-NH_3]^+$, m/z 861) starts to occur at low excitation energies and decreases at kinetic energies above 130 eV. At slightly higher kinetic energies than the onset of the loss of ammonia the fragmentation by loss of an FA plus ammonia

165

([M+NH$_4$-(FA+NH$_3$)]$^+$, m/z 605, 579 and 577) occurs and becomes more dominant. Neutral loss of a fatty acid only is not observed; the loss of fatty acid neutrals is always accompanied by the loss of ammonia. This confirms the inference that the DAGs present in the sample can be discriminated from DAG fragments on the basis of the cation (*vide supra*).

The dashed curve in **Figure 4** gives the intensity ratio of the fragments due to neutral loss of a fatty acid plus ammonia from the β-position to the equivalent loss from the α or γ-position. The intensity ratio of the DAG fragment ions is constant (0.47 ± 0.02) at all energies resulting in a survival yield of the parent ion between 0 and 50%. This indicates that the intensity ratio of the DAG fragments can only be used to derive the position of the fatty acyl chains on the glycerol backbone of triglycerides, when collision energies within this range are used. We have noted that the consistent difference in abundance of the [M+NH$_4$-(FA+NH$_3$)]$^+$ ions observed here does not agree with the observation of a small difference in intensity by Cheng *et al.* [16]. This is possibly related to the higher excitation energy and the different time scales that were used in Cheng's experiments compared to ours.

Breakdown of m/z 878

Legend:
- ···△··· 878; X = TAG55:1 + NH4+
- ─■─ 861; X - NH3
- ─✳─ 605; X - (C16:0 + NH3)
- ─✕─ 579; X - (C18:1 + NH3)
- ─●─ 577; X - (C18:0) + NH3)
- ···□··· 2*579/(577+ 605)

Figure 4 *Energy resolved fragmentation diagram of the ammonium adduct of α-palmitoyl-β-oleoyl-γ-stearoylglycerol (m/z 878). The kinetic collision energy was varied by changing the resonant excitation time. (Vpp: 17.4 V) Three spectra were summed per data point.*

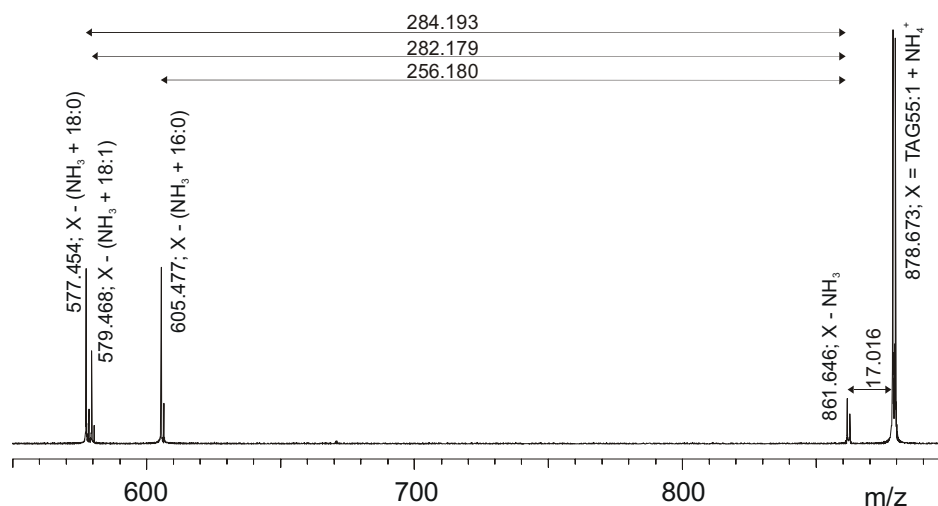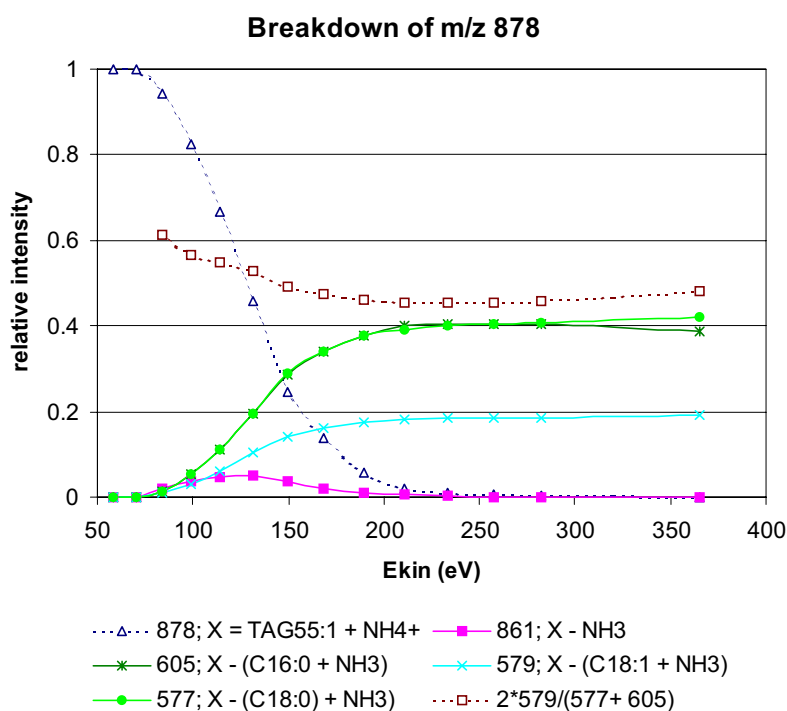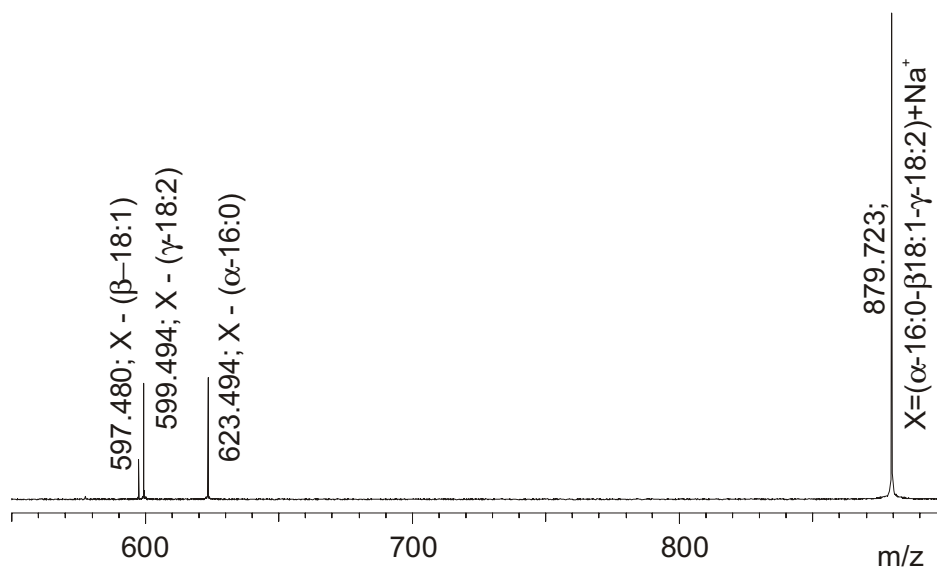**Figure 5** *CAD-MSMS spectrum of sodium-cationised α-palmitoyl-β-oleoyl-γ-linoleoylglycerol (m/z 879). Resonant excitation time: 150 μs; kinetic collision energy: 130 eV. Three spectra were summed.*

In order to test the second criterion, the ammonium adduct of α-palmitoyl-β-oleoyl-γ-linoleoylglycerol ([TAG55:3+NH$_4$]$^+$) was subjected to collision induced dissociated MSMS (data not shown). In addition to fragment peaks that originate from loss of ammonia ([M+NH$_4$-NH$_3$]$^+$) and ammonia plus one of the fatty acids ([M+NH$_4$-(NH$_3$+FA)]$^+$), the spectrum shows a peak resulting from the loss of ammonia plus water ([M+NH$_4$-(NH$_3$+H$_2$O)]$^+$) from the pseudo-molecular ion. It is likely that the loss of water is related to the presence of the doubly unsaturated linoleoyl chain, and its bivinylic hydrogen at C-11, which is known to be acidic. We consider the loss of water plus ammonia as a complicating factor in the interpretation of the CID-MSMS spectra of unknown (oxygenated) TAGs. CID-MSMS experiments carried out at a variety of kinetic energies of the parent ion (data not shown) indicate a strong energy dependence of the intensity ratio of the DAG fragments. To alleviate the problems with ammoniated ions, CID-MSMS of sodium adducts of standard TAGs was performed to investigate the energy-dependence and substituent-dependence of the DAG fragment intensity ratio. **Figure 5** shows the CID-MSMS spectrum of the sodium adduct of α-palmitoyl-β-oleoyl-γ-linoleoylglycerol. Three fragment ions are observed in this spectrum, which are attributed to loss of palmitic acid (m/z 623.494), linoleic acid (m/z 599.494) and oleic acid (597.480). The intensity ratio of the DAG fragment peaks was found to be constant at 0.29 ± 0.03 at collision energies corresponding to a 90% to 10% survival yield. Similarly the DAG fragment peak intensity ratio

for α-palmitoyl-β,γ-distearoylglycerol, and α-palmitoyl-β-oleoyl-γ-stearoyl-glycerol were found to be 0.34 ± 0.04 and 0.350 ± 0.002 respectively. These results indicate that low-energy CID-MSMS of sodium adducts of TAGs can be used to determine the position of fatty acyl chains on the glycerol backbone.

7.4.2 *MSMS of TAGs from the unaged egg sample*

The previous MSMS experiments were carried out on commercially available, chemically pure compounds. Complications are expected when MSMS is used to study the TAGs in complex mixtures such as light-aged egg. First of all the MSMS spectrum will be more complicated because the peaks are likely to originate from a mixture of compounds with the same elemental composition (in this case the same number of C-atoms and unsaturations). Secondly, when a mixture of TAGs with different degrees of unsaturation is analysed the second isotope peak (containing two ^{13}C atoms) of a TAG-n:(x+1) contributes to the mono-isotopic peak of a TAG-n:x. Unfortunately the resolution of the FTMS data obtained in broadband mode is not sufficient for baseline resolution of these two ions because of the small mass difference of 0.010 amu. This implies that MSMS of such a peak will not only give fragments of the TAG-n:x but also of the TAG-n:(x+1). Fortunately, the fragments from the second isotope peak of the TAG-n:(x+1) can be identified on the basis of their isotope pattern. Fragment peaks at m/z values higher than approximately two third of the m/z of the parent ion will have a second isotope peak that is higher than the first isotope peak. An example of this phenomenon will be given in the description of the MSMS results obtained on trimethylsilyl derivatised light-aged egg–only sample (*vide infra*). Fragment peaks at m/z values lower than approximately half the m/z of the parent ion will have a second isotope peak that is lower than the first isotope peak but still higher than would be expected for fragments of TAG-n:x at that m/z. In the mass window close to the m/z of the parent ion fragments from the second isotope peak of the TAG-n:(x+1) cannot be identified easily.

The purest and most elegant solution of this problem is isolation at high resolution. This puts strong requirements on the performance of the Arbitrary Waveform Generator (AWG) used to apply the SWIFT waveform. Van Rooij [21] has shown that the FOM AWG was successfully used to isolate the tenth isotope peak (10 ^{13}C atoms per molecule) of the 15[+] charge state of Cytochrome-C. High resolution isolation of the peak of interest was not applied here. Mass peaks were selected in which the contribution of the second isotope peak of a compound 2 Da lighter than the one of interest is negligible.

For example, **Figure 6** shows the CID-MSMS spectrum of the peak at m/z 879.759 in the spectrum of unexposed egg-only tempera. The spectrum shows

that this TAG55:3 peak does not originate from one pure compound but from a mixture of triglycerides. The low abundance of fragment ion at m/z 625.510 indicates that a small fraction of palmitoleoyl (16:1; exact mass 254.225) containing triglycerides must be present. The absence of a fragment formed by loss of stearic acid suggests that the majority of the palmitoleoyl (16:1) containing triglycerides must also contain two oleoyl groups. α-Palmitoleoyl-β,γ-dilinoleoylglycerol is reported to occur in egg at low relative abundance [23]. The presence of dilinoleoyl-palmitoleoyl-glycerol in the sample can only partly account for the observation that the intensity of the fragment formed by loss of oleic acid $[M+Na-(18:1)]^+$ (m/z 597.489) is significantly higher than that of the $[M+Na-(18:2)]^+$ (m/z 599.507). Hence the spectrum indicates that the main constituent of the TAG55:3 in egg is α-palmitoyl-β-linoleoyl-γ-oleoylglycerol. This is confirmed by the literature [23].
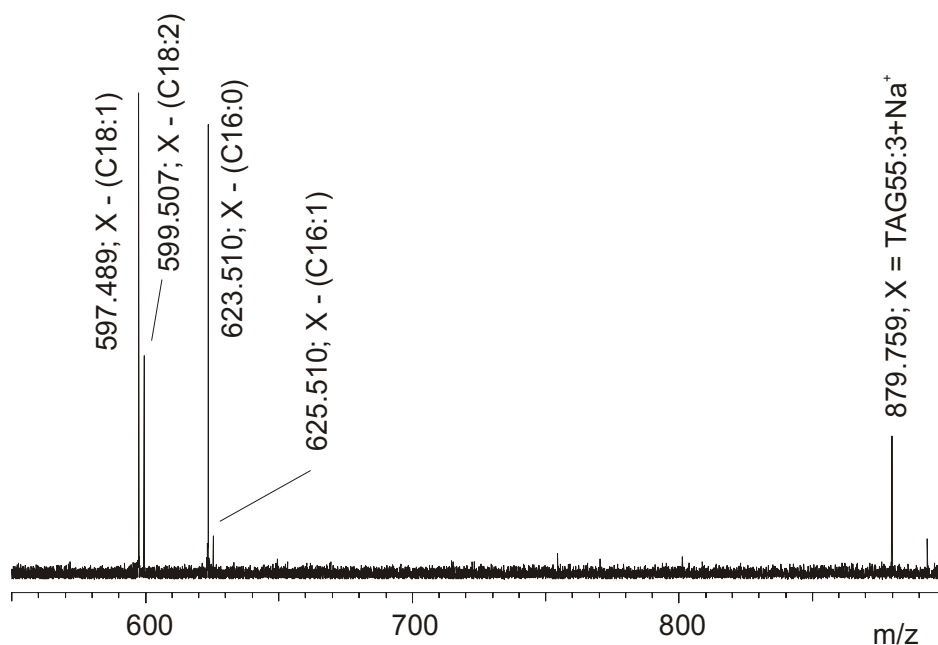
Figure 6 *CAD-MSMS spectrum of the peak at m/z 879 in the ESI-FTMS spectrum of unexposed egg-only tempera. Five spectra were summed.*

7.4.3 MSMS of oxygenated TAGs

The result of MSMS analysis of the $[(TAG55:3+O)+Na]^+$ peak at m/z 895 in the ESI-FTMS spectrum of light-aged egg-only tempera (21 days at 10,000 lx) is shown in **Figure 7A.** Two diglyceride fragment peaks appear in this MSMS spectrum, which are attributed to loss of palmitic (m/z 639.491) and oleic (m/z 613.477) acid moieties. On the basis of these two peaks it can be concluded that

169

the oxygen atom introduced upon light exposure must be part of a doubly unsaturated C18 fatty acid moiety.   Hence the fatty acid composition of the TAG55:3+O is 16:0/18:2+O/18:1; oxidation has taken place on the most unsaturated fatty acyl chain.
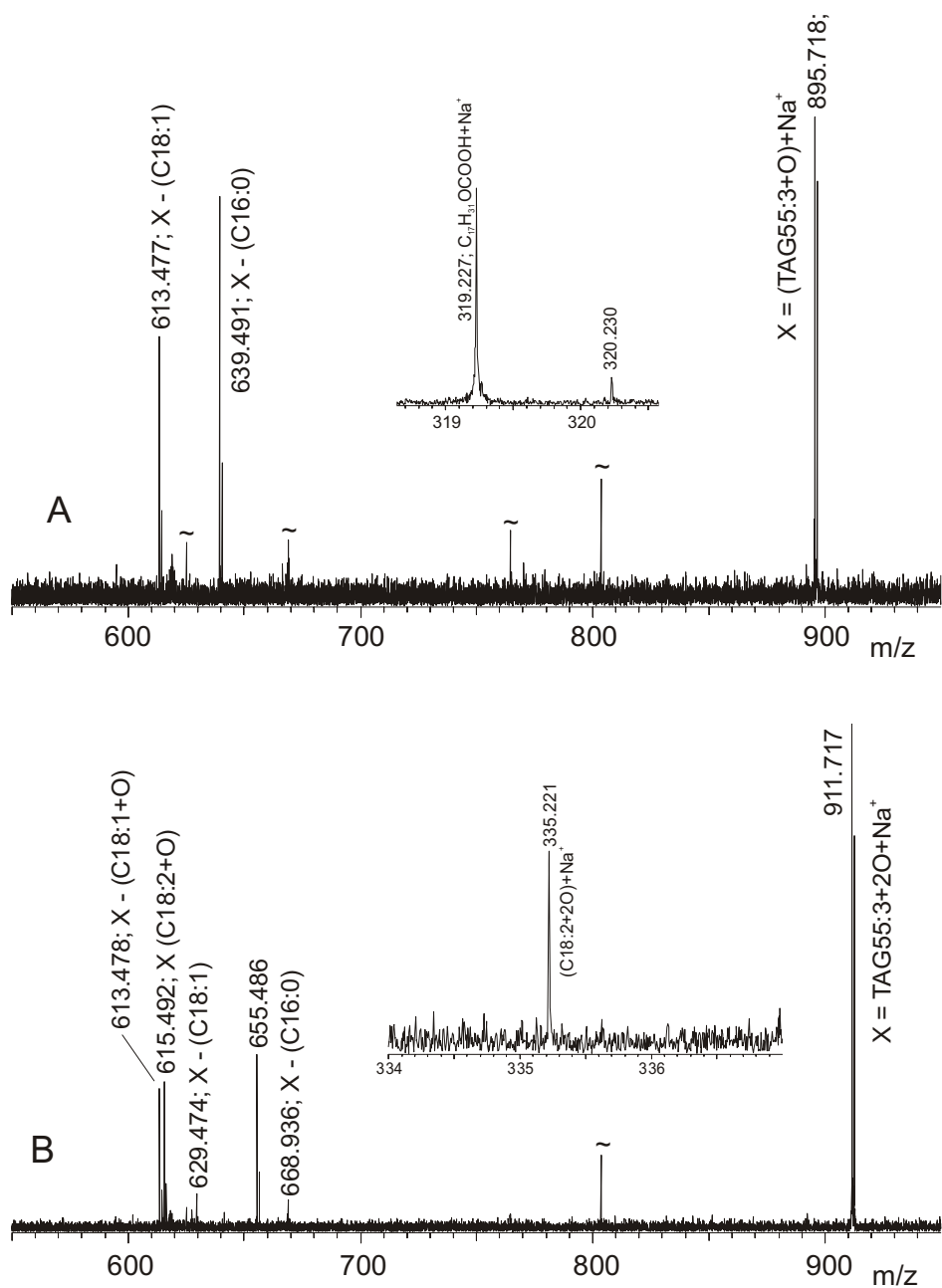
Figure 7 *CAD-MSMS spectra of the sodium adduct peaks of the singly oxygenated TAG-55:3+O (A) and the doubly oxygenated TAG-55:3+2O (B) from the ESI-FTMS spectrum of light-aged egg-only tempera. Twenty and fifty spectra were summed, respectively.*

A DAG fragment peak resulting from loss of a complementary oxygenated doubly unsaturated C18 FA moiety ($C_{17}H_{31}OCOOH$) is not observed in **Figure 7A**. At m/z 319.227, however, a peak is present (see inset), which is interpreted as the sodium adduct of such an oxygenated fatty acid ($[C_{17}H_{31}OCOOH+Na]^+$, exact mass 319.224). This indicates that the charge can also remain on an oxygenated fatty acid (instead of the glycerol backbone of the DAG fragment) by interaction between the sodium cation and oxygen containing functional groups on the oxidised fatty acyl chains. In relation to this it must be remarked that Na^+ adducts of unoxidised fatty acids are not observed in the MSMS spectra. The question whether the $[oxoFA+Na]^+$ ions are indicative of specific functionalities was not further investigated. The formation of $[oxoFA+Na]^+$ complicates the elucidation of the positional structure of the TAGs by using the ratios of the DAG fragments. More knowledge of the fragmentation of oxygenated TAG has to be generated before peak ratios can be used safely for this purpose.

The MSMS spectrum of the sodium cationised doubly oxygenated TAG55:3+2O (m/z 911.717) from the same sample of light-aged egg-only tempera is shown in **Figure 7B.** A DAG fragment peak resulting from loss of a palmitic acid moiety is observed at m/z 655.486. The DAG fragments at m/z 613.478 (mass difference with parent ion: 298.239) and m/z 615.492 (mass difference with parent ion: 296.225) are interpreted as the result of the loss of a singly oxygenated singly unsaturated C-18 FA moiety ($C_{17}H_{33}OCOOH$, exact mass 298.251) and a singly oxygenated doubly unsaturated C-18 FA moiety ($C_{17}H_{31}OCOOH$, exact mass 296.235), respectively. A ($[C_{17}H_{31}OCOOH+Na]^+$ peak is observed at m/z 319.226 (data not shown). These four peaks indicate that the TAG55:3+2O molecules have a fatty acid speciation 16:0/18:2+O/18:1+O. The peaks observed at m/z 335.221 and at m/z 629.474 are attributed to $[C_{17}H_{31}O_2COOH+Na]^+$ (exact mass 335.219) and $[M+Na-(18:1)]^+$, respectively. These peaks point to the presence of a different fatty acid speciation, viz. 16:0/18:2+2O/18:1.

The peak at m/z 925 in the mass spectrum of the light-aged egg sample consists of a doublet of TAG55:4+3O (m/z 925.687) and TAG57:2+O (m/z 925.778). Although the Arbitrary Waveform Generator can be used to apply a SWIFT pulse for the selection of only one of these peaks, the MSMS spectrum of the doublet at m/z 925, shown in **Figure 8**, demonstrates that this is not necessary for elucidation of the fatty acyl speciation of both oxidation products. The mass accuracy of the FTMSMS data is sufficient to determine whether a DAG fragment ion observed originates from the TAG55:4+3O or from the TAG57:2+O. The resulting assignment of the peaks in the MSMS spectrum is
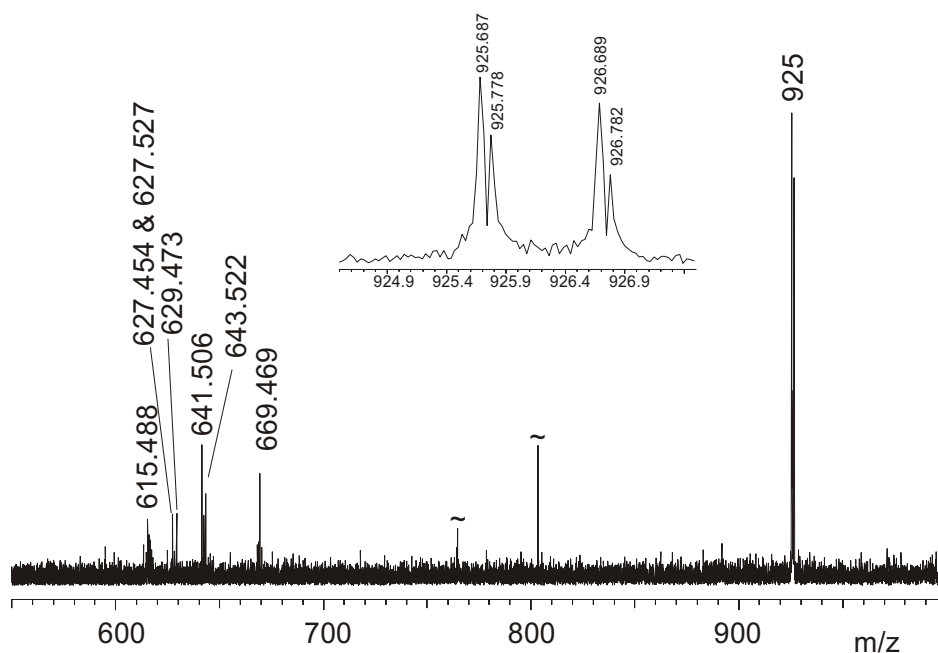
Figure 8 *CAD-MSMS spectra of the doublet of [TAG55:4+3O+Na]$^+$ and [(TAG57:2+O)+Na]$^+$ at m/z 925 in the ESI-FTMS spectrum of light-aged egg-only tempera. The inset shows that the peaks at m/z 925 and 926 consist of doublets. One hundred spectra were summed.*

given in **Table 2**. The first column in the table gives the peaks in the MSMS spectrum. The second and the third column give the mass differences of these peaks with each of the respective parent ions. The fourth column assigns the fragment peaks based on comparison of the observed mass differences with the exact mass of neutral (oxygenated) fatty acid moieties, given in the fifth column. Because most of the peaks in the spectrum originate from fragmentation of the TAG55:4+3O, most information is obtained on this compound. It contains native 16:0 and 18:1, singly oxygenated 18:1, 18:2 and 18:3, and doubly and triply oxygenated 18:3. The TAG57:2+O contains unaltered 18:0 and 18:1 and 18:1+O fatty acid moieties. Hence, there are four TAGs with different fatty acid speciations that contribute to the TAG55:4+3O. On the basis of the DAG fragments there is one possible fatty acid speciation for the TAG57:2+O peak. These assignments are specified in the lower part of **Table 2**. The fact that a $[C_{17}H_{31}O_2COOH+Na]^+$ peak is observed at very low intensity, and the absence of a $[(TAG57:2+O)+Na-(18:2+O)]^+$ peak in the spectrum make the presence of a 18:2+O fatty acyl moiety in the TAG57:2+O very unlikely. The assignment which includes this possibility is therefore placed in parentheses in **Table 2**.

The previous examples have shown two types of ions that are formed upon fragmentation of (oxidised) TAGs, viz. $[TAG+Na-FA]^+$ and $[FA+Na]^+$ (oxygenated fatty acids only). When the triply oxygenated TAG55:3+3O is analysed by ESI-FTMSMS (data not shown), loss of smaller oxygen containing neutrals from the pseudo-molecular ion is observed. This points to fragmentation of one of the oxygenated fatty acyl chains. The potential of such fragmentations as markers for specific functionalities that are introduced upon oxidation of TAGs was not explored further, because extensive research with standards of oxidised TAGs would have been required.

Table 2 *Assignment of peaks in the FTMSMS spectrum of the doublet at m/z 925.*

Peak	Δm with parent I	Δm with parent II	Assignment	Exact mass (difference)
925.687 ParentI	0	n.r.	TAG-55:4+3O+Na$^+$	925.710
925.778 ParentII	n.r.	0	TAG-57:2+O+Na$^+$	925.783
669.469	256.218	256.309	I-16:0	(256.240)
643.522	282.165	282.256	II-18:1	(282.256)
643.447	282.240	282.331	I-18:1	(282.256)
641.506	284.181	284.272	II-18:0	(284.272)
629.473	296.214	296.305	I-{18:2+O}	(296.235)
627.527 *	298.160	298.251	II-{18:1+O}	(298.251)
627.454	298.233	298.324	I-{18:1+O}	(298.251)
615.488	310.199	310.290	I-{18:3+O}	(310.214)
613.484	312.203	312.294	I-{18:2+2O}	(312.230)
599.499 *	326.188	326.279	I-{18:3+3O}	(326.209)
321.243	n.r.	n.r.	18:1+O+Na$^+$	321.240
319.226 *	n.r.	n.r.	18:2+O+Na$^+$	319.224

Assignment of TAGs		Fatty acid speciation
TAG-55:4+3O+Na$^+$		16:0 / 18:1 / 18:3+3O
		16:0 / 18:1+O / 18:3+2O
		16:0 / 18:2 / 18:2 +2O
		16:0 / 18:1+2O / 18:3+O
TAG-57:2+O+Na$^+$		18:0 / 18:1 / 18:1+O
		(18:0 / 18:0 / 18:2+O)
* very small peak, n.r. = not relevant		

7.5 Part C: Trimethylsilyl derivatised light-aged egg

7.5.1 ESI-FTMS

The presence of hydroxyl (and hydroperoxyl) functionalities was further investigated by analysis of a trimethylsilylated (TMS) sample of light-aged egg-only tempera. Note that both hydroxyl and hydroperoxyl funtionalities are derivatised to trimethylsilyl ether (O-TMS) groups. The spectrum of the TMS derivatised sample is shown in **Figure 9**. Because ammonium acetate was used to facilitate cationisation, TAGs and DAGs are observed as ammonium adducts and phospholipids as protonated molecules. The assignment of the peaks is given in the last four columns of **Table 1**. In **Figure 9** peaks originating from TAGs with up to four TMS groups are observed, indicating that hydroxyl and/or hydroperoxyl functionalities are abundant in the light-aged sample. The spectrum also shows peaks that are attributed to underivatised singly oxygenated TAG. This suggests that functionalities that cannot be TMS derivatised, such as epoxides and keto-groups, are present in the light-exposed sample. Conclusions regarding the significance of the relative abundance of TMS reactive groups and TMS unreactive groups are difficult to draw because comparative data on the ionisation efficiency of TMS derivatised and underivatised oxygenated TAGs are not available. Peaks of the oxo-TAGs that have taken up an odd number of TMS groups (1 or 3) show a higher intensity than the oxo-TAGs that have taken up an even number of TMS groups (2 or 4). This can be taken as a strong indication that progressed oxidation of unsaturated TAGs involves the formation of a dihydroxyl functionality after initial take-up of one oxygen atom.

The DAGs are also observed as (ammonium adducts of) trimethylsilylated compounds. Underivatised DAGs were not detected. The peak at m/z 772.631 can be attributed in two ways. It can originate from an oxidative cleavage product ($[(TAG44:1+3O)+NH_4]^+$; exact mass 772.630) or from a doubly trimethylsilylated DAG37:2+O ($[(DAG37:2+O+2TMS)+NH_4]^+$; exact mass 772.630). The latter is most probable because the TAG44:1+3O is not observed in the FTMS spectrum of the underivatised sample. At m/z 870.683 a small peak is present that is attributed to the TMS derivatised TAG46:2+3O ($[(TAG46:2+3O+TMS)+NH_4]^+$; exact mass 870.685). This is the only evidence for TMS derivatised oxidative cleavage products in the FTMS spectrum. Other oxidative cleavage products are mainly observed as underivatised compounds, which indicates that they do not contain hydroxyl, hydroperoxyl or carboxylic

16-DAY LIGHT-AGED, SILYLATED

A

LPC24:1+TMS

LPC26:1+TMS

DAG37:1+TMS

DAG39:x+TMS

DAG39:x+O+TMS

DAG37:x+O+2TMS

TAG46:x+2O

DAPC44:1

TAG46:x+3O

× 4

550 600 650 700 750 800

B

DAPC42:1+O+TMS

TAG53:x

TAG55:x

TAG55:x+O

TAG57:x

TAG55:x+2O

TAG57:x+O

TAG53:x+O+TMS

TAG55:x+O+TMS

TAG55:x+2O+TMS

TAG55:x+2O+2TMS

TAG55:x+3O+2TMS

TAG55:x+3O+3TMS

TAG55:x+4O+3TMS

TAG57:x+3O+3TMS

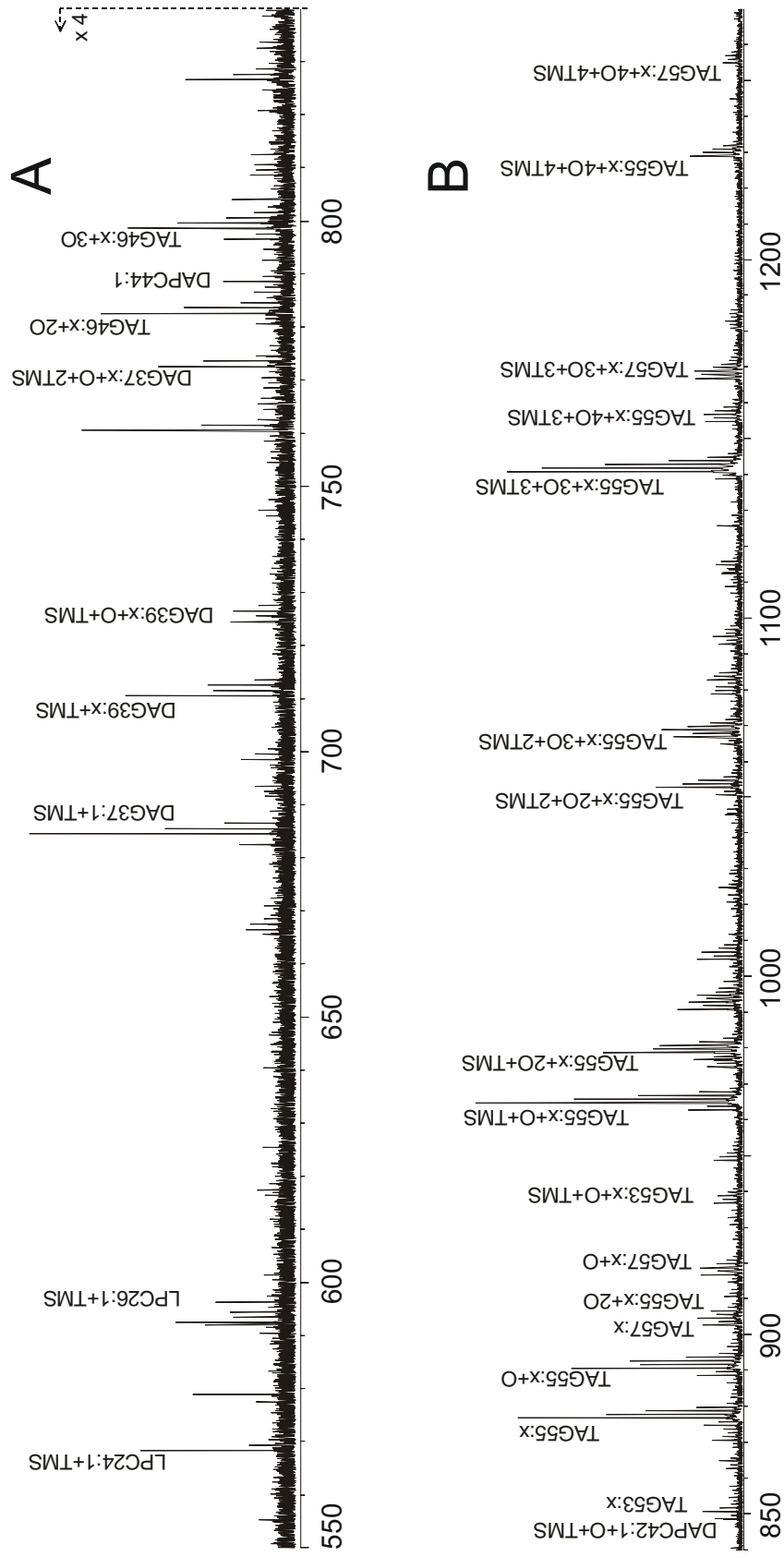TAG55:x+4O+4TMS

TAG57:x+4O+4TMS

850 900 1000 1100 1200

Figure 9 *ESI-FTMS spectrum of trimethylsilyl derivatised sample of 16-day light-aged egg-only tempera, m/z 550-840 (A) and m/z 840-1270 (B). Five hundred spectra were summed*

acid functionalities. Hence, they must contain epoxide, epidioxide, keto or aldehyde functionalities. Oxidative cleavage products of polyunsaturated fatty acid methyl esters are reported in the literature [26] to contain mainly aldehyde groups and smaller amounts of oxygen-free oxidative cleavage product.

The LPCs detected in the underivatised sample are now present as trimethylsilylated species. DAPCs are observed at the same masses as in the spectrum of the underivatised sample, which proves that the DAPCs are not derivatised on the phosphate group. Only one peak (at m/z 848.613) is present in the spectrum which can be attributed to a TMS derivatised oxygenated DAPC42:1 ($[(DAPC42:1+O+TMS)+NH_4]^+$; exact mass 848.620). Other peaks of oxygenated DAPCs, either derivatised or underivatised are not identified. In general we have noted that the sensitivity of the analytical process decreases upon derivatisation.

7.5.2 ESI-FTMSMS of TMS derivatised light-aged egg

Figure 10A shows the MSMS spectrum of a peak identified as TMS derivatised TAG55:2+2O (m/z 985.789). The DAG fragment peaks originate from loss of 16:0, 18:0 18:1, 18:1+O, and 18:1+O+TMS fatty acid neutrals from the parent ion. The insets (m/z 727-731 and m/z 613-617) show that small peaks are present at one or two mass units lower than the fragment peaks (F_1 and F_2). In both cases the F_x-2 peak is lower than the F_x-1 peak. These peaks illustrate the statement above that fragments of the second isotope peak of a TAG with one less unsaturation can be identified on the basis of the isotope ratios. The partial mass spectrum of the cluster of peaks from which the m/z 985 peak was isolated (**Figure 10B**) shows that the m/z 983 peak is relatively high so that a significant contribution of the second isotope peak ($^{13}C_2$) to the m/z 985 can be expected. The theoretical intensity of the second isotope peak of TAG55:3+2O+TMS is indicated by the arrow.

In addition to the DAG fragments the MSMS spectrum (**Figure 10A**) contains relatively intense peaks that are attributed to TMS derivatised oxygenated fatty acid fragments. The $[(18:1+2O+TMS)+Na]^+$ (exact mass: 409.274) peak at m/z 409.281 for instance indicates that also 18:1+2O+TMS fatty acyl moieties are present in the parent ion. The peak at m/z 408 originates from the contribution of the second isotope peak of $[(TAG55:3+2O+TMS)+Na]^+$ to the m/z 985 peak isolated for MSMS, and is interpreted as the first isotope peak ($^{13}C_1$) of the $[(18:2+2O+TMS)+Na]^+$ fragment. The expected isotope ratio (all-^{12}C:$^{13}C_1$:$^{13}C_2$) of a cluster of fragment ions that derives from the second isotope peak of a $[(TAG55:3+2O+TMS)+Na]^+$ parent ion is 0.40:0.47:0.13. Hence, the
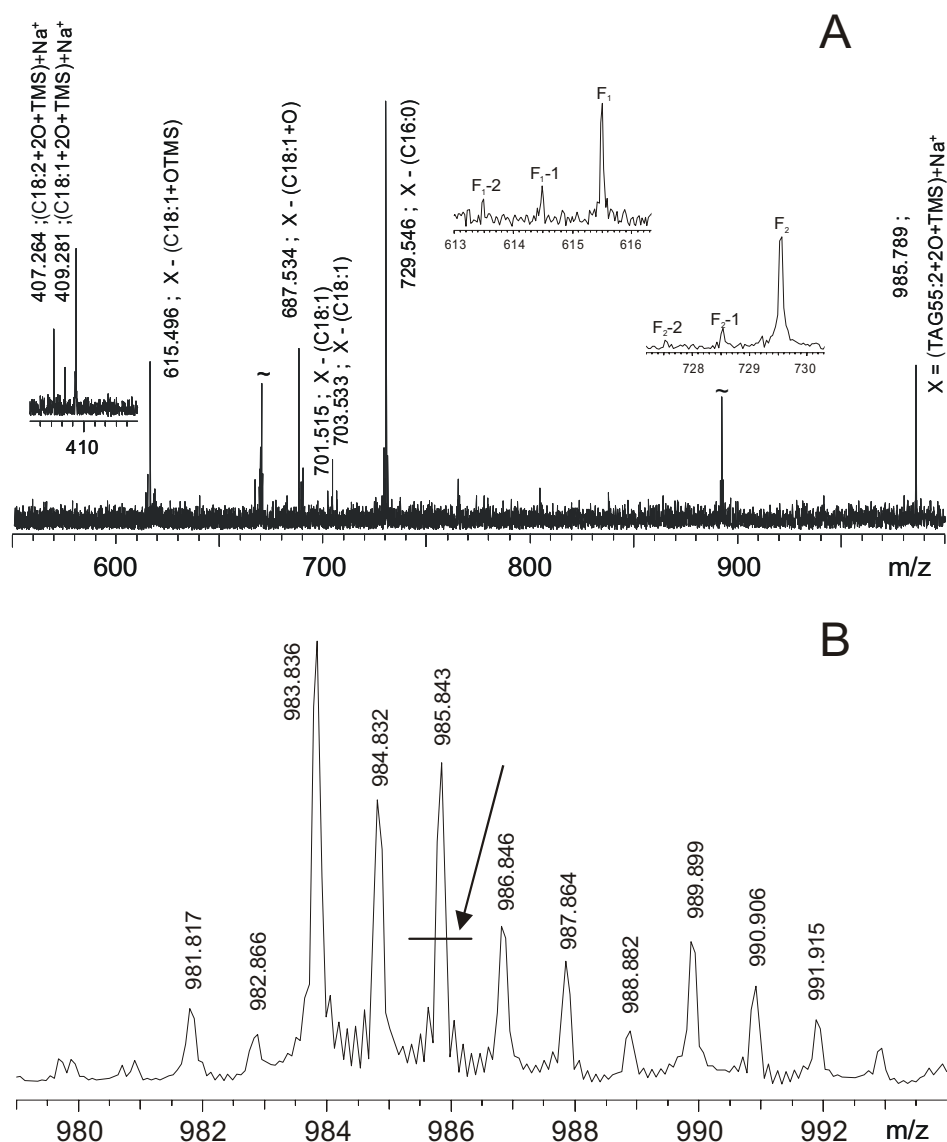
Figure 10 *CAD-MSMS spectrum of the TMS derivatised TAG55:2+2O (A) {F1 = the [TAG55:2+2O+TMS+Na-16:0]⁺ fragment peak and F2 = the [TAG55:2+2O+TMS+Na-18:1]⁺ fragment peak}, and the partial ESI-FTMS spectrum of the cluster of peaks from which the m/z 985 peak was isolated (B). In both cases 20 spectra were summed.*

$[(18:2+2O+TMS)+Na]^+$ (exact mass: 407.258) peak at m/z 407.264 derives mainly from the $[(TAG55:2+2O+TMS)+Na]^+$ parent ion.

Given the fact that more than three fatty acids are found as fragments or neutral losses from the TAG55:2+2O+TMS, it must be concluded that the peak at m/z 985.789 in the spectrum of TMS derivatised light-aged egg originates from a mixture of compounds. Although there is a great variety of TAGs that can be constructed theoretically with these fatty acids, there are only three combinations

which match the composition of the TAG55:2+2O+TMS. Based on the intensity of the fragment ions, two main constituents, viz. 16:0/18:1/(18:1+2O+TMS) and 16:0/(18:1+O+TMS)/(18:1+O),   and   one   minor   constituent,   viz. 16:0/(18:2+2O+TMS)/18:0 are identified. The literature indicates that the more saturated fatty acyl chains most often occupy the sn-1 (and sn-3) positions. Our data do not allow conclusions regarding the position of the fatty acyl chains.

The results presented in this section indicate that the MSMS of TMS derivatised oxygenated TAGs produces similar fragments as MSMS of underivatised oxygenated TAGs.   In both cases (TMS derivatised) DAG fragments and cationised (TMS derivatised) multiply oxygenated fatty acids are observed.   In relation to this we point to the MSMS of the (singly TMS derivatised) [(TAG55:3+3O+TMS)+Na]$^+$ ion that also shows fragmentation of an oxygenated fatty acyl chain.

7.6 *The potential of ESI-FTMS(MS) as a tool for the investigation of glycerolipids*

The ESI-FTMS results described here clearly show that the high resolution of the FTMS data allows unambiguous identification of a great variety of glycerolipids and their oxidation products based on their exact mass. In the case of a mixture of (oxidised) DAGs, TAGs, LPCs and DAPCs, the class of glycerolipids, the total number of carbon atoms, the number of unsaturations and the degree of oxygenation can be derived from an ESI mass spectrum that has been obtained in a few minutes. In this way ESI-FTMS with its vastly superior resolving power can be seen as an alternative for GC and LC. In the case of the light-aged egg-only tempera 125 components of different molecular mass were detected by ESI-FTMS.

Structural information on TAGs is obtained by tandem mass spectrometry (ESI-FTMSMS). As shown above, the fatty acid speciation of TAGs and isobaric oxidised TAGs can be derived from CID-MSMS results. ESI-FTMSMS of simple TAGs, which contain fatty acyl groups with more or less equivalent polarity allows discrimination between sn-2 and sn-1 or sn-3 substituents. Sn-1 and sn-3 substituents cannot be discriminated and hence the different enantiomeric forms of TAGs cannot be addressed by the ESI-FTMSMS methodology. Conventional elaborate methods and separation on chiral columns have to be used to investigate the stereo-isomers of glycerolipids [35, 36].

ESI-FTMSMS is a valuable tool in the investigation of lipid oxidation because the MSMS spectra of oxidised triacylglycerols make it possible to derive information on the fatty acid moieties where oxygenation has taken place. The high resolution of the FTMSMS data is indispensable for the interpretation of the spectra of oxygenated egg glycerolipids in our dosimeters.

For the determination of the fatty acid distribution in phosphatidylcholines (and other glycerophospholipids), a similar ESI-FTMSMS approach can be used. It must be noted that information on the fatty acyl chains is best obtained using negative ion FTMSMS. Marto *et al.* [14] have explored the application of negative ion MALDI-FTMSMS for the structure elucidation of glycerophospholipids. Hoischen *et al.* [37] have applied negative ion ESI-MS-CID-MS (on a quadrupole instrument) for the structural characterisation of phospholipids.

Structural information on the fatty acyl chains can be obtained by high energy CID-MSMS. Examples of this approach have not been shown here. Cheng *et al.* [16], however, have shown that charge remote fragmentation of TAGs yields detailed information, such as the position of double bonds in the fatty acyl chains. The high resolution of the FTMS further extends this potential of ESI-MS to the structure elucidation of glycerolipid oxidation products. The functional groups introduced upon oxidation can be assessed by derivatisation prior to ESI-FTMS analysis. The example in this paper shows that ESI-FTMSMS of oxygenated TAGs which contain TMS derivatised hydro(pero)xyl functionalities yields useful structural information on the fatty acid speciation. A variety of very selective silyl based derivatisation reagents is available. The combined use of ESI-FTMSMS with more specific derivatisation of functionalities can be of great value for the in-depth investigation of the oxidation of unsaturated glycerolipids.

If complete characterisation of mixtures of oxidised TAGs is an aim, ESI-FTMS(MS) can be used as a complementary technique to GCMS. Van den Berg [38] has shown that combined transesterification and silylation of oxidised oils followed by GCMS analysis can give valuable information on the functionalities introduced upon oxidation. If such information is combined with ESI-FTMS(MS) data on the same (TMS derivatised, but not transesterified) samples, integral characterisation of the TAG fraction oxidised oils can be attained. Obviously, the use of ESI-FTMS(MS) in combination with LC (for separation on the basis of functional groups) will be very powerful as well.

The value of ESI-FTMS to obtain qualitative information on complicated mixtures of glycerolipids is clear. For more quantitative information relative ionisation efficiencies of the components must be known, just like they have to be known for GC and HPLC [3]. Knowledge is being built up on proton affinities of

saturated fatty acid esters [39]. Duffin *et al.* [15] have determined relative ionisation efficiencies (electrospray) for saturated TAGs with different numbers of carbon atoms in the range of TAG51 till TAG69. They also determined that the presence of unsaturations in TAG69 decreased the ionisation efficiency. The response was found to be linear with concentration over four orders of magnitude. Such knowledge is useful for the interpretation of ESI mass spectra of clean samples of simple TAGs. However, it is not sufficient to guarantee robust quantification when a great variety of mixtures is studied, because matrix effects play a role in the ionisation efficiency of the analytes. Hence, ESI can only be used quantitatively for well-defined solutions of analyte mixtures.

7.7 Conclusions

The combined use of ESI with quadrupole accumulation and an open cylindrical ICR-cell facilitated the detection of a great variety of glycerolipids and their oxidation products extracted from a complex matrix such as egg. The efficient and relatively stable ion production of ESI is an advantage for structural studies by MSMS and gives ESI a distinct advantage over MALDI where the signal intensity often depends on "sweet spots". Sample preparation for ESI is not more complicated than for MALDI.

When ammonium acetate is used for cationisation of the sample, DAG pseudomolecular ions can be discriminated from diglyceride fragment ions of oxygenated TAGs and DAPCs, so that hydrolytic processes and oxidative processes in triglycerides can be followed simultaneously. Thus, the ESI-FTMS methodology is very useful to study changes in triglycerides and phospholipids in complex mixtures.

Due to the higher sensitivity of the present ESI-FTMS methodology a greater variety of components was detected in untreated egg and light-aged egg compared with MALDI-FTMS. There are strong indications that the untreated egg contains TAG59:3-7 and TAG61:4-7, which are not reported in the literature. In the light-aged egg-only tempera oxidative cleavage products of TAGs result mainly from loss of C_8 and C_9 moieties and thus indicate that photo-oxidation is the major process in the light ageing of the egg-only tempera. The oxidative cleavage products are likely to contain carbonyl functionalities. Oxidatively cleaved PCs are also observed, which probably contain carboxylic acid functionalities.

ESI-FTMSMS of TAGs reveals their fatty acid composition. In the case of simple triacylglycerols the relative intensities of the diglyceride fragment ions indicates which fatty acyl group is present on the sn-2 position. The MSMS results obtained on selected peaks in the ESI-FTMS spectrum of light-aged egg-only tempera indicated the number of oxygen atom inserted in each of the fatty acyl chains of an oxidised TAG. Up to triple oxygenation of FA residues was observed. Not only the more sensitive 18:2 and 18:3 fatty acid residues, but also 18:1 fatty acyl groups were found to be oxygenated.

Derivatisation of light-aged samples before ESI-FTMS analysis allows identification of hydro(pero)xyl functionalities introduced in the fatty acyl side chains as a result of photo-oxidation. The results presented show that oxidised TAGs contain functionalities that can be trimethylsilylated (hydroxyl or hydroperoxyl) as well as functionalities that are not trimethylsilylated (e.g. epoxide, keto and aldehyde).
MSMS of the TMS derivatised TAG oxidation products was applied successfully. The main fragmentation pathway of trimethylsilylated oxygenated TAGs is formation of DAG fragments.

References

1   Gornall, D. A., and Kuksis, A., 'Molecular species of glycerophosphatides and triglycerides of egg yolk lipoproteins', *Canadian Journal of Biochemistry* **49** (1971) 51-60.

2   Singleton, J. A., and Pattee, H. E., 'Characterization of peanut oil triacylglycerols by HPLC, GLC and EIMS', *The Journal of the American Oil Chemists' Society* **64** (4) (1987) 534-538.

3   Rezanka, T., and Mares, P., 'Determination of plant triacylglycerols using capillary gas chromatography, high-perfomance liquid chromatography and mass spectrometry', *Journal of Chromatography* **542** (1991) 145-159.

4   Sjövall, O., Kuksis, A., Marai, L., and Myher, J. J., 'Elution factors of sybthetic oxotriacylglycerols as an aid in identification of peroxidized natural triacylglycerols by reverse-phase high-performance liquid chromatography with electrospray mass spectrometry', *Lipids* **32** (11) (1997) 1211-1218.

5   Taguchi, R., Hayakawa, J., Takeuchi, Y., and Ishida, M., 'Two-dimensional analysis of phospholipids by capillary liquid chromatography/electrospray ionization mass spectrometry', *Journal of Mass Spectrometry* **35** (2000) 953-966.

6   Ravandi, A., Kuksis, A., Myher, J. J., and Maraj, L., 'Determination of lipid ester ozonides and core aldehydes by high-performance liquid chromatography with on-line mass spectrometry', *Journal of Biochemical and Biophysical Methods* **30** (1995) 271-285.

7   Christie, W. W., 'Advances in lipid methodology - Four' in The Oily Press Lipid Library, ed. Christie, W. W., Vol. 8, The Oily Press, Ayr, Scotland (1997) 301.

8   Christie, W. W., *Gas chromatography and lipids. A practical guide*, Vol. 1 The Oily Press, Ayr, Scotland (1989) 307 pp.

9   Christie, W. W., 'Advances in lipid methodology - One' in The Oily Press Lipid Library, ed. Christie, W. W., Vol. 2, The Oily Press, Ayr, Scotland (1992) 369.

10   Christie, W. W., 'Advances in lipid methodology - Two' in The Oily Press Lipid Library, ed. Christie, W. W., Vol. 4, The Oily Press, Ayr, Scotland (1993) 335.

11   Christie, W. W., 'Advances in lipid methodology - Three' in The Oily Press Lipid Library, ed. Christie, W. W., Vol. 7, The Oily Press, Ayr, Scotland (1996) 377.

12   van den Brink, O. F., O'Connor, P. B., Duursma, M. C., Peulvé, S., Heeren, R. M. A., and Boon, J. J., 'Analysis of Egg Lipids and Their Oxidation Products by MALDI-FTMS' in *45th ASMS Conference on Mass Spectrometry and Allied Topics*, Palm Springs, CA, USA (1997) 1372.

13   van den Brink, O. F., O'Connor, P. B., Duursma, M. C., Heeren, R. M. A., Peulvé, S., and Boon, J. J., 'Analysis of oxygenated egg lipids in tempera paint by MALDI FT-ICR-MS(MS)' in *14th International Conference on Mass Spectrometry*, ed. E.J. Karjalainen, A.E. Hesso, J.E. Jalonen, and U.P. Karjalainen, Advances in Mass Spectrometry, Vol. 14, Elsevier, Tampere, Finland (1997) POSTER C05 TUPO076.

14   Marto, J. A., White, F. M., Seldomridge, S., and Marshall, A. G., 'Structural characterization of phospholipids by matrix assisted laser desorption/ionization Fourier transform ion cyclotron resonance mass spectrometry', *Analytical Chemistry* **67** (1995) 3979-3984.

15   Duffin, K. L., Henion, J. D., and Shieh, J. J., 'Electrospray and Tandem Mass Spectrometric Characterization of Acylglycerol Mixtures That Are Dissolved in Nonpolar Solvents', *Analytical Chemistry* **63** (1991) 1781-1788.

16   Cheng, C., Gross, M. L., and Pittenauer, E., 'Complete stuctural elucidation of triacylglycerols by tandem sector mass spectrometry', *Analytical Chemistry* **70** (1998) 4417-4426.

17   Heeren, R. M. A., and Boon, J. J., 'Rapid microscale analyses with an external ion source Fourier transform ion cyclotron resonance mass spectrometer', *International Journal of Mass Spectrometry and Ion Processes* **157/158** (1996) 391-403.

18   Heeren, R. M. A., 'Design and performance of a thermostated open cell for FT-ICR-MS', *in preparation* (2001).

19 Koster, S., Duursma, M. C., Boon, J. J., and Heeren, R. M. A., 'Endgroup determination of synthetic polymers by electrospray ionization Fourier transform ion cyclotron resonance mass spectrometry', *Journal of the American Society for Mass Spectrometry* **11** (2000) 536-543.

20 Heeren, R. M. A., and Vekey, K., 'A novel method to determine collisional energy transfer by Fourier transform ion cyclotron resonance mass spectrometry', *Rapid Communications in Mass Spectrometry* **12** (1998) 1175-1181.

21 van Rooij, G. J., *Laser desorption analysis in trapped ion mass spectrometry systems*, PhD Thesis, University of Amsterdam (1999).

22 van den Brink, O. F., Boon, J. J., O'Connor, P. B., Duursma, M. C., and Heeren, R. M. A., 'Matrix-assisted laser desorption/ionization Fourier transform mass spectrometric analysis of oxygenated triglycerides and phosphatidylcholines in egg tempera paint systems for environmental monitoring of museum conditions', *Journal of Mass Spectrometry* **36** (2001) 479-492.

23 Kuksis, A., 'Yolk lipids', *Biochimica et Biophysica Acta* **1124** (1992) 205-222.

24 O'Connor, P. B., Heeren, R. M. A., Duursma, M. C., Rooij, G. J. v., Hage, E. R. E. v. d., and Boon, J. J., 'Analysis of polymers using FTMS' in *44th ASMS Conference on Mass Spectrometry*, Portland, Oregon, USA (1996) 654.

25 Frankel, E. N., Neff, W. E., and Selke, E., 'Analysis of autoxidised fats by gas chromatography-mass spectrometry: IX. Homolytic vs. heterolytic cleavage of primary and secondary oxidation products', *Lipids* **19** (10) (1984) 790-800.

26 Frankel, E. N., *Lipid oxidation*, Vol. 10 The Oily Press, Dundee, Scotland (1998) 303 pp.

27 Neff, W. E., Frankel, E. N., and Miyashita, K., 'Autoxidation of polyunsaturated triacylglycerols. I. Trilinoleoylglycerol', *Lipids* **25** (1990) 33-39.

28 Schieberle, P., and Grosch, W., 'Decomposition of lioleic acid hydroperoxides', *Zeitschrift für Lebensmittel-Untersuchung und -Forschung* **173** (1981) 192-198.

29 Cho, S.-Y., Miyashita, K., Miyazawa, T., Fujimoto, K., and Kaneda, T., 'Autoxidation of ethyl eicosapentaenoate and docosahexaenoate under light irradiation', *Nippon Suisan Gakkaishi* **53** (5) (1987) 813-817.

30 Zimmerman, G. A., Prescott, S. M., and McIntyre, T. M., 'Oxidatively fragmented phospholipids as inflammatory mediators: The dark side of polyunsaturated lipids', *The Journal of Nutrition* **125** (1995) 1661S-1665S.

31 Tanaka, T., Tokumura, A., and Tsukatani, H., 'Platelet-activating factor (PAF)-like phospholipids formed during peroxidation of phosphatidylcholines from different foodstuffs', *Bioscience, Biotechnology and Biochemistry* **59** (8) (1995) 1389-1393.

32   Odlyha, M., Cohen, N. S., Foster, G. M., Campana, R., Boon, J.J., Van den Brink, O.F., Peulvé, S., Bacci, M., Picollo, M., and Porcinai, S., 'ERA, Environmental Research for Art Conservation' Final Report for the European Commission. University of London, Birkbeck College (London, U.K.), FOM Institute for Atomic and Molecular Physics (Amsterdam, NL) and Istituto di Ricerca sulle Onde Elettromagnetiche, CNR (Florence, IT), (1999) 210 + xc pp.

33   van den Brink, O. F., Eijkel, G. B., and Boon, J. J., 'Dosimetry of paintings: Determination of the degree of chemical change in museum exposed test paintings by mass spectrometry', *Thermochimica Acta* **365** (1-2) (2000) 1-23.

34   Marto, J. A.,1997   Correction of paper "Structural Characterization of phospholipids by matrix assisted laser desorption/ionization fourier transform ion cyclotron resonance mass spectrometry" personal communication.

35   Myher, J. J., Kuksis, A., Geher, K., Park, P. W., and -Schade, D. A. D., 'Stereospecific analysis of triacylglycerols rich in long-chain polyunsaturated fatty acids', *Lipids* **31** (2) (1996) 207-215.

36   Itabashi, Y., and Kuksis, A., 'Reassessment of stereochemical configuration of natural phosphatidylcholines by chiral phase high performance liquid chromatography and electrospray mass spectrometry', *Analytical Biochemistry* **254** (1997) 49-56.

37   Hoischen, C., Ihn, W., Gura, K., and Gumpert, J., 'Structural characterization of molecular phospholipid species in cytoplasmic membranes of the cell wall-less Streptomyces hygroscopicus L form by use of Electrospray Ionization coupled with Collision-Induced Dissociation Mass Spectrometry', *Journal of Bacteriology* **179** (11) (1997) 3437-3442.

38   van den Berg, J. D. J., 'Determination of the degree of hydrolysis of oil paint samples using a two-step derivatisation method and on-column GC/MS', *Progress in Organic Coatings* **41** (1-3) (2001) 143-155.

39   Evans, J., Nicol, G., and Munson, B., 'Proton affinities of saturated aliphatic methyl esters', *Journal of the American Society for Mass Spectrometry* **11** (2000) 789-796.

8. Recommendations for further work on paint-based dosimetry and outlook

Although suggestions for further research and development are usually not included in a thesis such as this, the experience with exposure and analysis of the paint-based dosimeters, which has been gained in the ERA project allows the formulation of the recommendations and outlook presented in this chapter. The tempera paint-based dosimeters are now ready for further development and validation to make paint-based dosimetry a viable method for the evaluation of museum macro- and micro-environments on the large scale. The respective sections of this chapter present recommendations for the construction, readout, calibration and exposure of paint-based dosimeters.

It must be noted that some of the recommendations are currently being applied in a new project which aims at further development of paint-based dosimetry (MIMIC, Microclimate Monitoring in Cultural Heritage Preservation) [1, 2]. In addition, paint-based dosimeters which are similar to the ones used in the ERA project have been used in a study of the effects of laser cleaning of paintings in the framework of the European CRAFT-project "Advanced workstation for controlled laser cleaning of artworks" [3, 4].

8.1 Composition and size of the paint-based dosimeters

The test paintings used in the first field study of the ERA project were very large and their appearance was criticised by the management some of the museums where they were exposed [5]. In fact, the size and appearance of the test painting were the reason that the test painting in the Rijksmuseum Nightwatch room was placed where visitors could not easily see it. Reduction of the size of the test paintings will aid their acceptation by the museums and galleries. The size can be reduced by using smaller test strips. The recent application of fibre-optics in colorimetry [6, 7] allows smaller sample areas to be used for colour measurement. Very small samples can be analysed by DTMS and TGA. It must be stressed, however, that reduction in the sample size puts requirements on the homogeneity of the pigment/binder ratio of the paint systems. This applies for both surface and

bulk analysis. In the case of bulk analysis additional requirements are homogeneity of the paint layer thickness and reproducible sampling, so that the surface/volume ratio is constant for all samples. Hence, the preparation of the paint-based dosimeters must be standardised. This is an important reason to involve experienced industrial partners in the preparation of the test systems.

The present set of paint systems consisted exclusively of tempera paints with no or a single pigment. For future exploration of paint-based dosimetry it is recommended that the study be extended to a greater variety of systems, which include mixed pigments, varnished systems, other binding media, and various supports. After such an extended study, the most relevant and informative systems can be selected. The number of test systems in a test painting is then reduced so that the size of the test painting is reduced and the efficiency of paint-based dosimetry is improved.

8.2 *Readout of the dosimeters*

The robustness of paint-based dosimetry would not only benefit from standardisation of the paint formulation and preparation of the dosimeters, but also from standardisation of the readout of the dosimeters. Clearly, this applies for each of the techniques used to evaluate the changes of the physico-chemical properties of the dosimeters. As the work described here is restricted to the mass spectrometric analysis of the paint systems, the recommendations for readout of the dosimeters will focus on mass spectrometry.

In the methodology described in **Chapter 2**, samples are analysed integrally by DTMS. Hence, all components of the paint, lipids, proteins and (in)organic pigments, are subjected to analysis. As shown in **Chapters 2 and 3**, comparative DTMS analysis highlights the changes in the lipidic fraction of the paints. Lipophilic extraction of the paint samples before analysis by DTMS will further enhance the focus of the methodology on changes in the lipidic part. DTMS analysis of extracts has a distinct advantage in the case of systems that contain inorganic pigments, which may produce a great variety of interfering peaks upon pyrolysis, such as Naples yellow and lead chromate. It will also be advantageous for the analysis of paint systems such as the smalt tempera, which complicate the experimental process, in this case by the formation of glass on the filament of the DTMS probe. Preliminary tests with the light ageing series of the lead white tempera paint indicate that the discriminatory power of the lead white tempera paint system is greatly improved by analysis of dichloromethane/ethanol extracts of the exposed samples [4, 8]. The consistency of the results as

determined by the jack-knife method also increased upon extraction of the samples prior to analysis. In addition, the analysis of extracts instead of whole samples was found to cause less contamination of the instrument and require less instrument time. Although the preparation of the extracts introduces an extra, time consuming, step in the analytical methodology, it makes the practical methodology suitable for automation.

The analysis of the egg tempera binding medium can be focused on the glycerolipids by the use of other mass spectrometric ionisation techniques such as matrix-assisted laser desorption/ionisation (MALDI) and electrospray ionisation (ESI) which produce pseudo-molecular ions of triglycerides and phosphatidylcholines. **Chapters 6 and 7** have shown that analysis of such ions by Fourier transform ion cyclotron resonance mass spectrometry (FTMS) yields highly detailed spectra, which allow identification of chemical changes on the basis of differences in exact mass. The MALDI-FTMS data allow quantification of the oxidative changes induced in a series of extracts of light-aged egg-only tempera samples by determination of the degree of oxygenation of the triglycerides and phospholipids (**Chapter 6**). Using ESI-FTMS both hydrolytic and oxidative changes in triglycerides can be identified (**Chapter 7**). Of the two ionisation techniques mentioned here, MALDI combined with time-of-flight mass spectrometry (ToF-MS) is currently used for high-throughput analysis, and probably the most suitable for automation. Although analysis of the extracts of paint systems by MALDI- (and ESI-) MS techniques implies loss of information on other lipidic components of the binding medium, such as cholesterol and mastic triterpenoids, the increase in information on the triglycerides and phosphatidylcholines is enormous. A Comparison of the assays will be necessary to determine which approach yields the most information.

Probably, the environmentally induced changes observed in the paint systems take place mainly in the top layer of the paint, close to the exposed surface. It is therefore likely that the sensitivity of paint-based dosimetry can be enhanced by focussing on the changes in the surface. Preliminary investigations aimed at the analysis of the surface of egg tempera paint systems by MALDI-ToFMS produced spectra of triglycerides and phospholipids [9]. The development of this methodology for the readout of paint-based dosimeters would only require standardisation of the matrix application and hence be very suitable for automation. It must be remarked however that this methodology would also make the systems more sensitive to contamination, because it is a surface analysis technique.

8.3 Calibration of the paint based dosimeters

As mentioned in the **Chapter 3**, each of the tempera paints has a different starting point in its chemical state in terms of degree of oxidation and degree of hydrolysis. These differences, together with the varying degrees of catalytic action of each of the pigments on the environmentally induced chemical reactions constitute differences among the pigmented temperas in their response to the environmental factors. The dosimetric ranking results of nine different test systems presented in **Chapter 4** clearly illustrate this. In principle, this phenomenon can be used to deconvolve the ageing processes that effect the chemical composition of the exposed dosimeters. In this way the chemical representation of the effect of the museum environment can be used to reconstruct the most important (major) characteristics of the museum conditions. The current calibration set is too small, however, to allow this deconvolution.

The level used for the artificial light ageing to obtain a calibration set of paint-based dosimeters was 18,000 lx. This light intensity is many times higher than actual light intensities in museums and galleries. For future work exposure at lower, more realistic levels is recommended, so that the reciprocity principle can be tested. This will contribute to the understanding of the results obtained on paint-based dosimeters.

If larger training sets, including a variety of or combinations of environmental factors, are used, then a better calibration can be obtained, and observed differences can be used to indicate which of the environmental factors dominates in causing the chemical change. The calibration of the tempera test systems against light was conducted at a low RH of 27-28%. Calibration at a range of (higher) relative humidity values would be useful. Moreover, given the dramatic changes observed in the dosimeters observed upon exposure to high NO_x/SO_2 levels, more detailed investigation of these pollutants is recommended. Exposure in the ERA project was at a single value of NO_x and SO_2 and it was performed in the dark. To provide more detailed information, calibration against a range of values of NO_x and SO_2 in combination with controlled light intensity, relative humidity and temperature would be advisable. In addition studies of the effects of CO_2 and pollutants such as ozone on the dosimeters are recommended. Artificial ageing experiments involving atmospheric pollutants will be carried out in the MIMIC project.

8.4 Large-scale field exposure

A next step in the development of paint-based dosimetry could be a large-scale field exposure, which includes a range of sites with controlled and uncontrolled conditions and which would include measurement of relevant environmental conditions, including air quality, of the sites. Results obtained on field-exposed dosimeters could then be combined with records of the environmental conditions at the field sites. If the data set is large enough, data can be used as input for an expert system that correlates the results obtained on the exposed dosimeters with the conventional environmental data. Once the expert system is well trained, newly obtained dosimetric data on field sites can be put in and the expert system can be used to derive recommendations for improvement of the environmental conditions at these field sites (on the basis of the analytical/dosimetric results obtained on the paint-based dosimeters). It must be noted that the use of linear correlation methods such as principal component analysis and discriminant analysis will give rise to some fundamental problems in the correlation of the environmental factors with the dosimetric results. (It is for instance unknown whether the degree of change in paint shows a logarithmic, exponential or linear dependence of the number of visitors at a site, and hence it is not clear how the number of visitors should be specified in the data for linear correlation.) For this reason, it is recommended that non-linear correlation tools such as neural networks be explored for the development of expert systems. Clearly, the application of such tools can be used to identify correlated effects among the results of different analytical techniques.

The results of the three-months' survey in the Rijksmuseum reported in **Chapter 4** clearly show that exposure of the paint-based dosimeters for shorter periods than the nine months used in the first survey also leads to discrimination among the exposure sites. Three-months' surveys can be used to study seasonal effects.

References

1   Odlyha, M., van den Brink, O. F., Boon, J. J., Bacci, M., and Cohen, N. S., 'Environmental Research for Art Conservation: a new risk assessment tool.' in *4th European Conference for Protection, Conservation and Enhancement of European Cultural Heritage*, Strassbourg, France (2000) submitted.

2   Odlyha, M., van den Brink, O. F., Boon, J. J., Bacci, M., and Cohen, N. S., 'Damage assessment of storage and display conditions for painted works of art', *Journal of Thermal Analysis* **submitted** (2001).

3   Scholten, J. H., Teule, J. M., Zafiropulos, V., and Heeren, R. M. A., 'Advanced workstation for controlled laser cleaning of paintings' in *Optics and Lasers in Biomedicine and Culture: Contributions to the Fifth Internatinal Conference on Optics within Life Sciences OWLS V*, ed. C. Fotakis, T.G. Papazoglou, and C. Kalpouzos, Springer, Iraklion, Crete, Greece (1998) 184-187.

4   Teule, J. M., van den Brink, O. F., and Heeren, R. M. A., 'Advanced workstation for controlled laser cleaning of artworks (ENV4-CT98-0787)', ed. Teule, J. M., van den Brink, O. F., and Heeren, R. M. A., Hengelo and Amsterdam, The Netherlands (2001).

5   Hackney, S., Comment on mock paintings for dosimetry (1996) personal communication.

6   Bacci, M., 'UV-VIS-NIR, FT-IR, and FORS spectroscopies' in *Modern Analytical Methods in Art and Archeology*, ed. E. Ciliberto and G. Spoto, Chemical Analysis Series, Vol. 155, John Wiley & Sons, Inc., (2000).

7   Bacci, M., Casini, A., Lotti, F., Picollo, M., and Porcinai, S., 'Non-invasive spectroscopic methods for the characterisation of painted surfaces' in *6th International conference on non-destructive testing and microanalysis for the diagnostics and conservation of the cultural and environmental heritage*, Rome (1999) 5-13.

8   Heeren, R. M. A., and van den Brink, O. F., *Advanced workstation for controlled laser cleaning of artworks (ENV4-CT98-0787)*. Amsterdam: FOM-AMOLF, Midterm Project Review for European Commission (2000).

9   van den Brink, O. F., Duursma, M. C., Oonk, S., Eijkel, G. B., Boon, J. J., and Heeren, R. M. A., 'Probing changes in the lipid composition on the surface of laser treated artist paints by MALDI-MS.' in *49th ASMS Conference on Mass Spectrometry and Allied Topics*, ed. A.B. Giordani, Elsevier, Chicago, IL, USA (2001) in press.

Summary

Paintings change and decay slowly as a result of continuous interactions with their environment. In order to increase the life-time of the paintings, and thus preserve the cultural heritage for future generations conservation departments of museums pay a lot of attention to the control and monitoring of the museum environment.

The indoor environment of museums and galleries is subject to fluctuations in parameters such as relative humidity, temperature, light intensity and levels of pollutants such as nitrogen oxides. The indoor conditions in museums and galleries are studied by monitoring of a number of these factors. However, it is important not just to measure these variables, but also to investigate the actual damage that is caused by each of these factors. And even more important, to investigate the damage resulting from their synergistic action which may well differ from the damage caused by the individual factors. Individual paintings are themselves dosimeters of damage incurred upon exposure to their environment. The most effective way of assessing the overall damage to works of art in a given environment would be to measure changes with time in the objects themselves. This is possible with non-invasive and non-destructive techniques such as colorimetry. A disadvantage of such an approach is that damage must already be present in order to detect it, and hence that the paintings cannot be used as early-warning systems. A second disadvantage is that the effects of previous storage conditions and conservation treatments cannot be discriminated from the response of the painting to the present or near-past conditions.

Therefore, the idea was conceived in the ERA project to produce mock paintings of known composition and history which function as paint-based dosimeters that can be analysed by a variety of destructive and non-destructive techniques in order to determine the integrated effect of their exposure to the environment. The rationale and methodology of the project and the choice of the materials used are described in the **first chapter** of this thesis. The twin-track exposure of the paint-based dosimeters to predefined laboratory conditions and the environmental conditions of five selected European museums is also described in this chapter. These museum-exposure sites included rooms where environmental factors were controlled as well as rooms with uncontrolled environments. After exposure the paint-based dosimeters were analysed by a

variety of techniques which includes thermo-analytical and mechanical testing (Birkbeck College, University of London, England) and visible spectroscopic analysis (CNR-IROE, Florence, Italy). The research reported in this thesis was focused on the characterisation and semi-quantitative comparison of the molecular changes in the exposed paint-based dosimeters by mass spectrometric techniques.

Chapter 2 shows the methodology that was applied to determine the degree of chemical change in exposed paint-based dosimeters. DTMS, being a multi-component mass spectrometric finger-printing technique, was used to visualise chemical changes in the great variety of lipid constituents of the egg tempera binding medium. Oxidation and hydrolysis were identified as the most important processes that take place upon exposure of the test systems. The multivariate technique of discriminant analysis (DA) was used to quantify the difference between the mass spectrum of exposed paint systems and their unexposed controls. A procedure is described in **Chapter 3**, which tests the efficacy of the various test systems, i.e. paints with different pigments, produced in the project. In general, the paints pigmented with inorganic pigments score a lower efficacy than the unpigmented test systems. The homogeneity of a paint greatly improves the efficacy of a dosimeter.

Results obtained on the dosimeters that were exposed to laboratory conditions of light, thermal and NO_x/SO_2 concentrations clearly show that different environmental factors affect the paint systems in different ways. In all cases a positive correlation of the degree of chemical change with the duration of light exposure was observed. The data presented in **Chapters 3 and 4** show that each of the paints has its own response to the environmental conditions in the museums where they were exposed.

Results obtained on the paints with inorganic pigments classify the Tate Gallery (Clore gallery) as the best field site in terms of environmentally induced change. This is attributed to a better air quality. At the time of exposure the Tate Gallery was the only site where carbon filters were used to remove air pollutants from the inlet air of the air-conditioning system. In many cases, the uncontrolled environments of the Alcázar (Segovia, Spain) and Sandham Chapel (Burghclere, England) were found to show the largest chemical differences compared to the unexposed controls. In all cases the changes in the field-exposed dosimeters were much greater than would be expected on the basis of the reciprocity principle for light ageing (which states that the extent of damage on a system is proportional to the product of light intensity and exposure time). The dosimeter that was exposed in the Depot "Oost" of the Rijksmuseum (Amsterdam, NL), which is an almost dark site, consistently showed a significant change in the chemical composition. This is another indication that other factors than light alone contribute

significantly to the molecular changes of the tempera paints. The fact that the dosimeters are strongly affected by exposure to nitrogen oxides and sulphur oxides in the dark further confirms this observation.

Chapter 4 also reports an additional survey carried out at nine sites in the Rijksmuseum (Amsterdam, The Netherlands). The results of this survey supported the impression of the Rijksmuseum Conservation Department that there was a distinct difference in the environmental quality between the older part of the museum and the newer South wing.

In order to validate the analysis of paint-based dosimeters by DTMS and DA, the nature of the ageing processes have been investigated in more detail using advanced mass spectrometric techniques. The fate of cholesterol in egg tempera paint was investigated by tandem mass spectrometry (**Chapter 5**). A few cholesterol oxidation products, including 5,6-epoxycholestan-3-ol and 3-hydroxycholest-5-en-7-one, were positively identified in light-aged egg binding medium. Cholesterol is not a good marker for egg as binding medium in paintings, given the fast rate of oxidation of cholesterol in the egg tempera paint matrix. The cholesterol oxidation products would be better tracers.

Oxygenation of glycerolipids was unambiguously identified as an ageing process using MALDI-FTMS. Native and oxygenated phosphatidylcholines and triglycerides were detected simultaneously. The degree of oxygenation of the egg triglycerides and egg lecithin could be determined using the high resolution of the FTMS data. This work is reported in **Chapter 6**.

ESI-FTMSMS was applied for a further in-depth investigation of the changes in the glycerolipids (**Chapter 7**). It was possible to obtain structural information on the fatty acyl chains of triglycerides where oxidation had taken place. Trimethylsilyl derivatisation of samples prior to ESI-FTMS analysis allowed the identification of hydro(pero)xyl groups.

The results described in this thesis show that the principle of paint-based dosimetry of the museum environment is valid. Experience gained with paint-based dosimeters allows the formulation of recommendations for further development of the paint-based dosimetry (**Chapter 8**). One of these recommendations is to calibrate the dosimeters against combinations of environmental factors. This can be accomplished by exposure of the dosimeters to predefined combinations of environmental factors in the laboratory. In addition, results obtained on field-exposed dosimeters could be used as input for an expert system that correlates the results obtained on the dosimeters (i.e. the molecular change) with records of conventional environmental data, such as temperature, relative humidity and concentrations of air pollutants. A large-scale field exposure programme requires a further standardisation of the preparation of paint-based dosimeters.

Samenvatting

Geschilderd cultureel erfgoed staat voortdurend bloot aan invloeden van de omgeving. Als gevolg hiervan veranderen de eigenschappen van de kunstvoorwerpen. De meest opvallende veranderingen in schilderijen zijn craquelurevorming, verfverlies en verkleuring.

Teneinde de 'houdbaarheid' van schilderijen te verlengen en zodoende de kunstvoorwerpen voor volgende generaties te bewaren, wordt in de museumwereld veel aandacht besteed aan het beheersen en bewaken van de kwaliteit van de museumomgeving. Veelal gebeurt dat laatste door verschillende factoren zoals temperatuur, luchtvochtigheid en lichtintensiteit te meten. Hoewel het meten van de afzonderlijke factoren zeer informatief is, kleeft er een aantal nadelen aan deze benadering. Ten eerste geeft het geen inzicht in de processen die zich in een schilderij afspelen als gevolg van de blootstelling aan zijn omgeving. Zelfs als zou de relatie tussen verandering van een omgevingsfactor en de conditie van een schilderij bekend zijn, dan zou het uiteindelijke effect van het alle processen nog niet voorspeld worden door eenvoudige optelling van de afzonderlijke effecten. Dit vindt zijn oorsprong in het feit dat het gecombineerde effect van twee of meerdere factoren synergetisch of antagonistisch kan zijn. Ten tweede wordt bij deze benadering geen rekening gehouden met 'onverwachte' onbekende factoren, zoals plotselinge luchtverontreiniging door een onbekende bron. In de introductie van dit proefschrift worden deze nadelen verder toegelicht.

In het ERA project (Environmental Research for Art Conservation), waarvan het onderzoek in dit proefschrift deel heeft uitgemaakt, benaderen we het nauwkeurig volgen van de kwaliteit van de museumomgeving op een schilderij-georiënteerde manier. We zien het schilderij zelf als een dosimeter, die de effecten van de museumomgeving op zijn fysische en chemische conditie integreert. De chemische en fysische processen, die aan de basis liggen van het verval kunnen door analyse van schilderijmonsters gevolgd worden. Omdat het onpraktisch en bovendien ethisch onwenselijk zou zijn om dat op authentieke kunstwerken te doen, zijn er in het kader van het ERA project schilderij-achtige dosimetrische sensors ontwikkeld die bestaan uit eitemperaverf met een aantal verschillende pigmenten. De eitemperaverf is bereid volgens een oud Italiaans verfrecept.

Allereerst werden de testsystemen in een laboratorium blootgesteld aan vooraf gedefinieerde omgevingscondities. Zo werden series van lichtverouderde

en thermisch verouderde monsters verkregen. Van elk van de testsystemen werd ook een monster blootgesteld aan NO_x en SO_2. In tweede instantie werden dosimetrische schilderij-sensors gedurende een periode van negen maanden in vijf Europese musea opgehangen. De onderzochte ruimtes in deze musea verschilden in kwaliteit variërend van geklimatiseerd tot geheel niet geklimatiseerd. De veranderingen in de verf van de dosimetrische testsystemen zijn door de partners in het ERA project op verschillende manieren geanalyseerd. Veranderingen in de spectroscopische eigenschappen, zoals kleurveranderingen, zijn gemeten door de Italiaanse partners. De Engelse partners hebben zich voornamelijk op thermisch-analytische en mechanisch-analytische technieken geconcentreerd. Dit proefschrift rapporteert het werk uitgevoerd bij het FOM-Instituut voor Atoom- en Molecuulfysica en behandelt de karakterisering en semi-kwantitatieve vergelijking van de moleculaire veranderingen opgespoord met massaspectrometrische technieken. **Hoofdstuk 2** beschrijft de toegepaste methodologie van directe temperatuursopgeloste massaspectrometrie (DTMS) en multivariate analyse (DA) van de daaruit voortkomende data, die gebruikt is om de aard en mate van de chemische veranderingen vast te stellen. Oxidatie en hydrolyse blijken de belangrijkste processen die plaatsvinden bij de veroudering van eitemperaverf. **Hoofdstuk 3** evalueert de bruikbaarheid van de testsystemen en rapporteert de dosimetrische resultaten die ermee zijn verkregen, zowel na kunstmatige veroudering als na blootstelling in de musea. Homogeniteit van de verf is een belangrijke factor voor de bruikbaarheid van de testsystemen als ze moeten worden uitgelezen met behulp van de in **Hoofdstuk 2** beschreven methodologie. De data in **Hoofdstuk 3 en 4** laten ook zien dat de verschillende temperaverven verschillend reageren op dezelfde omgevingsomstandigheden. De respons van de verf als dosimetrisch systeem blijkt in belangrijke mate bepaald te worden door de pigmenten.

De temperaverf dosimeters die gepigmenteerd zijn met anorganische pigmenten wijzen de *Tate Gallery (Clore Gallery)* consequent aan als de beste locatie wanneer het gaat om de omgevingsgeïnduceerde veranderingen. Dit wordt toegeschreven aan de luchtkwaliteit in de *Tate Gallery.* Alleen daar werden toentertijd koolstoffilters gebruikt bij de luchtinlaat. In veel gevallen laten de dosimeters die blootgesteld zijn in de niet-geklimatiseerde omgeving van de *Alcázar* (Segovia, Spanje) en *Sandham Chapel* (Burghclere, Engeland), de grootste chemische verandering zien.

In alle gevallen is de mate van chemische verandering in de dosimeters groter dan verwacht op basis van het reciprociteitsprincipe voor lichtveroudering. Dit principe gaat ervan uit dat de schade aan een (verf)systeem evenredig is met het product van de lichtintensiteit en de duur van blootstelling. Zelfs de dosimeter die is blootgesteld in de vrijwel donkere omgeving van het Rijksmuseum Depot

196

'Oost' laat een belangrijke mate van chemische verandering zien. Dit is een sterke aanwijzing dat andere factoren dan de lichtintensiteit een belangrijke rol spelen in de omgevingsgeïnduceerde veroudering van de verfsystemen. Deze gedachtegang wordt bevestigd door het feit dat blootstelling aan stikstofoxiden en zwaveloxiden in het donker een sterke aantasting van de dosimeters tot gevolg heeft.

Naast de blootstelling in vijf Europese musea is er een tweede test uitgevoerd. **Hoofdstuk 4** rapporteert ook een dosimetrische verkenning van negen locaties in het Rijksmuseum te Amsterdam. De resultaten van die verkenning bevestigen het vermoeden van de conserveringsafdeling van het Rijksmuseum dat er een milieukwaliteitsverschil zou bestaan tussen het oude gedeelte van het museum en de nieuwere Zuidvleugel.

Er zijn diverse diepte-onderzoeken verricht naar de moleculaire veranderingen in de lipiden, die in de dosimeters een rol spelen als indicatorstoffen. Een voorbeeld hiervan is het onderzoek naar het lot van cholesterol in eitemperaverf dat in **Hoofdstuk 5** beschreven wordt. Met behulp van directe temperatuursopgeloste tandem massaspectrometrie (DTMSMS) zijn 5,6-epoxycholestaan-3-ol en 3-hydroxycholest-5-en-7-on geïdentificeerd als verouderingsproducten van cholesterol. Aangezien de oxidatie van cholesterol in de eitempera snel verloopt en zelfs versneld wordt door de aanwezigheid van pigmenten is cholesterol zelf geen goede indicator voor het gebruik van ei als bindmiddel in schilderijen. Oxidatieproducten van cholesterol zijn mogelijk betere markers.

Veranderingen in de glycerolipiden zijn bestudeerd met *matrix-assisted laser desorption/ionisation Fourier transform ion cyclotron resonance mass spectrometry* (MALDI-FTMS). Met deze techniek konden triglyceriden, fosfolipiden en hun verouderingsproducten simultaan en snel geanalyseerd worden. Door de hoogte van het oplossend vermogen (massa/lading schaal) en de massanauwkeurigheid van de door toepassing van deze techniek verkregen data kon oxidatie ondubbelzinnig geïdentificeerd worden als deel van het verouderingsproces en was het mogelijk de oxidatiegraad van de triglyceriden en fosfolipiden in lichtverouderde temperaverf te bepalen (**Hoofdstuk 6**).

Diepgaander onderzoek van geoxideerde triglyceriden werd uitgevoerd met behulp van electrospray-ionisatie Fourier-transformatie tandem massaspectrometrie (ESI-FTMSMS). Dit is beschreven in **Hoofdstuk 7**. Botsingsgeïnduceerde fragmentatie van pseudo-moleculaire ionen van triglyceriden laat zien op welke van de drie vetzuurstaarten van een triglyceride oxidatie heeft plaatsgevonden. ESI-FTMS(MS) van een trimethylsilyl-gederivatiseerd lichtverouderd eitemperamonster maakt het mogelijk om de hydro(pero)xyl groepen in de vetzuurstaarten te identificeren.

Tijdens het onderzoek is ervaring opgedaan die aanleiding geeft tot het doen van de in **Hoofdstuk 8** beschreven aanbevelingen voor verdere ontwikkeling van de dosimetrische verfsystemen en het 'uitlezen' daarvan. Een belangrijke aanbeveling is de kalibratie van de dosimetrische verfsystemen voor combinaties van omgevingsfactoren. Dit kan verwezenlijkt worden door de verfsystemen in een laboratorium bloot te stellen aan combinaties van factoren. Een andere manier van kalibreren bestaat uit de ontwikkeling van een expertsysteem voor de koppeling van conventionele omgevingsparameters, zoals temperatuur, luchtvochtigheid en concentratie van luchtverontreiniging aan de moleculaire veranderingen in dosimeters die in musea zijn blootgesteld. De verdere ontwikkeling van de standaardisatie van verfdosimeters is een belangrijke voorwaarde voor dergelijke grootschalige tests.

De resultaten beschreven in dit proefschrift tonen aan dat het principe van schilderijdosimetrie werkt.

Dankwoord

Als je geruime tijd bent bezig geweest met je promotieonderzoek en de verslaglegging daarvan, zijn er heel veel mensen die je wilt bedanken. Het is duidelijk dat de positieve sfeer waarin ik op AMOLF heb gewerkt, te danken is aan de instelling van de mensen die er werken en die altijd bereid zijn om je te helpen. Hoewel er veel AMOLFers zijn die ik in dat verband zou kunnen noemen, beperk ik mij hier tot diegenen met wie ik een kamer gedeeld heb of met wie ik nauw heb samengewerkt in het kader van het ERA-project. Zij die niet genoemd worden kunnen zich troosten met de gedachte dat zelfs mijn beste vrienden genoegen moeten nemen met een persoonlijke krabbel die ik voorin dit boekje plaats voordat zij het van mij ontvangen.

Ik probeer antichronologisch te werk te gaan en begin dus met mijn zusje Mariska (Ris) en promotor Jaap Boon, die terwijl ik dit schrijf hun creativiteit botvieren op de omslag van het boekje. Jaap dank ik daarnaast in het bijzonder voor de ronduit voortreffelijke wijze waarop hij mij heeft begeleid. Jaap, jouw enthousiasme voor de wetenschap werkt zeer inspirerend. Mede door jouw ontspannen begeleiding en de vrijheid die jij je mensen geeft, heb ik altijd met plezier mijn onderzoek kunnen doen. Ik prijs me gelukkig dat ik meer dan zes jaar met iemand mocht samenwerken waar ik het ook persoonlijk zo goed mee kan vinden.

Annebeth en Marlies, jullie hebben de afgelopen weken enorm veel werk hebben verricht om het boekje drukklaar te krijgen en daarmee mijn lijden verlicht. Ik waardeer jullie nimmer aflatende zorg voor kwaliteit bijzonder. Ik hoop dat jullie inmiddels geen allergie hebben ontwikkeld voor zinnen als "Misschien moeten we dat nog even aanpassen". Iliya, dank dank dank, dat je me op het allerlaatste moment, *nota bene* op je vrije middag, nog met de technische problemen van de omslag hebt geholpen.

Marc, jij was de afgelopen zes jaar mijn grote steun en toeverlaat op alles wat geen sector-instrument is. Zonder jouw hulp had ik veel leuke experimenten niet kunnen doen. Jij hebt niet alleen de instrumenten maar middels de fitness (zowel buiten als binnen de muren van het lab) ook mij in goede conditie gehouden. Overigens, wat denk je, is een FTMS zo'n krachtig apparaat omdat het zo duur is?

Jos en Sjerrie, doorzetters, wat was dat afzien hé, die eindeloze meetseries met temperamonsters op de DTMS. Met goede wil en humor werkten we door en

door, soms tot in de kleine uurtjes. Voorlopig even geen nopjes, sietjes en pbcu's meer.

Gert, ik denk dat er niemand is met wie ik zoveel gesproken heb zonder hem/haar aan te kijken als met jou. Of had jij het niet tegen mij en ik niet tegen jou? Altijd kon ik bij je terecht als ik weer eens met de handen in het haar zat vanwege software en/of hardware problemen. We hebben samen met Linda en daarna met Donna veel lol gehad in dat concertzaaltje op 1.27. Zo'n prettig microklimaat is van groot belang voor de creativiteit.

'Native speakers' Donna, Liz, Alan, Leslie, Rodger and Pete, thanks a lot for your good company and for your help when I was looking for the right words, which often resulted in very intesting discussions.

Ex-kamergenoten Gies, Inez, Ivana, Nick, Jorrit, Sannie, Sjorsje, en KJ bedankt voor de leuke tijd die we hadden in het kippenhok. We zaten elkaar wel eens in de weg, maar dat kon ook niet anders in zo'n klein hok en het was dan ook voornamelijk fysiek van aard. (Af en toe ook akoestisch, als ik weer eens een uur of langer met Marianne aan de telefoon was.)

Ron, ik heb veel geleerd van jouw lessen in pragmatiek en de aangename discussies over de technische kant van de massaspectrometrie. Bij dat laatste onderwerp is ook Piet belangrijk geweest. Ik maak van de gelegenheid gebruik om te zeggen dat heb genoten van de partijtjes pingpong met hem aan de koffietafel, zonder balletje en batje, maar met woord en geest. Alle (oud)Macromollers, Jan, Vincent, Janine, Parisz, Erik, Gerard, Muriel, Jaap vdW, Tina, Ad, Sophie, Leo (françois mayonaise), Lidwien, Katrien, Petra, Marcel, Stefan, Wim, Chris (de oorzaak van mijn komst naar AMOLF), Dominique, Beatrice, Xinghua en Ahmed. bedankt voor jullie collegialiteit en gezelligheid.

Marianne Odlyha and also Marcello Picollo, Mauro Bacci, and Neil Cohen, it was a great pleasure to work with you in the ERA-team. Met de persoon van Arie Wallert, bedank ik alle mensen van het restauratieatelier van het Rijksmuseum die mij geholpen hebben met de dosimetrische verkenningen van de museumomgeving aldaar, of zoals Arie het noemt het 'sensortjes plukken'.

Dit boekje is een MOLART report en niet voor niets. Het was me een groot genoegen om deel uit te maken van zo'n divers project. Ik dank alle Molartists van verschillende pluimage voor de prettige samenwerking.

Het slot van dit dankwoord is gereserveerd voor mijn ouders. Papa en mama, zonder jullie liefde, vertrouwen en bescherming had ik niet eens aan deze promotie kunnen beginnen. Jullie zijn geweldige kanjers! Dat mag best wel eens gezegd en, zoals in dit geval, gedrukt worden.

Oscar,   Amsterdam, oktober 2001

Curriculum Vitae

De auteur van dit proefschrift werd op 7 juli 1969 geboren in Bilthoven. Hij behaalde in 1987 het VWO diploma (Gymnasium) en begon in hetzelfde jaar met de studie Scheikunde aan de Universiteit Utrecht. In 1994 behaalde hij, na een hoofdvak Analytische Chemie gevolgd te hebben, het doctoraal examen (met genoegen). In het begin van 1995 begon hij op het FOM-Instituut voor Atoom en Molecuulfysica te Amsterdam aan het promotieonderzoek voor het EU project *'Environmental Research for Art conservation'* (ERA) dat in dit proefschrift gerapporteerd wordt. In januari 1999 ging hij bij hetzelfde instituut als onderzoeker werken aan het Europese CRAFT project *'Advanced Workstation for Controlled Laser Cleaning of Artworks'* en nam daarbij de wetenschappelijke coördinatie van dat project op zich. Momenteel werkt hij als massaspectrometrie-specialist bij Akzo Nobel - Chemicals Research Arnhem.